frontiers | Research Topics

Advances in theranostics of CNS injuries and diseases: From basic research to clinical practice

Edited by
Bo Li, Guangzhi Ning and Ping Zheng

Coordinated by
Jian Hao

Published in
Frontiers in Neuroscience

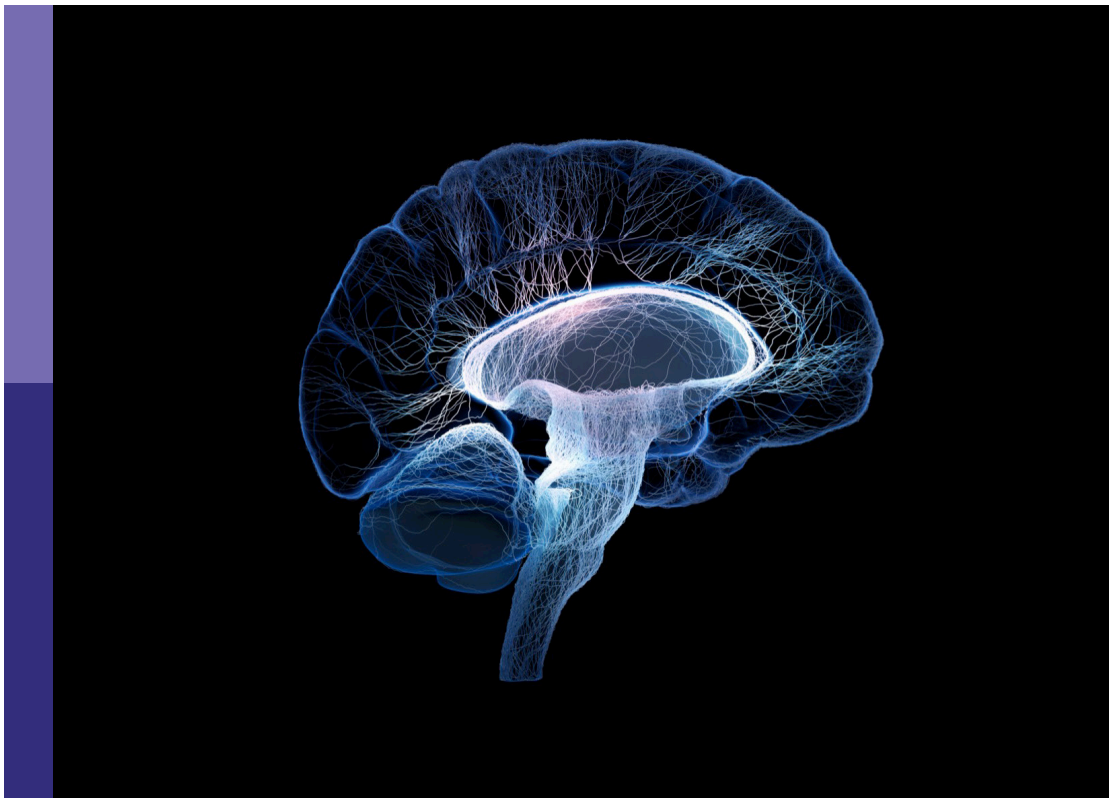

ISSN 1664-8714
ISBN 978-2-8325-3353-6
DOI 10.3389/978-2-8325-3353-6

About Frontiers

Frontiers is more than just an open access publisher of scholarly articles: it is a pioneering approach to the world of academia, radically improving the way scholarly research is managed. The grand vision of Frontiers is a world where all people have an equal opportunity to seek, share and generate knowledge. Frontiers provides immediate and permanent online open access to all its publications, but this alone is not enough to realize our grand goals.

Frontiers journal series

The Frontiers journal series is a multi-tier and interdisciplinary set of open-access, online journals, promising a paradigm shift from the current review, selection and dissemination processes in academic publishing. All Frontiers journals are driven by researchers for researchers; therefore, they constitute a service to the scholarly community. At the same time, the *Frontiers journal series* operates on a revolutionary invention, the tiered publishing system, initially addressing specific communities of scholars, and gradually climbing up to broader public understanding, thus serving the interests of the lay society, too.

Dedication to quality

Each Frontiers article is a landmark of the highest quality, thanks to genuinely collaborative interactions between authors and review editors, who include some of the world's best academicians. Research must be certified by peers before entering a stream of knowledge that may eventually reach the public - and shape society; therefore, Frontiers only applies the most rigorous and unbiased reviews. Frontiers revolutionizes research publishing by freely delivering the most outstanding research, evaluated with no bias from both the academic and social point of view. By applying the most advanced information technologies, Frontiers is catapulting scholarly publishing into a new generation.

What are Frontiers Research Topics?

Frontiers Research Topics are very popular trademarks of the *Frontiers journals series*: they are collections of at least ten articles, all centered on a particular subject. With their unique mix of varied contributions from Original Research to Review Articles, Frontiers Research Topics unify the most influential researchers, the latest key findings and historical advances in a hot research area.

Find out more on how to host your own Frontiers Research Topic or contribute to one as an author by contacting the Frontiers editorial office: frontiersin.org/about/contact

Advances in theranostics of CNS injuries and diseases: from basic research to clinical practice

Topic editors
Bo Li — Sun Yat-sen University, China
Guangzhi Ning — Tianjin Medical University General Hospital, China
Ping Zheng — University Hospital Münster, Germany

Topic Coordinator
Jian Hao — The Second Affiliated Hospital of Guangzhou Medical University, China

Citation
Li, B., Ning, G., Zheng, P., Hao, J., eds. (2023). *Advances in theranostics of CNS injuries and diseases: From basic research to clinical practice*. Lausanne: Frontiers Media SA. doi: 10.3389/978-2-8325-3353-6

Table of contents

frontiers | Frontiers in Neuroscience

TYPE Editorial
PUBLISHED 15 August 2023
DOI 10.3389/fnins.2023.1255751

OPEN ACCESS

EDITED BY
Guo-Yuan Yang,
Shanghai Jiao Tong University, China

REVIEWED BY
Andre Marolop Pangihutan Siahaan,
Universitas Sumatera Utara, Indonesia
Martin Susanto,
University of North Sumatra, Indonesia

*CORRESPONDENCE
Bo Li
libo_career@163.com
Guangzhi Ning
ningquangzhi@foxmail.com

†These authors have contributed equally to this work

RECEIVED 09 July 2023
ACCEPTED 01 August 2023
PUBLISHED 15 August 2023

CITATION
Li B, Hao J, Zheng P and Ning G (2023) Editorial: Advances in theranostics of CNS injuries and diseases: from basic research to clinical practice. *Front. Neurosci.* 17:1255751. doi: 10.3389/fnins.2023.1255751

Editorial: Advances in theranostics of CNS injuries and diseases: from basic research to clinical practice

Bo Li[1*†], Jian Hao[2†], Ping Zheng[3†] and Guangzhi Ning[4*]

[1]Department of Orthopedics, Sun Yat-Sen Memorial Hospital of Sun Yat-Sen University, Guangzhou, China, [2]Department of Orthopedics, The Second Aliated Hospital, Guangzhou Medical University, Guangzhou, China, [3]Department of Neurosurgery, Shanghai Pudong New Area People's Hospital, Shanghai, China, [4]Department of Orthopedics, Tianjin Medical University General Hospital, Tianjin, China

KEYWORDS

spinal cord injury-induced immune deficiency syndrome, kyphotic cervical spondylotic myelopathy, traumatic brain injury, acute ischemic stroke, acute cerebral hemorrhage, moyamoya disease

Editorial on the Research Topic
Advances in theranostics of CNS injuries and diseases: from basic research to clinical practice

Amid global aging populations, industrialization, and the continued occurrence of diseases and disasters, the incidence of Central Nervous System (CNS) diseases is on the rise. Injuries to the CNS such as stroke, traumatic brain injury, and spinal cord injury are often irreparable, leading to long-term disability. This research theme focuses on the forefront and progress of CNS injury research in these areas, aiming to summarize the studies on the mechanisms of CNS injury and the clinical application of advanced treatments. This editorial seeks to provide an overview of some key research achievements in this field recently, offering a novel perspective on the treatment of CNS injuries.

In the research "*CCR7-mediated T follicular helper cell differentiation is associated with the pathogenesis and immune microenvironment of spinal cord injury-induced immune deficiency syndrome*", the role of chemokine receptor CCR7 in T follicular helper cells and its relationship to spinal cord injury was probed. The downregulation of CCR7 was found in acute spinal cord injury and was linked to an altered immune microenvironment, characterized by suppressed T cell signaling and activated chemokine pathways. Thus, CCR7 can potentially be used to identify acute spinal cord injury patients and guide treatment decisions (Li et al.).

Highlighting the importance of surgical strategies in treating kyphotic cervical spondylotic myelopathy (KCSM), a study compared the efficacy of anterior decompression with fusion (ADF) vs. posterior decompression with fixation (PDF). In the study, 117 KCSM patients underwent either ADF or PDF, and cervical alignment parameters were analyzed pre and post-surgery. Results indicated that both ADF and PDF provided neurological improvement and significant reduction in axial symptoms, but ADF was more effective in improving cervical alignment. The study underscores the importance of considering each approach's pros and cons when deciding on a surgical plan for KCSM patients (Du et al.).

In a study underscoring the potential of predictive modeling in managing traumatic brain injury (TBI), a genetic algorithm modified back propagation neural network was employed to predict motor function in TBI patients. Using the Fugl-Meyer assessment scale, data from 463 TBI patients was analyzed to create the model. Key findings suggest the model showed a strong correlation of 0.95 between predicted and actual motor function outcomes. This suggests the potential of this model as a tool for risk and prognosis assessment, and aiding clinical decision-making for TBI patients (Dang et al.).

In a study aimed at understanding mortality rates and risk factors in acute ischemic stroke (AIS) patients undergoing endovascular thrombectomy (EVT), analysis of 245 patients found that early mortality occurred in 22.8% of cases. Key determinants of early mortality were recanalization status, NIHSS score 24 h post-EVT, and symptomatic intracerebral hemorrhage, underscoring their importance in mortality prediction. These findings highlight the need for careful monitoring and targeted interventions for these risk factors in AIS patients undergoing EVT (Chen et al.).

In the study "*The impact of blood pressure variability on prognosis and underlying mechanism in acute cerebral hemorrhage*", researchers evaluated 120 ICH patients post-antihypertensive treatment. They discovered high systolic blood pressure variability within 1 and 24 h linked to poor 90-day mRS scores. The findings also suggested a negative correlation between 24-h SBP variability and cerebral blood flow. This study could guide individualized antihypertensive treatment strategies for acute ICH patients (Sun et al.).

Highlighting the importance of thalamic structure and anastomosis in the progression of moyamoya disease (MMD), a retrospective study was conducted titled "*Thalamic structure and anastomosis in different hemispheres of moyamoya disease*". The study compared subcortical gray matter volume and angiographic features in symptomatic and asymptomatic hemispheres of MMD patients. Findings demonstrated significant differences in thalamic volume and the incidence of thalamic anastomosis between these hemispheres, suggesting a potential role in predicting stroke risk and understanding disease evolution in MMD patients (Hu et al.).

To understand genetic factors linked to Alzheimer's disease (AD) onset, researchers carried out a study titled "*Identification of candidate genes associated with clinical onset of Alzheimer's disease*". They utilized microarray data from post-mortem brains of AD patients and healthy controls to identify differentially expressed genes. They discovered 19 potential genes associated with symptomatic AD, four of which (VSNL1, RTN1, FGF12, and ENC1) were identified as critical. These findings could help pinpoint high-risk individuals prone to early AD onset (Liao et al.).

In a systematic review titled "*The prevalence and risk factors of anxiety in multiple sclerosis*", researchers analyzed studies to determine anxiety prevalence in MS patients and its associated risk factors. They found that around 36% of MS patients suffer from anxiety. Significant risk factors included age, gender, cohabitation, past psychiatric history, depression, lack of MS medication adherence, relapsing-remitting MS, and baseline EDSS score. This could aid in identifying MS patients at a higher risk of anxiety (Zhang et al.).

In the study "*Functional investigation and two-sample Mendelian randomization study of neuropathic pain hub genes obtained by WGCNA analysis*", researchers leveraged weighted gene co-expression network analysis (WGCNA) and differential expression to uncover neuropathic pain-associated genes. Key findings showed genes IL2, SMELL, CCL4, among others, correlated with cytokine receptor binding, chemokine pathways, and the JAK-STAT cascade. The link between IL2 and neuropathic pain was further validated by a Mendelian randomization study, helping to identify high-risk individuals (Zeng et al.).

The nine investigations included in this Research Topic delve into crucial facets of spinal cord and brain injuries, as well as neurodegenerative diseases. Each study unveils potential diagnostic markers, therapeutic strategies, and understanding disease mechanisms. They explore everything from chemokine receptors in spinal cord injury to predictive modeling in traumatic brain injury, individualized antihypertensive treatment strategies in cerebral hemorrhage, to genetic risk factors in Alzheimer's disease onset. Such comprehensive studies are crucial for devising more effective and personalized treatment plans, and for enhancing our understanding of these debilitating conditions.

Author contributions

BL: Writing—original draft. JH: Writing—review and editing. PZ: Writing—original draft. GN: Writing—original draft.

Conflict of interest

The authors declare that the research was conducted in the absence of any commercial or financial relationships that could be construed as a potential conflict of interest.

Publisher's note

frontiers | Frontiers in Neuroscience

TYPE Original Research
PUBLISHED 14 October 2022
DOI 10.3389/fnins.2022.1019406

OPEN ACCESS

EDITED BY
Bo Li,
Sun Yat-sen University, China

REVIEWED BY
Pankaj Gaur,
Georgetown University, United States
Wenyuan Shen,
Tianjin Medical University, China

*CORRESPONDENCE
Zhiming Cui
zhimingcuispine@163.com

†These authors have contributed equally to this work

SPECIALTY SECTION
This article was submitted to Translational Neuroscience, a section of the journal Frontiers in Neuroscience

RECEIVED 15 August 2022
ACCEPTED 20 September 2022
PUBLISHED 14 October 2022

CITATION
Li C, Wu C, Xu G, Liu Y, Chen J, Zhang J, Hong H, Ji C and Cui Z (2022) CCR7-mediated T follicular helper cell differentiation is associated with the pathogenesis and immune microenvironment of spinal cord injury-induced immune deficiency syndrome.
Front. Neurosci. 16:1019406.
doi: 10.3389/fnins.2022.1019406

CCR7-mediated T follicular helper cell differentiation is associated with the pathogenesis and immune microenvironment of spinal cord injury-induced immune deficiency syndrome

Chaochen Li[1,2,3†], Chunshuai Wu[1,2,3†], Guanhua Xu[1], Yang Liu[1], Jiajia Chen[1], Jinlong Zhang[1], Hongxiang Hong[1], Chunyan Ji[1,2,3] and Zhiming Cui[1,2,3*]

[1]The First People's Hospital of Nantong, The Second Affiliated Hospital of Nantong University, Nantong University, Nantong, China, [2]Key Laboratory for Restoration Mechanism and Clinical Translation of Spinal Cord Injury, Nantong, China, [3]Research Institute for Spine and Spinal Cord Disease of Nantong University, Nantong, China

Spinal cord injury-induced immune deficiency syndrome (SCI-IDS) is a disorder characterized by systemic immunosuppression secondary to SCI that dramatically increases the likelihood of infection and is difficult to treat. T follicular helper (Tfh) cells regulated by chemokine receptor CCR7 are associated with SCI-IDS after acute SCI. The present study explored the roles of CCR7 in SCI-IDS occurrence and immune microenvironment composition. Gene expression profile data of peripheral blood leukocytes from SCI and non-SCI subjects were collected from the Gene Expression Omnibus database. According to differential gene expression analysis, a protein-protein interaction (PPI) network, and risk model construction, the CCR7 expression level was prominently related to acute SCI and CCR7 expression was significantly downregulated after acute SCI. Next, we constructed a clinical prediction model and used it to identify patients with acute SCI. Using Gene Ontology (GO) analysis and gene set enrichment analysis (GSEA), we discovered that immune-related biological processes, such as T cell receptor signaling pathway, were suppressed, whereas chemokine-related signaling pathways were activated after acute SCI. Immune infiltration analysis performed using single sample GSEA and CIBERSORT suggested that Tfh cell function was significantly correlated with the CCR7 expression levels and was considerably reduced after acute SCI. Acute SCI was divided into two subtypes, and we integrated multiple classifiers to analyze and

elucidate the immunomodulatory relationships in both subtypes jointly. The results suggested that CCR7 suppresses the immunodeficiency phenotype by activating the chemokine signaling pathway in Tfh cells. In conclusion, CCR7 exhibits potential as a diagnostic marker for acute SCI.

KEYWORDS

spinal cord injury-induced immune deficiency syndrome, immune microenvironment, CCR7, biomarker, machine learning

Introduction

Spinal cord injury (SCI) is a common, serious injury associated with severe outcomes and high financial burden that causes SCI-induced immune deficiency syndrome (IDS) (Laginha et al., 2016; Wu et al., 2021). SCI-IDS can dramatically increase a patient's susceptibility to pathogenic infections, including pneumonia, and delay wound healing, leading to increased morbidity, mortality, and complications (Sekhon and Fehlings, 2001; Riegger et al., 2007; Failli et al., 2012). Clinical research on death causes in SCI patients has emphasized the prevalence of pathogenic infections in these patients. In a 70-year study in the UK, the major cause of death in SCI patients was infections, such as pneumonia (23.5% of all deaths), with another 7.8% of deaths caused by urinary tract infections and unexplained sepsis (Savic et al., 2017). In the Czech Republic, the cause of death in SCI patients within the first year was peripheral infections (24.4%), and after 1 year, peripheral infections remained the main reason for their death, including pulmonary infections (14%), urinary tract infections (10.3%), sepsis of unknown origin (6.5%), and pressure sores (12.1%) (Kriz et al., 2021). Further, infection and associated hyperthermia can impair central nervous system (CNS) function after SCI (Inamasu et al., 2003; Meisel et al., 2004). Thus, clinically relevant infections are normal after SCI and significantly affect SCI prognosis.

Rapid and accurate diagnosis of SCI and mitigation of clinically pertinent infections of patients would ensure SCI patients' recovery and their wellbeing. However, no quantitative diagnostic indicators for acute SCI are available. Acute SCI diagnosis is based on the 2011 International Standard for Neurological Classification of Spinal Cord Injury issued by the International Society for Spinal Cord Injury and the American Spinal Cord Injury Association (ASIA), ASIA Disability Classification, and comprehensive evaluation of conventional magnetic resonance images (Hulme et al., 2017; Rodrigues et al., 2018). The scoring criteria are based on the patient's neurological damage and are used to determine patient prognosis based on clinical experience, which is subjective, and diagnosis is difficult as traumatic SCI frequently appears in multiple injuries (Galeiras Vazquez et al., 2017). Further, although SCI-IDS can be treated to improve the outcome of SCI by eliminating the major factors contributing to poor recovery, the precise immune mechanism is unknown and no therapeutic target is available (Meisel et al., 2005).

Current research suggests that the balanced interaction of the CNS with the immune system can be disturbed after SCI, which is an essential mechanism of escalation to SCI-IDS and infection (Meisel et al., 2005). Following SCI, supraspinal control of the sympathetic nervous system is damaged and sympathetic nerves are dysfunctional, leading to the rapid release of glucocorticoids from the adrenal glands, thus damaging immune function (Prüss et al., 2017). In patients with SCI above T6 thoracic level, sympathetic hyperreflexia is observed, which leads to an abnormal increase in norepinephrine in the spleen and the activation of beta-adrenergic receptors on lymphocytes, leading to consistent immunosuppression (Lucin et al., 2007; Zha et al., 2014).

Various treatment approaches for SCI-IDS, including androgen receptor therapy, glucocorticoids, and neuromodulation, have been tested, but have low clinical usability because of limited sensitivity and specificity (Shi et al., 2013; Koopman et al., 2016; Ueno et al., 2016; Pavlov and Tracey, 2017). A recent study revealed that the spleen can serve as a therapeutic target to restore immune homeostasis of the body after immunosuppression following high-segment SCI (Noble et al., 2018). Notably, incompletely SCI, such as moderate to severe spinal cord contusions, can dramatically alter the level-dependence of SCI-IDS (Hong et al., 2019). However, these previous studies did not focus on differential immune cell expression and did not explore the underlying molecular mechanisms. Further research is needed to explore the pathogenesis of SCI-IDS to improve its diagnosis and treatment.

In the recent field of immune microenvironment research, T follicular helper (Tfh) cells have garnered attention because of their important roles in immune system establishment and functional refinement. Peripheral immunosuppression and impaired Tfh cell function are closely associated in

patients with severe CNS injury (Quattrocchi et al., 1991). Evidence indicates that Tfh cells have significant effects on the immunosuppressive process. For example, Tfh cells cause serious immune deficiencies due to aging (Almanan et al., 2020) and in patients with chronic inflammatory breast cancer, Tfh cells have been found to convert immunosuppression into an antitumor humoral response (Gu-Trantien et al., 2017). Tfh cells represent a particular CD4 + T cell subset of the lymph nodes and spleen and they contribute to information transfer in B cell differentiation, B cell activation, and germinal center formation (Crotty, 2014). The chemokine receptors CXCR5 and CCR7 allow the migration of Tfh cells to the T cell–B cell border for Tfh cell differentiation and maturation (Meli et al., 2016; Vinuesa et al., 2016). It has been demonstrated that that CCR7 is associated with the pathological processes of immunosuppressive diseases. For example, in myeloid cells, overexpression of CCR7 facilitated the targeted transfer of macrophages to the lymph nodes, thereby mediating immunosuppression (Yu et al., 2021).

This study aimed to identifying peripheral blood markers for accurate diagnosis of acute SCI and to interpreting changes in the immune microenvironment of SCI-IDS, using a high-throughput multi-omics approach. The potential association of CCR7 with SCI-IDS pathogenesis and changes in the immune microenvironment were examined using bioinformatics analyses, including differential gene expression analysis, protein-protein interaction (PPI) network analysis, scale-free network centrality analysis, clinical prediction model construction, functional enrichment analysis, molecular subtype analysis, and immune infiltration analysis combined with machine learning model analysis.

Materials and methods

Data sources and preprocessing

Chip-based RNA-sequencing data from peripheral blood leukocytes of acute SCI patients and controls (GSE151371) (Kyritsis et al., 2021) were collected from the Gene Expression Omnibus (GEO) database.[1] The dataset comprises data from 10 healthy control subjects (HC group), 10 trauma patients without CNS injury (TC group), and 38 acute SCI patients (SCI group). The mRNA data were $\log_2$ transformed after filtering a minimum of 70% valid values. Quantile normalization of the data was carried out using the Bioconductor package limma. Clinical data from the SCI patients, including censored data such as the ASIA impairment scale, were acquired from Kyritsis et al. (2021) (**Table 1**).

1 https://www.ncbi.nlm.nih.gov/geo/

TABLE 1 Baseline information.

Characteristic	SCI	HC	TC
n*	38	10	10
Status, n (%)			
non-SCI	0 (0%)	10 (17.2%)	10 (17.2%)
SCI	38 (65.5%)	0 (0%)	0 (0%)
Gender, n (%)			
Female	13 (22.4%)	2 (3.4%)	4 (6.9%)
Male	25 (43.1%)	8 (13.8%)	6 (10.3%)
Race, n (%)			
Asian	3 (5.2%)	0 (0%)	1 (1.7%)
Black or African-American	3 (5.2%)	2 (3.4%)	0 (0%)
Hispanic	17 (29.3%)	4 (6.9%)	4 (6.9%)
Other	0 (0%)	0 (0%)	3 (5.2%)
Unknown	10 (17.2%)	4 (6.9%)	2 (3.4%)
White	5 (8.6%)	0 (0%)	0 (0%)
Prior CNS pathology, n (%)			
No	21 (36.2%)	10 (17.2%)	10 (17.2%)
Unknown	5 (8.6%)	0 (0%)	0 (0%)
Yes	12 (20.7%)	0 (0%)	0 (0%)
Traumatic brain injury, n (%)			
No	28 (48.3%)	10 (17.2%)	10 (17.2%)
Unknown	2 (3.4%)	0 (0%)	0 (0%)
Yes	8 (13.8%)	0 (0%)	0 (0%)
Neurological level, n (%)			
Cervical	18 (31%)	0 (0%)	0 (0%)
Lumbar	2 (3.4%)	0 (0%)	0 (0%)
Thoracic	10 (17.2%)	0 (0%)	0 (0%)
Unknown	8 (13.8%)	10 (17.2%)	10 (17.2%)
Age (mean ± SD)	55.26 ± 20	49.44 ± 12.2	41.7 ± 17.98
Time of injury (median (IQR))**	23 (17, 43)		20 (19.25, 22.25)

*n, number of samples. **IQR, interquartile range.

Differential gene expression analysis

Differential gene expression among the HC, TC, and SCI groups was analyzed using the R package limma (Phipson et al., 2016) based on cutoffs of $|\log \text{fold change}| \geq 1.5$ and adjusted $p < 0.05$. In addition, differential expression between pairs of groups (HC vs. TC, HC vs. SCI, and TC vs. SCI) was analyzed. Only those genes with significant and specific changes in expression after SCI were selected ($n = 555$).

Protein-protein interaction network construction

A PPI network of the differentially expressed genes was constructed using the STRING 11.5 database

(Szklarczyk et al., 2019), with a confidence level of 0.7. To identifying highly connected subnetworks, the MCODE clustering algorithm with default parameters was applied to the network in Cytoscape (version:3.9.1) (Shannon et al., 2003). Genes in the top 2 clusters were considered as hub genes for downstream analysis. In a PPI network, node strength indicates the importance of a node according to the strength of its connections to the other network nodes. Degree centrality, betweenness centrality, closeness centrality, and stress centrality of nodes were selected as metrics of node centrality, and we calculated the degree of node centrality for each node in the PPI network using Cytoscape. Then, the intersection of the top 5 results of the four centrality analyses was taken.

Construction of risk models and nomogram prediction models

We created risk models to analyze the correlation between differentially expressed genes and acute SCI. First, we determined key genes related to acute SCI through univariate LR analysis. Second, the least absolute shrinkage and selection operator regression was applied in dimensionality reduction analysis to verify key genes related to acute SCI. Then, odds ratios, 95% confidence intervals and p-values were determined using univariate and multivariate LR. We selected only significant variables ($p < 0.05$) after multivariate LR analysis to develop nomogram prediction models for acute SCI. Model performance was evaluated using receiver operating characteristic curve (ROC) and calibration curves, representing the probability that the classifier will correctly label a new patient.

Gene set enrichment analysis (GSEA) and functional enrichment analysis

GSEA is a computational approach to analyze if any specific gene set shows statistically significant differences between two biological states and frequently applied in estimating changes in pathways and biological process activity in expression dataset samples (Subramanian et al., 2005). Differences in biological processes between groups were investigated by GSEA using the clusterProfiler package (Yu et al., 2012) and the GSE151371 dataset. Gene Ontology (GO) term enrichment and Kyoto Encyclopedia of Genes and Genomes (KEGG) pathway enrichment analyses of the 555 differentially expressed genes were conducted using the clusterProfiler package.

Immune infiltration analysis

Immune cell infiltration levels in the HC, TC, and SCI groups were estimated using single-sample (ss) GSEA in the GSVA (Hanzelmann et al., 2013) R package. ssGSEA determines the immune cell population in a sample base on gene expression data (Subramanian et al., 2005). CIBERSORT, an analytical tool developed by Newman et al. (2019) that estimates cell type abundance in a mixed cell population based on gene expression data, was used to validate immune infiltration results.

Analysis of molecular subtypes and their immune microenvironments

To identify the acute SCI subtypes, univariable LR was applied to identify genes related to ASIA levels in the SCI group, with a cutoff of $p < 0.05$. Then, the R package ConsensusClusterPlus (Wilkerson and Hayes, 2010) (reps = 1,000 bootstraps, pItem = 0.8, pFeature = 0.8) was used for class discovery. An average pairwise consensus matrix of consensus clusters, a delta plot of the relative change of the area under the consensus cumulative distribution function (CDF) curve, and the average silhouette distance of the consensus clusters were used to determine the number of clusters. Principal coordinate analysis was used to validate the molecular subtype analysis results. We selected two acute SCI clusters based on consensus clustering. To analyze the immune microenvironment in the two consensus molecular subtypes, we profiled the immune infiltration analysis in each subtype.

Immune infiltration feature identification

Patients with acute SCI were classified according to the ASIA impairment scale, with grades A, B, and C forming the ASIA-high group and grades D and E forming the ASIA-low group. Appropriate immune infiltrating cells in each subtype related to ASIA levels were selected based on ensemble models, such as extremely logistic regression (LR), a gradient boosting decision tree (GBDT), a random forest (RF), or extreme gradient boosting (XGBoost). Infiltrating immune cell importance scores were computed based on these models. Next, we obtained the immune infiltrating cells ($|\log \text{fold change}| \geq 0.25$ and false discovery rate < 0.05) between the ASIA-high and ASIA-low groups in the two molecular subtypes using the Wilcoxon test. The intersection of results of the five methods (LR, GBDT, RF, XGBoost, and the Wilcoxon test) was taken as the final immune infiltrating cells associated with ASIA levels.

Correlation analysis between immune microenvironment and acute spinal cord injury

To analyze the correlations between the immune microenvironment and acute SCI, first, correlations

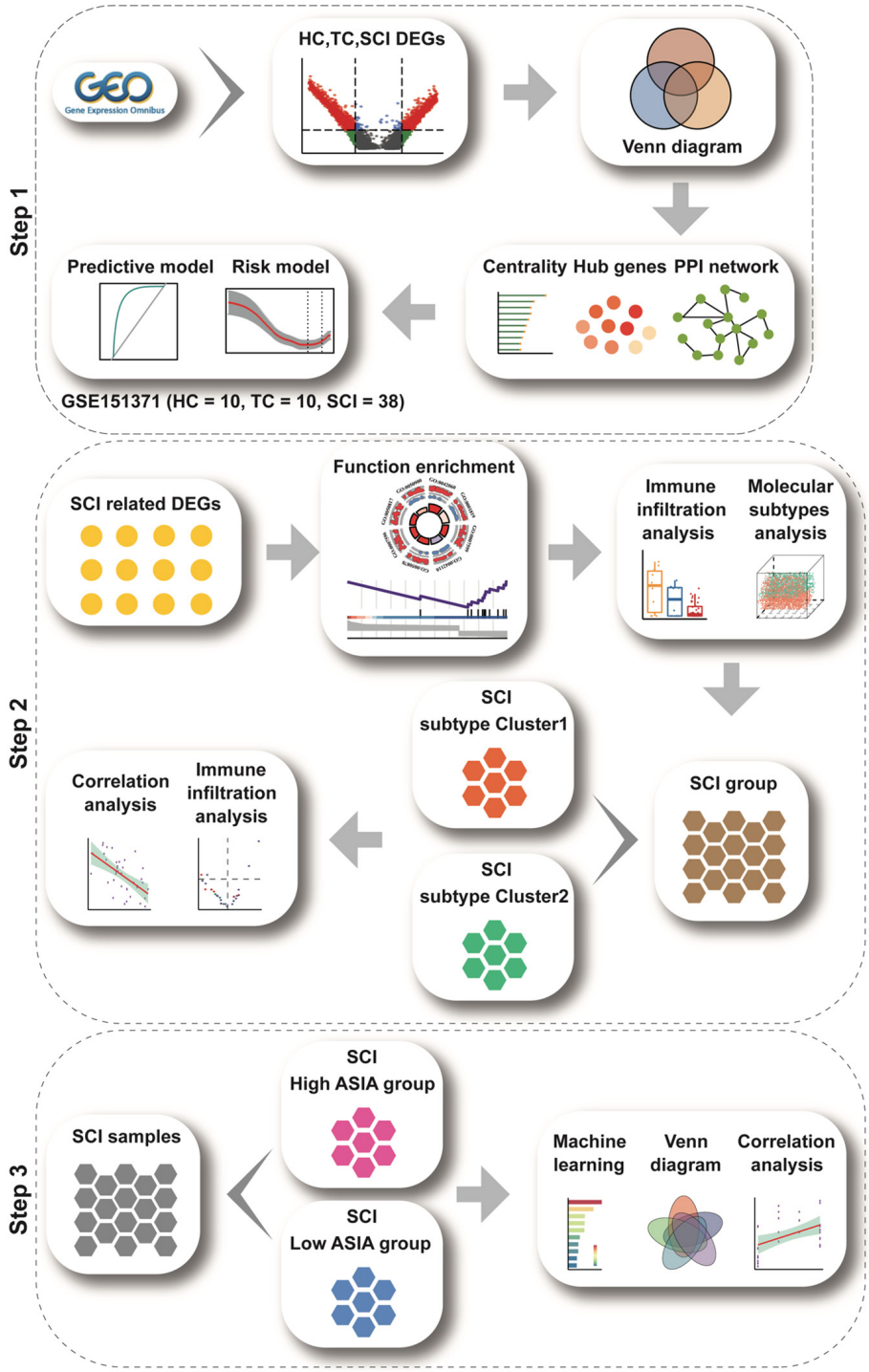

FIGURE 1
Study flow chart. The study flow chart is divided into three main sections according to the study sequence. Each icon represents schematically an analysis or a collection of data to be analyzed.

between a potential biomarkers (CCR7) and two acute SCI molecular subtypes (Cluster1, Cluster2) were determined using Spearman's correlation analysis. Next, Spearman correlation analysis between the potential biomarker and final immune infiltrating cells associated with ASIA levels was conducted.

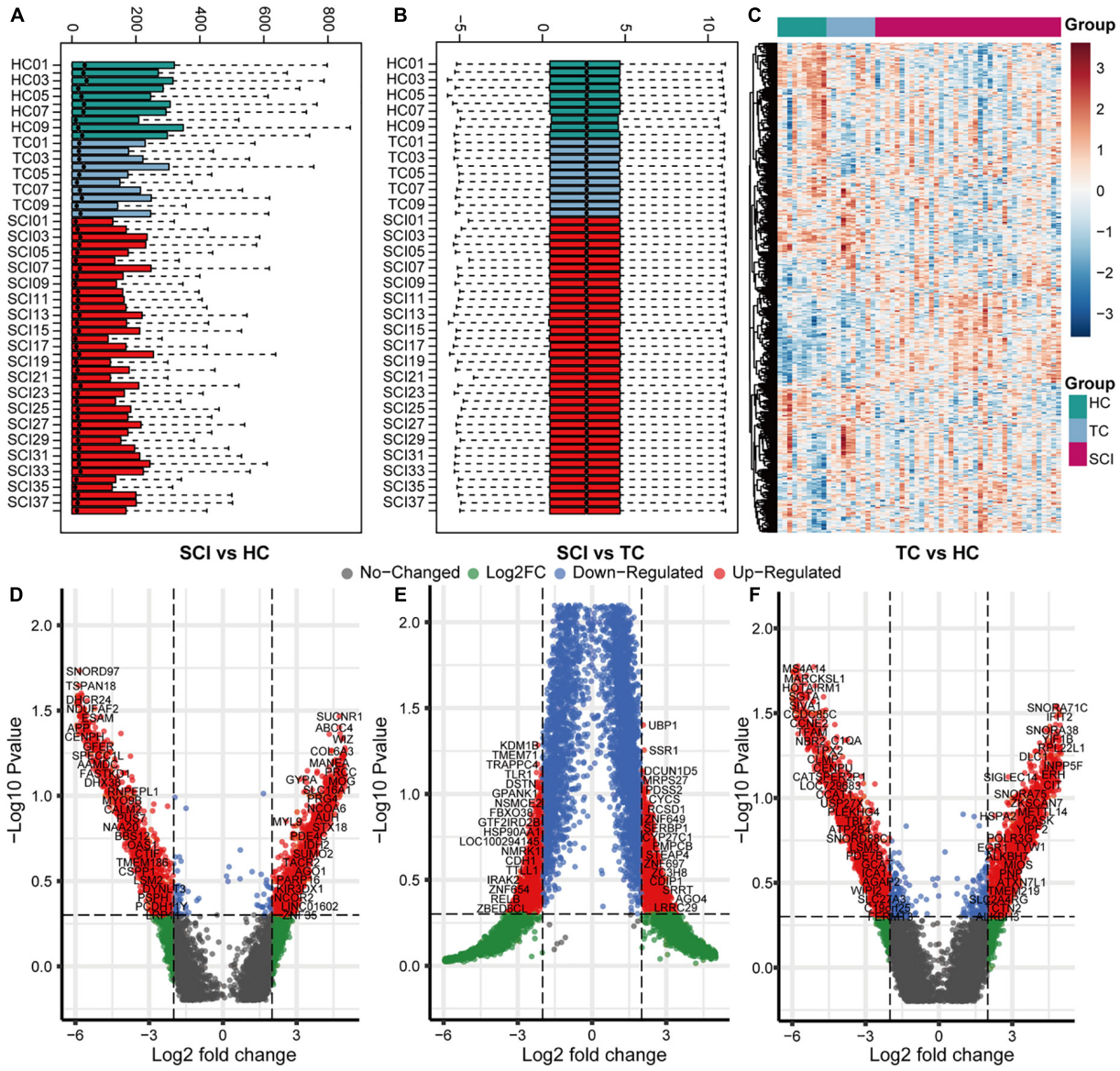

FIGURE 2
Overall gene expression profiles of peripheral blood leukocytes in acute SCI patients. **(A,B)** GSE151371 chip data before and after background correction. **(C)** Heatmap of the overall expression of GSE151371 chip data. **(D–F)** Volcano plots of differentially expressed genes between the SCI and HC groups, SCI and TC groups, and TC and HC groups.

Statistical analysis

The R software (version 4.2.0) was used for data processing and analyses. For comparing two groups of continuous variables, the independent Student's *t*-test was used for normally distributed data and the Mann-Whitney *U*-test (Wilcoxon rank-sum test) for non-normally distributed data. The chi-square test or Fisher's exact test was used to compare two groups of categorical variables. Correlation coefficients of differentially expressed genes were determined using Spearman correlation analysis. All *p*-values were two-sided, and $p < 0.05$ was considered statistically significant.

Results

Differential gene expression analysis

A flow chart of the study is presented in Figure 1.

To analyze the overall gene expression profile of patients with acute SCI, we comprehensively analyzed RNA-sequencing

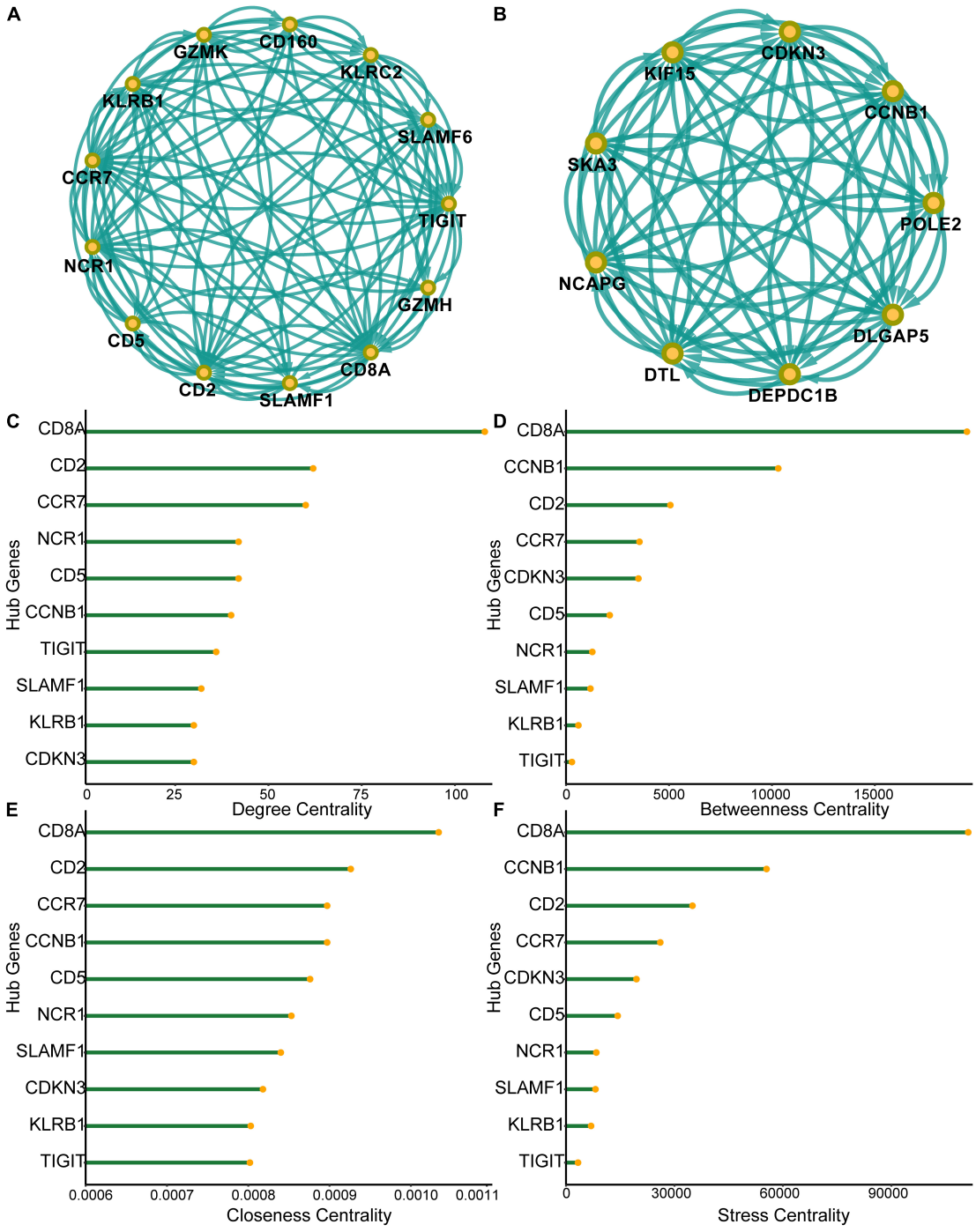

FIGURE 3
Protein-protein interaction (PPI) network of differentially expressed genes. **(A)** Subnetworks of the top-ranked PPI network. **(B)** Subnetworks of the second-ranked PPI network. **(C–F)** Analysis of degree centrality, betweenness centrality, closeness centrality and stress centrality in the top two PPI network subnetworks.

data from peripheral blood leukocytes of subjects in the HC, TC, and SCI groups in the GSE151371 dataset, using background correction (Figures 2A–C). To evaluate the molecular mechanisms of the changes induced by acute SCI, differentially expressed genes among the three groups were identified (Figures 2D–F). We found 555 genes that were significantly altered specifically in the SCI population based on cutoffs of |log fold change| ≥ 1.5 (Supplementary Table 1) and

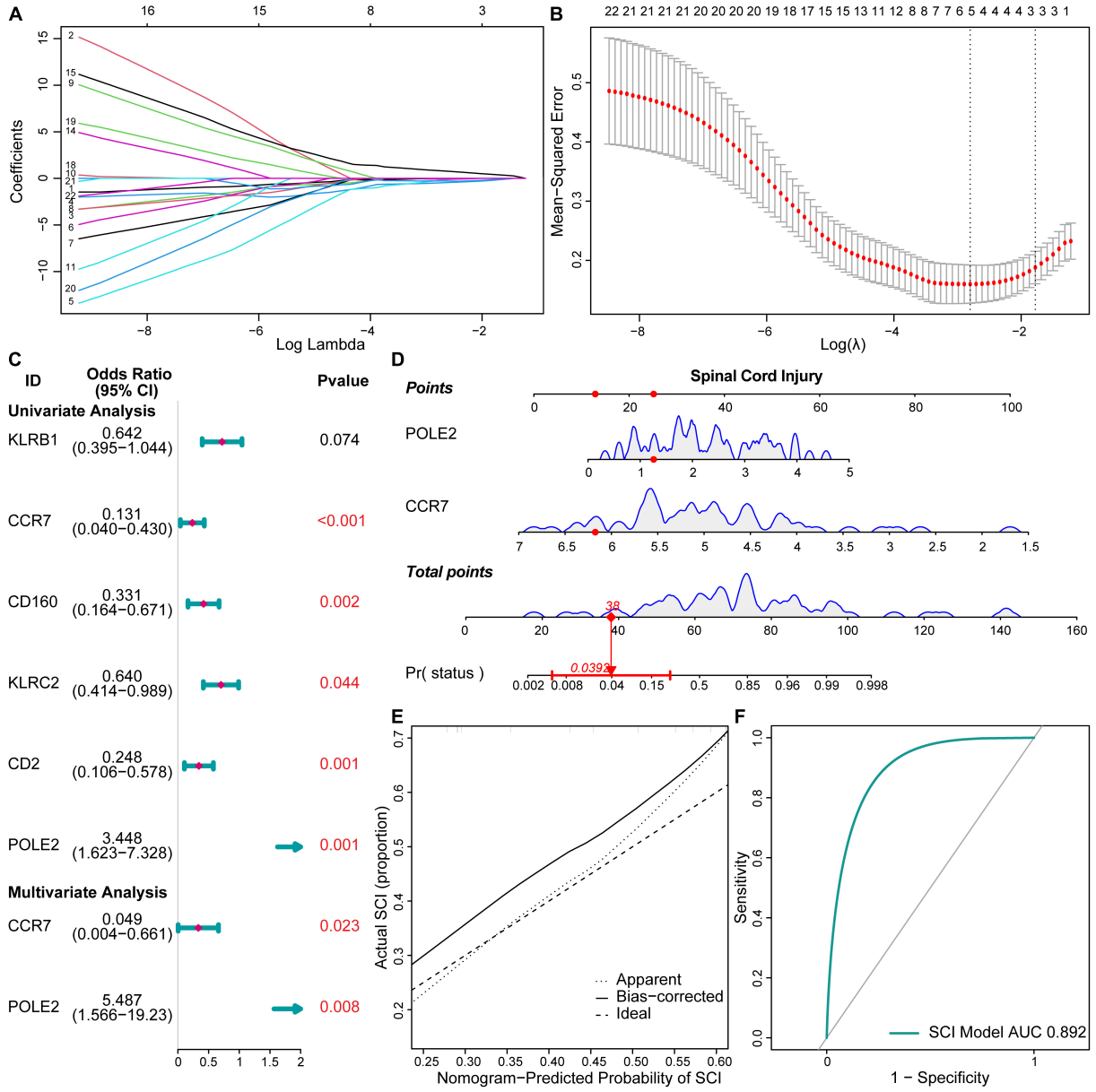

FIGURE 4
Risk models and clinical prediction models for acute SCI. **(A,B)** Least absolute shrinkage and selection operator regression identified key genes in acute SCI. **(C)** Forest plot for logistic regression. **(D)** Nomogram prediction model. **(E)** Calibration curve for the nomogram prediction model. **(F)** Receiver operating characteristic (ROC) curve of the nomogram prediction model.

a false discovery rate and adjusted $p \leq 0.05$ (Supplementary Figure 1).

Protein-protein interaction network analysis

A PPI network of the 555 differentially expressed genes was constructed based on the STRING database to identify differences between the SCI and control groups. Four hundred and seventy-seven genes were mapped to the network, of which 477 genes were interconnected with an average local clustering coefficient of 4.65. From the PPI network, 15 MCODE modules were identified (see Supplementary Appendix for details). To quantify the importance of the differentially expressed genes in the PPI network, the two most important MCODE components were extracted for further analysis (22 hub genes) (Figures 3A,B). The top 10 genes in the PPI network in terms of degree centrality, betweenness centrality, proximity centrality, and stress centrality are shown in Figures 3C–F. Three of the

22 hub genes, *CD8A*, *CD2*, and *CCR7*, were found in the top 5 results of the four centrality analyses, suggesting that they may be crucial in acute SCI.

Construction of risk models and nomogram prediction models

We constructed a risk model to determine the risk factors of acute SCI. We found that CCR7 and POLE2 were independent risk factors for the development of acute SCI (**Figures 4A–C**). A nomogram plot containing these two predictors was constructed, with an area under the ROC curve of 0.892 (**Figures 4D,F**). Calibration curves corroborated the good performance of the nomogram (**Figure 4E**). To evaluate the clinical application potential of the prediction model, we randomly selected a sample from a healthy subject for prediction, and the prediction results suggested that the probability of acute SCI onset in this subject was 3.92% (**Figure 4D**). Although multivariate LR suggested that *POLE2* and *CCR7* are independent risk factors for acute SCI, *POLE2* does not play a key role in acute SCI according to the PPI network analysis. Based on all these results, we finally selected *CCR7* for further study.

Gene set enrichment analysis and functional enrichment analysis

GSEA-GO and GSEA-KEGG are enrichment methods to identify classes of genes or proteins that are over-represented in a large set of genes or proteins. The top 5 terms identified in GSEA are listed in **Table 2**. GSEA-GO enrichment results revealed that antigen receptor-mediated signaling pathway regulation, T cell receptor signaling pathway, and leukocyte mediated cytotoxicity, were suppressed after acute SCI ($p < 0.01$) (**Figures 5A,B**). GSEA-KEGG enrichment results revealed that the chemokine signaling pathway and other chemokine-related pathways were activated after acute SCI ($p < 0.01$) (**Figures 5C,D**).

Unlike GSEA-GO and GSEA-KEGG, original GO and KEGG enrichment analyses are based on hypergeometric distributions. To accurately obtain functional changes after SCI, GOs and KEGG enrichment analyses were performed to test the stability of the GSEA enrichment results (**Table 3**). The results indicated that the top 5 functions related to immunity in GO biological processes, namely positive regulation of cytokine production, T cell activation, leukocyte migration, antigen receptor-mediated signaling pathway regulation, and leukocyte chemotaxis, were significantly enriched (**Supplementary Figures 2A–D**). The 555 differentially expressed genes were mapped to the KEGG pathways, and the top 15 enriched KEGG pathways are shown in **Supplementary Figures 2E,F**. Taken together, the data suggested that peripheral immune function was suppressed and chemokine-related signaling pathways were activated after acute SCI.

TABLE 2 Top five terms in GSEA.

Category	ID	Enrichment score	Normalized enrichment score	*P*
BP	GO:0009611	4.65E-01	2.99E + 00	1.49E-03
BP	GO:0042060	5.06E-01	3.10E + 00	1.53E-03
BP	GO:0007596	6.48E-01	3.23E + 00	1.55E-03
BP	GO:0050817	6.48E-01	3.23E + 00	1.55E-03
BP	GO:0050878	4.86E-01	2.78E + 00	1.56E-03
MF	GO:0005509	4.20E-01	2.30E + 00	1.56E-03
MF	GO:0030545	4.55E-01	1.98E + 00	3.18E-03
MF	GO:0030546	4.55E-01	1.98E + 00	3.18E-03
MF	GO:0048018	4.55E-01	1.98E + 00	3.18E-03
MF	GO:0038023	−2.44E-01	−2.19E + 00	3.31E-03
CC	GO:0005615	3.11E-01	2.84E + 00	1.30E-03
CC	GO:0099503	4.00E-01	2.90E + 00	1.45E-03
CC	GO:0030141	4.43E-01	3.13E + 00	1.46E-03
CC	GO:0031091	6.40E-01	2.92E + 00	1.58E-03
CC	GO:0031983	4.55E-01	2.39E + 00	1.59E-03
KEGG	hsa04062	4.90E-01	1.99E + 00	3.29E-03
KEGG	hsa04510	4.73E-01	1.86E + 00	1.35E-02
KEGG	hsa04015	4.59E-01	1.81E + 00	2.02E-02
KEGG	hsa05132	4.40E-01	1.73E + 00	2.53E-02
KEGG	hsa04810	4.54E-01	1.65E + 00	4.16E-02

Immune infiltration analysis between SCI and control groups

The gene functional annotation results suggested that peripheral immune function was suppressed after acute SCI. To explore the mechanism of SCI-IDS, immune cell infiltration abundance was measured using ssGSEA (**Figure 6A**). The results indicated that the levels of some immune infiltrating cells, including activated CD8 T cells, activated B cells, and CD56dim natural killer (NK) cells, were significantly decreased in the SCI group compared to the control group (non-SCI patients) ($p < 0.05$). The CIBERSORT algorithm was used to determine the abundance of peripheral immune infiltrating cells after acute SCI (**Figures 6B–G**). The results showed that naive B cells naive, CD8 T cells, CD4 memory resting T cells, activated NK cells, and activated dendritic cells contents were significantly decreased after acute SCI. The immune infiltration analysis results provided evidence for the development of SCI-IDS after acute SCI.

Establishment of molecular subtypes of acute spinal cord injury

Next, we performed molecular subtype analysis using unsupervised clustering to obtain a more accurate biomarker.

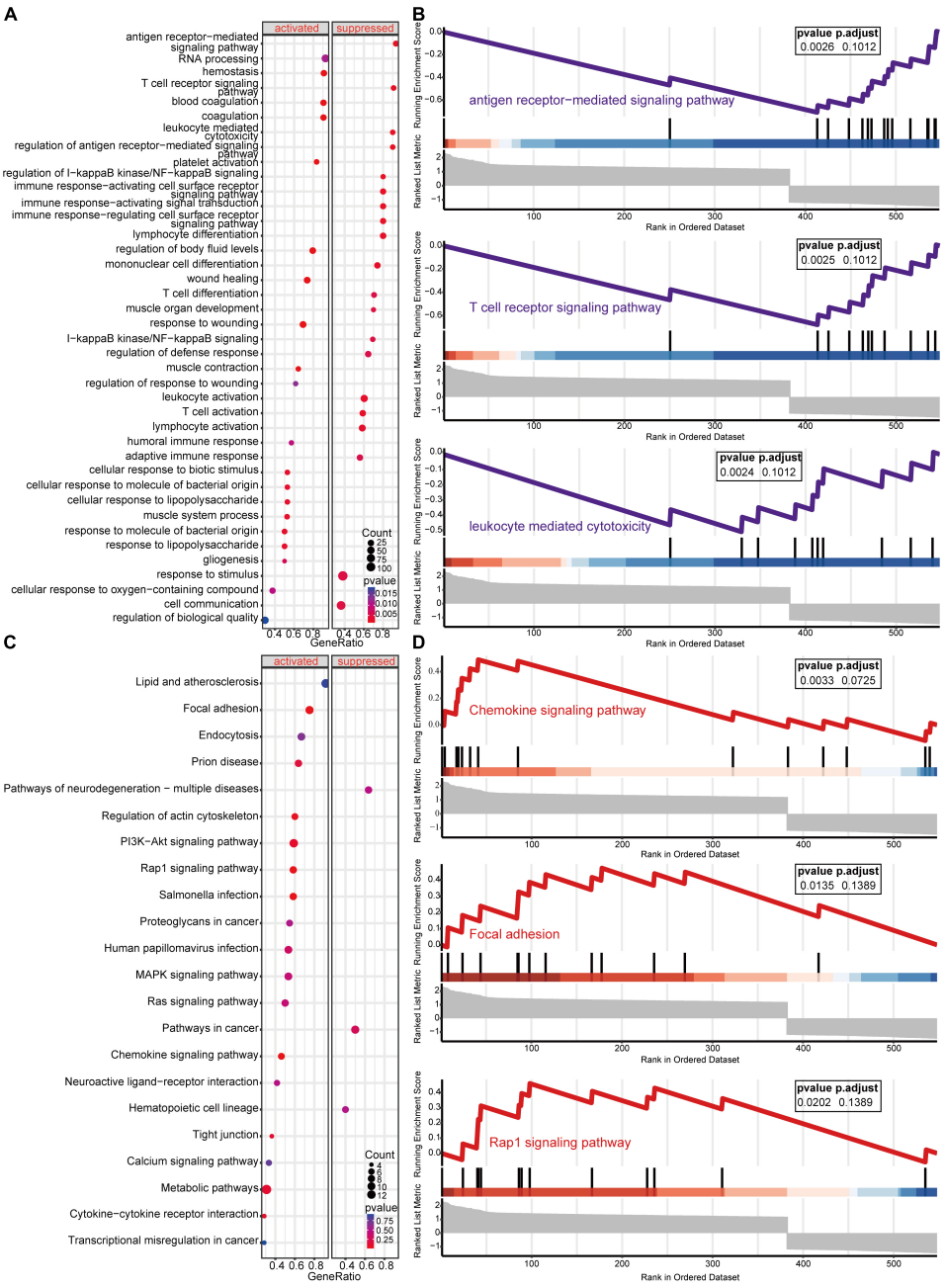

FIGURE 5
Gene set enrichment analysis (GSEA) of the experimental and control groups. **(A)** Bubble plot of GSEA-Gene Ontology (GO) analysis results. The horizontal coordinate indicates the gene ratio, the vertical coordinate the GO terms, dot size indicates gene number, dot color the *p*-value, left and right separation indicate activation and repression. **(B)** Clustering of the first three items of GSEA-GO terms. **(C)** Bubble plot of GSEA-KEGG results. The horizontal coordinate indicates the gene ratio, the vertical coordinate the GO terms, dot size indicates gene number, dot color the *p*-value, left and right separation indicate activation and repression. **(D)** GSEA-KEGG analysis of the first three clusters.

First, based on ASIA scores, a univariate LR analysis of the differentially expressed genes in the 38 acute SCI patients was conducted, and genes that were highly correlated with ASIA scores were screened out ($p < 0.05$) (see **Supplementary Appendix** for details). Next, we constructed the molecular subtypes of acute SCI based on the univariate LR results. CDF curves suggested that the optimal clustering of acute SCI was into two subtypes: Cluster 1 and Cluster 2 (**Figures 7A–C**). Principal coordinate analysis was used to validate the molecular subtype analysis results; the results indicated that Cluster 1 and Cluster 2 were well separated (**Figure 7D**).

Immune infiltration feature identification

To explore differences in the immune microenvironment between the two molecular acute SCI subtypes, we performed immune infiltration analysis of the two molecular subtypes separately. Base on the ASIA score, patients were categorized into two groups (ASIA-high and ASIA-low groups), followed by analysis of the differential immune cells infiltration in both groups using the Wilcoxon test, with a cutoff of false discovery rate < 0.05 (**Figures 8A,B**). The results suggested that memory B cells, CD8 central memory T cells, eosinophils, and type1 T helper cells were remarkably decreased in the ASIA-high group of the Cluster 1 subtype. In the Cluster 2 subtype, Tfh cells and type 1 T helper cells were significantly decreased, whereas regulatory T cells and activated dendritic cells were increased in the ASIA-high group.

In addition, correlations between immune infiltrating cells and ASIA scores in the two molecular subtypes were analyzed using four machine learning models, including LR, RF, GBDT, and XGBoost, for each subtype to obtain more accurate and stable results. These machine learning models are all classifier architectures and have good interpretability. We selected the top 5 immune infiltrating cells identified from the four machine learning models and took the intersection with the differentially expressed immune infiltrating cells (**Figures 8E–L**). Based on the combined results, we found that eosinophils were the key immune infiltrating cells that affected the ASIA score in subtype Cluster 1, and Tfh cells were the key immune infiltrating cells that affected the ASIA score in subtype Cluster 2 (**Figures 8C,D**).

Correlation analysis between the immune microenvironment and acute spinal cord injury

To explore the immune microenvironment regulatory network of the two acute SCI subtypes, we conducted a series of Spearman correlation analyses. The Spearman test was used because the data did not follow a strictly normal distribution. First, we investigated the correlation of chemokine receptor CCR7 with acute SCI molecular subtypes and key immune infiltrating cells in both molecular subtypes. The results suggested that CCR7 was not significantly correlated with molecular subtypes Cluster 1 and eosinophils ($p > 0.05$), negatively correlated with molecular subtype Cluster 2 ($R = -0.36$, $p = 0.044$), and positively correlated with Tfh cells ($R = 0.33$, $p = 0.044$) (**Figures 9G–J**). Second, the association of critical immune infiltrating cells with acute SCI molecular subtypes and ASIA scores was studied. There were no significant relationships between eosinophils and subtype Cluster 1 and ASIA scores ($p > 0.05$), and Cluster 2 and ASIA scores were positively correlated ($R = 0.46$, $p = 0.0064$), whereas Tfh cells and ASIA scores were negatively correlated ($R = -0.38$, $p = 0.029$) (**Figures 9C–F**). In addition, we explored the correlation between the subtypes and ASIA scores, and the results suggested that subtype Cluster 1 and ASIA scores were negatively correlated ($R = -0.47$, $p = 0.006$), whereas subtype Cluster 2 and ASIA scores were positively correlated ($R = 0.46$, $p = 0.0064$) (**Figures 9A,B**). Notably, CCR7 was negatively correlated with ASIA scores, and was significantly lowly expressed in the ASIA-high group (**Supplementary Figures 3A,B**). This suggested that the downregulation of CCR7 and suppression of Tfh cells after acute SCI cause an increase in the ASIA score.

TABLE 3 Top five terms in GO and KEGG enrichment analyses.

Category	ID	Description	*P*-value
BP	GO:0042060	Wound healing	6.97E-09
BP	GO:0001819	Positive regulation of cytokine production	2.62E-08
BP	GO:0007599	Hemostasis	9.72E-08
BP	GO:0042110	T cell activation	2.27E-07
BP	GO:0050878	Regulation of body fluid levels	2.73E-07
MF	GO:0140375	Immune receptor activity	6.31E-05
MF	GO:0023023	Major histocompatibility complex binding	2.34E-04
MF	GO:0005516	Calmodulin binding	5.16E-04
MF	GO:0001618	Virus receptor activity	5.84E-04
MF	GO:0140272	Exogenous protein binding	6.38E-04
CC	GO:0031091	Platelet alpha granule	1.49E-10
CC	GO:0031093	Platelet alpha granule lumen	1.36E-08
CC	GO:0034774	Secretory granule lumen	3.61E-06
CC	GO:0060205	Cytoplasmic vesicle lumen	4.24E-06
CC	GO:0031983	Vesicle lumen	4.71E-06
KEGG	hsa04610	Complement and coagulation cascades	9.21E-04
KEGG	hsa05202	Transcriptional misregulation in cancer	1.77E-03
KEGG	hsa04612	Antigen processing and presentation	2.16E-03
KEGG	hsa05414	Dilated cardiomyopathy	2.18E-03
KEGG	hsa04062	Chemokine signaling pathway	4.83E-03

Discussion

SCI is considered a common and severe illness with an increasing rate of disability and mortality, often with catastrophic consequences (Byra, 2016; Casper et al., 2018). The significant effects of immunosuppression on Tfh cells have attracted much attention (Yan et al., 2017). Using differential

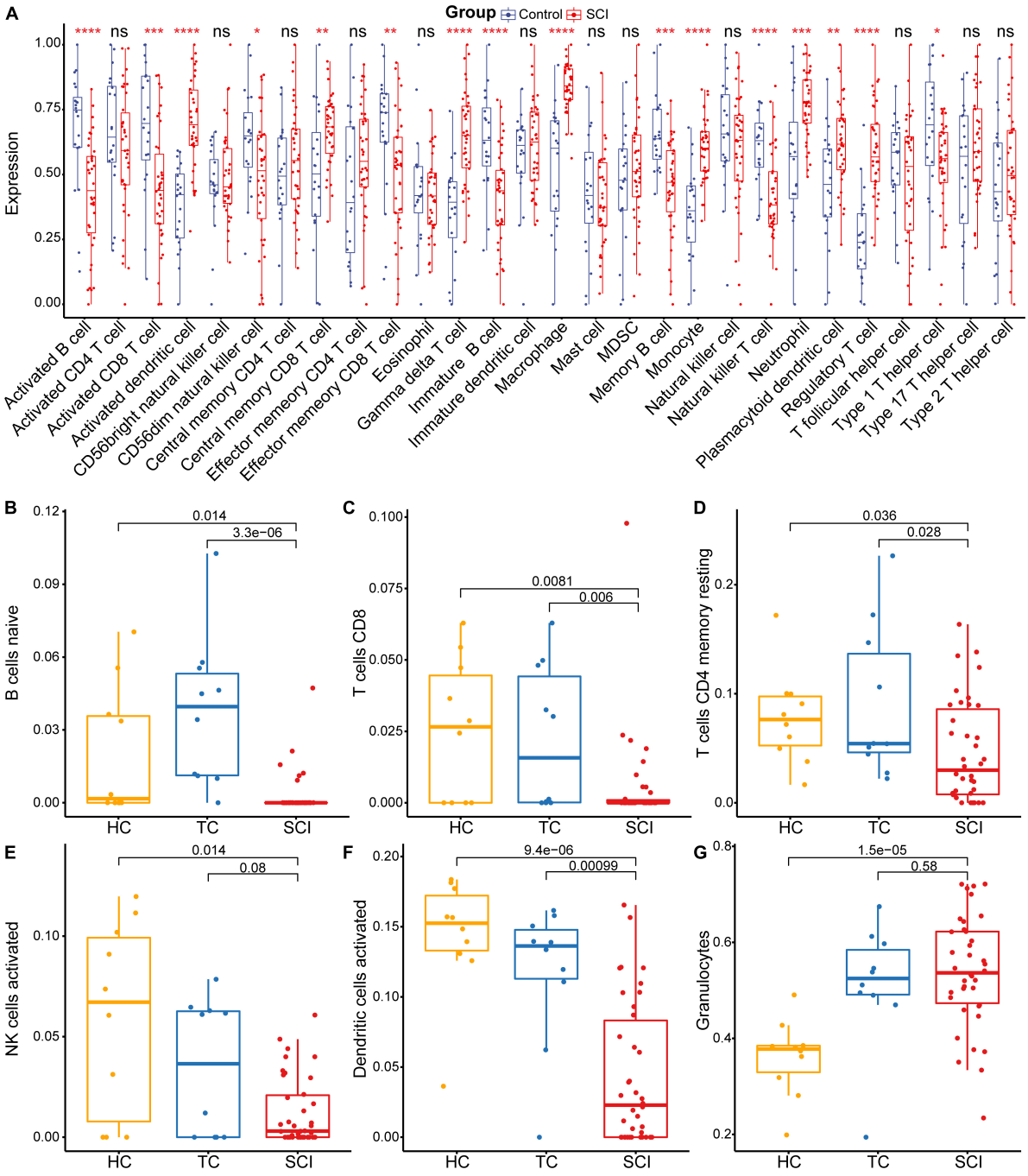

FIGURE 6
Acute SCI immune infiltration analysis. **(A)** Differential immune cell infiltration in the experimental and control groups based on ssGSEA. "ns" indicates $p \geq 0.05$, *$p < 0.05$, **$p < 0.01$, ***$p < 0.001$, and ****$p < 0.0001$. **(B–G)** Differential immune cell infiltration in the experimental and control groups according to CIBERSORT analysis. The number above the box indicates the p-value.

gene analysis, PPI network centrality analysis, and risk model construction, we identified CCR7 as a possible peripheral blood diagnostic markers for acute SCI and a therapeutic target for SCI-IDS. Next, we constructed predictive models by comparing the SCI and control groups (non-SCI subjects). We discovered that the biological processes and pathways related to the immune response were the most enriched in acute SCI. The immune infiltration results suggested that SCI-IDS occurred immediately after acute SCI. Next, we established two molecular subtypes if acute SCI and identified risk factors using supervised

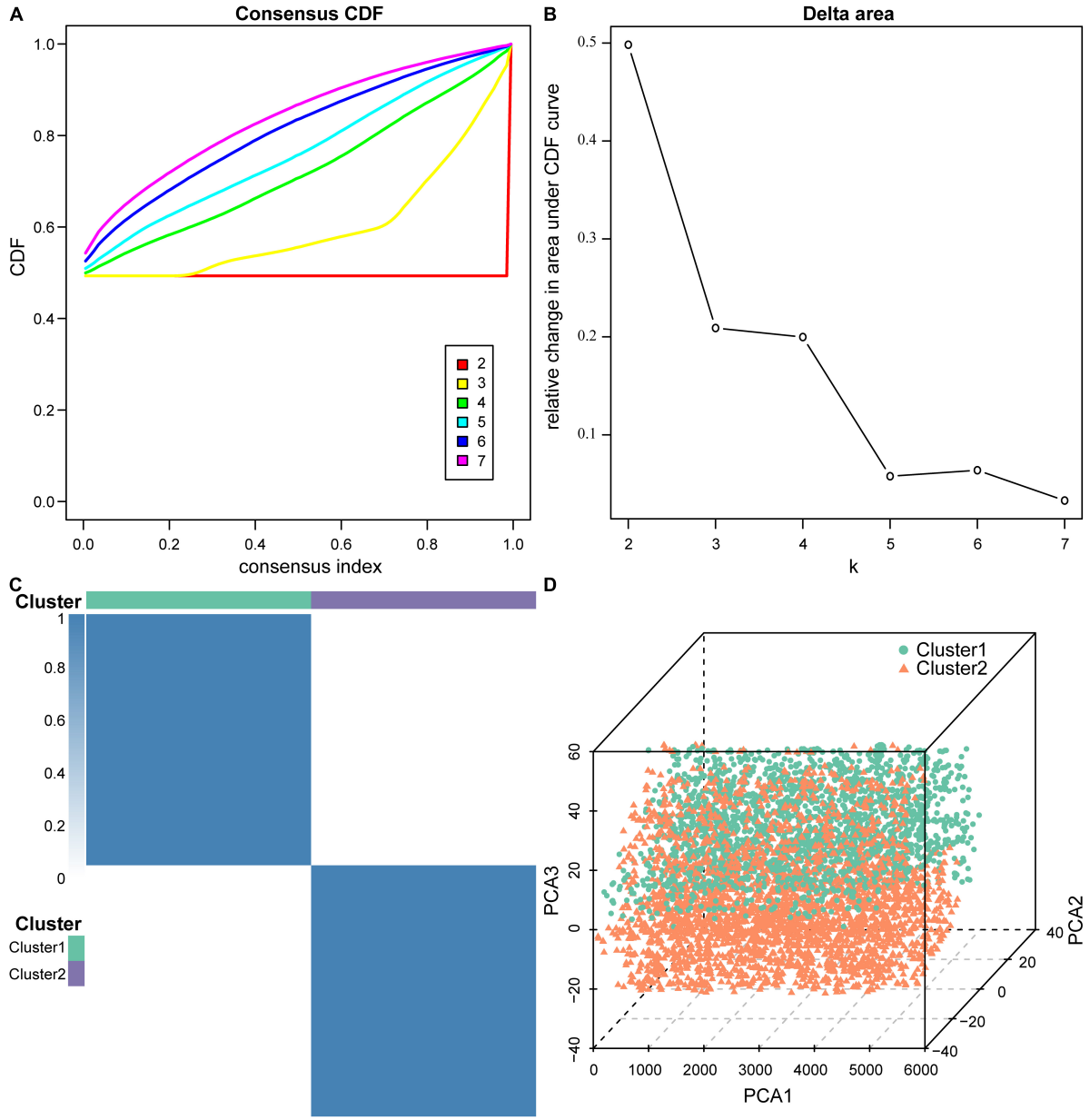

FIGURE 7
Molecular subtypes of acute SCI. **(A)** Cumulative distribution function (CDF) curve of consensus clustering of acute SCI-related genes. The horizontal coordinate indicates the consensus index, the vertical coordinate indicates the CDF index. **(B)** Relative change in the area under the CDF curve revealing two subtypes with the most stable trend of change. **(C)** Clustering heatmap of the subtypes of acute SCI-related genes. **(D)** Principal coordinate analysis plot for acute SCI-related molecular subtypes.

machine learning models. Unlike in acute SCI subtype Cluster 1, Tfh cells positively regulated by CCR7 in molecular subtype Cluster 2 significantly positively affected acute SCI prognosis.

Numerous studies have suggested the associations of various SCI-IDS symptoms with the functions of macrophages, NK cells, T cells and B cells (Cruse et al., 1992; Campagnolo et al., 1997; Furlan et al., 2006; Lucin et al., 2007; Riegger et al., 2009; Held et al., 2010). Therefore, sequencing data of human peripheral blood leukocytes were used in the present study. We normalized the GSE151371 chip data to eliminate data bias. Differential gene analysis revealed that 555 genes were significantly altered specifically in acute SCI. *CCR7* expression was downregulated after acute SCI and was one of the potential biomarkers based on differential expression analysis. As a chemokine receptor, CCR7 exerts remarkable effects on the differentiation of Tfh cells, the homing of lymphocytes, and the formation of germinal

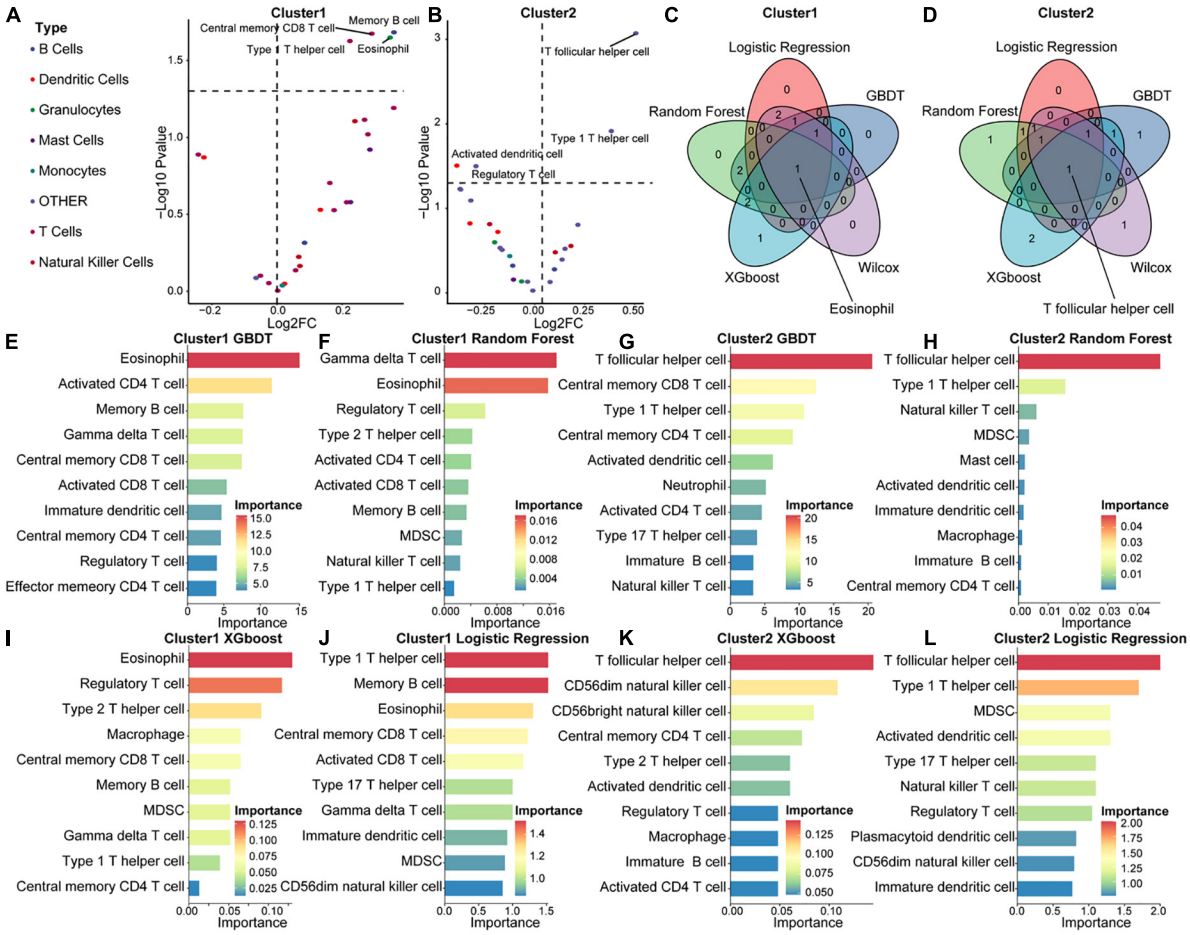

FIGURE 8
Immunological composition and feature identification analysis of the molecular subtypes of acute SCI. **(A,B)** Volcano plots of differential expression of immune infiltrating cells in ASIA-high and -low groups in acute SCI subtypes Cluster 1 and Cluster 2. **(C,D)** Venn diagrams of logistic regression (LR), random forest (RF), GBDT, XGboost, and Wilcoxon analyses in the acute SCI subtypes Cluster 1 and Cluster 2. **(E,F)** Histogram of GBDT and RF classifiers in the acute SCI subtype Cluster 1. The horizontal coordinates and colors indicate importance and the vertical coordinate indicates immune infiltrating cells. **(G,H)** Histogram of GBDT and RF classifiers in acute SCI subtype Cluster 2. The horizontal coordinates and colors indicate importance and the vertical coordinate indicates immune infiltrating cells. **(I,J)** Histogram of XGboost and LR classifiers in the acute SCI subtype Cluster 1. The horizontal coordinates and colors indicate importance and the vertical coordinate indicates immune infiltrating cells. **(K,L)** Histogram of XGboost and LR classifiers in the acute SCI subtype Cluster 2. The horizontal coordinates and colors indicate importance and the vertical coordinate indicates immune infiltrating cells.

centers (Forster et al., 1999; Hardtke et al., 2005; Arnold et al., 2007). CCR7 expression is significantly increased in patients with pancreatic cancer and induces intra-tumor angiogenesis and lymphangiogenesis through chemotactic interactions with its ligand, CCL21 (Zhao et al., 2011). CCR7 significantly affects multiple sclerosis relapse by regulating Tfh cell differentiation (Fan et al., 2015). Our research revealed the significant role of CCR7 in SCI-IDS.

From the PPI networks constructed in the current study, using sub-network extraction and centrality analysis, we identified *CD8A*, *CD2*, and *CCR7* as genes involved in acute SCI. The PPI analysis corroborated the importance of CCR7 in acute SCI from the scale-free network perspective. Both univariate and multivariate LRs suggested that CCR7 and POLE2 were significantly associated with acute SCI; however, only CCR7 showed high significance in both the scale-free network and linear regression, and was therefore selected as a potential biomarker for acute SCI. Its value in acute SCI and SCI-IDS diagnosis and treatment was further analyzed by constructing a clinical prediction model. GSEA-KEGG and KEGG functional enrichment analysis indicated that chemokine signaling and the PI3K/AKT pathway were significantly upregulated after acute SCI, suggesting an active chemokine cascade response. GSEA-GO and GO enrichment analysis indicated that chemokines became more active after acute SCI, while immune function was suppressed. Interestingly, a recent study showed that that chemokines play an important role in bone marrow failure caused by SCI (Carpenter et al., 2020). These results suggest that

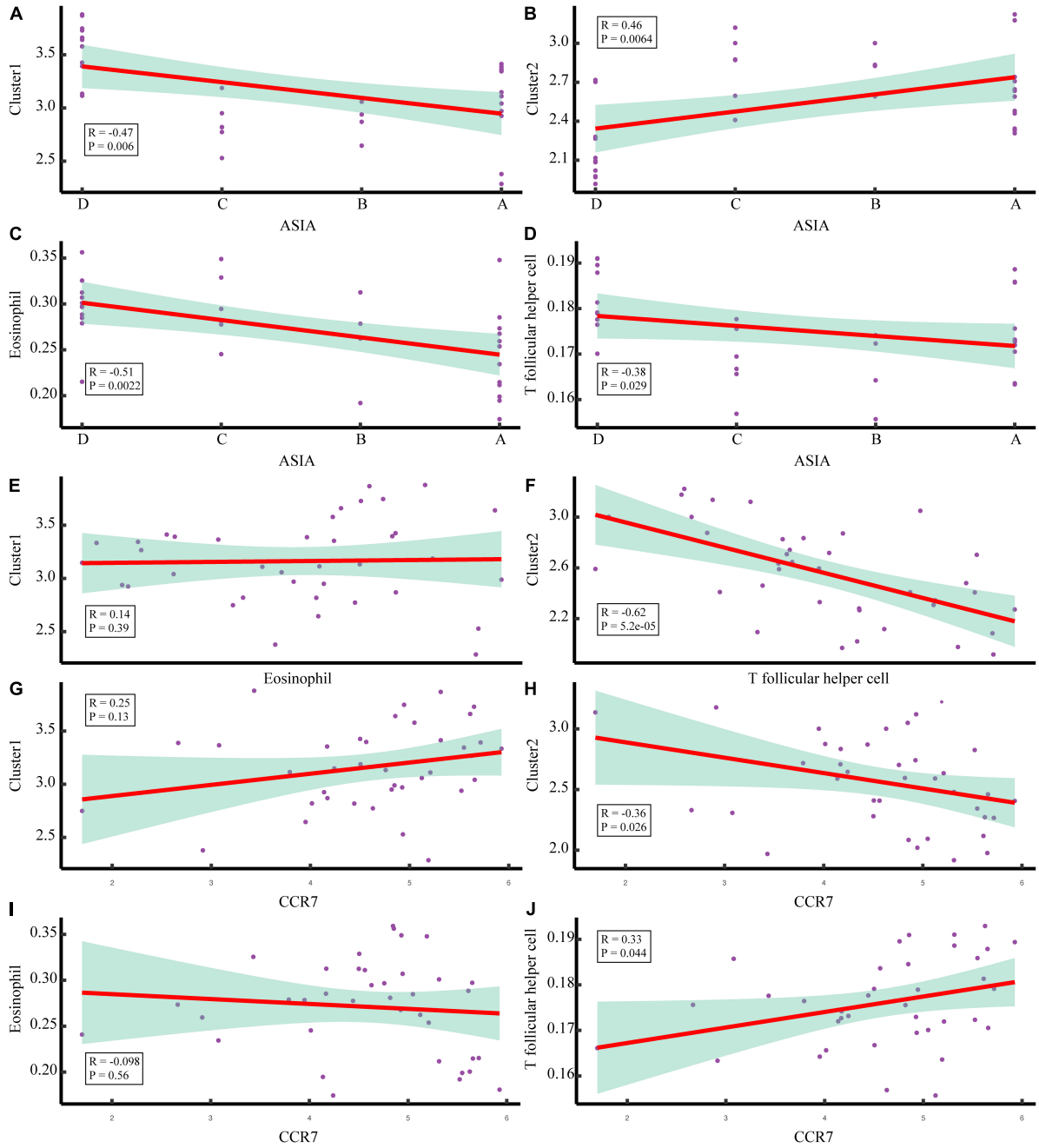

FIGURE 9
Correlation analysis of the molecular subtypes of acute SCI. **(A,B)** Scatter plot of correlation analysis between ASIA classification and the acute SCI molecular subtypes Cluster 1 and Cluster 2. **(C,D)** Scatter plot of correlation analysis between ASIA grading, eosinophils, and T follicular helper (Tfh) cells. **(E)** Correlation analysis of the acute SCI molecular subtype Cluster 1 and eosinophils. **(F)** Correlation analysis of the acute SCI molecular subtype Cluster 2 and Tfh cells. **(G,H)** Scatter plot of correlation analysis between CCR7 and the acute SCI molecular subtypes Cluster 1 and Cluster 2. **(I,J)** Scatter plot of correlation analysis between CCR7, eosinophils, and Tfh cells. R denotes the correlation coefficient, and *P* denotes the *p*-value.

chemokines may play a role in the immunosuppressive process after acute SCI.

Regarding immune infiltration, Tfh cell function was damaged in SCI patients compared to control patients, mainly in terms of a decreases in the proportions of mature B cells and NK cells. This finding is consistent with previously reported experimental results (Kliesch et al., 1996). Further, we found that activated B cells were significantly reduced

after acute SCI. It is well known that B cell maturation requires Tfh cell assistance to generate germinal centers, and CCR7-mediated effector cell migration also plays a key role in the formation of germinal centers (Salem et al., 2021). The downregulation of CCR7 after acute SCI may contribute to the impaired B cell activation. This was corroborated by the positive correlation between CCR7 expression and Tfh cell abundance. These evidences demonstrate the biomarker potential of CCR7 in SCI-IDS. Li et al. (2019) classified hepatocellular carcinoma into five immune subtypes, which can be targeted for treatment. Wang et al. (2021) classified SCI patients based on gene set variation analysis enrichment scores and found that Cluster 1 had the highest activity in the MAPK, NOTCH, MTOR, and WNT pathways. Similarly, we established two acute SCI subtypes and measured the correlation between ASIA scores and the two subtypes. Immunological infiltration was analyzed separately for the two subtypes. The results suggested that the two subtypes have different immunological characteristics. To identify the immune cells that exacerbate acute SCI disease, we built machine learning clusters in each of two molecular subtypes. Eosinophils and Tfh cells were found to play a major role in molecular subtype Cluster 1 and Cluster 2, respectively. There were no significant correlations between CCR7, Cluster 1, and eosinophils. This suggests that CCR7 is less suitable as a target for SCI-IDS of the molecular subtype Cluster 1. We found a reduced abundance of Tfh cells in the ASIA-high group of the molecular subtype Cluster 2, suggesting an effect of Tfh cells on neurological function in patients with acute SCI. Our results support that SCI-IDS aggravates acute SCI (Brommer et al., 2016). Moreover, CCR7 and the molecular subtype Cluster 2 were negatively correlated, whereas CCR7 and Tfh cells were positively correlated, suggesting that CCR7 plays an important role in the molecular subtype Cluster 2 and that downregulation of CCR7 after acute SCI causes a decrease in Tfh cell abundance. Tfh cells were negatively correlated with ASIA classification. This suggested that a decrease in Tfh abundance leads to an increase in the ASIA score. Combined with the functional enrichment findings that after acute SCI, peripheral immune function is suppressed and chemokine signaling pathways are activated, we suggest the following mechanism underlying the immune microenvironment changes in SCI-IDS: the downregulation of peripheral CCR7 after acute SCI leads to the downregulation of Tfh cells through chemokine signaling pathway, causing the development of SCI-IDS and aggravating acute SCI.

Currently, limited and diverse studies are present on the immune microenvironment in SCI-IDS. Exploring the pathogenesis and therapeutic direction of SCI-IDS and systematically interpreting the theory of the immune microenvironment can fill the gap of SCI-IDS in terms of targeted therapy and elaboration of multi-omics pathological mechanisms. We hoped our study to pave the way to precise diagnosis and targeted treatment of acute SCI to ultimately reduce the mortality rate of acute SCI patients, and to provide a theoretical basis for future studies.

The present study had some limitations. First, the research was based on bioinformatics analysis, and the findings must be validated in animal and human experiments and in clinical practice. Second, the number of samples included in each group was small. Third, although the clinical prediction model had a high degree of agreement (area under the ROC curve of 0.892), its detection power must be improved by combining data from different studies. Fourth, because of the heterogeneity of acute SCI and inadequate clinical data, not all acute SCI patients experience significant systemic immunosuppression, and additional immunosuppressive features of acute SCI patients should be examined in future subgroup analyses.

Conclusion

In conclusion, CCR7 was determined as a potential biomarker of acute SCI. CCR7 counteracts SCI-IDS by activating chemokine signaling in Tfh cells. We hope our finding will pave the way to an effective treatment for patients with acute SCI. The specific pathogenesis and molecular targets for SCI-IDS remain to be validated.

Data availability statement

The original contributions presented in this study are included in the article/**Supplementary material**, further inquiries can be directed to the corresponding author.

Author contributions

CL and CW helped in the conception and design, data acquisition, analysis and interpretation, and critical revision of the article and final approval. GX, YL, JC, JZ, HH, and CJ helped in the data acquisition and final approval. ZC helped in the data acquisition, analysis, and drafting and critical revision of the article and obtained final approval. All authors have approved the submitted version of the manuscript.

Funding

This study was supported by the National Natural Science Foundation of China (grant nos. 81771319, 82002394, 82202436), the Nantong Health Commission Research Project (grant no. MA2021016), and Medical Research Project of Jiangsu Commission of Health (grant no. ZDB2020004).

Acknowledgments

We would like to thank Editage (www.editage.cn) for English language editing.

Conflict of interest

The authors declare that the research was conducted in the absence of any commercial or financial relationships that could be construed as a potential conflict of interest.

Publisher's note

All claims expressed in this article are solely those of the authors and do not necessarily represent those of their affiliated organizations, or those of the publisher, the editors and the reviewers. Any product that may be evaluated in this article, or claim that may be made by its manufacturer, is not guaranteed or endorsed by the publisher.

Supplementary material

The Supplementary Material for this article can be found online at: https://www.frontiersin.org/articles/10.3389/fnins.2022.1019406/full#supplementary-material

SUPPLEMENTARY FIGURE 1
The intersection of differentially expressed genes after acute SCI. **(A)** A venn diagram of differentially expressed genes in the HC, TC, and SCI groups. **(B)** A venn diagram of up-regulated differentially expressed genes in the HC, TC, and SCI groups. **(C)** A venn diagram of down-regulated differentially expressed genes in the HC, TC, and SCI groups.

SUPPLEMENTARY FIGURE 2
Functional enrichment analysis of differential genes. **(A–C)** Bubble diagram of the first 15 biological processes, molecular functions, and cellular components items, with horizontal coordinates indicating GeneRatio, vertical coordinates indicating gene ontology (GO) terms, dot size indicating the number of genes, and dot color indicating adj *p*-value. **(D)** Circle diagram of the first eight biological processes items, with the outer circle dot color representing upregulated and downregulated genes and the inner circle color representing activation or repression of GO terms. **(E)** Bubble diagram of the first 15 KEGG pathways, with horizontal coordinates indicating GeneRatio, vertical coordinates indicating KEGG pathways, dot size indicating the number of genes, and dot color indicating adj *p*-value. **(F)** String diagram of the first eight KEGG pathways, the left outer half-circle represents genes within the pathways, the color indicates log fold changes (logFC), the right outer half-circle color indicates KEGG pathways, and the inner connecting line indicates the association of KEGG pathways with genes.

SUPPLEMENTARY FIGURE 3
Differential expression and correlation analysis of CCR7. **(A)** Scatter plot of correlation analysis between CCR7 and ASIA classification. *R* denotes the correlation coefficient, and *P* denotes the *p*-value. Despite the fact that $P < 0.05$ is considered significantly correlated, $P = 0.053$ is considered statistical error interference. Therefore, CCR7 and ASIA scores were still considered significantly correlated. **(B)** Differential expression of CCR7 in the ASIA-high and ASIA-low groups. The number above the box indicates the *p*-value.

References

Almanan, M., Raynor, J., Ogunsulire, I., Malyshkina, A., Mukherjee, S., Hummel, S. A., et al. (2020). IL-10-producing Tfh cells accumulate with age and link inflammation with age-related immune suppression. *Sci. Adv.* 6:eabb0806. doi: 10.1126/sciadv.abb0806

Arnold, C. N., Campbell, D. J., Lipp, M., and Butcher, E. C. (2007). The germinal center response is impaired in the absence of T cell-expressed CXCR5. *Eur. J. Immunol.* 37, 100–109. doi: 10.1002/eji.200636486

Brommer, B., Engel, O., Kopp, M. A., Watzlawick, R., Müller, S., Prüss, H., et al. (2016). Spinal cord injury-induced immune deficiency syndrome enhances infection susceptibility dependent on lesion level. *Brain* 139, 692–707. doi: 10.1093/brain/awv375

Byra, S. (2016). Posttraumatic growth in people with traumatic long-term spinal cord injury: predictive role of basic hope and coping. *Spinal Cord* 54, 478–482. doi: 10.1038/sc.2015.177

Campagnolo, D. I., Bartlett, J. A., Keller, S. E., Sanchez, W., and Oza, R. (1997). Impaired phagocytosis of Staphylococcus aureus in complete tetraplegics. *Am. J. Phys. Med. Rehabil.* 76, 276–280. doi: 10.1097/00002060-199707000-00005

Carpenter, R. S., Marbourg, J. M., Brennan, F. H., Mifflin, K. A., Hall, J. C. E., Jiang, R. R., et al. (2020). Spinal cord injury causes chronic bone marrow failure. *Nat. Commun.* 11:3702. doi: 10.1038/s41467-020-17564-z

Casper, D. S., Zmistowski, B., Schroeder, G. D., McKenzie, J. C., Mangan, J., Vatson, J., et al. (2018). Preinjury patient characteristics and postinjury neurological status are associated with mortality following spinal cord injury. *Spine* 43, 895–899. doi: 10.1097/BRS.0000000000002533

Crotty, S. (2014). T Follicular helper cell differentiation, function, and roles in disease. *Immunity* 41, 529–542. doi: 10.1016/j.immuni.2014.10.004

Cruse, J. M., Lewis, R. E., Bishop, G. R., Kliesch, W. F., and Gaitan, E. (1992). Neuroendocrine-immune interactions associated with loss and restoration of immune system function in spinal cord injury and stroke patients. *Immunol. Res.* 11, 104–116. doi: 10.1007/BF02918615

Failli, V., Kopp, M. A., Gericke, C., Martus, P., Klingbeil, S., Brommer, B., et al. (2012). Functional neurological recovery after spinal cord injury is impaired in patients with infections. *Brain* 135, 3238–3250. doi: 10.1093/brain/aws267

Fan, X., Jin, T., Zhao, S., Liu, C., Han, J., Jiang, X., et al. (2015). Circulating CCR7+ICOS+ memory T Follicular helper cells in patients with multiple sclerosis. *PLoS One* 10:e0134523. doi: 10.1371/journal.pone.0134523

Forster, R., Schubel, A., Breitfeld, D., Kremmer, E., Renner-Muller, I., Wolf, E., et al. (1999). CCR7 coordinates the primary immune response by establishing functional microenvironments in secondary lymphoid organs. *Cell* 99, 23–33. doi: 10.1016/s0092-8674(00)80059-8

Furlan, J. C., Krassioukov, A. V., and Fehlings, M. G. (2006). Hematologic abnormalities within the first week after acute isolated traumatic cervical spinal cord injury: a case-control cohort study. *Spine* 31, 2674–2683. doi: 10.1097/01.brs.0000244569.91204.01

Galeiras Vazquez, R., Ferreiro Velasco, M. E., Mourelo Farina, M., Montoto Marques, A., and Salvador de la Barrera, S. (2017). Update on traumatic acute spinal cord injury. *Med. Intensiva* 41, 237–247. doi: 10.1016/j.medin.2016.11.002

Gu-Trantien, C., Migliori, E., Buisseret, L., de Wind, A., Brohee, S., Garaud, S., et al. (2017). CXCL13-producing TFH cells link immune suppression and adaptive memory in human breast cancer. *JCI Insight* 2:e91487. doi: 10.1172/jci.insight.91487

Hanzelmann, S., Castelo, R., and Guinney, J. (2013). GSVA: gene set variation analysis for microarray and RNA-seq data. *BMC Bioinform.* 14:7. doi: 10.1186/1471-2105-14-7

Hardtke, S., Ohl, L., and Forster, R. (2005). Balanced expression of CXCR5 and CCR7 on follicular T helper cells determines their transient positioning to lymph node follicles and is essential for efficient B-cell help. *Blood* 106, 1924–1931. doi: 10.1182/blood-2004-11-4494

Held, K. S., Steward, O., Blanc, C., and Lane, T. E. (2010). Impaired immune responses following spinal cord injury lead to reduced ability to control viral infection. *Exp. Neurol.* 226, 242–253. doi: 10.1016/j.expneurol.2010.08.036

Hong, J., Chang, A., Liu, Y., Wang, J., and Fehlings, M. G. (2019). Incomplete spinal cord injury reverses the level-dependence of spinal cord injury immune deficiency syndrome. *Int. J. Mol. Sci.* 20:3762. doi: 10.3390/ijms20153762

Hulme, C. H., Brown, S. J., Fuller, H. R., Riddell, J., Osman, A., Chowdhury, J., et al. (2017). The developing landscape of diagnostic and prognostic biomarkers for spinal cord injury in cerebrospinal fluid and blood. *Spinal Cord* 55, 114–125. doi: 10.1038/sc.2016.174

Inamasu, J., Nakamura, Y., and Ichikizaki, K. (2003). Induced hypothermia in experimental traumatic spinal cord injury: an update. *J. Neurol. Sci.* 209, 55–60. doi: 10.1016/s0022-510x(02)00463-x

Kliesch, W. F., Cruse, J. M., Lewis, R. E., Bishop, G. R., Brackin, B., and Lampton, J. A. (1996). Restoration of depressed immune function in spinal cord injury patients receiving rehabilitation therapy. *Paraplegia* 34, 82–90. doi: 10.1038/sc.1996.14

Koopman, F. A., Chavan, S. S., Miljko, S., Grazio, S., Sokolovic, S., Schuurman, P. R., et al. (2016). Vagus nerve stimulation inhibits cytokine production and attenuates disease severity in rheumatoid arthritis. *Proc. Natl. Acad. Sci. U.S.A.* 113, 8284–8289. doi: 10.1073/pnas.1605635113

Kriz, J., Sediva, K., and Maly, M. (2021). Causes of death after spinal cord injury in the Czech Republic. *Spinal Cord* 59, 814–820. doi: 10.1038/s41393-020-00593-2

Kyritsis, N., Torres-Espín, A., Schupp, P. G., Huie, J. R., Chou, A., Duong-Fernandez, X., et al. (2021). Diagnostic blood RNA profiles for human acute spinal cord injury. *J. Exp. Med.* 218:e20201795. doi: 10.1084/jem.20201795

Laginha, I., Kopp, M. A., Druschel, C., Schaser, K.-D., Brommer, B., Hellmann, R. C., et al. (2016). Natural Killer (NK) Cell Functionality after human Spinal Cord Injury (SCI): protocol of a prospective, longitudinal study. *BMC Neurol.* 16:170. doi: 10.1186/s12883-016-0681-5

Li, W., Wang, H., Ma, Z., Zhang, J., Ou-yang, W., Qi, Y., et al. (2019). Multi-omics analysis of microenvironment characteristics and immune escape mechanisms of hepatocellular carcinoma. *Front. Oncol.* 9:1019. doi: 10.3389/fonc.2019.01019

Lucin, K. M., Sanders, V. M., Jones, T. B., Malarkey, W. B., and Popovich, P. G. (2007). Impaired antibody synthesis after spinal cord injury is level dependent and is due to sympathetic nervous system dysregulation. *Exp. Neurol.* 207, 75–84. doi: 10.1016/j.expneurol.2007.05.019

Meisel, C., Prass, K., Braun, J., Victorov, I., Wolf, T., Megow, D., et al. (2004). Preventive antibacterial treatment improves the general medical and neurological outcome in a mouse model of stroke. *Stroke* 35, 2–6. doi: 10.1161/01.STR.0000109041.89959.4C

Meisel, C., Schwab, J. M., Prass, K., Meisel, A., and Dirnagl, U. (2005). Central nervous system injury-induced immune deficiency syndrome. *Nat. Rev. Neurosci.* 6, 775–786. doi: 10.1038/nrn1765

Meli, A. P., Fontés, G., Avery, Danielle, T., Leddon, Scott, A., et al. (2016). The integrin LFA-1 controls T Follicular helper cell generation and maintenance. *Immunity* 45, 831–846. doi: 10.1016/j.immuni.2016.09.018

Newman, A. M., Steen, C. B., Liu, C. L., Gentles, A. J., Chaudhuri, A. A., Scherer, F., et al. (2019). Determining cell type abundance and expression from bulk tissues with digital cytometry. *Nat. Biotechnol.* 37, 773–782. doi: 10.1038/s41587-019-0114-2

Noble, B. T., Brennan, F. H., and Popovich, P. G. (2018). The spleen as a neuroimmune interface after spinal cord injury. *J. Neuroimmunol.* 321, 1–11. doi: 10.1016/j.jneuroim.2018.05.007

Pavlov, V. A., and Tracey, K. J. (2017). Neural regulation of immunity: molecular mechanisms and clinical translation. *Nat. Neurosci.* 20, 156–166. doi: 10.1038/nn.4477

Phipson, B., Lee, S., Majewski, I. J., Alexander, W. S., and Smyth, G. K. (2016). robust hyperparameter estimation protects against hypervariable genes and improves power to detect differential expression. *Ann. Appl. Stat.* 10, 946–963. doi: 10.1214/16-AOAS920

Prüss, H., Tedeschi, A., Thiriot, A., Lynch, L., Loughhead, S. M., Stutte, S., et al. (2017). Spinal cord injury-induced immunodeficiency is mediated by a sympathetic-neuroendocrine adrenal reflex. *Nat. Neurosci.* 20, 1549–1559. doi: 10.1038/nn.4643

Quattrocchi, K. B., Frank, E. H., Miller, C. H., Amin, A., Issel, B. W., and Wagner, F. C. Jr. (1991). Impairment of helper T-cell function and lymphokine-activated killer cytotoxicity following severe head injury. *J. Neurosurg.* 75, 766–773. doi: 10.3171/jns.1991.75.5.0766

Riegger, T., Conrad, S., Liu, K., Schluesener, H. J., Adibzahdeh, M., and Schwab, J. M. (2007). Spinal cord injury-induced immune depression syndrome (SCI-IDS). *Eur. J. Neurosci.* 25, 1743–1747. doi: 10.1111/j.1460-9568.2007.05447.x

Riegger, T., Conrad, S., Schluesener, H. J., Kaps, H. P., Badke, A., Baron, C., et al. (2009). Immune depression syndrome following human spinal cord injury (SCI): a pilot study. *Neuroscience* 158, 1194–1199. doi: 10.1016/j.neuroscience.2008.08.021

Rodrigues, L. F., Moura-Neto, V., and Tcls, E. S. (2018). Biomarkers in spinal cord injury: from prognosis to treatment. *Mol. Neurobiol.* 55, 6436–6448. doi: 10.1007/s12035-017-0858-y

Salem, A., Alotaibi, M., Mroueh, R., Basheer, H. A., and Afarinkia, K. (2021). CCR7 as a therapeutic target in Cancer. *Biochim. Biophys Acta Rev. Cancer* 1875:188499. doi: 10.1016/j.bbcan.2020.188499

Savic, G., DeVivo, M. J., Frankel, H. L., Jamous, M. A., Soni, B. M., and Charlifue, S. (2017). Causes of death after traumatic spinal cord injury—a 70-year British study. *Spinal Cord* 55, 891–897. doi: 10.1038/sc.2017.64

Sekhon, L. H., and Fehlings, M. G. (2001). Epidemiology, demographics, and pathophysiology of acute spinal cord injury. *Spine* 26:S2–S12. doi: 10.1097/00007632-200112151-00002

Shannon, P., Markiel, A., Ozier, O., Baliga, N. S., Wang, J. T., Ramage, D., et al. (2003). Cytoscape: a software environment for integrated models of biomolecular interaction networks. *Genome Res.* 13, 2498–2504. doi: 10.1101/gr.1239303

Shi, C., Flanagan, S. R., and Samadani, U. (2013). Vagus nerve stimulation to augment recovery from severe traumatic brain injury impeding consciousness: a prospective pilot clinical trial. *Neurol. Res.* 35, 263–276. doi: 10.1179/1743132813Y.0000000167

Subramanian, A., Tamayo, P., Mootha, V. K., Mukherjee, S., Ebert, B. L., Gillette, M. A., et al. (2005). Gene set enrichment analysis: a knowledge-based approach for interpreting genome-wide expression profiles. *Proc. Nat. Acad. Sci. U.S.A.* 102, 15545–15550. doi: 10.1073/pnas.0506580102

Szklarczyk, D., Gable, A. L., Lyon, D., Junge, A., Wyder, S., Huerta-Cepas, J., et al. (2019). STRING v11: protein-protein association networks with increased coverage, supporting functional discovery in genome-wide experimental datasets. *Nucleic Acids Res.* 47:D607–D613. doi: 10.1093/nar/gky1131

Ueno, M., Ueno-Nakamura, Y., Niehaus, J., Popovich, P. G., and Yoshida, Y. (2016). Silencing spinal interneurons inhibits immune suppressive autonomic reflexes caused by spinal cord injury. *Nat. Neurosci.* 19, 784–787. doi: 10.1038/nn.4289

Vinuesa, C. G., Linterman, M. A., Yu, D., and MacLennan, I. C. M. (2016). Follicular helper T cells. *Annu. Rev. Immunol.* 34, 335–368. doi: 10.1146/annurev-immunol-041015-055605

Wang, S., Xie, X., Li, C., Jia, J., and Chen, C. (2021). Integrative network analysis of N(6) methylation-related genes reveal potential therapeutic targets for spinal cord injury. *Math. Biosci. Eng.* 18, 8174–8187. doi: 10.3934/mbe.2021405

Wilkerson, M. D., and Hayes, D. N. (2010). ConsensusClusterPlus: a class discovery tool with confidence assessments and item tracking. *Bioinformatics* 26, 1572–1573. doi: 10.1093/bioinformatics/btq170

Wu, C., Yu, J., Xu, G., Gao, H., Sun, Y., Huang, J., et al. (2021). Bioinformatic analysis of the proteome in exosomes derived from plasma: exosomes involved in cholesterol metabolism process of patients with spinal cord injury in the acute phase. *Front. Neuroinform.* 15:662967. doi: 10.3389/fninf.2021.662967

Yan, L., de Leur, K., Hendriks, R. W., van der Laan, L. J. W., Shi, Y., Wang, L., et al. (2017). T Follicular helper cells as a new target for immunosuppressive therapies. *Front. Immunol.* 8:1510. doi: 10.3389/fimmu.2017.01510

Yu, G., Wang, L. G., Han, Y., and He, Q. Y. (2012). clusterProfiler: an R package for comparing biological themes among gene clusters. *OMICS* 16, 284–287. doi: 10.1089/omi.2011.0118

Yu, K., Hammerschmidt, S. I., Permanyer, M., Galla, M., Rothe, M., Zheng, X., et al. (2021). Targeted delivery of regulatory macrophages to lymph nodes

interferes with T cell priming by preventing the formation of stable immune synapses. *Cell Rep*. 35:109273. doi: 10.1016/j.celrep.2021.109273

Zha, J., Smith, A., Andreansky, S., Bracchi-Ricard, V., and Bethea, J. R. (2014). Chronic thoracic spinal cord injury impairs CD8+ T-cell function by up-regulating programmed cell death-1 expression. *J. Neuroinflammation* 11:65. doi: 10.1186/1742-2094-11-65

Zhao, B., Cui, K., Wang, C. L., Wang, A. L., Zhang, B., Zhou, W. Y., et al. (2011). The chemotactic interaction between CCL21 and its receptor, CCR7, facilitates the progression of pancreatic cancer via induction of angiogenesis and lymphangiogenesis. *J. Hepatobiliary Pancreat. Sci.* 18, 821–828. doi: 10.1007/s00534-011-0395-4

frontiers | Frontiers in Neuroscience

TYPE Original Research
PUBLISHED 23 November 2022
DOI 10.3389/fnins.2022.1029327

OPEN ACCESS

EDITED BY
Bo Li,
Sun Yat-sen University, China

REVIEWED BY
Masao Koda,
University of Tsukuba Hospital, Japan
Ming Yang,
Peking University People's Hospital, China

*CORRESPONDENCE
Rong Chen
chenrong52199@126.com
Li Zhang
13933058179@163.com

SPECIALTY SECTION
This article was submitted to Translational Neuroscience, a section of the journal Frontiers in Neuroscience

RECEIVED 27 August 2022
ACCEPTED 07 November 2022
PUBLISHED 23 November 2022

CITATION
Du W, Wang H-X, Zhang J-T, Wang F, Zhang X, Shen Y, Chen R and Zhang L (2022) Cervical alignment and clinical outcome of anterior decompression with fusion vs. posterior decompression with fixation in kyphotic cervical spondylotic myelopathy.
Front. Neurosci. 16:1029327.
doi: 10.3389/fnins.2022.1029327

Cervical alignment and clinical outcome of anterior decompression with fusion vs. posterior decompression with fixation in kyphotic cervical spondylotic myelopathy

Wei Du[1], Hai-Xu Wang[1], Jing-Tao Zhang[1], Feng Wang[1], Xu Zhang[1], Yong Shen[1], Rong Chen[2]* and Li Zhang[1]*

[1]Department of Orthopedics, The Third Hospital of Hebei Medical University, Shijiazhuang, China, [2]Department of Neurology, Hebei Key Laboratory of Vascular Homeostasis, Hebei Collaborative Innovation Center for Cardio-Cerebrovascular Disease, The Second Hospital of Hebei Medical University, Shijiazhuang, China

Background context: Cervical kyphosis is a common but potentially debilitating and challenging condition. There is controversy on the optimal surgical strategy for the treatment of kyphotic cervical spondylotic myelopathy (KCSM) using either anterior approach or posterior approach.

Introduction: The purpose of this study was to investigate the surgical efficacy of anterior decompression with fusion (ADF) vs. posterior decompression with fixation (PDF) for the treatment of KCSM, and to further analyze the changes of cervical spinal alignment parameters and axial symptoms (AS) severity after kyphotic correction.

Materials and methods: We retrospectively reviewed 117 patients with KCSM who had undergone ADF (58 patients) and PDF (59 patients) between January 2016 and December 2020. Cervical spinal alignment parameters, including curvature index (CI) and C2-7 Cobb angle, were measured on the PreOP and PostOP lateral radiographs. Recovery rate was calculated based on the Japanese Orthopedic Association (JOA) score. AS severity was quantified by Neck Disability Index (NDI). A *P*-value less than 0.05 was considered to be significant.

Results: The patient mean age, gender, presenting symptoms and follow-up time were similar between the two groups ($P > 0.05$). However, there were statistically significant differences ($P < 0.001$) between the two groups regarding the operation levels, operating time and intraoperative blood loss. Analysis of PostOP follow-up data showed significant differences ($P < 0.001$) in CI, correction of CI, C2-7 Cobb angle, and NDI between the two groups, whereas no significant differences in JOA score ($P = 0.16$) and recovery rate ($P = 0.14$). There were significant differences ($P < 0.001$) in CI, C2-7 Cobb angle, JOA score, and NDI between PreOP and PostOP follow-up in each

group. Correction of CI showed positive correlation with recovery of NDI in Group ADF (r = 0.51, $P < 0.001$), and in Group PDF (r = 0.45, $P < 0.001$).

Conclusion: Satisfied neurological improvement was obtained by ADF and PDF for patients with KCSM. Cervical kyphotic correction caused significant improvement of AS, and was more favorable with ADF than with PDF. Surgeons should pay full consideration of the merits and shortcomings of each approach when deciding on a surgical plan.

KEYWORDS

cervical spondylotic myelopathy, anterior decompression with fusion, posterior decompression with fixation, kyphotic correction, neurological improvement, axial symptoms

Introduction

Cervical spondylotic myelopathy (CSM), which is a degenerative disease associated with cervical cord compression, usually results in a stepwise deterioration of neurological function and life quality. In some patients with CSM, cervical kyphosis may develop because of the changes of intervertebral height and sagittal lordotic alignment, as well as progressive degeneration of the discs and facet joints. Cervical kyphosis is a common but potentially debilitating condition that can be challenging to treat (Sivaganesan and Kim, 2022). Although non-surgical treatments may have some short-term benefits in improving this disease, surgery remained to be pivotal to decompression of the spinal cord and correction of kyphosis using either anterior approach or posterior approach.

In the past several decades, anterior decompression with fusion (ADF) has become the gold standard treatment for cervical degenerative disease related with radiculopathy and myelopathy (Chang et al., 2022). The anterior approach is particularly effective for directly decompressing the spinal cord, removing anterior bony spurs and disc fragments, restoring intervertebral height, and correcting segmental kyphosis. The ADF-related complications are not rare, such as iatrogenic spinal cord injury, dysphagia, hoarseness, and air-way obstruction, cerebrospinal fluid leakage, graft failure, and pseudarthrosis (McCormick et al., 2020; Lannon and Kachur, 2021). In recent years, posterior decompression with fixation (PDF) had been demonstrated effectively to provide better clinical outcomes than laminoplasty alone for CSM accompanying local kyphosis or segmental instability (Abumi, 2015). Some PDF-related complications, which include compressive epidural hematoma, vertebral artery injury, iatrogenic spinal cord injury, dural tears, and implant failure, have also been observed (Li et al., 2022). The optimal surgical strategy for kyphotic cervical spondylotic myelopathy (KCSM) remains controversial for spine surgeons.

The purpose of this retrospective study was to investigate the surgical efficacy of anterior ADF vs. PDF for the treatment of KCSM, and to further analyze the changes of cervical spinal alignment parameters and axial symptoms severity after correction of kyphosis.

Materials and methods

Participants

We retrospectively reviewed 139 patients who suffered from KCSM at our medical center from January 2016 to December 2020. Among them, 72 patients had undergone ADF; while others, 67 patients had undergone PDF.

The inclusion criteria include patients who had at least 1–5 levels of cervical spinal cord compression with combined symptoms and signs of CSM; and kyphosis defined as an alignment of C2-7 Cobb angle less than 0° on lateral neutral radiograph. The exclusion criteria included (1) cervical trauma (n = 6 in Group ADF; n = 4 in Group PDF); (2) significant cervical anatomic deformity; (3) active infection; (4) rheumatoid arthritis; (5) neoplasm (n = 2 in Group ADF; n = 3 in Group PDF); (6) incomplete or poor quality pre- or post-operative magnetic resonance imaging (MRI) and X-rays (n = 4 in Group ADF; n = 1 in Group PDF); (7) loss to follow-up (n = 2 in Group ADF; n = 0 in Group PDF).

Finally, a total of 117 patients (58 patients in Group ADF; 59 patients in Group PDF) were included in this study. This study was approved by the Investigational Review Board at our institution, and informed consent was obtained from each patient.

Surgical techniques

The patients in Group ADF underwent anterior cervical discectomy and fusion (ACDF) under general anesthesia.

A standard right-sided approach through a transverse incision was used to expose the targeted segment based on the preoperative surgical planning. The compressive materials were removed, which included herniated disc, osteophytes and the posterior longitudinal ligament. The cartilaginous endplates were removed with a curette, and the bony endplates were protected simultaneously to prevent cage subsidence. The bilateral uncovertebral joints could be removed partially until release, but the vertebral artery must be taken care to avoid damage. The intervertebral space was properly distracted using a Caspar spreader, keeping the intervertebral space wide in anterior edge and narrow in posterior edge. An appropriate size Poly-ether-ether-ketone (PEEK) cage filled with excised osteophytes was implanted between vertebral bodies, and then the plate with normal cervical lordosis was fixed with screws inserted cranially and caudally.

Laminectomy with lateral mass screw fixation were performed in Group PDF by the same surgeon under general anesthesia. Screws (Medtronic Sofamor Danek, Memphis, TN, USA) were placed bilaterally with the Magerl technique (Pal et al., 2011), rods of appropriate size were selected and bent to match the normal cervical lordosis and secured to the lateral masses by screws, and then laminectomy were performed based on the preoperative surgical planning.

All patients stayed in bed for 1–3 days after surgery, and thereafter rehabilitation was instructed with a neck collar for 2 months. Anteroposterior, lateral, and flexion/extension lateral X-ray tests and MRI scans were routinely performed preoperatively. Routine X-ray tests were performed postoperatively at 3, 6, 12 months and then the last year.

Radiological assessments

PreOP and PostOP follow-up cervical alignments were measured three times on standing lateral X-ray with 200% magnification for accuracy by the first and second authors independently, and the mean value was used for analysis. The intraobserver errors were less than 5%. Curvature index (CI, **Figure 1**): "a1" was defined as the distance from the posterior inferior edge of the C3 vertebral body to line "AB," "a2, a3, and a4" using the same method; "AB" was defined as the distance from the posterior inferior edge of the C2 vertebral body to that of the C7 vertebral body. The correction of CI was calculated: PostOP CI–PreOP CI. C2-7 Cobb angle was the angle formed by the vertical lines of C2 and C7 inferior endplates in standing lateral radiographs (**Figure 2**).

Clinical assessment

Patient's neurological status was assessed using the Japanese Orthopedic Association (JOA) disability scale (Japanese Orthopedic Association, 1994). Neurological recovery rate was calculated using the Hirabayashi method: (PostOP JOA-PreOP JOA)/(17-PreOP JOA) × 100%. Recovery rates were graded as excellent (≥ 75%), good (50–74%), fair (25–49%), and poor (< 25%).

Axial symptom severity was quantified by Neck Disability Index (NDI, 0 = no disability, 50 = total disability) (Vernon and Mior, 1991). Subjects' scores were calculated and ranked according to the NDI ranking system (no disability, 0–4; mild disability, 5–14; moderate disability, 15–24; severe disability, 25–34; complete disability, ≥ 35).

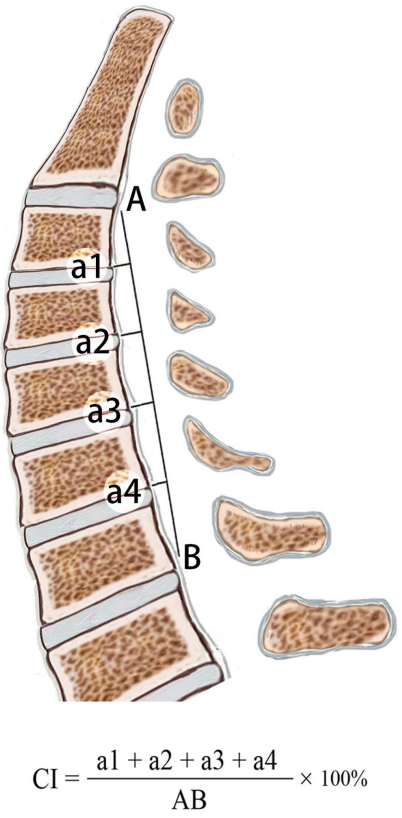

FIGURE 1
Calculation of the cervical curvature index (CI).

Statistical analysis

All statistical analysis was performed using IBM SPSS Statistics, version 21.0 (IBM Corp., Armonk, NY, USA). Continuous variables were expressed as means ± standard deviation. The Chi-square test was applied for qualitative data. A paired *t*-test was used to assess statistical significance between PreOP and PostOP parameters in each group. Statistical comparisons between Group ADF and PDF were performed in the PostOP follow-up CI, C2-7 Cobb angle, JOA score,

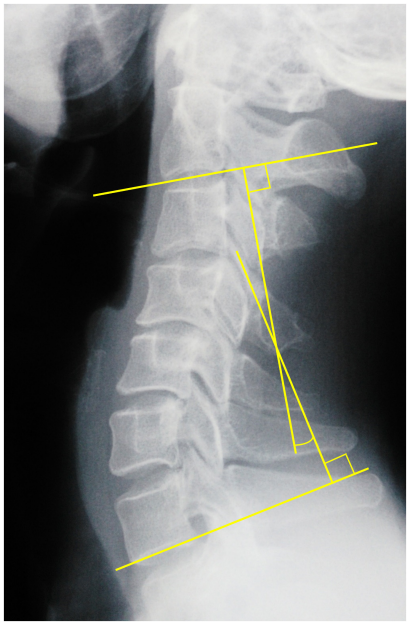

FIGURE 2
C2-7 Cobb angle measurement.

NDI, correction of CI, recovery rate and recovery of NDI using the independent sample t-test, and in the NDI ranking system using Mann–Whitney U test. The Chi-square test was performed in neurological recovery rate grade. Pearson's correlation coefficient was used to check the correlation between correction of CI and recovery of NDI in each group. A value of $P < 0.05$ was considered to be statistically significant.

Results

A total of 117 patients (58 patients in ADF group; 59 patients in PDF group) were included in this study (Table 1). The patient age, gender, presenting symptoms, and follow-up time were similar between the ADF and PDF groups ($P > 0.05$). However, there were statistically significant differences between the two groups regarding the operation levels ($U = 883$, $P < 0.001$), operating time ($t = 12.13$, $P < 0.001$), and intraoperative blood loss ($t = 22.77$, $P < 0.001$).

TABLE 1 Patient characteristics.

Characteristics	Group ADF	Group PDF
Total ($n = 117$)	58	59
Mean age (years)	60.47 ± 8.45 (45–74)	61.14 ± 7.17 (47–75)
Gender		
Male	42	39
Female	17	20
Operation levels*		
1 level	33	0
2 levels	21	1
3 levels	4	10
4 levels	0	31
5 levels	0	17
Presenting symptoms		
Weakness		
Upper extremity	45	47
Lower extremity	26	31
Extremity numbness hyperesthesia	34	35
Gait instability	38	40
Hyperreflexia	43	46
Hoffman sign	42	44
Babinski sign	21	25
Clonus	17	19
Operating time*	104.24 ± 24.96	151.86 ± 16.79
Intraoperative blood loss*	97.62 ± 29.72	357.80 ± 81.88
Follow-up time (year)	3.4 ± 0.9 (2–5)	3.6 ± 0.8 (2–5)

*Statistic tests: statistically significant differences between the two groups ($P < 0.001$).

Radiographic results

In Group ADF, there were statistically significant differences between the PreOP and PostOP data regarding CI ($t = 22.87$, $P < 0.001$), C2-7 Cobb angle ($t = 16.76$, $P < 0.001$) (Figures 3A–D). In Group PDF, there were statistically significant differences between PreOP and PostOP data regarding CI ($t = 16.95$, $P < 0.001$), C2-7 Cobb angle ($t = 13.09$, $P < 0.001$) (Figures 4A–D). Between the two groups, there were no significant differences regarding the PreOP CI and C2-7 Cobb angle ($P > 0.05$). There were also statistically significant differences regarding the PostOP CI ($t = 7.59$, $P < 0.001$), correction of CI ($t = 5.41$, $P < 0.001$) (Figure 5), C2-7 Cobb angle ($t = 6.39$, $P < 0.001$) (Table 2).

Functional outcomes

There were statistically significant differences between PreOP and PostOP JOA scores in Group ADF ($t = 26.09$; $P < 0.001$) and in Group PDF ($t = 26.31$, $P < 0.001$), respectively. Between the two groups, there were no significant differences regarding PreOP and PostOP JOA scores ($t = 0.37$, $P = 0.71$; $t = 1.40$, $P = 0.16$) (Table 3).

The improvement rates were 75.17 ± 14.33% after ADF and 71.20 ± 14.39% after PDF, respectively. There was no significant difference between the two groups regarding the recovery rate ($t = 1.50$, $P = 0.14$). Based on the neurological recovery rate grade, the neurological recovery was excellent in 31 (53.4%) patients and good in 27 (46.6%) patients in Group ADF. In Group PDF, the neurological recovery was excellent in 22 (37.3%) patients and good in 37 (62.7%). According to Pearson Chi-square test, there was no significant difference between the two groups regarding axial symptoms ($\chi^2 = 4.13$, $P = 0.25$).

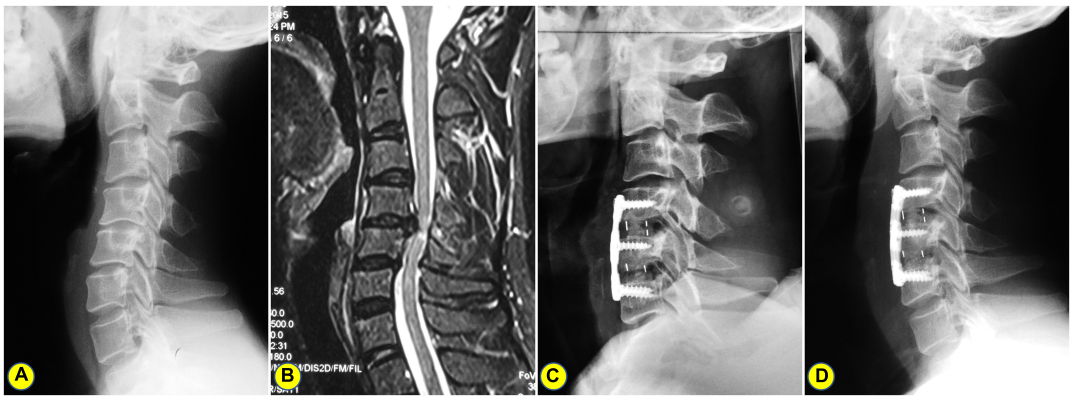

FIGURE 3
A 57-years-old man who underwent anterior cervical discectomy and fusion (ACDF). **(A)** The preoperative lateral X-ray shows the C2-7 Cobb angle and curvature index (CI) are 15° and 9.49%, respectively. **(B)** Preoperative magnetic resonance imaging (MRI) showing C4-6 spinal cord compression combined with kyphosis. **(C)** A postoperative lateral X-ray showing ACDF. **(D)** On the lateral X-ray of 2.5 years after surgery, the C2-7 Cobb angle and CI were 7° and 16.09%, respectively.

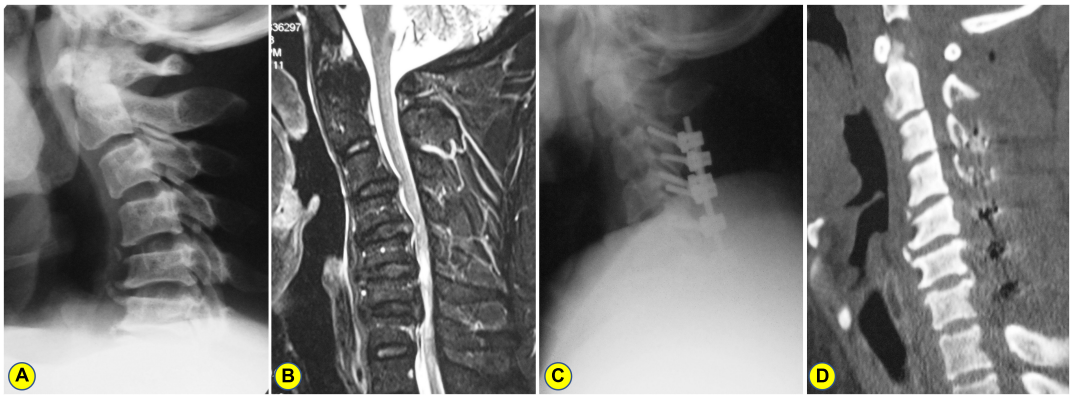

FIGURE 4
A 51-years-old man who underwent laminectomy with lateral mass screw fixation. **(A)** The preoperative lateral X-ray shows the C2-7 Cobb angle and curvature index (CI) are 17° and 9.45%, respectively. **(B)** Preoperative magnetic resonance imaging (MRI) showing C3–7 spinal cord compression combined with kyphosis. **(C)** A postoperative lateral X-ray showing laminectomy with lateral mass screw fixation. **(D)** On the CT image of 3 years after surgery, the C2-7 Cobb angle and CI were 6° and 13.09%, respectively.

Axial symptoms

There were statistically significant differences between PreOP and PostOP NDI in Group ADF ($t = 31.58$; $P < 0.001$) and in Group PDF ($t = 23.82$, $P < 0.001$), respectively. Between the two groups, there was significant differences regarding PostOP NDI ($t = 7.28$, $P < 0.001$). The recovery of NDI was 25.53 ± 6.34 after ADF and 19.20 ± 6.31 after PDF, respectively. There was a significant difference between the two groups regarding recovery of NDI ($t = 5.42$, $P < 0.001$). There were positive correlations between the CI correction and recovery of NDI in Group ADF ($r = 0.51$, $P < 0.001$), and in Group PDF ($r = 0.45$, $P < 0.001$) (Figure 6 and Table 4).

Based on the NDI ranking system, there was no disability in 24 patients, mild disability in 33 patients, and moderate disability in 1 patient in Group ADF. In Group PDF, there were no disabilities in 10 patients, mild disability in 32 patients, and moderate disability in 17 patients (Table 4). According to the Mann–Whitney U test, there was a significant difference between the two groups regarding axial symptoms ($U = 827$, $P < 0.001$).

Complications

Of a total of 58 patients in Group ADF, 14 patients (24.1%) suffered dysphagia, and 5 patients (8.6%) suffered hoarseness. However, dysphagia and hoarseness were relieved significantly after the above patients were given a low dose of glucocorticoid and dehydrant for 3 days.

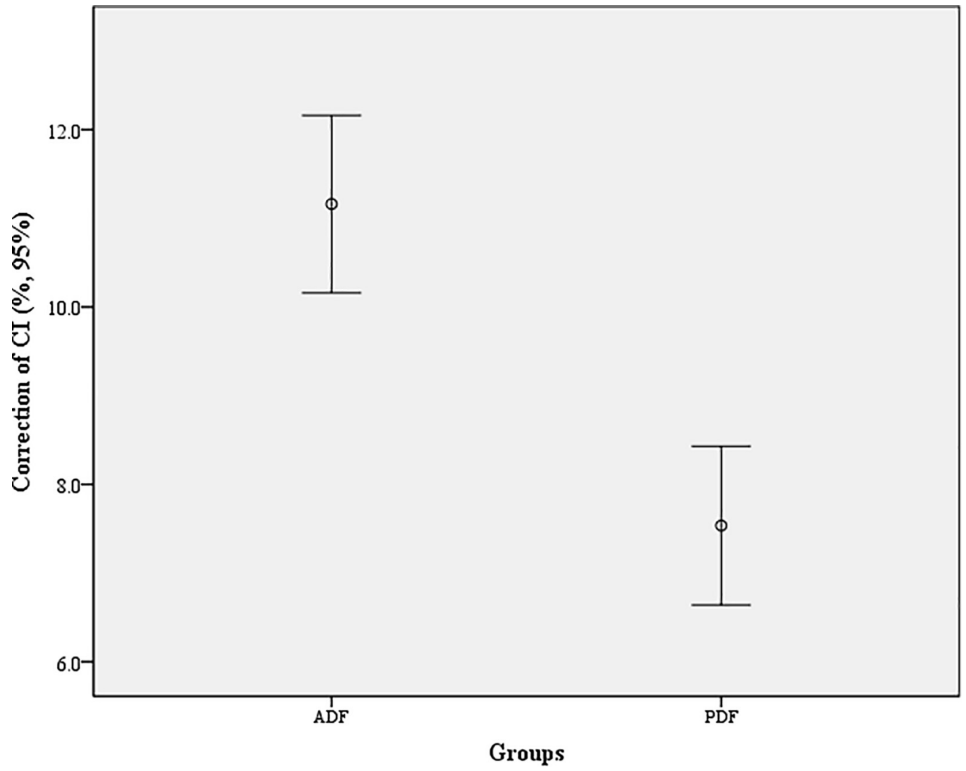

FIGURE 5
Correction of cervical curvature index (CI) in each group. The difference between the two groups for correction of CI was statistically significant (t = 5.41, P < 0.001).

TABLE 2 PreOP and PostOP follow-up cervical radiological data in each group.

Parameter	Group ADF (n = 58)	Group PDF (n = 59)	t-value*	*P-value*
CI (%)				
Preoperative	8.30 ± 2.36	8.17 ± 2.24	0.47	0.64
Postoperative follow-up	19.54 ± 2.87	15.71 ± 2.57	7.59	< 0.001
t-value*	22.87	16.95		
P-value	< 0.001	< 0.001		
Correction of CI (%)	11.16 ± 3.81	7.54 ± 3.44	5.41	< 0.001
C2-7 Cobb angle				
Preoperative	17.19 ± 4.63	16.69 ± 4.52	0.59	0.56
Postoperative follow-up	5.09 ± 2.97	8.15 ± 2.16	6.39	< 0.001
t-value*	16.76	13.09		
P-value*	< 0.001	< 0.001		

*t-test.

TABLE 3 PreOP and PostOP follow-up Japanese Orthopedic Association (JOA) score and neurological recovery rate in each group.

Parameter	Group ADF (n = 58)	Group PDF (n = 59)	Statistic value	*P-value*
JOA score*				
Preoperation	8.78 ± 1.38	8.86 ± 1.21	0.37	0.71
Postoperative follow-up	14.97 ± 1.17	14.66 ± 1.18	1.40	0.16
t-value	26.09	26.31		
P-value	< 0.001	< 0.001		
Recovery rate (%)*	75.17 ± 14.33	71.20 ± 14.39	1.50	0.14
Neurological recovery rate grade**				
Excellent (≥ 75%)	31	22	4.13	0.25
Good (50–74%)	27	37		
Fair (25–49%)	0	0		
Poor (< 25%)	0	0		

*t-test, **Pearson Chi-square test.

According to the recovery of NDI in Table 3, improvement of axial neck pain tended to be higher in Group ADF than in Group PDF, and the difference was significant (t = 5.42, P < 0.001). There were no major neurological or vascular complications, and wound complications in both groups.

Discussion

Currently, there is still a significant debate on the optimal surgical strategy for the treatment of KCSM using either anterior approach or posterior approach. Our study found that the cervical kyphotic correction can improve the severity of axial

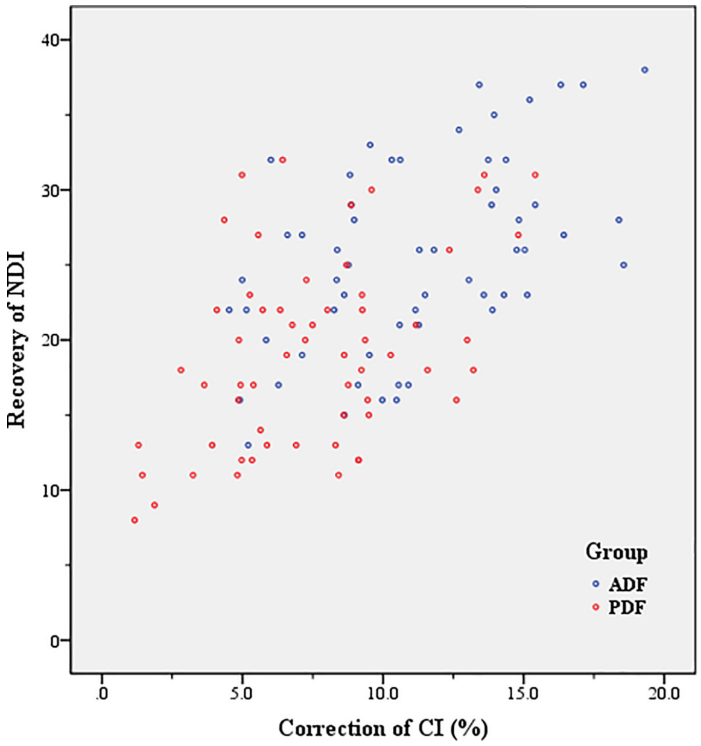

FIGURE 6
Correlation between correction of curvature index (CI) and recovery of Neck Disability Index (NDI) (Axial symptom severity) in Group anterior decompression with fusion (ADF) (r = 0.51, $P < 0.001$), and in Group posterior decompression with fixation (PDF) (r = 0.45, $P < 0.001$).

TABLE 4 PreOP and PostOP follow-up Axial symptom severity [neck disability index (NDI) scores] in each group.

Axial symptoms	Group ADF (n = 58)	Group PDF (n = 59)	Statistic value	*P-value*
NDI*				
Preoperation	32.09 ± 4.33	31.51 ± 4.57	0.70	0.49
Postoperative follow-up	6.55 ± 4.37	12.31 ± 4.17	7.28	< 0.001
t-value	31.58	23.82		
P-value	< 0.001	< 0.001		
Recovery of NDI	25.53 ± 6.34	19.20 ± 6.31	5.42	< 0.001
NDI ranking system**				
No disability (0–4)	24	10	827.00	< 0.001
Mild disability (5–14)	33	32		
Moderate disability (15–24)	1	17		
Severe disability (25–34)	0	0		
Complete disability (≥ 35)	0	0		

*t-test, **Mann–Whitney U test.

symptoms (AS), and was more favorable with ADF than with PDF. This study also confirms that the correction of CI is positively correlated with the recovery of AS. Surgeons should pay full consideration of the merits and shortcomings of each approach when deciding on a surgical plan for the CSM patients with kyphosis.

Options of surgical strategy for kyphotic cervical spondylotic myelopathy

Cervical kyphosis is a common but potentially debilitating and challenging condition. Surgical management for CSM patients with kyphosis aims to decompress the spinal cord and restore the normal sagittal alignment using either an anterior approach or a posterior approach. However, the above surgery-related complications include a high incidence of spinal cord injury, cerebrospinal fluid leakage, graft subsidence and extrusion, pseudarthrosis, fixation failures, and implant loosening (Ogura et al., 2021). Moreover, neurological recovery might be worsened because of the remaining anterior compression if the segmental instability and kyphotic deformity were not corrected effectively. The current evidence is not clear on whether anterior or posterior approach is superior for KCSM because of the shortcomings of each surgical approach.

Suda et al. (2003) thought that local kyphosis exceeding 13° was a relative contraindication for posterior decompression and that then anterior decompression for correcting the kyphotic

deformity should be recommended. Our early study (Du et al., 2014) showed that enlarged laminectomy with fixation (removing the inside edge of facet joints and decompressing the nerve foramina) was an effective strategy for improving neurological function, restoring the normal cervical lordosis, and decreasing the incidence of axial symptoms and C5 root palsy for multilevel cervical degenerative myelopathy (CDM) associated with kyphosis. In the present study, our results showed that both ADF and PDF produce similar neurological improvement, in agreement with the recent reports (Yoshii et al., 2020; Du et al., 2022). Therefore, we have good evidence that intraoperative adequate decompression of the spinal cord may be a pivotal factor in the early postoperative neurological recovery. Our results also showed a statistical difference between the two groups regarding the operation levels, and more operation levels were performed using PDF compared to ADF. Surgeons should pay full consideration of the merits and shortcomings of each approach when deciding on a surgical plan. ADF is more suitable for the KCSM patients who have less than 3 levels of spinal cord compression which need to be intervened. Nevertheless, PDF is more suitable for the KCSM patients who have 3 or more levels of spinal cord decompression.

Intraoperative consideration of anterior decompression with fusion vs. posterior decompression with fixation for kyphotic cervical spondylotic myelopathy

Surgery-related complications are relatively rare and mainly included compressive epidural hematoma, vertebral artery injury, dural tear, and iatrogenic spinal cord injury. Whether anterior or posterior approach is performed, the key point for the surgeon is spinal cord decompression with special attention to avoid iatrogenic spinal cord injury. Intraoperative neuromonitoring (IONM), including motor evoked potentials (MEPs), somatosensory evoked potentials (SSEPs), and electromyography (EMG), had gained popularity for the potential detection of neurological injury during spinal surgery (Mesregah et al., 2020). IONM afforded the surgical team an opportunity to perform rapid intervention and prevent injury progression or possibly to reverse impending neurological sequelae.

To avoid large amounts of bleeding and postoperative epidural hematoma, the surgeon must pay careful attention to hemostasis. For example, bipolar electrocautery and absorbable gelatin sponge were used for hemostasis in the epidural space, and bone edges were waxed as necessary. Tranexamic acid (TXA) can significantly reduce perioperative blood loss in cervical, thoracic, and lumbar laminectomy and fusion procedures, while demonstrating a minimal complication profile (Brown et al., 2022).

Lateral mass screw fixation is commonly used in the fusion and stabilization of the subaxial cervical spine. The accuracy of screw trajectory, screw length, technique of insertion, vertebral level, and size of the lateral mass affect the safety of lateral mass screw placement (Evans et al., 2022; Soliman et al., 2022). The main complications were lateral mass fracture and instrumental failure, resulting in screw breach into the ventral soft tissues, which may injure vertebral artery, roots and cervical sympathetic ganglion. With the progressive degeneration of facet joints, cervical lateral mass morphology may change. It is strongly necessary to assess the preoperative anatomical changes of cervical kyphosis using a 3D CT scan. For patients with severe cervical anatomical deformity, intraoperative CT navigation can enhance the safety of surgery (Sabri and York, 2021). Successful lateral mass screw placement still highly depends on the surgeon's experience. In the present study, there were no patients who developed the above surgery-related complications.

Correction of cervical kyphosis *via* anterior decompression with fusion vs. posterior decompression with fixation

Wu et al. (2021) found that cervical focal kyphosis correlated with worse myelopathy symptoms, and the threshold cervical focal kyphosis for severe myelopathy symptoms is predicted to be at about 7°. Progressive cervical kyphosis may result in cervical pain, which seriously decreases patients' quality of life. When the patient is supine during operation, cervical spine is elevated as high as possible to restore the cervical lordosis. Intraoperative cervical anterior or posterior fixation should keep to normal cervical physiologic lordosis. In the current study, cervical kyphosis can be corrected effectively by both ADF and PDF, and was more favorable with ADF than with PDF. We speculate that the cervical anterior column is more advantageous than the posterior column in the kyphotic correction.

Complications of anterior decompression with fusion vs. posterior decompression with fixation for kyphotic cervical spondylotic myelopathy

Dysphagia and hoarseness are the most common complications after ADF, with incidences ranging from

2.7–33.3% and 3–11%, respectively (Bakhsheshian et al., 2017; Nagoshi et al., 2017). The possible causes include postoperative soft tissue edema, postoperative hematoma, esophageal injury, cervical plate implanting, and the surrounding scar formation (Shen et al., 2018; Tetreault et al., 2022). In the current study, these complications usually occur in patients with multilevel spinal cord compression, longer operation times and short wide necks. However, dysphagia and hoarseness were relieved significantly after the patients were given a low dose of glucocorticoid and dehydrant.

The incidence of axial symptoms can be up to 29.91% after ACDF (Zhou et al., 2018) and 19.25% after laminoplasty (Chen et al., 2021). Postoperative neck pain alleviation may be related to the transient relief of facet joint pressure during the vertebral distraction procedure in ACDF (Xu et al., 2022). In the present study, cervical kyphotic correction causes significant improvement of axial symptoms postoperatively than preoperatively. The results show that improvement of axial symptoms is positively correlated with cervical kyphotic correction, and is more favorable with ADF than with PDF. Posterior decompression of spinal cord bases on disruption of the posterior tension band while cervical kyphosis is corrected. However, anterior decompression of spinal cord, as well as kyphosis correction, do not involve in disruption of the posterior tension band. We speculate that cervical kyphotic correction can change the bio-mechanical distribution of discs and facet joints, further resulting in postoperative neck pain alleviation.

Limitations of present study

This study has limitations. First, we only included the patients with KCSM. Second, all patients were selected from a single hospital and all operations were performed by the same surgical team, which may produce a selection bias. Third, only ACDF was selected for anterior approach, and only laminectomy with lateral mass screw fixation was selected for posterior approach. Fourth, our retrospective design has inherent weaknesses that may produce a statistical bias. Fifth, multi-center long-term clinical trials should be performed to ascertain the results of this study.

Conclusion

Satisfied neurological improvement was obtained by ADF and PDF for patients with KCSM. Cervical kyphotic correction caused significant improvement of AS, and was more favorable with ADF than with PDF. Surgeons should pay full consideration of the merits and shortcomings of each approach when deciding on a surgical plan. ADF is more suitable for the KCSM patients who have less than 3 levels of spinal cord compression which need to be intervened. Nevertheless, PDF is more suitable for the KCSM patients who have 3 or more levels of spinal cord decompression.

Data availability statement

The original contributions presented in this study are included in the article/supplementary material, further inquiries can be directed to the corresponding authors.

Ethics statement

The studies involving human participants were reviewed and approved by the Ethics Committee of The Third Hospital of Hebei Medical University. Written informed consent for participation was not required for this study in accordance with national legislation and institutional requirements.

Author contributions

WD participated in the study design, collection, interpretation, and writing of the manuscript. H-XW, J-TZ, and FW participated in the collection, interpretation, and analysis of the data. XZ and YS participated in revising of the manuscript. RC and LZ participated in the study design. All authors contributed to the article and approved the submitted version.

Funding

This study was funded by the Health Commission of Hebei Province (No. 20180407) and Natural Science Foundation of Hebei Province (No. H2022206432).

Conflict of interest

The authors declare that the research was conducted in the absence of any commercial or financial relationships that could be construed as a potential conflict of interest.

Publisher's note

References

Abumi, K. (2015). Cervical spondylotic myelopathy: Posterior decompression and pedicle screw fixation. *Eur. Spine J.* 24, 186–196. doi: 10.1007/s00586-015-3838-9

Bakhsheshian, J., Mehta, V. A., and Liu, J. C. (2017). Current diagnosis and management of cervical spondylotic myelopathy. *Glob. Spine J.* 7, 572–586. doi: 10.1177/2192568217699208

Brown, N. J., Choi, E. H., Gendreau, J. L., Ong, V., Himstead, A., Lien, B. V., et al. (2022). Association of tranexamic acid with decreased blood loss in patients undergoing laminectomy and fusion with posterior instrumentation: A systematic review and meta-analysis. *J. Neurosurg. Spine* 36, 686–693. doi: 10.3171/2021.7.SPINE202217

Chang, C. J., Liu, Y. F., Hsiao, Y. M., Huang, Y. H., Liu, K. C., Lin, R. M., et al. (2022). Comparison of anterior cervical discectomy and fusion versus artificial disc replacement for cervical spondylotic myelopathy: A meta-analysis. *J. Neurosurg. Spine* 22, 1–10. doi: 10.3171/2022.2.SPINE211500

Chen, T., Zhang, X., Meng, F., Zhang, T., Zhao, Y., Yan, J., et al. (2021). Open-door versus French-door laminoplasty for patients with multisegmental cervical spondylotic myelopathy: A systematic review and meta-analysis. *World Neurosurg.* 155, 82–93. doi: 10.1016/j.wneu.2021.08.032

Du, W., Wang, S., Wang, H., Zhang, J., Wang, F., Zhang, X., et al. (2022). Cervical alignment and clinical outcome of open-door laminoplasty vs. laminectomy and instrumentation in kyphotic multilevel cervical degenerative myelopathy. *Arch. Orthop. Trauma Surg.* 23. doi: 10.1007/s00402-021-04316-x [Epub ahead of print].

Du, W., Zhang, P., Shen, Y., Zhang, Y. Z., Ding, W. Y., and Ren, L. X. (2014). Enlarged laminectomy and lateral mass screw fixation for multilevel cervical degenerative myelopathy associated with kyphosis. *Spine J.* 14, 57–64. doi: 10.1016/j.spinee.2013.06.017

Evans, S., Nagassima Rodrigues Dos Reis, K., McDonnell, J. M., Ahern, D. P., Gibbons, D., and Butler, J. S. (2022). What is the superior screw fixation technique for posterior decompression and fusion in the management of cervical spondylotic myelopathy: Pedicle screw or lateral mass screw? *Clin. Spine Surg.* 35, 91–94. doi: 10.1097/BSD.0000000000001118

Japanese Orthopedic Association (1994). Scoring system for cervical myelopathy. *J. Jpn. Orthop. Assoc.* 68, 490–503.

Lannon, M., and Kachur, E. (2021). Degenerative cervical myelopathy: Clinical presentation, assessment, and natural history. *J. Clin. Med.* 10:3626. doi: 10.3390/jcm10163626

Li, X., Yu, H., Welle, K., Gathen, M., Zhang, L., Xiao, J., et al. (2022). Comparative effectiveness and safety of open-door laminoplasty, french-door laminoplasty, laminectomy and fusion, and laminectomy alone for multilevel degenerative cervical myelopathy: A bayesian network analysis. *Adv. Ther.* 39, 117–139. doi: 10.1007/s12325-021-01980-8

McCormick, J. R., Sama, A. J., Schiller, N. C., Butler, A. J., and Donnally, C. J. III (2020). Cervical spondylotic myelopathy: A guide to diagnosis and management. *J. Am. Board Fam. Med.* 33, 303–313. doi: 10.3122/jabfm.2020.02.190195

Mesregah, M. K., Buchanan, I. A., Formanek, B., Wang, J. C., and Buser, Z. (2020). Intra- and post-complications of cervical laminoplasty for the treatment of cervical myelopathy: An analysis of a nationwide database. *Spine (Phila Pa 1976)* 45, E1302–E1311. doi: 10.1097/BRS.0000000000003574

Nagoshi, N., Tetreault, L., Nakashima, H., Arnold, P. M., Barbagallo, G., Kopjar, B., et al. (2017). Risk factors for and clinical outcomes of dysphagia after anterior cervical surgery for degenerative cervical myelopathy: Results from the AOSpine International and North America studies. *J. Bone Joint Surg. Am.* 99, 1069–1077. doi: 10.2106/JBJS.16.00325

Ogura, Y., Dimar, J. R., Djurasovic, M., and Carreon, L. Y. (2021). Etiology and treatment of cervical kyphosis: State of the art review-a narrative review. *J. Spine Surg.* 7, 422–433. doi: 10.21037/jss-21-54

Pal, D., Bayley, E., Magaji, S. A., and Boszczyk, B. M. (2011). Freehand determination of the trajectory angle for cervical lateral mass screws: How accurate is it? *Eur. Spine J.* 20, 972–976. doi: 10.1007/s00586-011-1694-9

Sabri, S. A., and York, P. J. (2021). Preoperative planning for intraoperative navigation guidance. *Ann. Transl. Med.* 9:87. doi: 10.21037/atm-20-1369

Shen, Y., Du, W., Wang, L. F., Dong, Z., and Wang, F. (2018). Comparison of Zero-Profile device versus Plate-and-Cage implant in the treatment of symptomatic adjacent segment disease after anterior cervical discectomy and fusion: A minimum 2-year follow-up study. *World Neurosurg.* 115, e226–e232. doi: 10.1016/j.wneu.2018.04.019

Sivaganesan, A., and Kim, H. J. (2022). A review of indications, surgical technique, and outcomes for the cervical pedicle subtraction osteotomy. *J. Am. Acad. Orthop. Surg.* 30, e295–e300. doi: 10.5435/JAAOS-D-21-00177

Soliman, M. A. R., Khan, S., Ruggiero, N., Mariotti, B. L., Aguirre, A. O., Kuo, C. C., et al. (2022). Complications associated with subaxial placement of pedicle screws versus lateral mass screws in the cervical spine: Systematic review and meta-analysis comprising 1768 patients and 8636 screws. *Neurosurg. Rev.* 45, 1941–1950. doi: 10.1007/s10143-022-01750-2

Suda, K., Abumi, K., Ito, M., Shono, Y., Kaneda, K., and Fujiya, M. (2003). Local kyphosis reduces surgical outcomes of expansive open-door laminoplasty for cervical spondylotic myelopathy. *Spine (Phila Pa 1976)* 28, 1258–1262. doi: 10.1097/01.BRS.0000065487.82469.D9

Tetreault, L., Lange, S. F., Chotai, S., Lupo, M., Kryshtalskyj, M. T., Wilson, J. R., et al. (2022). A systematic review of definitions for dysphagia and dysphonia in patients treated surgically for degenerative cervical myelopathy. *Glob. Spine J.* 12, 1535–1545. doi: 10.1177/21925682211035714

Vernon, H., and Mior, S. (1991). The neck disability index: A study of reliability and validity. *J. Manip. Physiol. Ther.* 14, 409–415.

Wu, B., Liu, B., Sang, D., Cui, W., and Wang, D. (2021). The association between cervical focal kyphosis and myelopathy severity in patients with cervical spondylotic myelopathy before surgery. *Eur. Spine J.* 30, 1501–1508. doi: 10.1007/s00586-021-06771-x

Xu, C., Wang, R., Li, J., Zhong, H., Zhang, Z., Cui, C., et al. (2022). Intervertebral-spreader-assisted anterior cervical discectomy and fusion prevents postoperative axial pain by alleviating facet joint pressure. *J. Orthop. Surg. Res.* 17:91. doi: 10.1186/s13018-022-02983-z

Yoshii, T., Egawa, S., Chikuda, H., Wakao, N., Furuya, T., Kanchiku, T., et al. (2020). Comparison of anterior decompression with fusion and posterior decompression with fusion for cervical spondylotic myelopathy-A systematic review and meta-analysis. *J. Orthop. Sci.* 25, 938–945. doi: 10.1016/j.jos.2019.12.010

Zhou, J., Li, L., Li, T., and Xue, Y. (2018). Preoperative modic changes are related to axial symptoms after anterior cervical discectomy and fusion. *J. Pain Res.* 11, 2617–2623. doi: 10.2147/JPR.S172953

frontiers | Frontiers in Neuroscience

TYPE Original Research
PUBLISHED 05 December 2022
DOI 10.3389/fnins.2022.1035061

OPEN ACCESS

EDITED BY
Bo Li,
Sun Yat-sen Memorial Hospital, Sun Yat-sen University, China

REVIEWED BY
Yunzhong Cheng,
Beijing Chao-Yang Hospital, Capital Medical University, China
Antonino Tuttolomondo,
University of Palermo, Italy

*CORRESPONDENCE
Xiangrong Sun
sunxiangrong197407@163.com

†These authors have contributed equally to this work

SPECIALTY SECTION
This article was submitted to Translational Neuroscience, a section of the journal Frontiers in Neuroscience

RECEIVED 02 September 2022
ACCEPTED 07 November 2022
PUBLISHED 05 December 2022

CITATION
Sun X, Jv X, Mi Q, Yang Q, Chen T and Jiang G (2022) The effect of blood pressure variability on the prognosis of patients with acute cerebral hemorrhage: Possible mechanism. *Front. Neurosci.* 16:1035061. doi: 10.3389/fnins.2022.1035061

The effect of blood pressure variability on the prognosis of patients with acute cerebral hemorrhage: Possible mechanism

Xiangrong Sun[1]*†, Xinyue Jv[2]†, Qi Mi[3], Qian Yang[1], Tao Chen[4] and Guohui Jiang[1]

[1]Department of Neurology, Affiliated Hospital of North Sichuan Medical College, Nanchong, Sichuan, China, [2]Department of Neurology, The Third Affiliated Hospital of Chongqing Medical University, Chongqing, China, [3]Wusheng County People's Hospital, Wusheng, Sichuan, China, [4]Department of Neurosurgery, Guangyuan Central Hospital, Guangyuan, Sichuan, China

Background: Antihypertensive therapy in the acute phase of intracerebral hemorrhage (ICH) can reduce hematoma expansion. Numerous studies have demonstrated that blood pressure variability secondary to antihypertensive therapy has adverse effects on neurological outcomes, but the conclusions are diverse, and the mechanism of this occurrence is unknown. The aim of this research was to analyze the impact of blood pressure variability after antihypertensive treatment on the prognosis of patients with acute ICH, along with the possible mechanism.

Materials and methods: A total of 120 patients within 20 h of onset of ICH were divided into a good prognosis group (mRS $\leq$ 2 points) and a poor prognosis group (mRS $\geq$ 3 points) according to their 90-day mRS scores. The basic patient information, NIHSS score, GCS score, mRS score at 90 days after admission, head CT examination at admission and 24 h and CTP examination at 24 h were collected from some patients. The blood pressure values of patients were collected within 24 h, and multiple blood pressure variation (BPV) parameters within 1 and 24 h were calculated.

Results: (1) After excluding confounding factors such as age, whether the hematoma ruptured into the ventricle, confounding signs, amount of bleeding, edema around the hematoma, NIHSS on admission, operation or non-operation, and 24-h hematoma increment, the fourth quartile systolic blood pressure (SBP) maximum and minimum difference within 1 h [OR: 5.069, CI (1.036–24.813) P = 0.045] and coefficient of continuous variation (SV) within 24 h [OR: 2.912 CI (1.818–71.728) P = 0.009] were still independent factors affecting the 90-day mRS in ICH patients. (2) There was a negative correlation between SBP SV and CBF in terms of the difference between the contralateral side and the perihematomal region at 24 h (Rs = −0.692, P = 0.013).

Conclusion: Blood pressure variability after antihypertensive therapy in acute ICH is one of the influencing factors for 90-day mRS in patients. A 1-h dramatic drop in SBP and 24-h SBP SV may affect the long-term prognosis of patients by reducing whole cerebral perfusion.

KEYWORDS

cerebral hemorrhage, antihypertensive treatment, blood pressure variability, prognosis, brain CT perfusion

Preface

Elevated blood pressure in the acute phase of cerebral hemorrhage (ICH) patients is not only the cause of bleeding but also an important clinical manifestation (Fischer et al., 2014). High blood pressure in the hyperacute phase is the main factor causing rebleeding (Murthy et al., 2016; Qureshi and Qureshi, 2018). A large number of clinical studies have confirmed that controlling the increase in blood pressure in patients with ICH in the acute phase can effectively reduce hematoma expansion and prevent the deterioration of neurological deficit symptoms and the occurrence of adverse outcomes (Yamaguchi et al., 2018; Qureshi et al., 2020). Clinical guidelines (Chinese Society of Neurology et al., 2019) domestically and overseas recommend rapid intensive antihypertensive therapy in the acute phase as level A evidence. However, antihypertensive treatment does not provide the additional benefit of preventing hematoma expansion (Qureshi et al., 2020; Moullaali et al., 2022). Several studies have shown that blood pressure variability (BPV) after antihypertensive treatment is one of the risk factors for poor prognosis of patients (Manning et al., 2014; Chung et al., 2018; Qureshi et al., 2020), but the targets and outcomes of the studies are inconsistent, and the mechanism is still unclear.

Thus, we investigated the clinical data of hospitalized patients experiencing ICH within the past 2 years to observe whether the BPV caused by acute antihypertensive treatment affects the 90 mRS of patients and to explore the possible mechanism.

Objects and methods

Research objects

This was a prospective study. Written approval was obtained from the Medical Ethics Committee of our hospital. In addition to the diagnostic criteria set by the 2019 Chinese Guidelines for the Diagnosis and Treatment of Intracerebral Hemorrhage as the inclusion criteria, patients also met the following conditions: age $>$ 18 years old, onset $<$ 24 h, SBP $>$ 140 mmHg, neurological deficit symptoms, and imaging examination suggesting intracerebral hemorrhage. Exclusion criteria were intracerebral hemorrhage patients with onset $>$ 24 h or admission SBP $<$ 140 mmHg, subarachnoid hemorrhage, arteriovenous malformation, cerebrovascular amyloidosis, anticoagulant drugs, and secondary intracerebral hemorrhage due to vasculitis. Patients with severe illness and short-term death were also excluded.

Research method

Clinical intervention methods

Patients with cerebral hemorrhage were given intravenous antihypertensive therapy with urapidil and maintained for 24 h after admission. The goal was to reduce the 1-h systolic blood pressure as much as possible to 120–140 mmHg or 20% lower than that at admission. Blood pressure measurements were recorded during the first 24 h and every 5 min from admission until 30 min after admission, every 10 min from 30 min to 1 h after admission, and every hour from 1 to 24 h after admission, for a total of 34 times. The blood pressure variability index (BPV) was calculated. Basic clinical data were collected, and mRS scores were followed up for 3 months. It was defined good prognosis group (mRS $\leq$ 2 points) and a poor prognosis group (mRS $\geq$ 3 points).

Imaging examination

A GE Light VCT 64-slice spiral CT scanner and an AW4.5 independent workstation were used as imaging equipment. Head CT at admission and 24 h after admission was completed, and simultaneous CT perfusion (CTP) examination was performed in some patients. Hematoma volume was measured using the formula of Taguda and calculated in ml. The final result was calculated as the mean of the measured values of two attending physicians. The increase in hematoma at 24 h ($\triangle$ICH, ml) was calculated as the volume of hematoma at the 24-h reexamination (ml) $-$ the volume of hematoma at admission (ml).

TABLE 1 Univariate analysis of the baseline characteristics of subjects with intracerebral hemorrhage in the good and poor prognosis groups.

	Good prognosis ($n = 71$)	Poor prognosis ($n = 49$)	*P*-value
Sex	Male 45 (63.3%) Female 26 (36.7%)	Male 28 (57.1%) Female 21 (42.9%)	0.491
Age, years	58.45 ± 12.51	63.90 ± 11.59	0.017*
Onset to treat time, hours	4.85 ± 3.956	4.27 ± 2.812	0.379
Hematoma location			0.482
Supratentorial	61 (85.9%)	45 (91.8%)	
Subtentorial	10 (14.1%)	4 (0.02%)	
Broken into ventricle			0.004*
Yes	12 (16.9%)	20 (40.8%)	
No	59 (83.1%)	29 (59.2%)	
Mixed sign			0.017*
Yes	25 (35.2%)	28 (57.1%)	
No	46 (64.8%)	21 (42.9%)	
Hypertension			0.831
No	17 (23.9%)	13 (26.5%)	
Yes, Unmedicated	19 (26.8%)	10 (20.4%)	
Yes, Intermittent medication	21 (29.6%)	14 (28.6%)	
Yes, Regular medication	14 (19.7%)	12 (24.5%)	
Diabetes			0.546
No	67 (94.4%)	44 (89.8%)	
Yes, Unmedicated	3 (4.2%)	3 (6.1%)	
Yes, Intermittent medication	0 (0%)	1 (2.0%)	
Yes, Regular medication	1 (1.4%)	1 (2.0%)	
Treatment			0.022*
Conservative treatment	69 (97.2%)	41 (83.7%)	
Evacuation of the hematoma	2 (2.8%)	8 (16.3%)	
Antihypertensive treatment			0.96
Intensive antihypertensive	33 (46.5%)	23 (46.9%)	
Non-intensive antihypertensive treatment	38 (53.5%)	26 (53.1%)	
SBP on admission, mmHg	176.2 ± 19.94	177.88 ± 21.32	0.66
DBP on admission, mmHg	105.45 ± 16.31	101.94 ± 13.70	0.22
Hematoma on admission, ml	9.5 (3.8–15.75)	25 (10.3–42.75)	0.000*
Peripheral edema on admission, ml	3.2 (1.0–7.12)	8.5 (3.53–14.77)	0.000*
NIHSS on admission	8 (4–11)	18 (13–23)	0.000*
GCS on admission	14 (13–15)	11 (8–14)	0.000*
△ICH, ml	0.97 (0.11–2.75)	2.68 (0.55–3.81)	0.047*
△PHE, ml	0.77 (0.0–3.36)	1.45 (0.0–8.99)	0.160

Mean ± SD; Median (IQR), Median (interquartile spacing); PHE, Peripheral edema; △ICH, Hematoma enlargement at 24 h; △PHE, the enlargement of peripheral edema at 24 h. *The difference was statistically significant at $P < 0.05$.

The selection of regions of interest for head CTP included 3–4 regions of interest (ROIs) selected 1 cm along the edge of the hematoma and the contralateral mirror region. The perfusion parameters cerebral blood flow (CBF) and cerebral blood volume (CBV) were obtained.

TABLE 2 The effects of BPV on the prognosis of ICH patients.

	Good prognosis ($n = 71$)	Poor prognosis ($n = 49$)	*P*-value
1 h SBP			
Mean	160.06 ± 13.90	160.98 ± 47.34	0.723
Max-Min	36.25 ± 16.27	43.31 ± 21.88	0.023*
SD	12.02 ± 5.98	14.72 ± 7.39	0.029*
CV	0.75 ± 0.037	0.09 ± 0.046	0.034*
SV	28.56 (16.44–55.33)	41.27 (21.03–90.72)	0.051
24 h SBP			
Mean	147.23 ± 11.72	149.00 ± 9.88	0.388
Max-Min	62.99 ± 17.85	70.73 ± 21.66	0.034*
SD	15.78 ± 4.75	18.16 ± 5.65	0.014*
CV	0.11 ± 0.034	0.12 ± 0.039	0.031*
SV	67.89 (49.11–96.34)	89.61 (64.38–134.46)	0.009*

$\bar{x} \pm s$, Mean ± SD; Median (IQR), Median (interquartile spacing). *The difference was statistically significant at $P < 0.05$.

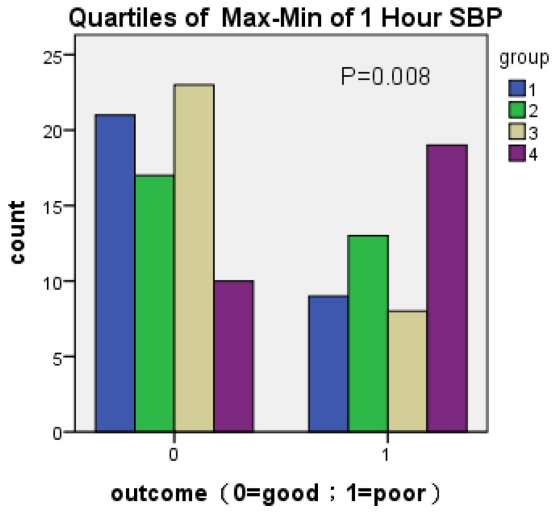

FIGURE 1
Quartiles of Max-Min of 1-h SBP (outcome: 0 = good; 1 = poor).

Statistical analysis

Microsoft Office Professional Plus 2013 was used to access all the data of the input after completion for BPV parameters, including the average (Mean), difference (Max − Min), standard deviation (SD), coefficient of variation (CV), and continuous variation (SV).

Statistical Product and Service Solutions (SPSS) 24.0 statistical packages were used for data analysis. In univariate analysis, an independent sample *t*-test was used to compare

the continuous variables with normal distribution between groups. The non-parametric Mann–Whitney *U* test was used for comparisons between groups if the distribution was not normal. Categorical variables were compared between groups using the chi-square test. Variables that were significantly different in univariate analysis were further included in multivariate binary logistic regression analysis to assess the association between the 90-day mRS score and BPV. In the comparison of continuous variables between the cerebral perfusion value and BPV, Pearson correlation analysis was used for those with a normal distribution. If the data did not conform to a normal distribution, Spearman correlation analysis was used. Statistical differences were observed at $P < 0.05$.

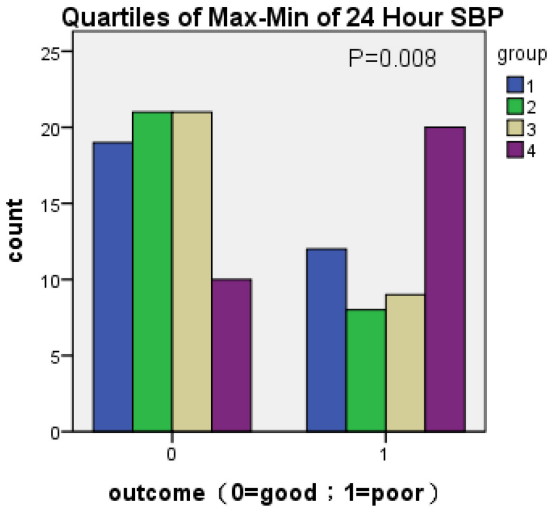

FIGURE 2
Quartiles of Max-Min of 24-h SBP (outcome: 0 = good; 1 = poor).

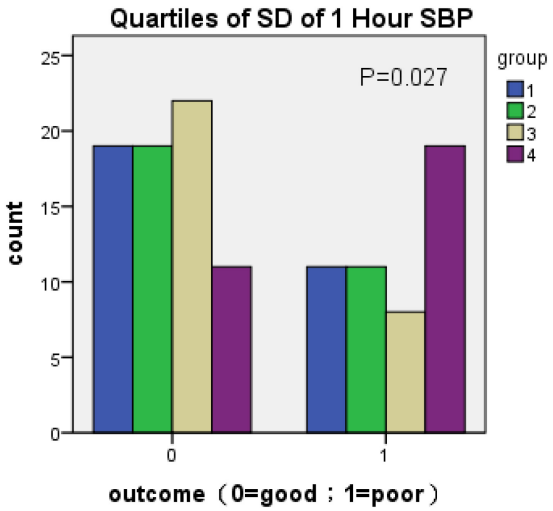

FIGURE 3
Quartiles of SD of 1-h SBP (outcome: 0 = good; 1 = poor).

Results

Demographic and clinical characteristics

A total of 120 patients were enrolled in this study, including 71 patients in the good prognosis group and 49 patients in the poor prognosis group. The results showed (Table 1) that age, rupture into the ventricle, confounding sign, treatment method, admission NIHSS score, admission GCS score, hematoma volume, and edema range at admission, and 24-h △ICH were all different between the two groups and were related factors affecting the prognosis.

Effects of blood pressure variation at different periods after antihypertensive treatment on the 90-day neurological outcome in patients with acute intracerebral hemorrhage

The effect of BPV at different time periods (within 1 and 24 h) on clinical outcomes was evaluated. The results showed (Table 2) that the SBP max-min, SD and CV of the two time periods and 24-h SBP SV were different between the good

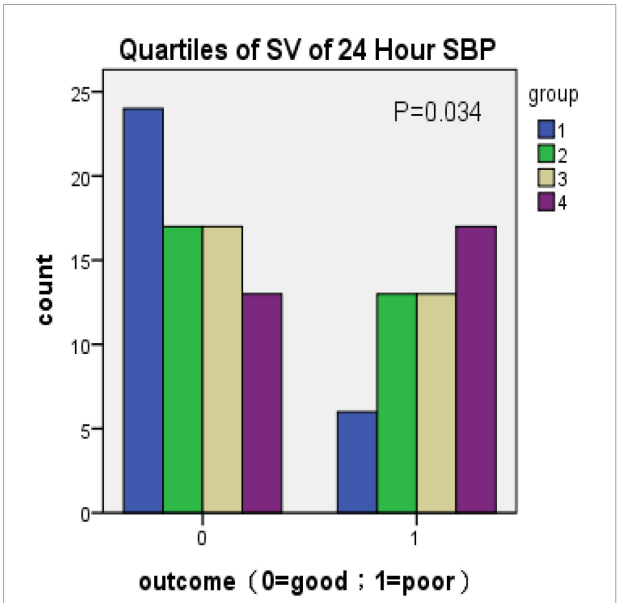

FIGURE 4
Quartiles of SV of 24-h SBP (outcome: 0 = good; 1 = poor).

TABLE 3 Multivariate logistic regression analysis of the prediction of different interval BPV parameters for poor prognosis.

	1-h SBP (MAX-MIN)		1-h SBPSD		24-h SBP (MAX-MIN)		24-h SBPSV	
	OR (CI)	*P*	OR (CI)	*P*	OR (CI)	*P*	OR (CI)	*P*
q1	–	0.232	–	0.301	–	0.157	–	0.08*
q2	2.41 (0.557–10.429)	0.239	0.92 (0.213–3.97)	0.911	0.392 (0.075–2.041)	0.266	4.674 (0.797–27.424)	0.088
q3	1.77 (0.333–9.417)	0.503	0.8 (0.167–3.85)	0.784	1.07 (0.262–4.368)	0.925	3.457 (0.768–29.189)	0.094
q4	5.069 (1.036–24.813)	0.045*	3.087 (0.684–13.93)	0.143	3.008 (0.67–13.498)	0.151	2.912 (1.818–71.728)	0.009*

Multiple independent variables including age, rupture into ventricle, confounding sign, first blood loss, NIHSS score, GCS score, and ΔICH were adjusted. q1–q4 interquartile range. *The difference was statistically significant at $P < 0.05$.

prognosis group and the poor prognosis group ($P < 0.05$). The 1-h SBP SV ($P < 0.1$) was included in the multivariate analysis.

There was no significant difference in diastolic blood pressure variation parameters between the two groups ($P > 0.05$, data not listed).

The interquartile blood pressure variation parameters on the adverse prognosis of intracerebral hemorrhage patients

Because there was no statistical difference in the above parameters obtained according to Table 2 in the multivariate analysis, the parameters of BPV with statistically significant differences were divided into four groups (q1–q4) according to the quartile as the boundary value. The R × C chi-square test was used to compare the incidence of poor prognosis in each group. The correlation between BPV and poor prognosis was analyzed by quartile group comparison. The results showed that 1 h SBP Max-Min ($\chi 2 = 11.746$, $P = 0.008$) 24 h SBP Max-Min ($\chi 2 = 11.908$, $P = 0.008$), 1 h SBP SD ($\chi 2 = 9.21$, $P = 0.027$), 24 h SBP SV ($\chi 2 = 8.658$, $P = 0.034$), suggesting that the above variables were correlated with prognosis (Figures 1–4 below for details).

Multivariate analysis of prognostic value of parameters in patients with intracerebral hemorrhage

Multivariate binary logistic regression analysis was used to evaluate the effect of BPV parameters in different time periods

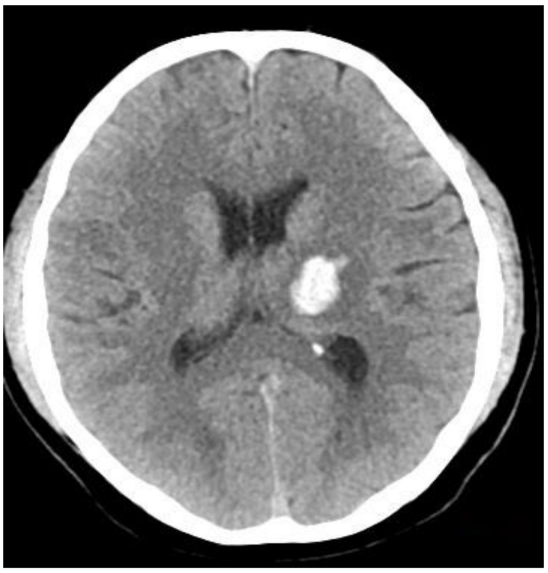

FIGURE 5
The hematoma area.

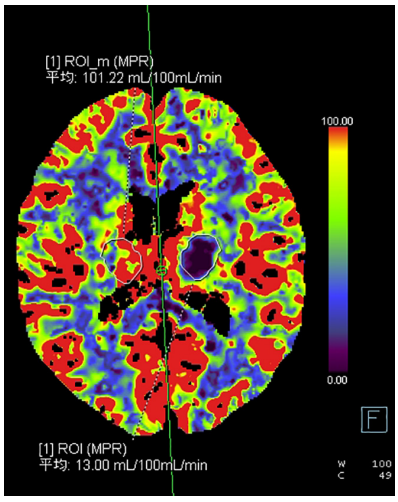

FIGURE 6
The hematoma marginal area on the CBF map.

and different intervals on the poor prognosis of neurological function in patients with acute intracerebral hemorrhage. The results showed that the 1-h Max-Min and 24-h SBP SV q4 regions were significantly associated with 90-day neurological outcomes (Table 3).

Effect of blood pressure variability on cerebral perfusion after antihypertensive treatment

Twenty-two patients were randomly selected to undergo a 24-h CT (Figure 5) scan and simultaneous perfusion (CTP) examination. CTP (Figures 6–8) showed a significant reduction in perfusion in the core area and periphery of the hematoma, as well as a significant reduction in CBF and CBV.

The Spearman correlation analysis of blood pressure variation parameters and cerebral perfusion parameters at each time period showed that the difference in CBF between the perihematoma and contralateral mirror area (contralateral to affected-side blood flow) was negatively correlated with 24 h SBP SV, while there was no statistically significant difference in the correlation analysis of CBF and CBV around the hematoma or CBF and CBV in the mirror area (Table 4).

A 43-year-old male presented with 3 h of numbness and immobility in the right limb. Head CT (Figure 5) showed cerebral hemorrhage in the left basal ganglia area. CTP (Figure 6) showed the hematoma area; CTP (Figure 7) showed the ROI and CBF values of the hematoma marginal area, cortical area, and corresponding mirror area; CTP (Figure 8) showed the CBV values in each ROI area.

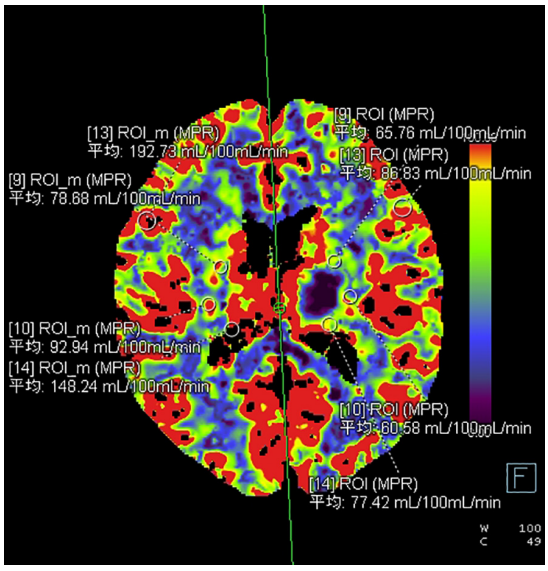

FIGURE 7
The ROI and CBF values of the hematoma marginal area, cortical area, and corresponding mirror area.

Discussion

In the past 10 years, a number of large-scale international clinical studies have confirmed that early intensive antihypertensive therapy can effectively control hematoma expansion and bring more obvious blood pressure fluctuations (blood pressure variability, BPV), which may have adverse effects on patients with ICH.

Chung et al. (2018) analyzed the Fast-Mag Trial (Field Administration of Stroke Therapy-Magnesium), a study of prehospital care. The patients with obvious blood pressure variability in the hyperacute phase (0–6 h) and acute phase (0–24 h) had a poor prognosis rate (mRS 3–6 scores) of 69.9%. Among them, SD, CV, and SV were all related to poor prognosis in the acute phase and hyperacute phase. The OR

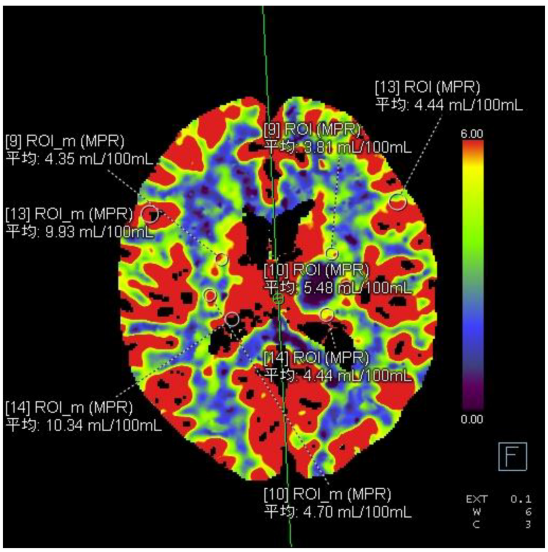

FIGURE 8
The CBV values in each ROI area.

TABLE 4 Spearman correlation analysis of the relationship between the 24-h SBP SV and the CBF difference and CBV difference.

Variables	Coefficient r	*P*-value
Healthy side CBF	−0.19	0.713
Healthy side CBV	−0.063	0.846
Affected side CBF	−0.049	0.880
Affected side CBV	0.021	0.948
CBF difference	−0.692	00.013*
CBV difference	−0.035	0.914

Cerebral blood flow (CBF) difference = healthy side CBF − affected side CBF; cerebral blood volume (CBV) difference = healthy side CBV − affected side CBV.

of the highest quintile was 3.73, the OR of the coefficient of variation was 4.78, and the OR of the SV was 3.39. Conclusion: blood pressure variability in the acute phase of ICH in the prehospital emergency room is an independent risk factor for poor prognosis, and it is also one of the targets of clinical treatment. Qureshi et al. (2020) retrospectively analyzed a clinical multicenter blood pressure control study from 2011 to 2015. The results showed that 228 patients with ICH whose initial blood pressure was equal to or greater than 220 mmHg were treated with intensive blood pressure control or standard blood pressure control. The proportion of neurological deterioration within 24 h in the intensive treatment group was higher than that in the non-intensive treatment group (15.5 vs. 6.8%; RR 2.28 [95% CI, 1.03–5.07]; $P = 0.04$). There was no significant difference in mortality or severe disability rate between the two groups (39.0 vs. 38.4%; RR 1.02 [95% CI, 0.73–1.78]; $P = 0.92$). This suggests that early and rapid lowering of blood pressure may be harmful. Manning et al. (2014) conducted a retrospective analysis of the INTERACT2 study, which showed that the maximum systolic blood pressure was in the hyperacute phase (24 h), and SD was a marker of death in the acute phase (2–7 days) and poor prognosis at 90 days (OR = 1.41, $P = 0.016$; OR = 1.57, $P = 0.012$). It is suggested that smooth and sustained control of blood pressure is needed in the ultra early stage. Liu W. et al. (2021) included 7 randomized controlled prospective studies with 5,201 participants in their meta-analysis. Increased SBP variability was associated with an increased risk of poor functional outcomes: The results are SD (OR: 1.38, $P = 0.001$), CV (OR: 1.98, $P = 0.017$), SV (OR: 1.30, $P = 0.006$), and the effect of SBP variability on the risk of poor functional outcomes in ICH patients was affected by country, study design, mean age, stroke type, outcome definition, and study quality.

The aim of our study was to observe the 90-day prognosis of patients with ICH after antihypertensive treatment. The results showed that after excluding other factors that clearly affect the prognosis of ICH, the top quartile of SBP 1-h max-min and 24-h SBP SV was still an independent risk factor for ICH patients with a poor prognosis at 90 days. We hypothesized that BPV affects clinical outcomes through the following mechanisms: 1. Destroy perihematomal perfusion. 2. Change the microcirculation of the whole brain.

Whether early lowering of blood pressure results in lower early cerebral perfusion remains controversial. On the basis of INTERACT1 and ATACH experiments, studies such as ICH ADAPT suggest that there is no significant correlation between the magnitude of blood pressure reduction and the relative cerebral blood flow around the hematoma (Powers et al., 2001). Moreover, the SBP in a small number of ICH patients is controlled at the target value within 24 h. The blood flow of the brain tissue around the hematoma can be maintained by autoregulation (Gould et al., 2014; Tanaka et al., 2014; Tamm et al., 2016). With the progress of INTERACT2 and ATACH2 experiments, Gould et al. (2014) demonstrated that the blood perfusion around the hematoma, perihematoma tissue area and watershed tissue area of early ICH (<2 h) was below the ischemic threshold by CTP, but there was no significant correlation between intensive hypotension and hypoperfusion area. In Our study, CTP of some patients was performed at the same time as reexamination of head CT 24 h after admission, and decreased CBF and CBV around the hematoma was found. **Table 3** showed that only the 1-h SBP Max-Min in the fourth quartile was associated with poor outcome, suggesting that the amplitude of blood pressure reduction is a factor of functional recovery. Kuang et al. (2015) showed the perihematomal ischemic injury in acute supratentorial large hematoma. Also found a synchronous decreased CBF and CBV around hematoma suggesting microcirculation compression. As a result, the autoregulation ability of cerebral perfusion in this region was weakened or disappeared. The sharp short-term drop in blood pressure again causes perihematoma hypoperfusion to aggravate neurological injury.

In addition, the above studies were limited to the hyperacute phase. Regarding sustained blood pressure reduction, a recent study by Morotti et al. (2022) showed that cerebral perfusion around the hematoma gradually decreased with the development of the disease, and 7-day CBF < 20 ml/100 g/min was shown to be an independent predictor of poor functional outcome (OR: 2.45, 95% CI 1.08-5-54, $p = 0.032$).

To further explore the relationship between BPV and cerebral perfusion, we performed correlation analysis on the related variation parameters affecting the poor prognosis of patients and ultimately showed that there was a negative correlation between 24-h SBP SV and the CBF difference between the healthy side and the affected side in patients with ICH; that is, the larger the 24-h SBP SV was, the smaller the CBF difference value. It is speculated that the reason for this phenomenon is that the cerebral perfusion around the hematoma loses its autoregulation ability early due to compression by the hematoma and edema and is less affected by blood pressure fluctuations.

Previous studies (Rickards and Tzeng, 2014; Kario, 2016) have demonstrated that cerebral hemodynamic variables (blood pressure and cerebral blood flow) have physiologically protective characteristics and can cause extensive damage to organ function. These apparently different outcomes may lie in the time scale of hemodynamic variability; short time-scale variability appears to be brain protective, whereas medium- and long-term fluctuations are associated with primary and secondary end-organ dysfunction. Blood pressure fluctuations can damage vascular endothelium and blood-brain barrier, increase small vessel resistance, and reduce brain cell

metabolism (Liu N. et al., 2021) resulting in decreased CBF. The change is systemic and as to healthy tissue is particularly significant compared to impaired blood circulation around the hematoma.

There was no significant difference in cerebral perfusion parameters between healthy brain areas and surrounding hematoma, which may be related to the small sample size or the fact that the difference did not reach statistical significance. Unfortunately, although 1-h SBP max-min is a poor prognostic factor in ICH patients, its role in cerebral perfusion is not clear due to the short time from admission to hospitalization.

Conclusion

The 1-h quartile difference in SBP and 24-h SBP SV are independent risk factors for poor prognosis in patients with intracerebral hemorrhage. Excessive hypotension and secondary continuous blood pressure fluctuations cause secondary brain injury through whole-brain perfusion and then aggravate the neurological impairment of patients with cerebral hemorrhage.

Data availability statement

The original contributions presented in this study are included in the article/supplementary material, further inquiries can be directed to the corresponding author.

Ethics statement

The studies involving human participants were reviewed and approved by the Ethics Committee of Affiliated Hospital of North Sichuan Medical College 2020ER194-1. The patients/participants provided their written informed consent to participate in this study. Written informed consent was obtained from the individual(s) for the publication of any potentially identifiable images or data included in this article.

Author contributions

XS: project design, declaration, experiment coordinating and organization, translation, and revision. XJ: data collection, analysis, and draft. QM, QY, and TC: clinical cases. GJ: project administration. All authors contributed to the article and approved the submitted version.

Funding

The work was supported by the Education Department of Sichuan Province (No. 16ZA0243).

Conflict of interest

The authors declare that the research was conducted in the absence of any commercial or financial relationships that could be construed as a potential conflict of interest.

Publisher's note

All claims expressed in this article are solely those of the authors and do not necessarily represent those of their affiliated organizations, or those of the publisher, the editors and the reviewers. Any product that may be evaluated in this article, or claim that may be made by its manufacturer, is not guaranteed or endorsed by the publisher.

References

Chinese Society of Neurology., Chinese Stroke Society, and Neurovascular Intervention Group of Chinese Society of Neurology (2019). Chinese guidelines for the diagnosis and treatment of cerebral hemorrhage. *Chin J. Neurol.* 52, 994–1005.

Chung, P. W., Kim, J. T., Sanossian, N., Starkmann, S., Hamilton, S., Gornbein, J., et al. (2018). Association Between Hyperacute Stage Blood Pressure Variability and Outcome in Patients With Spontaneous Intracerebral Hemorrhage. *Stroke* 49, 348–354. doi: 10.1161/STROKEAHA.117.017701

Fischer, U., Cooney, M. T., Bull, L. M., Silver, L. E., Chalmers, J., Anderson, C. S., et al. (2014). Acute post-stroke blood pressure relative to premorbid levels in intracerebral haemorrhage versus major ischaemic stroke: A population-based study. *Lancet Neurol.* 13, 374–384. doi: 10.1016/S1474-4422(14)70031-6

Gould, B., McCourt, R., Gioia, L. C., Kate, M., Hill, M. D., Asdaghi, N., et al. (2014). Acute Blood Pressure Reduction in Patients With Intracerebral Hemorrhage Does Not Result in Borderzone Region Hypoperfusion. *Stroke* 45, 2894–2899. doi: 10.1161/STROKEAHA.114.005614

Kario, K. (2016). Systemic Hemodynamic Atherothrombotic Syndrome and Resonance Hypothesis of Blood Pressure Variability: Triggering Cardiovascular Events. *Korean Circ.* 46, 456–467.

Kuang, Y., Chen, W., Zheng, K., Fu, J., Hu, Z., Yang, Y., et al. (2015). CT perfusion imaging evaluation on hemodynamic changes of acute spontaneous intracerebral hemorrhage surrounding tissues. *Zhonghua Yi Xue Za Zhi* 95, 3514–3518.

Liu, N., Xue, Y., Tang, J., Zhang, M., Ren, X., Fu, J. H., et al. (2021). Research progress of impaired cerebral hemodynamics in cerebral small vessel disease. *Chin. J. Contemp. Neurol. Neurosurg.* 21, 25–29.

Liu, W., Zhuang, X., and Zhang, L. (2021). Prognostic Value of Blood Pressure Variability for Patients With Acute or Subacute Intracerebral Hemorrhage: A Meta-Analysis of Prospective Studies. *Front. Neurol.* 11:6065–6094. doi: 10.3389/fneur.2021.606594

Manning, L., Hirakawa, Y., Arima, H., Wang, X., Chalmers, J., Wang, J., et al. (2014). Blood pressure variability and outcome after acute intracerebral haemorrhage: A post-hoc analysis of INTERACT2, a randomised controlled trial. *Lancet Neurol.* 13, 364–373. doi: 10.1016/S1474-4422(14)70018-3

Morotti, A., Busto, G., Boulouis, G., Scola, E., Bernardoni, A., Fiorenza, A., et al. (2022). Delayed perihematomal hypoperfusion is associated with poor outcome in intracerebral haemorrhage. *Eur. J. Clin. Invest.* 52:e13696. doi: 10.1111/eci.13696

Moullaali, T. J., Wang, X., Sandset, E. C., Woodhouse, L. J., Law, Z. K., Arima, H., et al. (2022). Early lowering of blood pressure after acute intracerebral haemorrhage: A systematic review and meta-analysis of individual patient data. *J. Neurol. Neurosurg. Psychiatry* 93, 6–13.

Murthy, S. B., Urday, S., Beslow, L. A., Dawson, J., Lees, K., Kimberly, W. T., et al. (2016). Rate of perihaematomal oedema expansion is associated with poor clinical outcomes in intracerebral haemorrhage. *J. Neurol. Neurosurg. Psychiatry* 87, 1169–1173. doi: 10.1136/jnnp-2016-313653

Powers, W. J., Zazulia, A. R., Videen, T. O., Adams, R. E., Yundt, K. D., Aiyagari, V., et al. (2001). Autoregulation of cerebral blood flow surrounding acute (6 to 22 hours) intracerebral hemorrhage. *Neurology* 57, 18–24. doi: 10.1212/wnl.57.1.18

Qureshi, A. I., Huang, W., Lobanova, I., Barsan, W. G., Hanley, D. F., Hsu, C. Y., et al. (2020). Outcomes of Intensive Systolic Blood Pressure Reduction in Patients With Intracerebral Hemorrhage and Excessively High Initial Systolic Blood Pressure: Post Hoc Analysis of a Randomized Clinical Trial. *JAMA Neurol.* 77, 1355–1365. doi: 10.1001/jamaneurol.2020.3075

Qureshi, A. I., and Qureshi, M. H. (2018). Acute hypertensive response in patients with intracerebral hemorrhage pathophysiology and treatment(Review). *J. Cereb. Blood Flow Metab.* 38, 1551–1563.

Rickards, C. A., and Tzeng, Y. C. (2014). Arterial pressure and cerebral blood flow variability: Friend or foe? A review. *Front. Physiol.* 5:120. doi: 10.3389/fphys.2014.00120

Tamm, A. S., McCourt, R., Gould, B., Kate, M., Kosior, J. C., Jeerakathil, T., et al. (2016). Cerebral Perfusion Pressure is Maintained in Acute Intracerebral Hemorrhage: A CT Perfusion Study. *AJNR Am. J. Neuroradiol.* 37, 244–251. doi: 10.3174/ajnr.A4532

Tanaka, E., Koga, M., Kobayashi, J., Kario, K., Kamiyama, K., Furui, E., et al. (2014). Blood pressure variability on antihypertensive therapy in acute intracerebral hemorrhage: The Stroke Acute Management with Urgent Risk-factor Assessment and Improvement-intracerebral hemorrhage study. *Stroke* 45, 2275–2279. doi: 10.1161/STROKEAHA.114.005420

Yamaguchi, Y., Koga, M., Sato, S., Yamagami, H., Todo, K., Okuda, S., et al. (2018). Early Achievement of Blood Pressure Lowering and Hematoma Growth in Acute Intracerebral Hemorrhage: Stroke Acute Management with Urgent Risk-Factor Assessment and Improvement-Intracerebral Hemorrhage Study. *Cerebrovasc. Dis.* 46, 116–122. doi: 10.1159/000492728

frontiers | Frontiers in Neuroscience

TYPE Original Research
PUBLISHED 20 December 2022
DOI 10.3389/fnins.2022.1034472

OPEN ACCESS

EDITED BY
Bo Li,
Department of Orthopedics, Sun Yat-sen Memorial Hospital, Sun Yat-sen University, China

REVIEWED BY
Angel Lee,
Hospital Angeles Pedregal, Mexico
Antonino Tuttolomondo,
University of Palermo, Italy

*CORRESPONDENCE
Xuxing Liao
✉ drliao210409@163.com
José Fidel Baizabal-Carvallo
✉ baizabaljf@hotmail.com

SPECIALTY SECTION
This article was submitted to Translational Neuroscience, a section of the journal Frontiers in Neuroscience

RECEIVED 01 September 2022
ACCEPTED 02 December 2022
PUBLISHED 20 December 2022

CITATION
Chen Y, Zhou S, Yang S, Mofatteh M, Hu Y, Wei H, Lai Y, Zeng Z, Yang Y, Yu J, Chen J, Sun X, Wei W, Nguyen TN, Baizabal-Carvallo JF and Liao X (2022) Developing and predicting of early mortality after endovascular thrombectomy in patients with acute ischemic stroke. *Front. Neurosci.* 16:1034472. doi: 10.3389/fnins.2022.1034472

Developing and predicting of early mortality after endovascular thrombectomy in patients with acute ischemic stroke

Yimin Chen[1], Sijie Zhou[2], Shuiquan Yang[1], Mohammad Mofatteh[3], Yuqian Hu[4], Hongquan Wei[5], Yuzheng Lai[6], Zhiyi Zeng[7], Yajie Yang[8], Junlin Yu[9], Juanmei Chen[10], Xi Sun[11,12], Wenlong Wei[1], Thanh N. Nguyen[13], José Fidel Baizabal-Carvallo[14,15]* and Xuxing Liao[2,16]*

[1]Department of Neurology and Advanced National Stroke Center, Foshan Sanshui District People's Hospital, Foshan, Guangdong, China, [2]Department of Surgery of Cerebrovascular Diseases, The First People's Hospital of Foshan, Foshan, Guangdong, China, [3]School of Medicine, Dentistry and Biomedical Sciences, Queen's University Belfast, Belfast, United Kingdom, [4]The First School of Clinical Medicine, Southern Medical University, Guangzhou, Guangdong, China, [5]Department of 120 Emergency Command Center, Foshan Sanshui District People's Hospital, Foshan, Guangdong, China, [6]Department of Neurology, Guangdong Provincial Hospital of Integrated Traditional Chinese and Western Medicine, Nanhai District Hospital of Traditional Chinese Medicine of Foshan City, Foshan, Guangdong, China, [7]Department of Scientific Research and Education, Foshan Sanshui District People's Hospital, Foshan, Guangdong, China, [8]The First School of Clinical Medicine, Southern Medical University, Foshan, China, [9]School of Laboratory Medicine and Biotechnology, Southern Medical University, Foshan, China, [10]Second Clinical College, Guangzhou Medical University, Guangzhou, China, [11]School of Medicine, Shaoguan University, Shaoguan, Guangdong, China, [12]Medical Intern, Foshan Sanshui District People's Hospital, Foshan, Guangdong, China, [13]Department of Neurology, Radiology, Boston University Chobanian & Avedisian School of Medicine, Boston, MA, United States, [14]Department of Neurology, Baylor College of Medicine, Parkinson's Disease Center and Movement Disorders Clinic, Houston, TX, United States, [15]Department of Sciences and Engineering, University of Guanajuato, León, Mexico, [16]Department of Neurosurgery and Advanced National Stroke Center, Foshan Sanshui District People's Hospital, Foshan, Guangdong, China

Background: Stroke is one of the leading causes of mortality across the world. However, there is a paucity of information regarding mortality rates and associated risk factors in patients with acute ischemic stroke (AIS) undergoing endovascular thrombectomy (EVT). In this study, we aimed to clarify these issues and analyzed previous publications related to mortality in patients treated with EVT.

Methods: We analyzed the survival of 245 consecutive patients treated with mechanical thrombectomy for AIS for which mortality information was obtained. Early mortality was defined as death occurring during hospitalization after EVT or within 7 days following hospital discharge from the stroke event.

Results: Early mortality occurred in 22.8% of cases in this cohort. Recanalization status (modified thrombolysis in cerebral infarction, mTICI)

(p = 0.002), National Institute of Health Stroke Scale Score (NIHSS) score 24-h after EVT ($p < 0.001$) and symptomatic intracerebral hemorrhage (sICH) ($p < 0.001$) were independently associated with early mortality. Age, sex, cardiovascular risk factors, NIHSS score pre-treatment, Alberta Stroke Program Early CT Score (ASPECTS), stroke subtype, site of arterial occlusion and timing form onset to recanalization did not have an independent influence on survival. Non-survivors had a shorter hospitalization ($p < 0.001$) but higher costs related to their hospitalization and outpatient care.

Conclusion: The recanalization status, NIHSS score 24-h after EVT and sICH were predictors of early mortality in AIS patients treated with EVT.

KEYWORDS

ischemic stroke, endovascular therapy, thrombectomy, intracranial hemorrhage, mortality

Introduction

Stroke is one of the leading causes of death and disability worldwide. For this reason, low mortality and good functional status are important goals in clinical trials assessing the outcome of patients with acute ischemic stroke (AIS). Mortality in patients with stroke may have diverse causes, but evidence shows that it may be linked to early neurological complications such as recurrent stroke, hemorrhagic transformation or malignant edema, as well as systemic complications in the days following the acute event (Langhorne et al., 2000; Indredavik et al., 2008; Linfante et al., 2015; Rohweder et al., 2015; Viderman et al., 2020). A large study enrolling 13,721 European patients showed that 25.2% of cases experienced one or more medical complications during the hospitalization in the days following AIS (Ingeman et al., 2011; Rocco et al., 2012).

Stroke severity at onset and patient age have been estimated as some of the most important predictive variables for prognosis and post-stroke complications (Ingall, 2004; Indredavik et al., 2008). Moreover, occlusion site plays also a major role, as large vessel occlusion (LVO), i.e., internal carotid artery and/or proximal middle cerebral artery have a worse prognosis compared with more distal or medium vessel occlusions (Karamchandani et al., 2021). For example, a study including 764 patients with LVO showed a 90-day mortality rate of 26% (Karamchandani et al., 2021). Older age, higher National Institute of Health Stroke Scale Score (NIHSS) at presentation and greater modified Rankin Score (mRS) at discharge were predictors of mortality; however, patients undergoing revascularization therapy showed a survival benefit (Karamchandani et al., 2021). As large vessel recanalization is a modified variable, efforts have been done to achieve expedited and effective recanalization in patients with AIS and LVO (Broderick et al., 2013; Ciccone et al., 2013; Kidwell et al., 2013). Since 2014, randomized clinical trials demonstrated the benefit of endovascular thrombectomy (EVT) compared with standard therapy by using novel stent retrievers in functional outcome, assessed by the modified Ranking Scale (mRS) at 90 days (Goyal et al., 2016). Therefore, EVT is currently considered the standard of care for AIS with LVO by most health agencies in developed and developing countries. However, mortality rate at 90 days did not differ in a meta-analysis of 1,287 patients (634 EVT; 653 controls) including five randomized clinical trials: MR CLEAN, ESCAPE, REVASCAT, SWIFT PRIME, and EXTEND IA (Goyal et al., 2016; Eskey et al., 2018).

We aimed to investigate early mortality following EVT. We defined early mortality as inpatient mortality after EVT or death within 7 days after hospice home discharge as some local customs preferred patients pass away at home.

Materials and methods

This retrospective study enrolled prospectively collected data of consecutive AIS patients with large vessel occlusion (LVO) who underwent EVT from October 2019 to February 2022 at two comprehensive stroke centers in China. Data were obtained from the Big Data Observatory Platform for Stroke in China and from the individual hospital data platforms. Inclusion criteria for this study were as follows: (1) EVT for patients with LVO including internal carotid artery (ICA), tandem, proximal middle cerebral artery (M1 and M2 segments), basilar artery, and other big vessels treated within 24 h of symptom onset; (2) age $\geq$ 18 years old. Patients with missing follow-up data were excluded. From 80 to 90% of patients underwent EVT using the SOLITAIRE system, the rest were treated with previous generation of devices, such as MERCI and PENUMBRA.

The following data were collected: age, sex, vascular risk factors [including hypertension, diabetes mellitus, coronary artery disease (CAD), atrial fibrillation (AF), prior stroke, chronic kidney disease (CKD), and dyslipidemia and smoking]. The NIHSS pre-treatment was calculated by stroke neurologists at each center. The Alberta Stroke Program Early CT Score (ASPECTS) before treatment was assessed on CT scans as reported by the site.

Door-to-needle time (DNT) and onset-to-needle time (ONT) were recorded for those receiving IV thrombolysis. Door-to-puncture time (DPT), door-to-recanalization time (DRT), puncture-to-recanalization time (PRT), and last known normal-to-puncture-time (LKNPT) were assessed for patients receiving EVT. Reperfusion was estimated with the modified thrombolysis in cerebral infarction (mTICI), accordingly as absent or minimal reperfusion: 0/1; partial arterial filling <50%: 2a; partial arterial filling: 2b; near complete reperfusion: 2c; and complete reperfusion: 3. Successful reperfusion was defined as mTICI post-EVT, 2b or 3. The NIHSS score was assessed 24-h following EVT. Symptomatic intracranial hemorrhage (sICH) was defined as intracranial hemorrhage associated with neurological deterioration post EVT manifested by an increase of ≥4 points in the NIHSS score (Rao et al., 2014).

Outcome measures

The outcome variable was "early mortality" defined as death during hospitalization following EVT or death within 7 days following hospice home discharge. We consider this time important, as it provides an opportunity window to decrease death when patients are still under thorough medical care. Mortality corresponded to a mRS of six. Stroke neurologists and nurses followed patients by telephone calls or in-person consultations to assess the patient's outcome.

Ethics

The Institutional Review Board of both hospitals approved the study protocol. Written informed consent from the participants' legal guardian/next of kin was obtained to perform the EVT.

Statistical analysis

We summarized data in percentages, means and standard deviations for normally distributed and medians with interquartile range (IQR) for non-normally distributed variables. The chi-square ($\chi 2$) and Fisher's exact tests were used to compare proportions between groups. The student's *t*-test and Mann–Whitney *U*-test were used to compare normally and non-normally distributed continuous variables, respectively. Statistically significant variables ($p < 0.05$) in the bivariate analysis were included as independent variables in a multivariate logistic regression model using a Wald backward method to assess their effect on the dependent variable: Early mortality. Elimination threshold from the final model was a p-value ≥ 0.10. Unstandardized B coefficients and exponentiation of B (ExpB) coefficient with 95% confidence intervals (CI) were used to provide an estimated weight of the independent variable. Goodness of fit of the final regression model was evaluated with the Hosmer–Lemeshow test, p-value < 0.05 was considered poor fit. Determination coefficients (R2) were calculated for the final regression model. If the *P*-value was less than 0.05, results were considered statistically significant. IBM SPSS version 26 (IBM-Armonk, NY) was used for statistical analyses.

Results

We enrolled 249 consecutive patients with AIS who underwent EVT. Four patients were excluded from the final analysis owing to loss to follow-up. A total of 245 patients were analyzed, among them, 56 patients died during the study period (22.8%). Patients who died had a median length (IQR) of hospitalization of 4 (2, 6) days.

Patients who died were on average 4.3 years older than those who survived ($p = 0.029$) and had a median of 5 points higher NIHSS score pre-treatment on admission ($p < 0.001$). This difference in NIHSS widened to 14 points, 24-h following EVT ($p < 0.001$) (**Table 1**). Patients who survived, achieved a much higher percent of optimal recanalization (mTICI ≥ 2b) compared to those who died: 91.53 vs. 60.7% ($P < 0.001$). The timing between symptom onset and initiation of reperfusion did not differ either, except for a shorter PRT ($p = 0.013$) in survivors. A total of 24 patients from the cohort suffered symptomatic intracerebral hemorrhage (sICH) (9.79%). The frequency of sICH was markedly higher in patients who did not survive 33.9 vs. 2.65% ($p < 0.001$). Length of hospitalization was shorter in patients who died as expected; however, costs of hospitalizations were higher in patients who died during the study period (**Table 1**). Other variables such as sex, cardiovascular risk factors, site of arterial occlusion, stroke subtypes and complicated lung infection did not differ between survivors and non-survivors.

In the multivariate logistic regression NIHSS score 24-h after EVT ($p < 0.001$), mTICI post-EVT ≥ 2b ($p = 0.002$); and sICH ($p < 0.001$) were significantly associated with early mortality (**Table 2**). Age, pre-treatment NIHSS score and PRT were excluded from the final regression model. Length and costs of hospitalization were not considered in the regression model as these variables depend on patient survival.

TABLE 1 Summary of demographic, clinical hemodynamic, and therapeutic features between non-surviving and surviving patients.

	Early mortality	Survival	X^2/t/z	*P*-value
Number	56	189		
Age (years), mean ± SD	67.82 ± 11.94	63.52 ± 13.09	2.200	0.029
Female, *n*%	17 (30.36)	57 (30.16)	0.001	0.977
Hypertension, *n*%	34 (60.71)	108 (57.14)	0.226	0.634
DM, *n*%	15 (26.79)	41 (21.69)	0.635	0.425
CAD, *n*%	12 (21.43)	29 (15.34)	1.148	0.284
AF, *n*%	21 (37.5)	64 (33.86)	0.252	0.615
Prior stroke, *n*%	13 (23.21)	36 (19.05)	0.469	0.494
CKD, *n*%	7 (12.50)	13 (6.88)	1.821	0.177
Dyslipidemia, *n*%	7 (12.50)	30 (15.87)	0.383	0.535
Smoker, *n*%	9 (16.07)	37 (19.58)	0.348	0.555
NIHSS pre-treatment (IQR)	20.00 (16.00, 22.00)	15.00 (11.00, 18.00)	5.416	<0.001
ASPECTS pre-treatment (IQR)	8.00 (8.00, 9.00)	9.00 (8.00, 9.00)	1.286	0.199
IV thrombolysis, *n*%	26 (46.43)	71 (37.57)	1.419	0.234
DNT (IQR)	52.00 (32.75, 59.75)	42.00 (31.50, 56.75)	1.487	0.137
ONT (IQR)	140.00 (89.00, 200.00)	135.00 (101.75, 178.75)	0.209	0.835
TOAST classification				
Large artery atherosclerosis	25 (44.6)	105 (55.6)	2.221	0.528
Cardioembolic	29 (51.8)	77 (40.7)		
Stroke other determined cause	1 (1.8)	3 (1.6)		
Undetermined cause	1 (1.8)	4 (2.1)		
Site of arterial occlusion				
Distal/terminal ICA, *n*%	14 (25.00)	30 (15.87)	8.785	0.118
MCA-M1, *n*%	14 (25.00)	87 (46.03)		
MCA-M2, *n*%	4 (7.14)	11 (5.82)		
Tandem, *n*%	9 (16.07)	27 (14.29)		
Basilar, *n*%	12 (21.43)	29 (15.34)		
Others, *n*%	3 (5.36)	5 (2.56)		
ICA and MCA-M1, *n*%	37 (84.09)	144 (76.19)	2.192	0.130
DPT (IQR), minute	145.00 (114.25, 196.00)	148.00 (116.00, 196.00)	0.151	0.880
DRT (IQR), minute	247.00 (171.25, 322.00)	231.00 (173.50, 285.00)	1.061	0.289
PRT (IQR), minute	85.00 (44.75, 121.50)	60.00 (40.00, 92.50)	2.492	0.006
LKNPT (IQR), minute	302.50 (208.75, 493.75)	310.00 (212.50, 440.50)	0.202	0.840
mTICI post-EVT ≥ 2b, *n*%	34 (60.71)	173 (91.53)	31.313	<0.001
NIHSS 24-h post-EVT	25.00 (21.25, 28.00)	11.00 (5.00, 15.00)	8.873	<0.001
Pulmonary infection, *n*%	28 (50.00)	79 (41.80)	1.181	0.277
sICH, *n*%	19 (33.93)	5 (2.65)	47.844	<0.001
Length of hospitalization (days) (IQR)	4.00 (2.00, 6.00)	14.00 (10.00, 23.00)	7.566	<0.001
Hospitalization costs (RMB) (IQR)	117455.52 (83506.09, 164035.68)	112.389.72 (87487.21, 153096.45)	0.414	0.679

AF, atrial fibrillation; ASPECTS, Alberta stroke program early CT score; CAD, coronary artery disease; CKD, chronic kidney disease; DM, diabetes mellitus; DPT, door-to-puncture time; DRT, door-to-recanalization time; EVT: endovascular thrombectomy; LKNPT, last-known normal-to-puncture time; mTICI, modified thrombolysis in cerebral infarction; NIHSS, National Institute of Health Stroke Scale/score; PRT, puncture-to-recanalization time; sICH, symptomatic Intracranial Hemorrhage; TOAST, trial of ORG 10,172 in acute stroke treatment.

Discussion

In the present study, early mortality was noted in 22.8% of patients who had undergone EVT for acute ischemic stroke. High mortality rates among patients treated with EVT is mostly observed in patients with LVO (Malhotra et al., 2017). These patients represent about one third of cases, but account for three fifths of post-stroke dependence and death (Malhotra et al., 2017). Compared with non-LVO patients, those with LVO had an estimated mortality rate of 26.2 vs. 1.3% (OR: 4.1; 95% CI: 2.5–6.6, $p < 0.0001$) (Malhotra et al., 2017). In a meta-analysis of randomized clinical trials of EVT vs. medical care alone, there was no difference in the mortality proportion between groups: 248/1,538 (16.12%) vs. 234/1,342 (17.43%), $p = 0.52$ (**Figure 1**; Rodrigues et al., 2016). These proportions were similar for trials published in 2013 where early generation devices were used for thrombectomy such as the Merci retriever, Penumbra system or aspiration systems. For trials published in 2015 and later, including MR CLEAN; REVASCAT, EXTEND-IA, SWIFT PRIME, ESCAPE, THRACE, and PISTE, modern stent retrievers were used in more than 86% of cases (Berkhemer et al., 2015; Campbell et al., 2015; Goyal et al., 2015; Jovin et al., 2015; Saver et al., 2015; Bracard et al., 2016; Mocco et al., 2016; Muir et al., 2017). The latter suggest that use of early vs. latter generation retrievers do not have a major influence on mortality.

Of note, outcomes of clinical trials of patients undergoing mechanical thrombectomy may differ from real life experience (Zaidat et al., 2018; Qureshi et al., 2020). A study enrolling 23,375 patients treated with mechanical thrombectomy, showed lower in-hospital mortality rates for those participating in a clinical trial ($n = 430$, 1.8%): OR 0.14; 95% CI: 0.03–0.71, $p < 0.001$ (Qureshi et al., 2020). This difference is key when generalizing results from clinical trials and observational studies to real life experience.

An important question is which variables can predict mortality in patients undergoing EVT. In our study, older age, greater clinical severity at presentation and at 24 h (NIHSS score), higher PRT, lower mTICI, and presence of sICH were observed in early mortality group patients. However, in the multivariate regression only higher NIHSS score at 24 h, lower mTICI and sICH were independently associated with early mortality. It is likely, however, that the NIHSS score at 24 h may depend on the degree of revascularization or early occurrence of sICH. A study of 111 patients with anterior and posterior AIS treated with EVT from 2012 to 2017, reported a mortality rate of 37.8% within 3 months following the procedure. Non-surviving patients had higher NIHSS scores at presentation, compared with survivors: 19.6 vs. 14.9 ($p < 0.002$), lower rates of revascularization: 50 vs. 78.3%, higher rates of hemorrhagic conversion: 47.6 vs. 21.7%, technical problems during the procedure: 26.2 vs. 7.4% and higher rates of cancer history (Awad et al., 2020). This study mirrors our results related to revascularization status and frequency of sICH. While we did not assess for technical problems, a longer PRT may reflect difficulties to achieve rapid recanalization in our study. A multidisciplinary well-coordinated team is helpful to shorten PRT (Chen et al., 2022b; Yang et al., 2022). An additional study also showed that higher NIHSS scores at baseline and lower rates of recanalization following EVT were consistently associated with inpatient mortality (Mouchtouris et al., 2019). Whereas when assessing mortality following EVT 6–16 h after last normal in the DEFUSE 3 (The Endovascular Therapy Following Imaging Evaluation for Ischemic Stroke 3) trial, age older than 75 years, NIHSS score of ≥20, wake-up stroke and diabetes predicted death within 90 days (Taussky et al., 2021). While the NIHSS score on arrival is important for prognosis in studies not undergoing an active recanalization procedure, it is likely that the 24-h NIHSS score has a greater weight as it reflects irreversible damage and, in some cases, life-threatening conditions such as sICH, severe edema, brain herniation, etc. We did not find ASPECTS as a predictor of mortality neither.

In our study, sICH was strongly associated with mortality; however, this has not been observed in all studies. For example, one retrospective study did not find an association between inpatient mortality and hemorrhagic conversion with significant mass effect (Mouchtouris et al., 2019). However, another study including 417 patients who had undergone successful recanalization showed a significant association between sICH and mortality (OR 9.51; 95% CI: 4.54–19.92). This variable had much greater weight on mortality at 3-months compared with age, poor pre-treatment collateral status, baseline blood glucose and the NIHSS score, which were also significant (Zhang et al., 2020). This is in accordance with the findings of our study, where sICH had the higher weight to predict early mortality. Moreover, sICH was more frequently present in our study compared with randomized clinical trials of EVT in AIS, with rates similar to those observed in the THERAPY trial, which enrolled 108 patients; 55 underwent EVT and 53 controls (**Figure 2**; Mocco et al., 2016). Increased peak body temperature (≥38°C) during the acute phase has been associated with increased risk of sICH and poorer outcome in stroke patients with large artery disease undergoing EVT (Chen et al., 2022a).

TABLE 2 Logistic regression analysis of statistically significant variables in the bivariate analysis.

Variables in the final equation	B	Exp^B coefficient	Exp^B 95% C.I.	Wald	*P*-value
NIHSS 24-h post-EVT	0.188	1.207	1.137–1.282	38.096	<0.001
mTICI post-EVT ≥ 2b	−1.556	0.211	0.080–0.559	9.801	0.002
sICH	2.308	10.05	2.965–34.062	13.728	<0.001

Constant: B = −3.802, Exp^B: 0.22, p = 0.000. Hosmer–Lemeshow: $X^2 = 5.343$ ($p = 0.618$). Variables excluded in the final model: age (p = 0.297) pre-treatment NIHSS score (p = 0.941), and puncture-to-recanalization time (PRT) (p = 0.556). Cox and Snell $R^2 = 0.392$; Nagelkerke $R^2 = 0.595$.

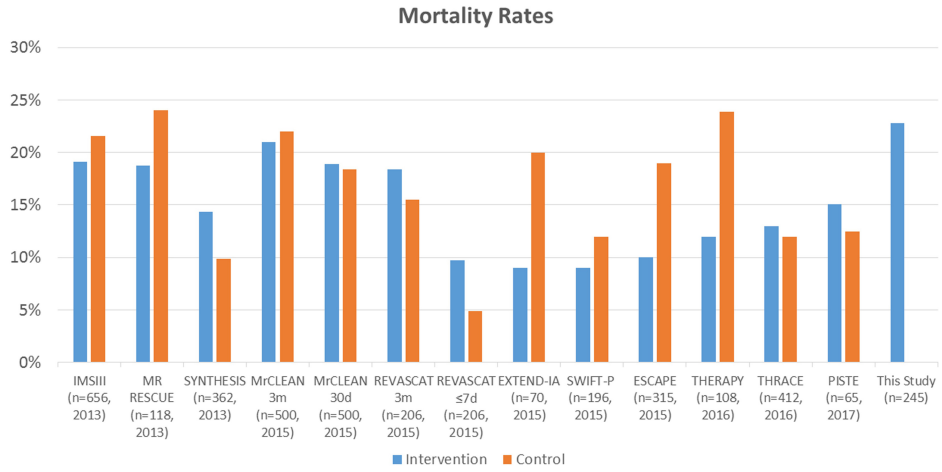

FIGURE 1
Summary of randomized clinical trials assessing the effect of endovascular thrombectomy (EVT) compared with standard care on mortality rates and this study. Blue: intervention and EVT. Orange: controls and standard therapy.

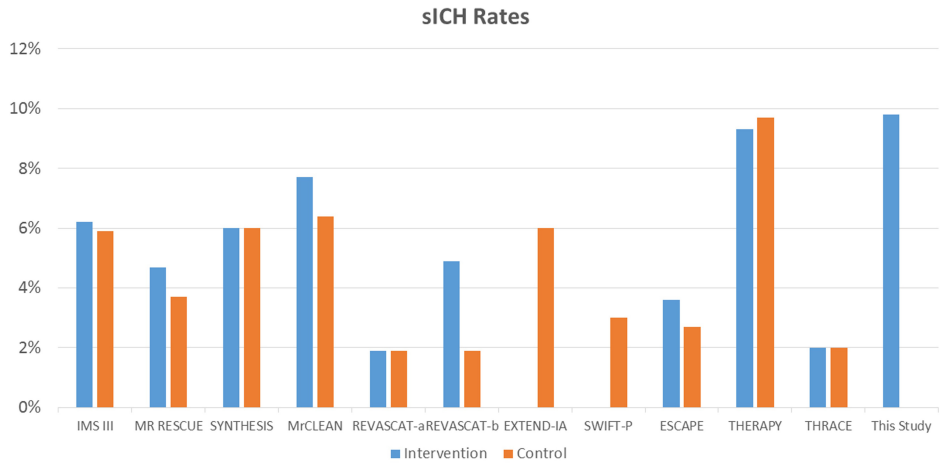

FIGURE 2
Summary of randomized clinical trials assessing the effect of endovascular thrombectomy compared with standard care on sICH rates and this study. Blue: intervention and EVT. Orange: controls and standard therapy. REVASCAT-a: SITS-MOST criteria; REVASCAT-b: ECASS II criteria. PISTE study: 0% sICH, not included in the figure.

In our study, we did not find a statistically significant difference in the rate of pulmonary infections in non-survivors compared with survivors. Pneumonia has been deemed as the most common cause of mortality up-to 1 year after AIS (Ingeman et al., 2011; Rocco et al., 2012). This data suggests that systemic complications may explain most of late mortality (i.e., after 3 months) in patients with AIS when a large proportion of patients have been already discharged from the hospital. Although non-survivors in our study had a shorter hospitalization time than survivors ($p < 0.001$), costs of hospitalization were higher for non-survivors.

Other variables may also influence the mortality rate in patients treated with EVT. For example, experience-performing EVT is another variable potentially influencing the outcome. In a Nationwide analysis in the US, it was estimated that for every 10 more proceduralist cases, patients had 4% lower inpatient mortality ($p < 0.0001$), and 3% greater odds of good outcome (Stein et al., 2021). In contrast, whether the risk of sICH has a link with the device used for thrombectomy or the technical experience of the treating physician should be further clarified. Moreover, patients undergoing AIS show a remarkable increase in serum inflammatory markers that may potentially increase the risk of death. Evidence has shown that high dose atorvastatin may decrease such markers and improve functional outcome (Tuttolomondo et al., 2016). The latter finding suggests that inflammation may have an important role in mortality in

AIS. However, other markers of inflammation such an arterial stiffness may also be explored in relation with early mortality in this scenario (Tuttolomondo et al., 2017; Zanoli et al., 2017).

Our study has limitations. It is a two-center study with a limited sample size. Further large-scale, multi-center investigations with larger sample sizes are required to verify these findings. Our study included patients of Asian origin and it is unclear whether these patients represent a population with a high risk of death after EVT. A recent study, for example, showed higher mortality rates in Blacks compared to White patients treated with EVT (Catapano et al., 2021). Another limitation is that we did not record the exact day an individual patient died and the cause of death on each case, these variables could be addressed in further studies. Despite these limitations, we were able to identify the factors associated with early mortality after EVT.

Conclusion

Early mortality occurred in 22.8% of the real-world cohort of patients treated with EVT. Poor recanalization following EVT, poor clinical recovery or deterioration at 24-h and sICH seem to have a major influence in this outcome. Although patients suffering early mortality had shorter hospitalization times, it may represent higher costs and a greater burden for health care systems.

Data availability statement

The original contributions presented in this study are included in the article/supplementary material, further inquiries can be directed to the corresponding authors.

Ethics statement

The studies involving human participants were reviewed and approved by The First People's Hospital of Foshan Review Board and Foshan Sanshui District People's Hospital Review Board. The patients/participants provided their written informed consent to participate in this study.

Author contributions

YC, JC, and XL: conception and design and drafting the manuscript. YC, SZ, SY, YH, HW, YL, ZZ, YY, JY, JC, XS, and WW: acquisition of data. MM and TNN: review and critique. JB-C: conception, drafting of the manuscript, review, and critique. All authors contributed to the article and approved the submitted version.

Funding

This study was supported by Foshan 14th Five-Year Plan Key Discipline Foundation, China, the Guangdong Provincial TCM Bureau Key Discipline Foundation, China, and Foshan Competitive Talent Support Project Fund (Brain-Heart Talent Project-Build the Brain-Heart Comorbidity Muti-disciplinary Medical Center).

Acknowledgments

We would like to thank all colleagues for data collection and patients for their contribution to the study.

Conflict of interest

The authors declare that the research was conducted in the absence of any commercial or financial relationships that could be construed as a potential conflict of interest.

Publisher's note

References

Awad, A. W., Kilburg, C., Ravindra, V. M., Scoville, J., Joyce, E., Grandhi, R., et al. (2020). Predicting death after thrombectomy in the treatment of acute stroke. *Front. Surg.* 7:16. doi: 10.3389/fsurg.2020.00016

Berkhemer, O. A., Fransen, P. S., Beumer, D., van den Berg, L. A., Lingsma, H. F., Yoo, A. J., et al. (2015). A randomized trial of intraarterial treatment for acute ischemic stroke. *N. Engl. J. Med.* 372, 11–20. doi: 10.1056/NEJMoa1411587

Bracard, S., Ducrocq, X., Mas, J. L., Soudant, M., Oppenheim, C., Moulin, T., et al. (2016). Mechanical thrombectomy after intravenous alteplase versus alteplase alone after stroke (THRACE): A randomised controlled trial. *Lancet Neurol.* 15, 1138–1147. doi: 10.1016/S1474-4422(16)30177-6

Broderick, J. P., Palesch, Y. Y., Demchuk, A. M., Yeatts, S. D., Khatri, P., Hill, M. D., et al. (2013). Endovascular therapy after intravenous t-PA versus t-PA alone for stroke. *N. Engl. J. Med.* 368, 893–903. doi: 10.1056/NEJMoa1214300

Campbell, B. C., Mitchell, P. J., Kleinig, T. J., Dewey, H. M., Churilov, L., Yassi, N., et al. (2015). Endovascular therapy for ischemic stroke with perfusion-imaging selection. *N. Engl. J. Med.* 372, 1009–1018. doi: 10.1056/NEJMoa1414792

Catapano, J. S., Rumalla, K., Srinivasan, V. M., Nguyen, C. L., Farhadi, D. S., Ngo, B., et al. (2021). Delays in presentation and mortality among Black patients with mechanical thrombectomy after large-vessel stroke at a US hospital. *Neurosurg. Focus* 51:E9. doi: 10.3171/2021.4.Focus2182

Chen, Y., Nguyen, T. N., Wellington, J., Mofatteh, M., Yao, W., Hu, Z., et al. (2022b). Shortening door-to-needle time by multidisciplinary collaboration and workflow optimization during the COVID-19 pandemic. *J. Stroke Cerebrovasc. Dis.* 31:106179. doi: 10.1016/j.jstrokecerebrovasdis.2021.106179

Chen, Y., Nguyen, T. N., Mofatteh, M., Abdalkader, M., Wellington, J., Yan, Z., et al. (2022a). Association of early increase in body temperature with symptomatic intracranial hemorrhage and unfavorable outcome following endovascular therapy in patients with large vessel occlusion stroke. *J. Integr. Neurosci.* 21:156. doi: 10.31083/j.jin2106156

Ciccone, A., Valvassori, L., Nichelatti, M., Sgoifo, A., Ponzio, M., Sterzi, R., et al. (2013). Endovascular treatment for acute ischemic stroke. *N. Engl. J. Med.* 368, 904–913. doi: 10.1056/NEJMoa1213701

Eskey, C. J., Meyers, P. M., Nguyen, T. N., Ansari, S. A., Jayaraman, M., McDougall, C. G., et al. (2018). Indications for the performance of intracranial endovascular neurointerventional procedures: A scientific statement from the American heart association. *Circulation* 137, e661–e689. doi: 10.1161/cir.0000000000000567

Goyal, M., Demchuk, A. M., Menon, B. K., Eesa, M., Rempel, J. L., Thornton, J., et al. (2015). Randomized assessment of rapid endovascular treatment of ischemic stroke. *N. Engl. J. Med.* 372, 1019–1030. doi: 10.1056/NEJMoa1414905

Goyal, M., Menon, B. K., van Zwam, W. H., Dippel, D. W., Mitchell, P. J., Demchuk, A. M., et al. (2016). Endovascular thrombectomy after large-vessel ischaemic stroke: A meta-analysis of individual patient data from five randomised trials. *Lancet* 387, 1723–1731. doi: 10.1016/s0140-6736(16)00163-x

Indredavik, B., Rohweder, G., Naalsund, E., and Lydersen, S. (2008). Medical complications in a comprehensive stroke unit and an early supported discharge service. *Stroke* 39, 414–420. doi: 10.1161/strokeaha.107.489294

Ingall, T. (2004). Stroke–incidence, mortality, morbidity and risk. *J. Insur. Med.* 36, 143–152.

Ingeman, A., Andersen, G., Hundborg, H. H., Svendsen, M. L., and Johnsen, S. P. (2011). In-hospital medical complications, length of stay, and mortality among stroke unit patients. *Stroke* 42, 3214–3218. doi: 10.1161/strokeaha.110.610881

Jovin, T. G., Chamorro, A., Cobo, E., de Miquel, M. A., Molina, C. A., Rovira, A., et al. (2015). Thrombectomy within 8 hours after symptom onset in ischemic stroke. *N. Engl. J. Med.* 372, 2296–2306. doi: 10.1056/NEJMoa1503780

Karamchandani, R. R., Rhoten, J. B., Strong, D., Chang, B., and Asimos, A. W. (2021). Mortality after large artery occlusion acute ischemic stroke. *Sci. Rep.* 11:10033. doi: 10.1038/s41598-021-89638-x

Kidwell, C. S., Jahan, R., Gornbein, J., Alger, J. R., Nenov, V., Ajani, Z., et al. (2013). A trial of imaging selection and endovascular treatment for ischemic stroke. *N. Engl. J. Med.* 368, 914–923. doi: 10.1056/NEJMoa1212793

Langhorne, P., Stott, D. J., Robertson, L., MacDonald, J., Jones, L., McAlpine, C., et al. (2000). Medical complications after stroke: A multicenter study. *Stroke* 31, 1223–1229. doi: 10.1161/01.str.31.6.1223

Linfante, I., Walker, G. R., Castonguay, A. C., Dabus, G., Starosciak, A. K., Yoo, A. J., et al. (2015). Predictors of mortality in acute ischemic stroke intervention: Analysis of the North American solitaire acute stroke registry. *Stroke* 46, 2305–2308. doi: 10.1161/strokeaha.115.009530

Malhotra, K., Gornbein, J., and Saver, J. L. (2017). Ischemic strokes due to large-vessel occlusions contribute disproportionately to stroke-related dependence and death: A review. *Front. Neurol.* 8:651. doi: 10.3389/fneur.2017.00651

Mocco, J., Zaidat, O. O., von Kummer, R., Yoo, A. J., Gupta, R., Lopes, D., et al. (2016). Aspiration thrombectomy after intravenous alteplase versus intravenous alteplase alone. *Stroke* 47, 2331–2338. doi: 10.1161/strokeaha.116.013372

Mouchtouris, N., Al Saiegh, F., Fitchett, E., Andrews, C. E., Lang, M. J., Ghosh, R., et al. (2019). Revascularization and functional outcomes after mechanical thrombectomy: An update to key metrics. *J. Neurosurg.* [Epub ahead of print].

Muir, K. W., Ford, G. A., Messow, C. M., Ford, I., Murray, A., Clifton, A., et al. (2017). Endovascular therapy for acute ischaemic stroke: The Pragmatic Ischaemic Stroke Thrombectomy Evaluation (PISTE) randomised, controlled trial. *J. Neurol. Neurosurg. Psychiatry* 88, 38–44. doi: 10.1136/jnnp-2016-314117

Qureshi, A. I., Singh, B., Huang, W., Du, Z., Lobanova, I., Liaqat, J., et al. (2020). Mechanical thrombectomy in acute ischemic stroke patients performed within and outside clinical trials in the united states. *Neurosurgery* 86, E2–E8. doi: 10.1093/neuros/nyz359

Rao, N. M., Levine, S. R., Gornbein, J. A., and Saver, J. L. (2014). Defining clinically relevant cerebral hemorrhage after thrombolytic therapy for stroke: Analysis of the National Institute of Neurological Disorders and Stroke tissue-type plasminogen activator trials. *Stroke* 45, 2728–2733. doi: 10.1161/strokeaha.114.005135

Rocco, A., Fam, G., Sykora, M., Diedler, J., Nagel, S., and Ringleb, P. (2012). Poststroke infections are an independent risk factor for poor functional outcome after three-months in thrombolysed stroke patients. *Int. J. Stroke* 8, 639–644. doi: 10.1111/j.1747-4949.2012.00822.x

Rodrigues, F. B., Neves, J. B., Caldeira, D., Ferro, J. M., Ferreira, J. J., and Costa, J. (2016). Endovascular treatment versus medical care alone for ischaemic stroke: Systematic review and meta-analysis. *BMJ* 353:i1754. doi: 10.1136/bmj.i1754

Rohweder, G., Ellekjær, H., Salvesen, Ø., Naalsund, E., and Indredavik, B. (2015). Functional outcome after common poststroke complications occurring in the first 90 days. *Stroke* 46, 65–70. doi: 10.1161/strokeaha.114.006667

Saver, J. L., Goyal, M., Bonafe, A., Diener, H. C., Levy, E. I., Pereira, V. M., et al. (2015). Stent-retriever thrombectomy after intravenous t-PA vs. t-PA alone in stroke. *N. Engl. J. Med.* 372, 2285–2295. doi: 10.1056/NEJMoa1415061

Stein, L. K., Mocco, J., Fifi, J., Jette, N., Tuhrim, S., and Dhamoon, M. S. (2021). Correlations between physician and hospital stroke thrombectomy volumes and outcomes: A nationwide analysis. *Stroke* 52, 2858–2865. doi: 10.1161/strokeaha.120.033312

Taussky, P., Agnoletto, G., Grandhi, R., Alexander, M. D., Wong, K. H., Albers, G. W., et al. (2021). Prediction of death after endovascular thrombectomy in the extended window: A secondary analysis of DEFUSE 3 ". *J. Neurointerv. Surg.* 13, 805–808. doi: 10.1136/neurintsurg-2020-016548

Tuttolomondo, A., Casuccio, A., Guercio, G., Maida, C., Del Cuore, A., Di Raimondo, D., et al. (2017). Arterial stiffness, endothelial and cognitive function in subjects with type 2 diabetes in accordance with absence or presence of diabetic foot syndrome. *Cardiovasc. Diabetol.* 16:2. doi: 10.1186/s12933-016-0483-5

Tuttolomondo, A., Di Raimondo, D., Pecoraro, R., Maida, C., Arnao, V., Della Corte, V., et al. (2016). Early high-dosage atorvastatin treatment improved serum immune-inflammatory markers and functional outcome in acute ischemic strokes classified as large artery atherosclerotic stroke: A randomized trial. *Medicine* 95:e3186. doi: 10.1097/MD.0000000000003186

Viderman, D., Issanov, A., Temirov, T., Goligher, E., and la Fleur, P. (2020). Outcome predictors of stroke mortality in the neurocritical care unit. *Front. Neurol.* 11:579733. doi: 10.3389/fneur.2020.579733

Yang, S., Yao, W., Siegler, J. E., Mofatteh, M., Wellington, J., Wu, J., et al. (2022). Shortening door-to-puncture time and improving patient outcome with workflow optimization in patients with acute ischemic stroke associated with large vessel occlusion. *BMC Emerg. Med.* 22:136. doi: 10.1186/s12873-022-00692-8

Zaidat, O. O., Castonguay, A. C., Gupta, R., Sun, C. J., Martin, C., Holloway, W. E., et al. (2018). North American solitaire stent retriever acute stroke registry: Post-marketing revascularization and clinical outcome results. *J. Neurointerv. Surg.* 10(Suppl. 1), i45–i49. doi: 10.1136/neurintsurg-2013-010895.rep

Zanoli, L., Boutouyrie, P., Fatuzzo, P., Granata, A., Lentini, P., Oztürk, K., et al. (2017). Inflammation and aortic stiffness: An individual participant data meta-analysis in patients with inflammatory bowel disease. *J. Am. Heart Assoc.* 6:e007003. doi: 10.1161/JAHA.117.007003

Zhang, X., Yuan, K., Wang, H., Gong, P., Jiang, T., Xie, Y., et al. (2020). Nomogram to predict mortality of endovascular thrombectomy for ischemic stroke despite successful recanalization. *J. Am. Heart Assoc.* 9:e014899. doi: 10.1161/jaha.119.014899

frontiers | Frontiers in Neuroscience

TYPE Original Research
PUBLISHED 20 December 2022
DOI 10.3389/fnins.2022.1060111

OPEN ACCESS

EDITED BY
Guangzhi Ning,
Tianjin Medical University General Hospital, China

REVIEWED BY
Li-Ching Wu,
National Central University, Taiwan
Jihu Sun,
Jiangsu Vocational College of Medicine, China
Wenzhen He,
The First Affiliated Hospital of Shantou University Medical College, China
Junliang Yuan,
Peking University Sixth Hospital, China

*CORRESPONDENCE
Jun Liu
liujun@gzhmu.edu.cn
Aiguo Xuan
xag2005@163.com
Shaoqing Yang
1069381104@qq.com

†These authors have contributed equally to this work

SPECIALTY SECTION
This article was submitted to Translational Neuroscience, a section of the journal Frontiers in Neuroscience

RECEIVED 02 October 2022
ACCEPTED 30 November 2022
PUBLISHED 20 December 2022

CITATION
Liao W, Luo H, Ruan Y, Mai Y, Liu C, Chen J, Yang S, Xuan A and Liu J (2022) Identification of candidate genes associated with clinical onset of Alzheimer's disease. *Front. Neurosci.* 16:1060111. doi: 10.3389/fnins.2022.1060111

Identification of candidate genes associated with clinical onset of Alzheimer's disease

Wang Liao[1†], Haoyu Luo[1†], Yuting Ruan[2], Yingren Mai[1], Chongxu Liu[1], Jiawei Chen[3], Shaoqing Yang[1*], Aiguo Xuan[4*] and Jun Liu[1*]

[1]Department of Neurology, The Second Affiliated Hospital, Guangzhou Medical University, Guangzhou, China, [2]Department of Rehabilitation, The Second Affiliated Hospital, Guangzhou Medical University, Guangzhou, China, [3]Guangzhou Medical University, Guangzhou, China, [4]School of Basic Medical Sciences, Guangzhou Medical University, Guangzhou, China

Background and objective: Alzheimer's disease (AD) is the most common type of dementia, with its pathology like beta-amyloid and phosphorylated tau beginning several years before the clinical onset. The aim is to identify genetic risk factors associated with the onset of AD.

Methods: We collected three microarray data of post-mortem brains of AD patients and the healthy from the GEO database and screened differentially expressed genes between AD and healthy control. GO/KEGG analysis was applied to identify AD-related pathways. Then we distinguished differential expressed genes between symptomatic and asymptomatic AD. Feature importance with logistic regression analysis is adopted to identify the most critical genes with symptomatic AD.

Results: Data was collected from three datasets, including 184 AD patients and 132 healthy controls. We found 66 genes to be differently expressed between AD and the control. The pathway enriched in the process of exocytosis, synapse, and metabolism and identified 19 candidate genes, four of which (VSNL1, RTN1, FGF12, and ENC1) are vital.

Conclusion: VSNL1, RTN1, FGF12, and ENC1 may be the essential genes that progress asymptomatic AD to symptomatic AD. Moreover, they may serve as genetic risk factors to identify high-risk individuals showing an earlier onset of AD.

KEYWORDS

Alzheimer's disease, genes, transcriptomic analysis, GEO, dementia

1 Introduction

Alzheimer's disease (AD) is a chronic degenerative disease characterized by the extracellular deposition of beta-amyloid and intracellular accumulation of phosphorylated tau protein (Spina et al., 2021). For older adults, AD is the most common cause of dementia, with an incidence rate of approximately 1.5% among people over 65 years old and nearly 50% among people over 90 years old (Scheltens et al., 2021). Interestingly, cognitive impairment of many AD patients occurs substantial years after pathological changes, such as amyloid and neurofibrillary tangles (NFTs). In contrast, more than 20% of the aged population have an amyloid deposition. Individuals with intact cognition and neuropathology consistent with AD were called asymptomatic AD (AsymAD) (Patel et al., 2019). AsymAD is distinguishable from normal aging based on neuropathology, brain imaging, and cerebrospinal fluid biomarkers (Ayodele et al., 2021). While some of these individuals progress to symptoms related to cognition, which deviate from mild cognitive impairment (MCI), and then to AD, not all do. They are, therefore, a heterogeneous group, representing those with prodromal AD and those impervious to AD despite having pathological hallmarks. These individuals are highly likely to develop symptomatic AD. Abundant evidence has demonstrated genetic risk factors of AD, such as APP, PSEN1, PSEN2, and apolipoprotein ε4 allele (APOE4) (Lefterov et al., 2019). However, transcriptomic changes in the brain, which might reveal AD vulnerability, are currently unknown. In the present study, we identified genetic risk factors for AD onset in asymptomatic and symptomatic individuals with clear signs of AD pathology at autopsy. Understanding the fundamental changes may shed light on specific biological mechanisms involved in early pathological hallmarks of AD, providing new therapeutic targets for early intervention.

2 Materials and methods

2.1 Data acquisition and processing

We searched the microarray sequencing datasets of AD patients' post-mortem brain samples for 5 years on the Gene Expression Omnibus database (GEO). Then we removed the datasets with incomplete annotation of platform annotation information. Finally, we selected three datasets of the same platform [GSE139384 (Morimoto et al., 2020), GSE118553 (Patel et al., 2019), and GSE132903 (Piras et al., 2019)]. We integrated the temporal lobe data in the post-mortem brains of 184 AD patients and 132 healthy people with ComBat package (**Supplementary Data Sheet 1**). All the above datasets were gathered using the Illumina HumanHT-12 V4.0 platform.

2.2 Screening of key differentially expressed genes

We screened the differentially expressed genes (DEGs) between AD patients and control in the processed new dataset using the limma R package. We first use the lmFit function to construct the linear model and then use the contrasts fit function to calculate the contrast of the model (estimated coefficient and standard error). Next, eBayes function to compute moderated t-statistic, moderated F-statistic, and log-odds of differential expression, and use the top table function (adjust.method is ' fdr ') to extract the gene table. Finally, the differential genes were screened by the standard of |logFoldChange| = 0.5, adjust P = 0.05, and displayed visually by ggplot2 and heatmap. Further, we performed weighted correlation network analysis (WGCNA) with the new dataset we got to identify the co-expression of hub genes.

2.3 Functional enrichment and pathway analysis of DEGs

All the DEGs were analyzed by GO (Gene ontology) and KEGG (Kyoto Encyclopedia of Genes and Genomes) enrichment analysis to investigate the biological mechanisms. With enrichgo and enrichKEGG functions in the clusterProfiler package, we analyzed the differential genes and logFC values to obtain significantly enriched gene functions and pathways. GO analysis was annotated by org.Hs.eg.db package, KEGG analysis set hsa as species information, p value and q value were set to 0.05, and visualize with barplot and GOChord. In order to reduce the poor enrichment results caused by the fixed threshold method for screening differential genes, we further performed GSEA analysis on the overall genes list with logFC value of the new dataset using the gseKEGG function in the clusterProfiler package, organism is hsa.

2.4 Establishment of PPI network

We input DEGs list into the String database[1] and obtained a protein interaction network diagram and data forms. Then, we downloaded the data tables and imported them into cytoscape software, using the cytohubba plug-in to calculate the key nodes. Based on the results of MCC algorithm, the interactive network diagrams of different colors are drawn according to the calculated scores.

1 https://cn.string-db.org

TABLE 1 Datasets characteristics.

Datasets	Tittle	Platform	Organism	Submission date	PMID	Samples
GSE139384	Synaptopathy in Kii ALS/PDC, a disease concept based on transcriptome analyses of human brains	GPL10558 (Illumina HumanHT-12 V4.0 expression beadchip)	*Homo sapiens*	October 25, 2019	32422904	6
GSE118553	Transcriptomic analysis of probable asymptomatic and symptomatic Alzheimer's brains			August 14, 2018	31063847	115
GSE132903	Transcriptome changes in the Alzheimer's middle temporal gyrus: importance of RNA metabolism and mitochondria-associated membrane (MAM) genes			June 18, 2019	31256118	195

2.5 Differential genes between symptomatic and asymptomatic AD

Differentially expressed genes were first analyzed between asymptomatic and symptomatic AD groups in the GSE118553 dataset to identify the genetic risk factors for symptomatic AD. We then overlapped these DEGs with AD-related DEGs derived from WGCNA. Feature importance with a logistic regression analysis were used to identify the predicted importance of the DEGs further. Specifically, we first sorted out the expression of immune-related differential expressed genes in the validation set. Next, the matrix was input into SPSS 26.0 software, and the binary logistic regression analysis with the forward conditional method was carried out with whether it was symptomatic AD as the dependent variable and the expression of each gene as the independent variable. Finally, the matrix of the key genes successfully incorporated into the model was input into the R language, the rms package was loaded, and the linear regression model between these genes and symptomatic AD was constructed using the lrm function. Then, the nomogram function was used to draw a nomogram representing the regression fitting to visually demonstrate the predictive power of these genes.

3 Results

3.1 Demographic characteristics and data processing

A total of 184 AD patients and 132 normal controls were included in this study. The demographic information is shown in **Tables 1**, **2**. After standardized processing and removing the batch effect, the distribution of the three datasets tends to be comparable, indicating that the processed data is highly uniform and quality (**Supplementary Figure 1**).

TABLE 2 Datasets clinical characteristics.

	Group		Gender		Age	
	AD	Control	Male	Female	≤85 years	>85 years
GSE139384	3	3	6	0	4	2
GSE118553	84	31	64	65	65	50
GSE132903	97	98	99	96	98	97

3.2 Identification of DEGs between AD patients and healthy

Nighty-two DEGs were found, including 68 down-regulated and 24 upregulated genes (**Figures 1A,B**). Next, we got the Median Absolute Deviation (MAD) of each gene, and the most minor top 30% genes were removed. Then we removed outlier genes and samples using the goodSampleGenes method in the R software package WGCNA (**Figure 2C**) and constructed a scale-free co-expression network. Then we evaluated the optimal power using the pick Soft Threshold function in the WGCNA package with a threshold of 0.9 (**Figure 2A**). As is shown in **Figure 2B**, the weighted gene network constructed with a power value of six has good connectivity. To classify genes with similar expression profiles into Gene modules, we set the gene tree's minimum size as 30, the sensitivity as 3, and the distance less than 0.25 to synthesize modules. Finally, 18 co-expression modules were obtained, and gene clustering maps and module vector clustering maps were shown in **Figures 2D,E** (the gray module is considered a gene set that cannot be assigned to any module). Next, clinical information of the dataset was included to clarify its correlation with the modules (**Figure 2F**). Finally, based on the truncation criteria with $|MM| > 0.8$ and $|GS| > 0.2$, we selected the top five modules with the highest coefficient as the key modules: turquoise, dark turquoise, blue, brown, and black modules. Among them, 585 genes with high connectivity were extracted as hub genes, intersecting with the previously obtained 92 DEGs. A total of 66 co-expressed differential genes were left (**Figure 2G**).

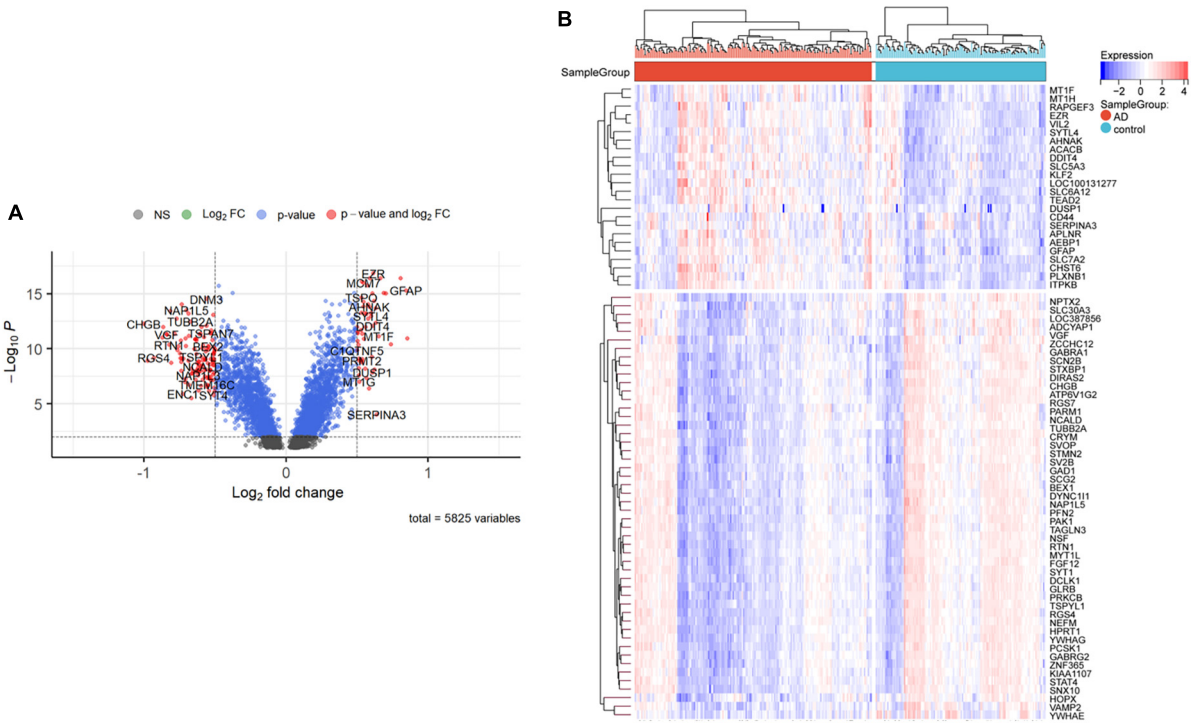

FIGURE 1
Differentially expressed genes between AD and control samples. **(A)** The right red genes represent significantly high expression in AD; the left red genes represent significantly high expression in control. **(B)** The heatmap shows the top 50 genes significantly expressed in AD or ND samples.

3.3 Enrichment of DEGs and protein interaction network

We analyzed these 66 DEGs in GO and KEGG databases. We found that the GO database enriched regulating exocytosis, synapse organization, presynapse, neuron projection terminus, and transport vesicle pathways. Moreover, it is enriched in protein kinase C binding, chloride transmembrane transporter activity, and SNARE binding pathways (Figure 3A). The GO plot package chord diagram showed that SYT13, PFN2, NSF, PCLO, SYP, PRKCB, VAMP2, VSNL1, and SYT1 were significantly enriched in multiple major pathways (Figure 3B). While in the KEGG database is enriched in GABAergic synapse, synaptic vesicle cycle, insulin secretion, morphine addiction, and vasopressin-regulated water reabsorption pathways (Figure 3C). To discuss the pathway enrichment of the whole sample more comprehensively, we further performed GSEA analysis. The results showed that these genes were significantly enriched in 21 pathways, especially those associated with Alzheimer's disease and neurodegenerative diseases (Table 3).

Next, 66 DEGs were further analyzed with STRING (Figure 4). After excluding 17 independent DEGs, we finally constructed a protein interaction network map according to the Maximal Clique Centrality (MCC) score, with the remaining 49 genes processed by Cytohubba. The top 10 hub genes are SYP, SYT1, GABRG2, GABRA1, SLC12A5, GAD1, SV2B, STMN2, VAMP2, and SCG2 (Table 4).

3.4 Gene expression profiling of symptomatic and asymptomatic AD

Firstly, we extracted the temporal lobe information from AsymAD (n = 32) and SymAD (n = 52) in GSE118553 dataset. Seven hundred and sixty-two DEGs were identified, including 30 upregulated genes and 732 down-regulated genes (Figures 5A,B). Then, we sequence overlapped these DEGs with 92 AD-specific DEGs and WGCNA hub genes and finally obtained 19 key genes, including VSNL1, TAGLN3, SYP, SVOP, SLC12A5, RTN1, PCSK1, PAK1, NSF, NEFM, NCALD, LOC387856, HPRT1, GABRG2, FGF12, ENC1, CHGB, CAP2, and ADCYAP1 (Figure 5C and Table 5).

3.5 VSNL1, RTN1, FGF12, and ENC1 might be genetic risk factors associated with AD onset

Next, we performed a stepwise logistic regression analysis of these 19 DEGs to identify symptomatic AD risk factors

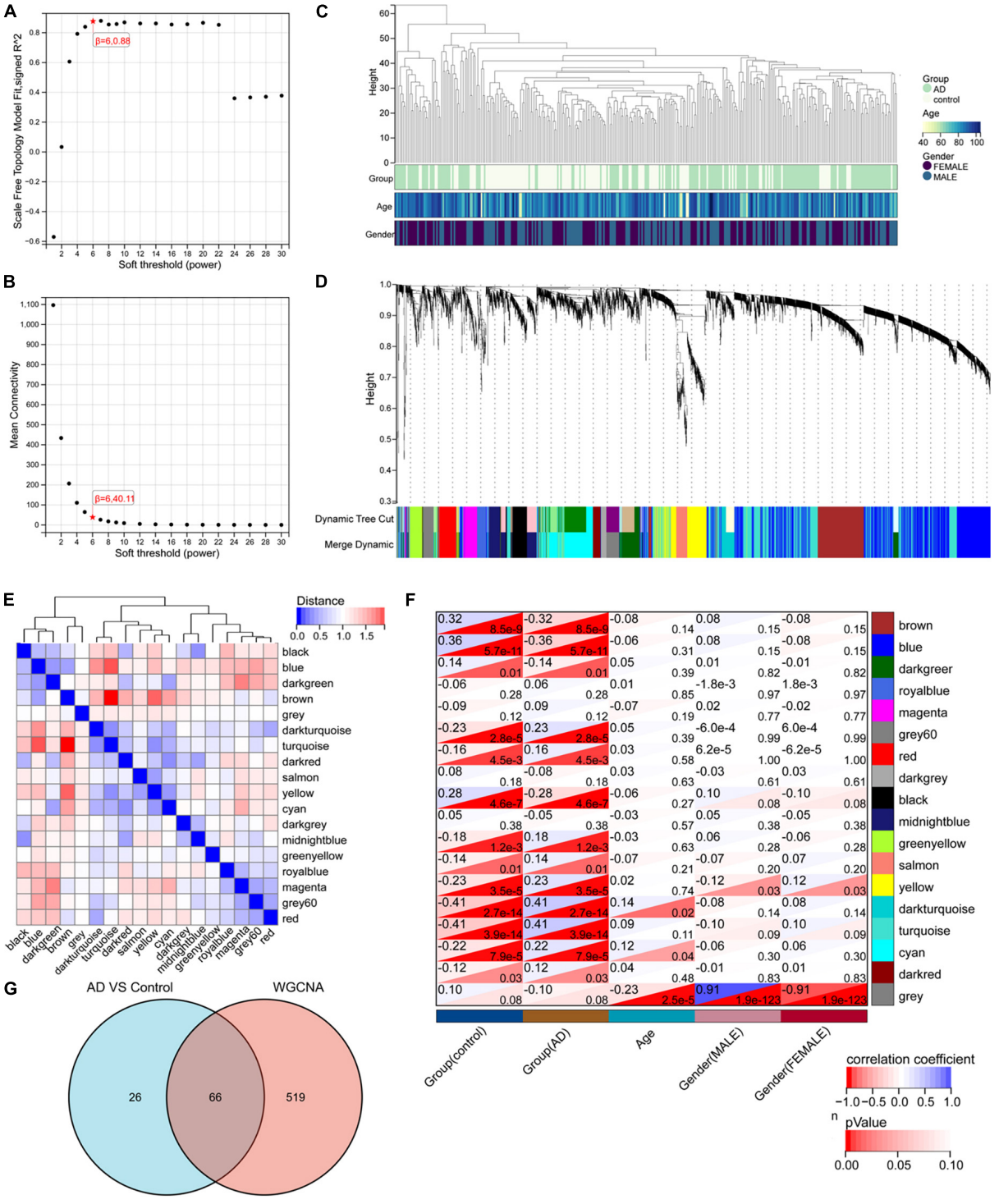

FIGURE 2
WGCNA analysis results. **(A)** The corresponding scale-free topological model fit indices at different soft threshold powers. **(B)** The corresponding mean connectivity values at other soft threshold powers. **(C)** Sample clustering. **(D)** Cluster dendrogram of genes. **(E)** Correlation map of vector clustering of 18 modules. **(F)** Correlation heatmap between modules and clinical features, the lower left corner of each grid is the *P*-value, and the upper right corner is the correlation coefficient. **(G)** The Wayne diagram of intersection with 585 hub genes obtained by WGCNA and 92 DEGs by limma.

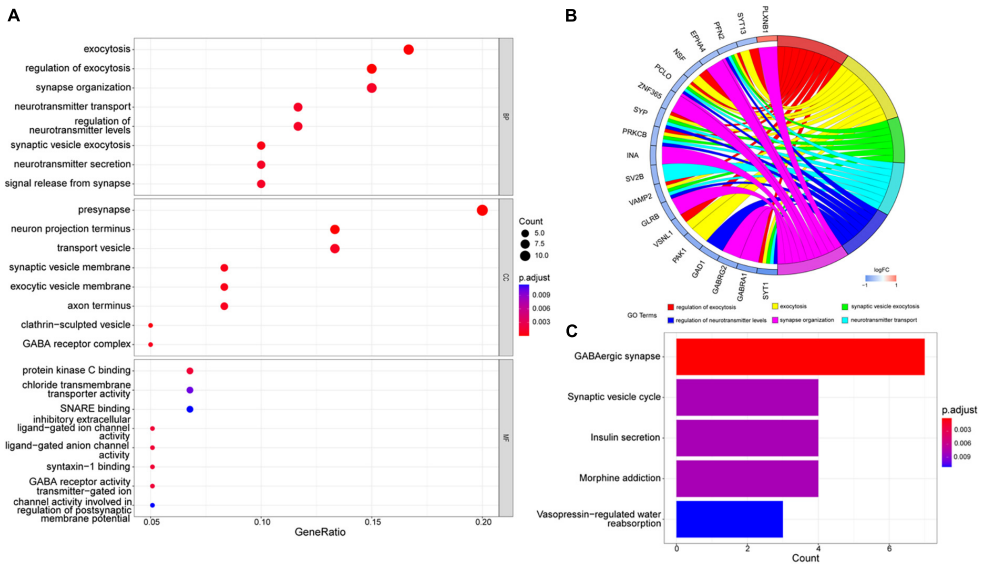

FIGURE 3
GO and KEGG enrichment analysis. **(A)** The most significant enrichment pathways in the GO database. **(B)** Chord diagram of GO enrichment analysis. **(C)** The most considerable enrichment pathways in the KEGG database.

TABLE 3 GSEA results.

ID	Description	setSize	Enrichment score	Adj. *P*-value
hsa05168	Herpes simplex virus 1 infection	467	0.284718529	8.72×10^{-5}
hsa05022	Pathways of neurodegeneration	434	−0.333872677	9.04×10^{-5}
hsa05010	Alzheimer's disease	345	−0.318194061	3.88×10^{-3}
hsa05014	Amyotrophic lateral sclerosis	320	−0.335493776	9.26×10^{-4}
hsa05016	Huntington disease	269	−0.363160142	3.04×10^{-4}
hsa05020	Prion disease	240	−0.398580749	3.67×10^{-5}
hsa05012	Parkinson's disease	232	−0.41709762	4.81×10^{-5}
hsa04024	cAMP signaling pathway	217	−0.315166868	4.24×10^{-2}
hsa03010	Ribosome	131	−0.360481409	4.24×10^{-2}
hsa00190	Oxidative phosphorylation	103	−0.505392372	2.21×10^{-5}
hsa04350	TGF-beta signaling pathway	92	0.417938926	1.33×10^{-3}
hsa04911	Insulin secretion	86	−0.432626299	1.24×10^{-2}
hsa04512	ECM-receptor interaction	86	0.363314004	4.22×10^{-2}
hsa04260	Cardiac muscle contraction	81	−0.4123577	3.67×10^{-2}
hsa04721	Synaptic vesicle cycle	78	−0.562303369	4.81×10^{-6}
hsa05120	Epithelial cell signaling in Helicobacter pylori infection	68	−0.44664597	2.13×10^{-2}
hsa05110	Vibrio cholerae infection	49	−0.547099768	1.48×10^{-3}
hsa00620	Pyruvate metabolism	46	−0.496786058	2.67×10^{-2}
hsa03050	Proteasome	45	−0.530909935	4.32×10^{-3}
hsa00020	Citrate cycle (TCA cycle)	30	−0.6441294	1.17×10^{-3}
hsa04966	Collecting duct acid secretion	27	−0.577941421	2.69×10^{-2}

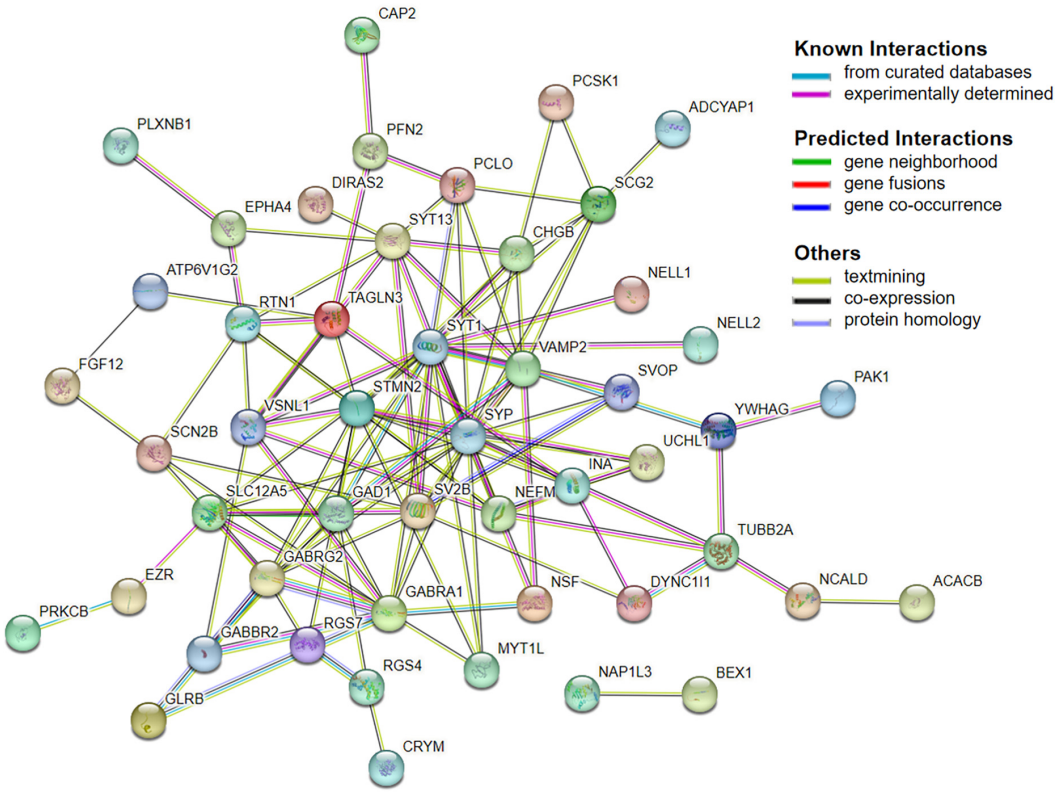

FIGURE 4
PPI network.

TABLE 4 Cytohubba results.

Gene name	Description	MCC	Degree	LogFC
SYP	Synaptophysin	398	18	−0.624723213
SYT1	Synaptotagmin-1	368	18	−0.972911963
GABRG2	Gamma-aminobutyric acid type B receptor subunit 2	280	11	−0.745760764
GABRA1	Gamma-aminobutyric acid receptor subunit alpha-1	266	12	−0.837374053
SLC12A5	Solute carrier family 12 member 5	241	7	−0.664705232
GAD1	Glutamate decarboxylase 1	157	9	−0.743098858
SV2B	Synaptic vesicle glycoprotein 2B	145	10	−0.665987783
STMN2	Stathmin-2	88	13	−0.640119418
VAMP2	Vesicle-associated membrane protein 2	81	10	−0.682915931
SCG2	Secretogranin-2	51	7	−0.665987783

and obtained four genes: VSNL1, RTN1, FGF12, and ENC1 (Table 6). Specifically, the goodness of fit and predictive ability of the model are as follows: (1) according to the Omnibus Test results, the chi-square value of the model is 54.070, and the p-value is <0.001, indicating that the model is statistically significant; (2) according to the results of Hosmer and Lemeshow Test, the p-value of the fitting model is 0.229 > 0.05, which indicates that the information in the current data has been fully extracted and the goodness of fit of the model is high; (3) according to the results of the classification table, the sensitivity of the model is 90.4% and the specificity is 80.4%. On the whole, it has a correct prediction rate of 88.1% for all samples, indicating that it has good predictive ability. Through the nomogram, we found that decreased VSNL1, RTN1, and increased FGF12 and ENC1 were positively correlated with disease risk (Figure 5D). Then, we

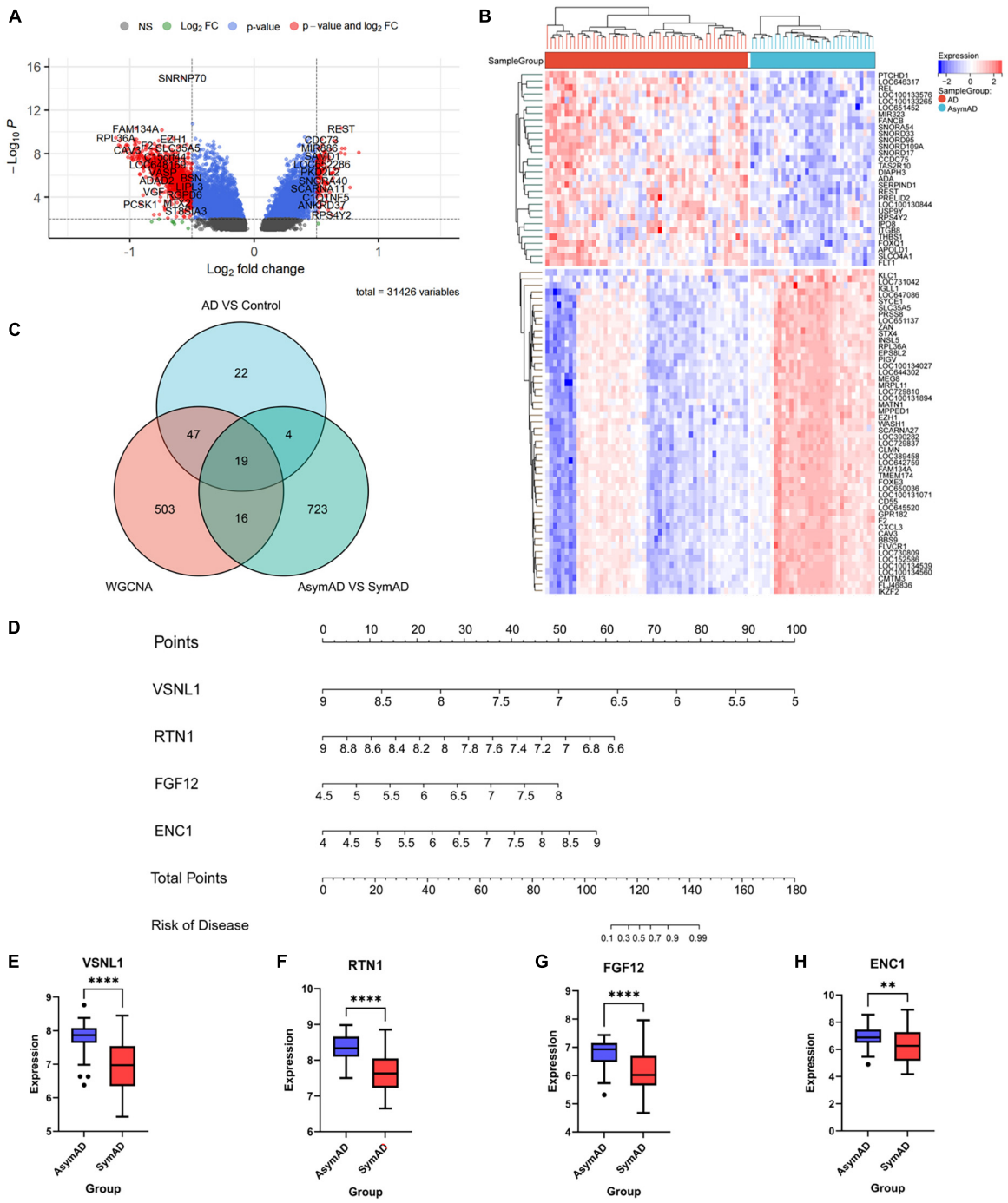

FIGURE 5
The gene expression difference between AsymAD and SymAD. **(A)** The right red genes represent significantly high expression in SymAD; the left red genes represent increased expression in AsymAD. **(B)** The heatmap shows the top 50 genes predominantly expressed in AsymAD or SymAD. **(C)** Wayne diagram to intersection DEGs of three difference analysis. **(D)** Nomogram of four essential genes. **(E–H)** Expression differences of four critical genes in AsymAD and SymAD group. ** means p-value < 0.01; **** means p-value < 0.0001.

further examined the expression levels of these four genes in disease grouping and observed that the expression of all these four genes was significantly lower in the SymAD group (Figures 5E–H).

4 Discussion

The present study analyzed three datasets of post-mortem brain samples of AD patients and the healthy. Since the

TABLE 5 Nineteen DEGs list.

Gene name	Description	LogFC	Adj. *P*-value
PCSK1	Phosphoenolpyruvate carboxykinase 1	−0.914236026	4.27×10^{-4}
CAP2	Cyclase associated actin cytoskeleton regulatory protein 2	−0.8927109	6.52×10^{-6}
LOC387856	Coiled-coil domain containing 184 (CCDC184)	−0.872134325	1.49×10^{-6}
VSNL1	Visinin like 1	−0.823806102	2.71×10^{-6}
PAK1	p21 (RAC1) activated kinase 1	−0.752922248	3.19×10^{-6}
GABRG2	Gamma-aminobutyric acid type A receptor subunit gamma 2	−0.751904972	9.59×10^{-6}
SLC12A5	Solute carrier family 12 member 5	−0.73219574	3.82×10^{-6}
ADCYAP1	Adenylate cyclase activating polypeptide 1	−0.716567516	1.08×10^{-3}
TAGLN3	Transgelin 3 (Neuronal protein NP2)	−0.715251481	2.70×10^{-6}
NCALD	Neurocalcin delta	−0.694917396	8.29×10^{-3}
SVOP	SV2 related protein	−0.666215273	1.93×10^{-4}
RTN1	Reticulon 1 (Neuroendocrine-specific protein)	−0.663450406	6.98×10^{-6}
FGF12	Fibroblast growth factor 12	−0.657390284	1.46×10^{-4}
ENC1	Ectodermal-neural cortex 1	−0.649388586	2.01×10^{-2}
CHGB	Chromogranin B	−0.645099164	5.03×10^{-6}
NSF	*N*-Ethylmaleimide sensitive factor, vesicle fusing ATPase	−0.62336505	4.38×10^{-6}
NEFM	Neurofilament medium chain	−0.609879042	2.56×10^{-3}
SYP	Synaptophysin	−0.599413737	4.34×10^{-6}
HPRT1	Hypoxanthine phosphoribosyltransferase 1	−0.587576219	7.57×10^{-6}

temporal lobe is demonstrated to be most related to AD, we extract the specific brain region for further analysis. A dataset with information on asymptomatic AD was applied for subsequent analysis of genetic risk factors and their onset. Differential analysis, WGCNA analysis, function enrichment pathway analysis, protein interaction network analysis, and logistic regression analysis were used to interpret the data. Finally, we found four essential genes closely related to AD, including VSNL1, RTN1, FGF12, and ENC1.

A lot of analytical methods have found many risk molecules associated with AD (Talwar et al., 2014). However, most recent studies still focus on genetic characteristics of early-onset or familial AD (Mold et al., 2020) and pay less attention to the gene expression of late-onset AD. Therefore, we firstly investigated the differential gene expression profiling between AD and the healthy. Among the 92 candidate genes, the most significantly upregulated genes were APLNR, GFAP, and AEBP1, while the most down-regulated genes were CHGB, SYT1, and RGS4. With further analysis by WGCNA, we finally obtained 66 differentially expressed genes.

Moreover, SYP and SYT1 were identified as top hub gene nodes in the protein interactions network, suggesting that these two genes play a vital role in the pathogenesis of AD. SYP has been widely demonstrated to cause cognitive disability. It mainly functions as a membrane protein of small synaptic vesicles in the central nerve system (Xiao et al., 2021). It directs the targeting of vesicle-specific membrane protein 2 (synaptobrevin) toward intracellular compartments (Chen et al., 2022). The other vital DEGs are SYT1, encoding synaptotagmin, integral membrane proteins of synaptic vesicles, and serves as a Ca^{2+} sensor in vesicular trafficking and exocytosis (Baker et al., 2018; Shi et al., 2020).

There are several canonical pathways in AD, including inflammatory responses, cholesterol, lipid metabolism, and endosomal vesicle recycling (Guerreiro and Hardy, 2014; Wang et al., 2021). Interestingly, metabolism and cellular biological functions were also observed in this study. It is noted that these DEGs were mainly enriched in exocytosis, synapse, and transport pathways in the GO database. Among them, the most enriched pathway in BPs is neurotransmitter transport and regulation of exocytosis. Apart from this, the most prominent pathway for enrichment in CCs is the presynapse and neuron projection terminus.

In contrast, protein kinase C binding and chloride transmembrane transporter activity are primarily significant pathways. Similarly, the most prominent enrichment in the KEGG database is the synapse, metabolism, and hormone-related pathways. All of the evidence mentioned above suggest that the DEGs between AD and controls are closely related to cell membrane function, transport, synapse, and metabolism.

TABLE 6 Logistic regression analysis of four key genes.

Variable	*B*	Std. err.	Wald	*P*	OR	95% CI
VSNL1	−5.058	1.588	10.147	0.001	0.006	0.000–0.143
RTN1	−5.208	1.768	8.682	0.003	0.005	0.000–0.175
FGF12	2.884	1.495	3.721	0.054	17.891	0.955–335.245
ENC1	2.347	0.851	7.607	0.006	10.458	1.973–55.444

Meanwhile, it is noted that AsymAD is a subtype of preclinical AD characterized as an asymptomatic at-risk state for AD, where beta-amyloids in the brain and CSF are thought to be the primary evidence (Mantzavinos and Alexiou, 2017). Basic scientists indicate that alterations in neurons, microglia, and astroglia drive the disease's insidious progression before cognitive impairment appear (Elahi et al., 2020). In addition, data obtained through imaging studies with PiB-PET also suggests that Aβ deposits may appear up to two decades before the onset of clinical manifestations of dementia. There is growing evidence that pathological changes in AD have occurred 10 years before symptoms arise, but not all AsymADs will translate into SymADs. AsymADs are not the necessary stage of AD. Therefore, in the second part, we discussed the difference between AsymAD and SymAD to find the risk factors for converting AsymAD to SymAD and provide targets for subsequent drug treatment.

In the comparative analysis of AsymAD and SymAD, we obtained 19 genes by intersection. Among them, compared with AD genes through GeneCards[2] and MalaCards[3] databases, we found that CAP2, VSNL1, PAK1, SYP, ENC1, NEFM, ADCYAP1, SVOP, CHGB are related to Alzheimer's disease; LOC387856 (CCDC184) and SYP are associated with dementia. Finally, according to logistic regression analysis, four molecules most related to clinical transformation (VSNL1, RTN1, FGF12, and ENC1) were screened out.

Visinin-like 1 (VSNL1) is a member of a subfamily of neuronal calcium sensor proteins. The encoded visinin-like protein 1 (VILIP-1) upregulates functional α4β2 nicotinic/acetylcholine receptors in hippocampal neurons (Recabarren and Alarcon, 2017). Several studies have shown that in patients with early symptomatic AD, the level of VILIP-1 in cerebrospinal fluid is closely related to whole and regional brain atrophy and is associated with amyloid load in normal individuals in cognition (Tarawneh et al., 2012). Moreover, VILIP-1 influences the intracellular neuronal signaling pathways involved in synaptic plasticity in the central nervous system. It also participates in cyclic nucleotide cascades, nicotinic signaling, and Ca^{2+} homeostasis, leading to neuronal loss (Groblewska et al., 2015). In this study, the expression of VSNL1 in SymAD was significantly downregulated, which was consistent with the results of Mirza and Rajeh (2017).

Reticulon 1 (RTN1) is an endoplasmic reticulum stress protein in the reticulon family involved in endocrine secretion and membrane trafficking. RTN1 is expressed predominantly in neuroendocrine tissues. Its function is mainly implicated in DNA binding or epigenetic modification, neuronal differentiation, and neurodegenerative diseases such as AD (Recabarren and Alarcon, 2017). Considerable evidence suggests that all RTN proteins and receptor NgR are engaged in the pathology change of AD by regulating the beta-site amyloid precursor protein-cleaving enzyme 1 (BACE1) function or APP processing, and thereby product amyloid β in the brain (Kulczynska-Przybik et al., 2021). Previous studies have observed a significant decrease in RTN1 expression in the frontal cortex of AD patients (Kim et al., 2000). Similarly, it was also significantly downregulated in the temporal cortex of symptomatic AD patients here.

The fibroblast growth factor 12 (FGF12) encodes the growth factor family protein involved in nervous system development and the positive regulation of voltage-gated sodium channel activity (Siekierska et al., 2016). FGF family members possess broad cell survival activities and are involved in various biological processes, including embryonic development, cell growth, morphogenesis, tissue repair, tumor growth, and invasion. The PI3K-Akt and apoptotic pathways in fibroblasts are the most relevant pathways to this gene. Gene Ontology annotations closely related FGF12 to growth factor activity and transmembrane transporter binding. This gene has been shown to play an essential role in the pathogenesis of epileptic encephalopathy (Deciphering Developmental Disorders Study, 2017).

The ectodermal-neural Cortex 1 (ENC1) gene is highly expressed in developing neurons and plays a role in the oxidative stress response as a regulator of the transcription factor Nrf2. This gene encodes a member of the kelch-related family of actin-binding proteins, which is implicated in neurite development and neuronal process formation during neuronal differentiation. In addition, ENC1 is upregulated *in vitro* models of neural injuries, such as oxygen-glucose deprivation or toxic intracellular protein aggregation and endoplasmic reticulum stress. Among its related pathways are the glucocorticoid receptor and wnt signaling pathway. Furthermore, based on cognitive, pathological, and genomic data, ENC1 was identified as a potential risk factor in cognitive performance and neuropathological burden in the aging population (White et al., 2017). Similar to other studies, we found a significant decrease in ENC1 expression in the temporal cortex of symptomatic AD patients (Wang et al., 2022).

In addition to the expression changes, the SNP loci of these genes are also worthy of further study. In previous researches, Hollingworth et al. (2012) found that VSNL1 (rs4038131) showed the most robust association with AD

2 https://www.genecards.org

3 https://www.malacards.org

symptoms compared to controls. White et al. (2017) announced that rs76662990G locus in ENC1 was associated with slower cognitive decline in multiple domains. However, there is little evidence for the genetic locus associated with the risk of symptomatic AD, and more analysis and experimental studies are needed to gradually discover the mechanism behind it.

It is worth noting that our integrated dataset included a total of 184 patients with AD and 132 non-AD participants. The number of samples investigated ranged from 6 to 195 cases across the studies. There was no statistical difference among datasets in age. In the same way, we found that a total of 6 data sets obtained from the same platform (GPL10558) were included in the study of Zhang et al. (2019), of which the minimum sample size was 13, and the maximum was as many as 106. The three datasets we selected were also sequenced by using the same platform. Additionally, a total of 4 microarray data sets were included in the study of Yin et al. (2016). The small sample consisted of 22 cases of hepatocellular carcinoma and 21 liver tissue while the large sample covered 225 cases of hepatocellular carcinoma and 220 liver tissue. They also claimed that there was no significant difference between the datasets. We are trying to include as many datasets as possible. Sample size imbalance is inevitable as a consequence which is one of the drawbacks of such research. Researchers need to further think about how to solve this problem to improve the accuracy of analysis.

The result of the present study provides new insight into the earliest biological changes occurring in the brain before the manifestation of clinical AD symptoms. It offers new potential therapeutic targets for early disease intervention. VSNL1, RTN1, FGF12, and ENC1 may be the essential genes that progress asymptomatic AD to symptomatic AD. Moreover, they may serve as genetic risk factors to identify high-risk individuals showing an earlier onset of AD.

Data availability statement

The original contributions presented in this study are included in this article/**Supplementary material**, further inquiries can be directed to the corresponding authors.

Author contributions

JL, SY, and AX conceived and designed the study. YR and YM analyzed the data and composition of figures. WL and HL drafted the manuscript. All authors were involved in writing of the manuscript, gave final approval of the version, and agreed to be accountable for all aspects of the work.

Funding

This study was supported by the grant from the National Natural Science Foundation of China (Nos. 82171178 and 82101271) and the Natural Science Foundation of Guangdong Province (Nos. 2021A1515010705 and 2020A1515110317).

Conflict of interest

The authors declare that the research was conducted in the absence of any commercial or financial relationships that could be construed as a potential conflict of interest.

Publisher's note

Supplementary material

The Supplementary Material for this article can be found online at: https://www.frontiersin.org/articles/10.3389/fnins.2022.1060111/full#supplementary-material

SUPPLEMENTARY FIGURE 1
Data standardization and quality control. **(A,B)** The PCA graph before and after data set processing. **(C,D)** The density map before and after data set processing. **(E)** The box plot of comparison between AD group and control group after dataset processing.

References

Ayodele, T., Rogaeva, E., Kurup, J. T., Beecham, G., and Reitz, C. (2021). Early-Onset Alzheimer's disease: What is missing in research? *Curr. Neurol. Neurosci. Rep.* 21:4.

Baker, K., Gordon, S. L., Melland, H., Bumbak, F., Scott, D. J., Jiang, T. J., et al. (2018). SYT1-associated neurodevelopmental disorder: A case series. *Brain* 141, 2576–2591. doi: 10.1093/brain/awy209

Chen, G., Wang, M., Zhu, P., Wang, G., and Hu, T. (2022). Adverse effects of SYP-3343 on zebrafish development via ROS-mediated mitochondrial dysfunction. *J. Hazard. Mater.* 437:129382. doi: 10.1016/j.jhazmat.2022.129382

Deciphering Developmental Disorders Study (2017). Prevalence and architecture of de novo mutations in developmental disorders. *Nature* 542, 433–438.

Elahi, F. M., Casaletto, K. B., La Joie, R., Walters, S. M., Harvey, D., Wolf, A., et al. (2020). Plasma biomarkers of astrocytic and neuronal dysfunction in early- and late-onset Alzheimer's disease. *Alzheimers Dement.* 16, 681–695. doi: 10.1016/j.jalz.2019.09.004

Groblewska, M., Muszyński, P., Wojtulewska-Supron, A., Kulczyńska-Przybik, A., and Mroczko, B. (2015). The role of Visinin-Like Protein-1 in the pathophysiology of Alzheimer's disease. *J. Alzheimers Dis.* 47, 17–32.

Guerreiro, R., and Hardy, J. (2014). Genetics of Alzheimer's disease. *Neurotherapeutics* 11, 732–737.

Hollingworth, P., Sweet, R., Sims, R., Harold, D., Russo, G., Abraham, R., et al. (2012). Genome-wide association study of Alzheimer's disease with psychotic symptoms. *Mol. Psychiatry* 17, 1316–1327.

Kim, S. H., Yoo, B. C., Broers, J. L., Cairns, N., and Lubec, G. (2000). Neuroendocrine-specific protein C, a marker of neuronal differentiation, is reduced in brain of patients with Down syndrome and Alzheimer's disease. *Biochem. Biophys. Res. Commun.* 276, 329–334. doi: 10.1006/bbrc.2000.3464

Kulczynska-Przybik, A., Mroczko, P., Dulewicz, M., and Mroczko, B. (2021). The Implication of Reticulons (RTNs) in neurodegenerative diseases: From molecular mechanisms to potential diagnostic and therapeutic approaches. *Int. J. Mol. Sci.* 22:4630. doi: 10.3390/ijms22094630

Lefterov, I., Wolfe, C. M., Fitz, N. F., Nam, K. N., Letronne, F., Biedrzycki, R. J., et al. (2019). APOE2 orchestrated differences in transcriptomic and lipidomic profiles of postmortem AD brain. *Alzheimers Res. Ther.* 11:113. doi: 10.1186/s13195-019-0558-0

Mantzavinos, V., and Alexiou, A. (2017). Biomarkers for Alzheimer's disease diagnosis. *Curr. Alzheimer Res.* 14, 1149–1154.

Mirza, Z., and Rajeh, N. (2017). Identification of electrophysiological changes in Alzheimer's disease: A microarray based transcriptomics and molecular pathway analysis study. *CNS Neurol. Disord. Drug Targets* 16, 1027–1038. doi: 10.2174/1871527316666171023153837

Mold, M., Linhart, C., Gómez-Ramírez, J., Villegas-Lanau, A., and Exley, C. (2020). Aluminum and amyloid-β in familial Alzheimer's disease. *J. Alzheimers Dis.* 73, 1627–1635.

Morimoto, S., Ishikawa, M., Watanabe, H., Isoda, M., Takao, M., Nakamura, S., et al. (2020). Brain transcriptome analysis links deficiencies of stress-responsive proteins to the Pathomechanism of Kii ALS/PDC. *Antioxidants* 9:423. doi: 10.3390/antiox9050423

Patel, H., Hodges, A. K., Curtis, C., Lee, S. H., Troakes, C., Dobson, R. J. B., et al. (2019). Transcriptomic analysis of probable asymptomatic and symptomatic Alzheimer brains. *Brain Behav. Immun.* 80, 644–656.

Piras, I. S., Krate, J., Delvaux, E., Nolz, J., Mastroeni, D. F., Persico, A. M., et al. (2019). Transcriptome changes in the Alzheimer's disease middle temporal Gyrus: Importance of RNA metabolism and mitochondria-associated membrane genes. *J. Alzheimers Dis.* 70, 691–713. doi: 10.3233/JAD-181113

Recabarren, D., and Alarcon, M. (2017). Gene networks in neurodegenerative disorders. *Life Sci.* 183, 83–97.

Scheltens, P., De Strooper, B., Kivipelto, M., Holstege, H., Chételat, G., Teunissen, C. E., et al. (2021). Alzheimer's disease. *Lancet* 397, 1577–1590.

Shi, Z., Zhang, K., Zhou, H., Jiang, L., Xie, B., and Wang, R. (2020). Increased miR-34c mediates synaptic deficits by targeting synaptotagmin 1 through ROS-JNK-p53 pathway in Alzheimer's disease. *Aging Cell* 19:e13125.

Siekierska, A., Isrie, M., Liu, Y., Scheldeman, C., Vanthillo, N., Lagae, L., et al. (2016). Gain-of-function FHF1 mutation causes early-onset epileptic encephalopathy with cerebellar atrophy. *Neurology* 86, 2162–2170. doi: 10.1212/WNL.0000000000002752

Spina, S., La Joie, R., Petersen, C., Nolan, A. L., Cuevas, D., Cosme, C., et al. (2021). Comorbid neuropathological diagnoses in early versus late-onset Alzheimer's disease. *Brain* 144, 2186–2198. doi: 10.1093/brain/awab099

Talwar, P., Silla, Y., Grover, S., Gupta, M., Agarwal, R., Kushwaha, S., et al. (2014). Genomic convergence and network analysis approach to identify candidate genes in Alzheimer's disease. *BMC Genomics* 15:199. doi: 10.1186/1471-2164-15-199

Tarawneh, R., Lee, J. M., Ladenson, J. H., Morris, J. C., and Holtzman, D. M. (2012). CSF VILIP-1 predicts rates of cognitive decline in early Alzheimer disease. *Neurology* 78, 709–719.

Wang, H., Bennett, D. A., De Jager, P. L., Zhang, Q. Y., and Zhang, H. Y. (2021). Genome-wide epistasis analysis for Alzheimer's disease and implications for genetic risk prediction. *Alzheimers Res. Ther.* 13:55.

Wang, H., Zhang, Y., Zheng, C., Yang, S., Chen, X., Wang, H., et al. (2022). A 3-Gene-based diagnostic signature in Alzheimer's disease. *Eur. Neurol.* 85, 6–13. doi: 10.1159/000518727

White, C. C., Yang, H. S., Yu, L., Chibnik, L. B., Dawe, R. J., Yang, J., et al. (2017). Identification of genes associated with dissociation of cognitive performance and neuropathological burden: Multistep analysis of genetic, epigenetic, and transcriptional data. *PLoS Med.* 14:e1002287. doi: 10.1371/journal.pmed.1002287

Xiao, Z., Yao, S., Wang, Z. M., Zhu, D. M., Bie, Y. N., Zhang, S. Z., et al. (2021). Multiparametric MRI features predict the SYP gene expression in low-grade glioma patients: A machine learning-based radiomics analysis. *Front. Oncol.* 11:663451. doi: 10.3389/fonc.2021.663451

Yin, F., Shu, L., Liu, X., Li, T., Peng, T., Nan, Y., et al. (2016). Microarray-based identification of genes associated with cancer progression and prognosis in hepatocellular carcinoma. *J. Exp. Clin. Cancer Res.* 35:127.

Zhang, S., Wu, Z., Xie, J., Yang, Y., Wang, L., and Qiu, H. (2019). DNA methylation exploration for ARDS: A multi-omics and multi-microarray interrelated analysis. *J. Transl. Med.* 17:345. doi: 10.1186/s12967-019-2090-1

frontiers | Frontiers in Neuroscience

TYPE Original Research
PUBLISHED 09 January 2023
DOI 10.3389/fnins.2022.1058137

OPEN ACCESS

EDITED BY
Guangzhi Ning,
Tianjin Medical University General Hospital, China

REVIEWED BY
Jianjian Zhang,
Wuhan University, China
Bin Xu,
Fudan University, China

*CORRESPONDENCE
Ruiliang Bai
✉ ruiliangbai@zju.edu.cn
Lin Wang
✉ dr_wang@zju.edu.cn

†These authors have contributed equally to this work

SPECIALTY SECTION
This article was submitted to Translational Neuroscience, a section of the journal Frontiers in Neuroscience

RECEIVED 30 September 2022
ACCEPTED 30 November 2022
PUBLISHED 09 January 2023

CITATION
Hu J, Wang Y, Tong Y, Lin G, Li Y, Chen J, Xu D, Wang L and Bai R (2023) Thalamic structure and anastomosis in different hemispheres of moyamoya disease. *Front. Neurosci.* 16:1058137. doi: 10.3389/fnins.2022.1058137

Thalamic structure and anastomosis in different hemispheres of moyamoya disease

Junwen Hu[1,2†], Yongjie Wang[1,2†], Yun Tong[3†], Gaojun Lin[4], Yin Li[1,2], Jingyin Chen[1,2], Duo Xu[5], Lin Wang[1,2*] and Ruiliang Bai[6,7,8*]

[1]Department of Neurosurgery, The Second Affiliated Hospital, Zhejiang University School of Medicine, Hangzhou, China, [2]Clinical Research Center for Neurological Diseases of Zhejiang, Hangzhou, China, [3]Affiliated Cixi Hospital of Wenzhou Medical University, Ningbo, China, [4]Zhejiang University School of Medicine, Hangzhou, China, [5]Department of Radiology, The Second Affiliated Hospital, Zhejiang University School of Medicine, Hangzhou, China, [6]Key Laboratory of Biomedical Engineering of Ministry of Education, College of Biomedical Engineering and Instrument Science, Zhejiang University, Hangzhou, China, [7]Department of Physical Medicine and Rehabilitation of the Affiliated Sir Run Run Shaw Hospital and Interdisciplinary Institute of Neuroscience and Technology, Zhejiang University School of Medicine, Hangzhou, China, [8]MOE Frontier Science Center for Brain Science and Brain-Machine Integration, School of Brain Science and Brain Medicine, Zhejiang University, Hangzhou, China

Objective: The progression of the asymptomatic hemisphere of moyamoya disease (MMD) is largely unknown. In this study, we investigated the differences in subcortical gray matter structure and angiographic features between asymptomatic and symptomatic hemispheres in patients with MMD.

Methods: We retrospectively reviewed patients with MMD in consecutive cases in our center. We compared subcortical gray matter volume and three types of collaterals (lenticulostriate anastomosis, thalamic anastomosis, and choroidal anastomosis) between symptomatic and asymptomatic hemispheres. Symptomatic hemispheres were classified as ischemic hemisphere (i-hemisphere) and hemorrhagic hemisphere (h-hemisphere). Asymptomatic hemispheres were classified as contralateral asymptomatic hemisphere of i-hemisphere (ai-hemisphere), contralateral asymptomatic hemisphere of h-hemisphere (ah-hemisphere), bilateral asymptomatic hemispheres in asymptomatic group (aa-hemisphere).

Results: A total of 117 MMD patients were reviewed, and 49 of them met the inclusion criteria, with 98 hemispheres being analyzed. The thalamic volume was found to differ significantly between the i- and ai-hemispheres (P = 0.010), between the i- and ah-hemispheres (P = 0.004), as well as between the h- and ai-hemispheres (P = 0.002), between the h- and ah-hemispheres ($P < 0.001$). There was a higher incidence of thalamic anastomosis in the ai-hemispheres than i-hemispheres (31.3% vs. 6.3%, P = 0.070), and in the ah-hemispheres than h-hemispheres (29.6% vs. 11.1%, P = 0.088). Additionally, the hemispheres with thalamic anastomosis had a significantly greater volume than those without thalamic anastomosis (P = 0.024). Univariate and multivariate logistic regression analysis showed that thalamic volume was closely associated with thalamic anastomosis.

Conclusion: The thalamic volume and the incidence of thalamic anastomosis increase in asymptomatic hemispheres and decrease in symptomatic hemispheres. Combining these two characteristics may be helpful in assessing the risk of stroke in the asymptomatic hemispheres of MMD as well as understanding the pathological evolution of the disease.

KEYWORDS

moyamoya disease, brain structure, cerebral angiography, anastomosis, thalamus

Introduction

Moyamoya disease (MMD) is a type of chronic cerebrovascular disease characterized by progressive steno-occlusive changes at the terminal of the internal carotid arteries and the puff of smoke-like vascular network at the base of the brain (Suzuki and Takaku, 1969). Cerebral ischemia and intracranial hemorrhage are the two primary phenotypes of MMD. Despite the development of abnormal vessels on both sides of the brain, patients with MMD do not always have bilateral symptoms (Sun et al., 2022). Thus, there is a distinction between the symptomatic and asymptomatic hemispheres. Considering the potential for an asymptomatic hemisphere to become symptomatic as the disease advances (Kuroda et al., 2007), researchers are keen to understand the progression of the asymptomatic hemisphere (He et al., 2020; Lai et al., 2022).

"Moyamoya" vessels are the notably dilated perforating arteries in the basal ganglia and thalamus that conduct an important collateral circulation (Kuroda and AMORE Study Group, 2015). Abnormal circulation leads to structural changes in the brain. Lenticulostriate, thalamic, and choroidal anastomosis are the three primary collateral patterns of MMD, which have been described in detail in the symptomatic hemispheres (Funaki et al., 2018; Fujimura et al., 2019). However, the knowledge of the collateral circles in the asymptomatic hemisphere is still not known.

The aim of this study was to explore the differences of subcortical gray matter structure and angiographic features between asymptomatic and symptomatic hemispheres in patients with MMD. Clarifying the structural and angiographic characteristics of the asymptomatic hemisphere would be helpful to further understand the natural course of MMD and guide management of the asymptomatic hemispheres.

Materials and methods

Study design and cohort

We retrospectively reviewed consecutive patients diagnosed with MMD who visited our institution between July 2020 and May 2022. The diagnostic criteria were based on digital subtraction angiography (DSA) or magnetic resonance angiography (MRA) which were in accordance with the guideline (Clinical Guidelines Committee and Surgeons Branch of Chinese Medical Doctor Association, 2017). We enrolled adult patients with right-handed, no revascularization surgery before, and who had been free from ischemic/hemorrhagic attack for at least 1 month (Fujimura et al., 2019).

The exclusion criteria were as follows: (1) imaging data did not meet the imaging protocols or angiography lost; (2) hemorrhagic MMD attributed to ruptured intracranial aneurysms or which side of the brain suffering from hemorrhage could not be distinguished; (3) infarction or lesion in subcortical gray matter was excluded, which was considered to affect the structure of the subcortical region. The patients' inclusion and exclusion flowchart was displayed in **Figure 1**. The Human Research Ethics Committee of the Second Affiliated Hospital of Zhejiang University approved this study (ID: 2020-064). Informed consent was obtained from every participant.

According to the clinical presentations and radiological findings, the included MMD patients were divided into ischemic group, hemorrhagic group, and asymptomatic group (without neurological symptoms or only with mild and unspecific symptoms such as headache or dizziness, and with negative findings on MR images). Their hemispheres were classified into five types proposed by Sun et al. (2022): ischemic hemisphere (i-hemisphere), hemorrhagic hemisphere (h-hemisphere), contralateral asymptomatic hemisphere of i-hemisphere (ai-hemisphere), contralateral asymptomatic hemisphere of h-hemisphere (ah-hemisphere), and bilateral asymptomatic hemispheres in asymptomatic group (aa-hemisphere) (**Figure 1**).

Imaging protocol and processing

The MR imaging was completed on a 3T MR scanner (Discovery MR750, GE, Boston, MA, USA) with an 8-channel head coil. T1-weighted images (T1WI) were collected through 3D fast spoiled gradient-echo with repetition time (TR), 7.4 ms; echo time (TE), 3.1 ms; flip angle (FA),

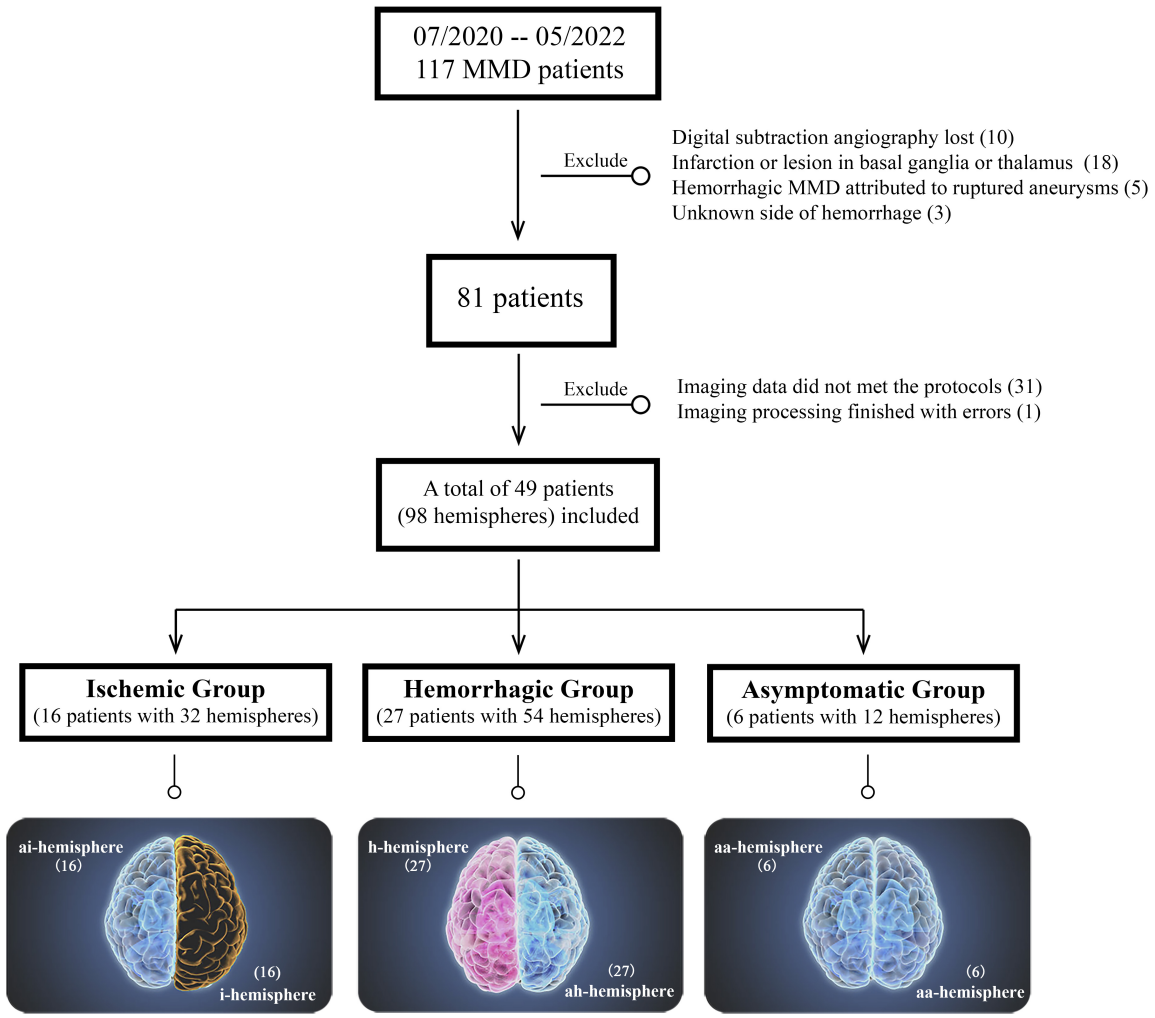

FIGURE 1
Patients' inclusion and exclusion flowchart. The bottom is the classification of different hemispheres in moyamoya disease (MMD).

8°; field of view (FOV), 256 mm × 256 mm; slices, 170; voxel size, 0.8 mm × 0.8 mm × 1.0 mm. T2-Flair images were acquired with TR, 8,400 ms; TE, 145.3 ms; FA, 90°; FOV, 512 mm × 512 mm; slices, 40; voxel size, 0.39 mm × 0.39 mm × 4.0 mm. Though it takes more scanning time for T1WI with high resolution, we get a more accurate structure of the subcortical gray matter. Time-of-flight MRA images were obtained by TR, 21 ms; TE, 2.5 ms; FA, 20°; FOV, 512 mm × 512 mm; slices, 129; voxel size, 0.39 mm × 0.39 mm × 1.4 mm.

Subcortical segmentation and volume calculation of T1WI were processed by FreeSurfer *v*6.0[1] with the "recon-all" pipeline to automatically perform 31 processing steps for each subject, the technical details of these procedures were described in prior publications (Reuter et al., 2012). The volume of the subcortical gray matter (including basal ganglia, thalamus, and hippocampus) of each subject was then extracted. To control for the difference in brain size among subjects and the difference between the left and right hemispheres, the volume of basal ganglia, thalamus, and hippocampus were represented as a ratio to total subcortical gray matter volume.

Collaterals evaluation

Three types of collaterals were classified according to previous research, which was named lenticulostriate anastomosis, thalamic anastomosis, and choroidal anastomosis, respectively (Funaki et al., 2018). Lenticulostriate anastomosis was defined as the anastomosis between the lenticulostriate artery and the cortex through the medial end of the medullary

1 http://surfer.nmr.mgh.harvard.edu

artery (meMedA) with at least 1 artery extending beyond the level of the pericallosal artery. Thalamic anastomosis was defined as the anastomosis between the thalamic perforator and the meMedA or the insular artery with at least 1 perforator extending beyond the position of the medial posterior choroidal artery (ChA). The last type was choroidal anastomosis, which was the anastomosis between the ChA and the meMedA with ChA deviated from the peripheral portion of the lateral ventricle (**Figure 2**; Funaki et al., 2018; Ge et al., 2020).

Each hemisphere of all patients was reviewed by two experienced neurosurgeons (Dr. Hu and Dr. Li) who were completely blinded to the patients' clinical information through the anteroposterior and lateral views on DSA. If there was any difference, another senior neurosurgeon (Dr. Wang) was invited to discuss and reach a final consensus.

Statistical analysis

Continuous variables were presented as the mean ± SD. The *t*-tests and Mann–Whitney *U* tests were used as appropriate when performed to determine group difference. The difference in the subcortical volume between groups was compared using the one-way ANOVA tests. The proportion of positive anastomosis and other categorical variables between groups were compared by the chi-square test. All variables from the univariate analysis using binary logistic regression with a $P < 0.15$ were further moved into a forward-stepwise multivariate analysis. Analyses were performed using SPSS *v*25 software (IBM, Armonk, NY, USA) and GraphPad Prism *v*8.0 (GraphPad Software, San Diego, CA, USA). Two-sided values of $P < 0.05$ was considered as statistically significant. All data generated and analyzed are available on reasonable request.

Results

In this consecutive cohort of 117 patients with MMD, 10 patients had no documented DSA data; 18 patients had significant lesion in subcortical gray matter region; five patients had hemorrhage due to ruptured aneurysm; In three patients it was unable to distinguish the side of hemorrhage because of the equal volume of intraventricular hemorrhage in both sides; 31 patients did not met the imaging protocols of high-resolution T1WI; and 1 patient had an unknown error when performing image processing. The aforementioned patients were excluded from this study.

Finally, 49 patients with 98 hemispheres were enrolled. Among them, there were 16 patients in the ischemic group (including both 16 i- and ai-hemispheres) with symptoms including transient ischemic attack (n = 7, 43.8%), cerebral ischemia (n = 7, 43.8%), and paresthesia (n = 2, 12.5%). Twenty-seven patients were hemorrhagic MMD (including both 27 h- and ah-hemispheres) with the most frequent manifestation was primary intraventricular hemorrhage (IVH) (n = 9, 33.3%), followed by IVH with intracerebral hemorrhage (ICH) (n = 8, 29.6%), subarachnoid hemorrhage (SAH) (n = 3, 11.1%), IVH with SAH (n = 2, 7.4%), and ICH only (n = 5, 18.5%). And 6 cases in the asymptomatic group with 12 aa-hemispheres.

A total of 12 patients were ischemic MMD with symptoms including transient ischemic attack (n = 6, 27.3%), cerebral ischemia (n = 1, 4.5%), dizziness (n = 4, 18.2%), and headache (n = 1, 4.5%). A total of 10 patients were hemorrhagic MMD with the most frequent manifestation was primary IVH (n = 5, 22.7%), followed by IVH with ICH (n = 2, 9.1%), IVH with subarachnoid hemorrhage (n = 1, 4.5%), and ICH only (n = 2, 23.9%).

Demographical and clinical characteristics

Table 1 summarizes the baseline characteristics of 49 patients enrolled in this study. The percentage of females was 85.7% (42/49) in total. There was no statistical difference in age, gender, body mass index (BMI), other personal/medical histories and Suzuki stage between the groups, except modified Rankin Scale (mRS) at admission (P = 0.006).

Subcortical volume between different MMD hemispheres

A significant difference was noted in thalamic volume between the i- and ai-hemispheres (P = 0.010), the i- and ah-hemispheres (P = 0.004), the h- and ai-hemispheres (P = 0.002), as well as the h- and ah-hemispheres ($P < 0.001$) (**Figure 3A**). The putamen also displayed a significant difference between the i- and ai-hemispheres (P = 0.030), and the i- and ah-hemispheres (P = 0.034) (**Figure 3B**). As for other subcortical gray matter volumes, no statistical differences were found between the groups (**Figures 3C–F**). The total subcortical gray matter volume did not differ statistically between the different groups (**Supplementary Figure 1**).

Collateral feature in different hemispheres

We observed lenticulostriate anastomosis was found in 24.9% of hemispheres, thalamic anastomosis in 19.0% of hemispheres, and choroidal anastomosis in 38.6% of hemispheres. There were no significant differences in the incidence of lenticulostriate anastomosis among the groups (**Figure 4A**). A difference toward statistical significance in the

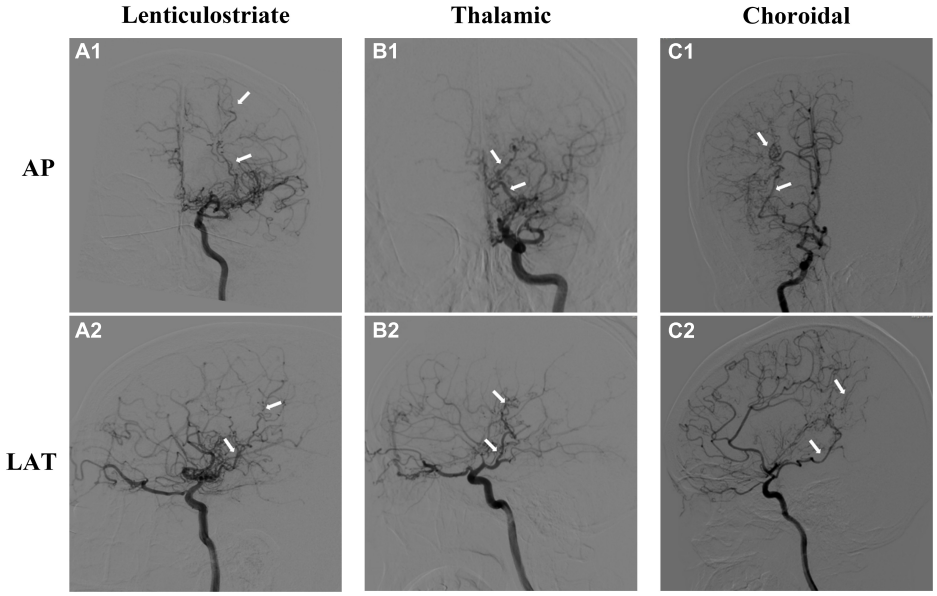

FIGURE 2
Three types of moyamoya disease (MMD) collaterals. The upper is the anteroposterior (AP) view of angiographic images, and the lower is the lateral (LAT) view. **(A1,A2)** Lenticulostriate anastomosis; **(B1,B2)** thalamic anastomosis; **(C1,C2)** choroidal anastomosis. The dilated and extended arteries are labeled with white arrows.

TABLE 1 Baseline characteristics of enrolled MMD patients.

	Ischemic group (16)	Hemorrhagic group (27)	Asymptomatic group (6)	*P*-value
Age (years)	45.9 ± 8.8	45.8 ± 7.5	46.3 ± 9.7	0.990
Gender (men/women)	2/14	5/22	0/6	0.488
BMI (kg/m^2)	22.9 ± 2.3	23.1 ± 3.4	24.4 ± 4.1	0.577
Smoking (%)	2 (12.5%)	5 (18.5%)	0 (0%)	0.488
Alcohol (%)	1 (6.3%)	5 (18.5%)	0 (0%)	0.307
Hypertension (%)	6 (37.5%)	4 (18.2%)	1 (16.7%)	0.212
Diabetes mellitus (%)	1 (6.3%)	3 (11.1%)	2 (33.3%)	0.218
Hyperlipidemia (%)	5 (31.3%)	10 (45.5%)	1 (16.7%)	0.623
mRS at admission				0.006*
0	4	18	6	
1	10	5	0	
2	2	4	0	
Suzuki stage[#]				0.801
1	0	0	0	
2	2	5	2	
3	4	8	2	
4	7	9	2	
5	1	4	0	
6	2	1	0	

MMD, moyamoya disease; BMI, body mass index; mRS, modified Rankin Scale. *$P < 0.01$. [#]The Suzuki stage was evaluated in both hemispheres and displayed the higher value here.

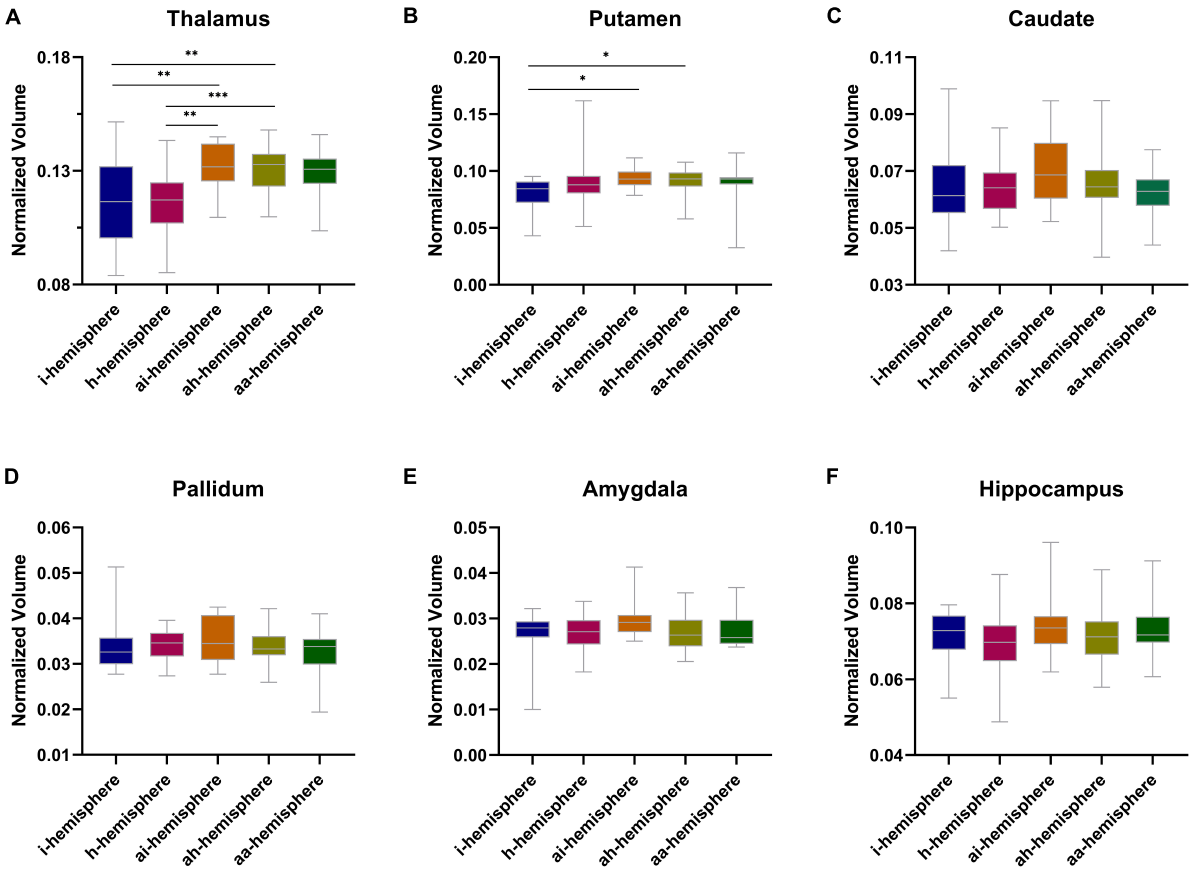

FIGURE 3
(A–F) Normalized subcortical gray matter volume between different hemispheres in moyamoya disease (MMD). $^{*}P < 0.05$, $^{**}P < 0.01$, $^{***}P < 0.001$.

incidence of thalamic anastomosis was noted between the i- and ai-hemispheres (6.3% vs. 31.3%, $P = 0.070$), and between the h- and ah-hemispheres (11.1% vs. 29.6%, $P = 0.088$) (Figure 4B). The h-hemispheres had a significantly higher incidence of choroidal anastomosis than the i-hemispheres (18.8% vs. 51.9%, $P = 0.032$) (Figure 4C). Table 2 showed every P-value between the different hemispheres.

Higher thalamic volume in hemispheres with thalamic anastomosis

The thalamic volumes of the hemispheres with and without thalamic anastomosis was further compared. The results indicated that the hemispheres with thalamic anastomosis had significantly greater volume than those without this anastomosis ($P = 0.024$) (Figure 4D). In addition, the results of univariate logistic analysis found that gender (OR, 0.36; 95% CI: 0.11–1.24; $P = 0.105$), BMI (OR, 1.16; 95% CI: 0.98–1.36; $P = 0.077$) and thalamic volume (OR, 1.59; 95% CI: 1.05–2.42; $P = 0.029$) were associated with thalamic anastomosis. Furthermore, the multivariate logistic analysis indicated that thalamic volume (OR, 1.68; 95% CI: 1.07–2.63; $P = 0.024$) was the only factor that related to thalamic anastomosis (Table 3).

Discussion

Identifying the brain volume, which is an important component of brain structure (Salinas et al., 2021), as well as angiographic features is an essential part of the research on MMD, as it can provide further information about the pathogenesis and neuropathology of the disease (Kazumata et al., 2019, 2020; Tahedl, 2020; Sun et al., 2022). However, previous studies have focused primarily on the symptomatic hemisphere. There has been no comparative study of the hemispheres with different characteristics, which is important for exploring the progression of MMD. Moreover, the proliferation of abnormal blood vessels in MMD initially develops at the skull base, which has a close relationship with the central core. Thus, we designed this study to examine the

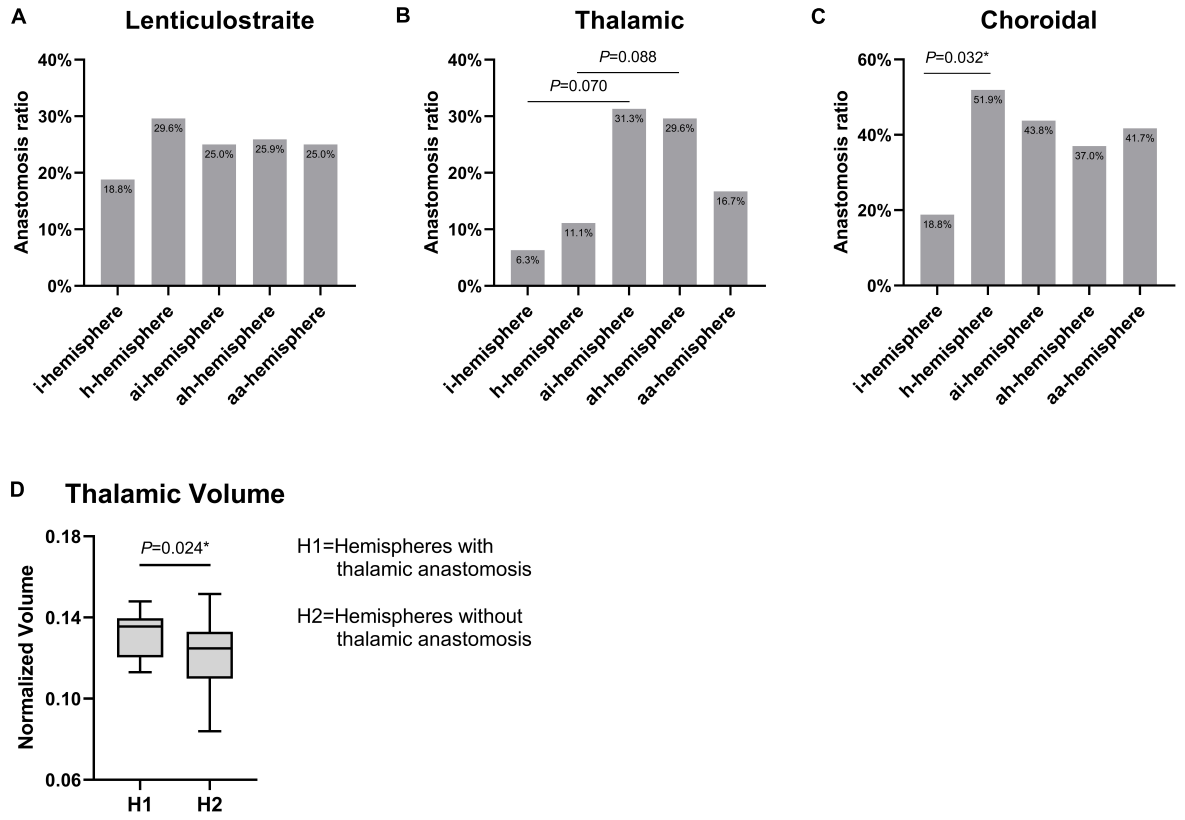

FIGURE 4
(A–C) Comparison of three types of collateral features among different hemispheres in moyamoya disease (MMD). **(D)** The difference of thalamic volume between hemispheres with thalamic anastomosis and those without thalamic anastomosis. *$P < 0.05$.

subcortical gray matter volume and collateral anastomosis in the different hemispheres of MMD, as well as the relationship between the two features.

Cerebral blood supply and hemodynamics are closely related to the brain structure (Zonneveld et al., 2015), decreased cerebral perfusion may contribute to brain atrophy (Alosco et al., 2013). Moon et al. (2020) demonstrated that subcortical gray matter volume decreases in patients with MMD using high-resolution imaging, but due to the small sample size and combined analyses of the symptomatic and asymptomatic hemispheres, the decreased volume had no statistical difference from healthy controls. Our study first examined subcortical gray matter volume between the different types of hemispheres in MMD and found that the thalamic volume in the symptomatic hemispheres (i- and h-hemispheres) was significantly smaller than that in contralateral asymptomatic hemispheres (ai- and ah-hemispheres).

We next investigated the angiographic feature between the hemispheres. The proportion of three different types of collateral anastomosis in this cohort was comparable to that of previous studies (Funaki et al., 2018; Fujimura et al., 2019). There was, for example, no difference between hemorrhagic and ischemic MMD in the incidence of lenticulostriate anastomosis, and hemorrhagic MMD had a significantly higher rate of choroidal anastomosis. Interestingly, the thalamic anastomosis rate in the symptomatic hemispheres (i- and h-hemispheres) was lower than that in the contralateral asymptomatic hemisphere (ai- and ah-hemispheres). Due to the limited sample size, the difference was not statistically significant, but the trend was evident.

Increased thalamic volume and the incidence of thalamic anastomosis in the asymptomatic hemisphere prompted us to explore the relationship between the two characteristics. Thalamic anastomosis arises from the thalamotuberal artery and thalamoperforating artery, which originate from the posterior communicating artery and posterior cerebral artery, respectively (Funaki et al., 2018). Both of these vessels are the primary blood supply of the thalamus (Bordes et al., 2020). The univariate and multivariate logistic analysis showed that there was a strong correlation between the thalamic volume and the incidence of thalamic anastomosis. Additionally, it has also been demonstrated in a previous study that increased cerebral blood flow corresponds to a larger brain volume (Erickson et al., 2011). Thus, we suggested that the thalamic volume increases as a result of the development of thalamic anastomosis.

TABLE 2 Comparison of three types of collateral feature in different hemispheres.

	i-hemispheres	h-hemispheres	ai-hemispheres	ah-hemispheres
Lenticulostriate anastomosis				
i-hemispheres	/	/	/	/
h-hemispheres	0.340			
ai-hemispheres	0.500	0.515		
ah-hemispheres	0.442	0.500	0.621	
aa-hemispheres	0.521	0.544	0.672	0.640
Thalamic anastomosis				
i-hemispheres	/	/	/	/
h-hemispheres	0.521			
ai-hemispheres	0.070	0.101		
ah-hemispheres	0.069	0.088	0.587	
aa-hemispheres	0.389	0.494	0.334	0.332
Choroidal anastomosis				
i-hemispheres	/	/	/	/
h-hemispheres	0.032*			
ai-hemispheres	0.126	0.422		
ah-hemispheres	0.180	0.206	0.453	
aa-hemispheres	0.183	0.406	0.609	0.528

*$P < 0.05$.

The results of this study can be interpreted in two different ways. The first is that the hemispheres with a small thalamic volume and a lower incidence of thalamic anastomosis are more likely to suffer a stroke. The second assumption is that in the symptomatic hemispheres, thalamic anastomosis contracts after a stroke attack, which further causes atrophy of the thalamus. While in the ai- and ah-hemispheres, the thalamic volume and thalamic anastomosis are better preserved. Therefore, the combination of these two characteristics may provide insight into the risk of stroke in the asymptomatic hemispheres of MMD and the pathological development of the disease.

TABLE 3 Univariate and multivariate logistic regression analysis of factors associated with thalamic anastomosis.

Variables	Univariate		Multivariate	
	OR (95% CI)	*P*-value	OR (95% CI)	*P*-value
Age	0.98 (0.92–1.05)	0.586		
Gender	**0.36 (0.11–1.24)**	**0.105**	**2.84 (0.76–10.54)**	**0.120**
BMI	**1.16 (0.98–1.36)**	**0.077**	**1.18 (0.99–1.40)**	**0.061**
Smoking	0.54 (0.15–1.97)	0.353		
Alcohol	0.69 (0.17–2.82)	0.601		
Hypertension	0.77 (0.24–2.43)	0.653		
Diabetes mellitus	1.75 (0.20–15.14)	0.611		
Hyperlipidemia	1.45 (0.47–4.47)	0.513		
mRS at admission	0.82 (0.39–1.72)	0.593		
Suzuki stage	1.19 (0.79–1.79)	0.420		
Thalamic volume	**1.59 (1.05–2.42)**	**0.029***	**1.68 (1.07–2.63)**	**0.024***

OR, odds ratio; CI, confidence interval; BMI, body mass index; mRS, modified Rankin Scale. *$P < 0.05$.
The bold values indicate that three variables were analyzed in a univariate analysis with a $P < 0.15$ and are further analyzed in a multivariate analysis.

There are several limitations to be noted. Firstly, after taking into account certain factors that may influence the results of this study, the sample size appears to be small, which, in turn, limits the generalizability of the findings. A multicenter, large-sample study is needed to verify our results. Secondly, all of the patients included in this study were independent in their daily lives (scores between 0 and 2 on mRS), which might lead to a selection bias. Thirdly, Fujimura et al. (2019) have classified three types of anastomosis into two grades; however, it is unknown whether each grade has a different thalamic volume.

Conclusion

In adult patients with MMD, the thalamic volume and the incidence of thalamic anastomosis increase in asymptomatic hemispheres and decrease in symptomatic hemispheres. Combining these two characteristics may be helpful in assessing the risk of stroke in the asymptomatic hemispheres of MMD as well as understanding the pathological evolution of the disease.

Data availability statement

The raw data supporting the conclusions of this article will be made available by the authors, without undue reservation.

Ethics statement

The studies involving human participants were reviewed and approved by the Human Research Ethics Committee of the Second Affiliated Hospital of Zhejiang University (ID: 2020-064). The patients/participants provided their written informed consent to participate in this study.

Author contributions

JH and YW wrote the manuscript and collected the data. YT revised the manuscript. GL helped to evaluate statistical results. YL and JC assisted in writing the manuscript and contributed to the analysis of data. DX assisted in the MRI scan. JH, YL, and LW reviewed all imaging data. LW and RB conceived and designed the manuscript. All authors contributed to this article and approved the submitted version.

Funding

The National Natural Science Foundation of China provided the funding for this work (grant number 81870910), as well as the Key R&D Program of Zhejiang (No. 2022C03133).

Acknowledgments

We would like to thank Bai Lab of ZIINT from Zhejiang University for providing a robust and powerful database environment.

Conflict of interest

The authors declare that the research was conducted in the absence of any commercial or financial relationships that could be construed as a potential conflict of interest.

Publisher's note

All claims expressed in this article are solely those of the authors and do not necessarily represent those of their affiliated organizations, or those of the publisher, the editors and the reviewers. Any product that may be evaluated in this article, or claim that may be made by its manufacturer, is not guaranteed or endorsed by the publisher.

Supplementary material

The Supplementary Material for this article can be found online at: https://www.frontiersin.org/articles/10.3389/fnins.2022.1058137/full#supplementary-material

References

Alosco, M. L., Gunstad, J., Jerskey, B. A., Xu, X., Clark, U. S., Hassenstab, J., et al. (2013). The adverse effects of reduced cerebral perfusion on cognition and brain structure in older adults with cardiovascular disease. *Brain Behav.* 3, 626–636. doi: 10.1002/brb3.171

Bordes, S., Werner, C., Mathkour, M., McCormack, E., Iwanaga, J., Loukas, M., et al. (2020). Arterial supply of the thalamus: A comprehensive review. *World Neurosurg.* 137, 310–318. doi: 10.1016/j.wneu.2020.01.237

Clinical Guidelines Committee and Surgeons Branch of Chinese Medical Doctor Association (2017). Consensus of Chinese experts on the diagnosis and treatment of moyamoya disease and moyamoya syndrome. *Chin. J. Neurosur.* 33, 541–547. doi: 10.1186/s13023-019-1137-y

Erickson, K. I., Voss, M. W., Prakash, R. S., Basak, C., Szabo, A., Chaddock, L., et al. (2011). Exercise training increases size of hippocampus and improves memory. *Proc. Natl. Acad. Sci. U.S.A.* 108, 3017–3022. doi: 10.1073/pnas.1015950108

Fujimura, M., Funaki, T., Houkin, K., Takahashi, J. C., Kuroda, S., Tomata, Y., et al. (2019). Intrinsic development of choroidal and thalamic collaterals in hemorrhagic-onset moyamoya disease: case-control study of the Japan Adult Moyamoya Trial. *J. Neurosurg.* 130, 1453–1459. doi: 10.3171/2017.11.JNS171990

Funaki, T., Takahashi, J. C., Houkin, K., Kuroda, S., Takeuchi, S., Fujimura, M., et al. (2018). Angiographic features of hemorrhagic moyamoya disease with high recurrence risk: a supplementary analysis of the Japan Adult Moyamoya Trial. *J. Neurosurg.* 128, 777–784. doi: 10.3171/2016.11.JNS161650

Ge, P., Zhang, Q., Ye, X., Liu, X., Deng, X., Wang, J., et al. (2020). Different subtypes of collateral vessels in hemorrhagic moyamoya disease with p.R4810K variant. *BMC Neurol.* 20:308. doi: 10.1186/s12883-020-01884-0

He, S., Duan, R., Liu, Z., Ye, X., Yuan, L., Li, T., et al. (2020). Characteristics of cognitive impairment in adult asymptomatic moyamoya disease. *BMC Neurol.* 20:322. doi: 10.1186/s12883-020-01898-8

Kazumata, K., Tha, K. K., Tokairin, K., Ito, M., Uchino, H., Kawabori, M., et al. (2019). Brain structure, connectivity, and cognitive changes following revascularization surgery in adult moyamoya disease. *Neurosurgery* 85, E943–E952. doi: 10.1093/neuros/nyz176

Kazumata, K., Tokairin, K., Ito, M., Uchino, H., Sugiyama, T., Kawabori, M., et al. (2020). Combined structural and diffusion tensor imaging detection of ischemic injury in moyamoya disease: relation to disease advancement and cerebral hypoperfusion. *J. Neurosurg.* 134, 1155–1164. doi: 10.3171/2020.1.JNS193260

Kuroda, S., and AMORE Study Group (2015). Asymptomatic moyamoya disease: Literature review and ongoing AMORE study. *Neurol. Med. Chir. (Tokyo)* 55, 194–198. doi: 10.2176/nmc.ra.2014-0305

Kuroda, S., Hashimoto, N., Yoshimoto, T., and Iwasaki, Y. (2007). Research committee on moyamoya disease in J. Radiological findings, clinical course, and outcome in asymptomatic moyamoya disease: results of multicenter survey in Japan. *Stroke* 38, 1430–1435. doi: 10.1161/STROKEAHA.106.478297

Lai, P. M. R., Gomez-Paz, S., Patel, N. J., Frerichs, K. U., Thomas, A. J., Aziz-Sultan, M. A., et al. (2022). Asymptomatic moyamoya disease in a north american

adult cohort. *World Neurosurg.* 161, e146–e153. doi: 10.1016/j.wneu.2022.01.076

Moon, H. C., Oh, B. H., Cheong, C., Kim, W. S., Min, K. S., Kim, Y. G., et al. (2020). Precentral and cerebellar atrophic changes in moyamoya disease using 7-T magnetic resonance imaging. *Acta Radiol.* 61, 487–495. doi: 10.1177/0284185119866808

Reuter, M., Schmansky, N. J., Rosas, H. D., and Fischl, B. (2012). Within-subject template estimation for unbiased longitudinal image analysis. *Neuroimage* 61, 1402–1418. doi: 10.1016/j.neuroimage.2012.02.084

Salinas, J., O'Donnell, A., Kojis, D. J., Pase, M. P., DeCarli, C., Rentz, D. M., et al. (2021). Association of social support with brain volume and cognition. *JAMA Netw. Open* 4:e2121122. doi: 10.1001/jamanetworkopen.2021.21122

Sun, H., Li, W., Xia, C., Ren, Y., Ma, L., Xiao, A., et al. (2022). Angiographic and hemodynamic features in asymptomatic hemispheres of patients with moyamoya disease. *Stroke* 53, 210–217. doi: 10.1161/STROKEAHA.121.035296

Suzuki, J., and Takaku, A. (1969). Cerebrovascular "moyamoya" disease. Disease showing abnormal net-like vessels in base of brain. *Arch. Neurol.* 20, 288–299. doi: 10.1001/archneur.1969.00480090076012

Tahedl, M. (2020). Towards individualized cortical thickness assessment for clinical routine. *J. Transl. Med.* 18:151. doi: 10.1186/s12967-020-02317-9

Zonneveld, H. I., Loehrer, E. A., Hofman, A., Niessen, W. J., van der Lugt, A., Krestin, G. P., et al. (2015). The bidirectional association between reduced cerebral blood flow and brain atrophy in the general population. *J. Cereb. Blood Flow Metab.* 35, 1882–1887. doi: 10.1038/jcbfm.2015.157

frontiers | Frontiers in Neuroscience

TYPE Original Research
PUBLISHED 19 January 2023
DOI 10.3389/fnins.2022.1031712

OPEN ACCESS

EDITED BY
Bo Li,
Sun Yat-sen University, China

REVIEWED BY
Weitao Man,
Tsinghua University, China
Chunlei Shan,
Shanghai University of Traditional Chinese Medicine, China

*CORRESPONDENCE
Shouwei Yue
✉ shouweiy@sdu.edu.cn
Hao Zhang
✉ crrczh2020@163.com

SPECIALTY SECTION
This article was submitted to Translational Neuroscience, a section of the journal Frontiers in Neuroscience

RECEIVED 30 August 2022
ACCEPTED 30 December 2022
PUBLISHED 19 January 2023

CITATION
Dang H, Su W, Tang Z, Yue S and Zhang H (2023) Prediction of motor function in patients with traumatic brain injury using genetic algorithms modified back propagation neural network: a data-based study. *Front. Neurosci.* 16:1031712. doi: 10.3389/fnins.2022.1031712

Prediction of motor function in patients with traumatic brain injury using genetic algorithms modified back propagation neural network: a data-based study

Hui Dang[1,2,3], Wenlong Su[2,3], Zhiqing Tang[2], Shouwei Yue[1]* and Hao Zhang[2,1,3]*

[1]Cheeloo College of Medicine, Shandong University, Jinan, Shandong, China, [2]China Rehabilitation Research Center, Beijing, China, [3]School of Health and Life Sciences, University of Health and Rehabilitation Sciences, Qingdao, Shandong, China

Objective: Traumatic brain injury (TBI) is one of the leading causes of death and disability worldwide. In this study, the characteristics of the patients, who were admitted to the China Rehabilitation Research Center, were elucidated in the TBI database, and a prediction model based on the Fugl-Meyer assessment scale (FMA) was established using this database.

Methods: A retrospective analysis of 463 TBI patients, who were hospitalized from June 2016 to June 2020, was performed. The data of the patients used for this study included the age and gender of the patients, course of TBI, complications, and concurrent dysfunctions, which were assessed using FMA and other measures. The information was collected at the time of admission to the hospital and 1 month after hospitalization. After 1 month, a prediction model, based on the correlation analyses and a 1-layer genetic algorithms modified back propagation (GA-BP) neural network with 175 patients, was established to predict the FMA. The correlations between the predicted and actual values of 58 patients (prediction set) were described.

Results: Most of the TBI patients, included in this study, had severe conditions (70%). The main causes of the TBI were car accidents (56.59%), while the most common complication and dysfunctions were hydrocephalus (46.44%) and cognitive and motor dysfunction (65.23 and 63.50%), respectively. A total of 233 patients were used in the prediction model, studying the 11 prognostic factors, such as gender, course of the disease, epilepsy, and hydrocephalus. The correlation between the predicted and the actual value of 58 patients was R^2 = 0.95.

Conclusion: The genetic algorithms modified back propagation neural network can predict motor function in patients with traumatic brain injury, which can be used as a reference for risk and prognosis assessment and guide clinical decision-making.

KEYWORDS

TBI, back propagation neural network, prediction model, FMA, database

1. Introduction

Traumatic brain injury (TBI) is not a one-time event but a condition, which is one of the leading causes of death and disability worldwide. This disease can develop among people of any age, often causing labor loss (Brain and Spinal Injury Center, 2021). With the development of medicine, the survival rate of patients, suffering from multi-degree TBI, increased and the number of disabilities in patients decreased, improving the quality of patients' life and their social issues (Pickelsimer et al., 2006). It is essential to predict the functional outcome, which improves the therapeutic schedule and adjusts personal livelihood (Yu et al., 2015).

In the previous studies, which predicted the mortality and GCS score, the indicators, such as GCS score, pupil response, and laboratory examination, were mainly identified in the acute phase after trauma (Roberts et al., 2004; Hukkelhoven et al., 2005; Perel et al., 2006, 2008; Rogers et al., 2010; Subaiya et al., 2012; Ercole et al., 2021). As compared to the patients in the acute phase, those in the chronic phase tended to be stable with decreased cerebral edema, and fewer acute intracranial lesions, which were favorable factors for the prediction of prognosis. However, many factors, such as rehabilitation therapies, location of the lesion, limb complications, etc., might affect the outcome of motor function.

As dysfunction is a common outcome of moderate to severe TBI. The alleviation of dysfunction and improvement of the quality of life are the primary research focus. The indicators, including GCS and pupil response, are not suitable for the prediction of outcomes in the chronic phase. Therefore, the degree of dysfunction in the patients with TBI, especially the motor function, is needed to be predicted (Perel et al., 2008; Reith et al., 2017). In the current clinical practices, the rehabilitation assessment, such as the functional independence measure (FIM), which assesses the overall prognosis of living ability, and the Fugl-Myer assessment scale (FMA), which assesses the motor function, might be used to cope with this deficiency (Ottenbacher et al., 1996; Segal et al., 1996; Zarshenas et al., 2019). The current study focused on the FMA and its effects on the upper and lower limbs.

Corticosteroid Randomization After Significant Head Injury (CRASH) and International Traumatic Brain Injury Clinical Trials Prognosis and Analysis Task (IMPACT) are relatively mature models, which can predict the outcome of TBI; their prognostic potential has been evaluated (Boyd et al., 1987; Dodds et al., 1993; Edwards et al., 2005; Rogers et al., 2010; Ercole et al., 2021). The foundation and validation of the prediction model are based on TBI clinical trials, including Collaborative European Neurotrauma Effectiveness Research in TBI (CENTER-TBI), Translational Research, and Clinical Knowledge in TBI (TRACK-TBI), and Japan Neurotrauma Database (JNTDB) (Steyerberg et al., 2008; Maeda et al., 2019; Gao et al., 2020). Based on the available data, the prediction models were built using statistical models, such as correlation, regression, non-linear fitting, and artificial neural networks (ANN) analyses. Although the previously established model could not predict FMA in the patients with dysfunction after TBI, these methods can be used to establish a prediction model.

The backpropagation (BP) neural model is one of the most common and mature models based on ANN. A large number of studies have used ANN to predict the prognosis and complications of TBI. However, these models focus on the outcome prediction, such as mortality, rather than the function prediction. This study aimed to use the BP neural network model for predicting the FMA outcome in TBI patients in the chronic phase.

2. Methodology

2.1. Research design

In this study, the measures were retrospectively analyzed at the time of the patient's admission to the Beijing Boai hospital and during hospitalization. The possible indicators, which were related to the motor function of the patients, were also analyzed. The demographic information of the patients, excluding their personal information, was collected. The study was approved by the Medical Ethics Committee of China Rehabilitation Research Center (No. 2021-026-1).

2.2. Data source and population

A total of 463 TBI patients, who were admitted to the China Rehabilitation Research Center from June 2016 to June 2020, were enrolled in this study. According to the International Statistical Classification of Diseases and Related Health Problems-tenth edition (ICD-10),the diagnosis of the hospitalized patients in this study included TBI (S06.902), traumatic intracranial hematoma (S06.806), diffuse axonal injury (S06.204), concussion (S06.001), subdural hematoma (S06.501), epidural hematoma (S06.401), traumatic subarachnoid hemorrhage (S06.601), and brain contusion and laceration (S06.201).

TABLE 1 The information of predictive factors.

	Overall (n = 233)	Male (n = 171)	Female (n = 62)
Course of disease (d)			
<30	11 (4.72%)	7 (4.09%)	4 (6.45%)
30∼90	68 (29.18%)	55 (32.16%)	13 (20.97%)
90∼180	70 (30.04%)	49 (28.65%)	21 (33.87%)
180∼365	45 (19.31%)	27 (15.79%)	18 (29.03%)
>365	39 (16.74%)	33 (19.30%)	6 (9.68%)
Complications and dysfunctions			
Hydrocephalus	85 (36.48%)	60 (35.09%)	25 (40.32%)
Epilepsy	57 (24.46%)	47 (27.49%)	10 (16.13%)
Aphasia	110 (47.21%)	78 (45.61%)	32 (51.61%)
Other*	82 (35.19%)	52 (30.41%)	30 (48.39%)
Treatment			
Tracheotomy	147 (63.09%)	107 (62.57%)	40 (64.52%)
Rehabilitation therapy	182 (78.11%)	128 (74.85%)	54 (87.10%)
Admission assessment			
FMA	57.59 ± 33.94	60.12 ± 33.86	50.63 ± 33.47
FMB	6.67 ± 4.75	6.86 ± 4.71	6.12 ± 4.87

*Other, including disuse syndrome, shoulder subluxation or shoulder-hand syndrome; FMA, Fugl-Myer assessment scale; FMB, balance subscale of the Fugl-Meyer test.

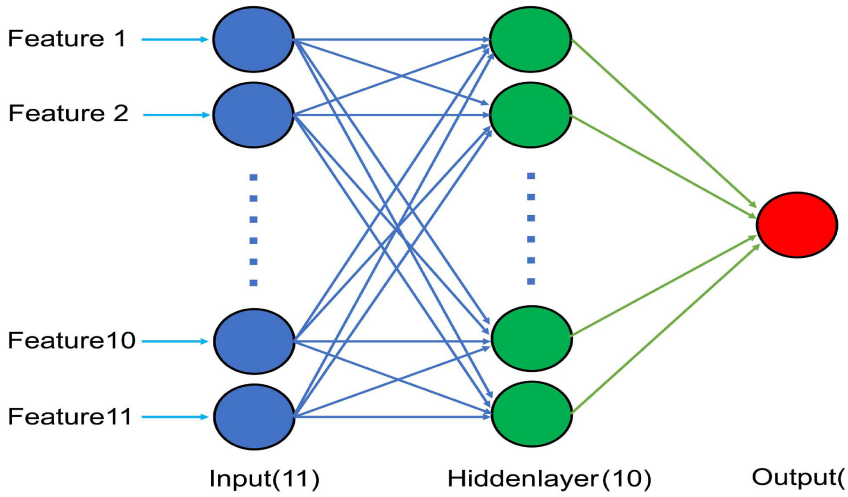

FIGURE 1
Schematic diagram of the optimal BP neural network model with 11 input nodes, 10 nodes in a hidden layer, and a single output node.

The criteria for the inclusion of patients in this included (1) definitive diagnosis of TBI; (2) complete availability of required data; and (3) the patients performed physical and occupying therapy during hospitalization. The criteria for the exclusion of patients from this included (1) the patients with the disorders of consciousness; (2) the patients in unstable periods; (3) the patients with dyskinesia caused by fractures or any other reason; (4) the patients, who were hospitalized for less than 4 weeks; and (5) the patients, who did not cooperate due to other reasons.

2.3. Data preparation

In this study, the data of the patient's age, gender, course of TBI, years of education, marital status, occupation, place of residence (urban or rural), history of tobacco and alcohol use, medical history, injury location, cause of injury, lesion laterality, type of surgery, skull defect, clinical symptoms, diagnosis, tracheotomy, complications, such as epilepsy, hydrocephalus and aphasia, mental or emotional disorders, motor dysfunction, such as shoulder subluxation, shoulder-hand syndrome, disuse syndrome, and joint spasm, and rehabilitation therapies, etc., was collected. The measures, including Fugl-Meyer balance scale (FMB), Hand Practicability assessment scale, Mini-Mental State Examination Scale (MMSE), and Fugl-Meyer assessment scale (FMA), were calculated at the time of the patient's admission to the hospital, and the FMA scores were calculated after 4 weeks of admission.

Data scoring: TBI was given scores, ranging from 1 to 5 for $<$1 month, 1–3 months, 3–6 months, 4 months–1 years, and $>$1 year, respectively. The male and female patients were indicated by 0 and 1, respectively. The presence and absence of other complications or treatments were indicated by 1 and 0, respectively. Pearson correlation was performed using SPSS 25 for determining the factors related to the outcome (4 weeks after admission), which were also included in the establishment of the prognosis model. For each input and output item, the score was recorded as $P_{(initial)}$, while the highest score was recorded as $P_{(maximum)}$. The score of each patient was calculated as $P = P_{(initial)}/P_{(maximum)}$. The scores of all items were used as input in the predicting model.

2.4. Data analysis and model construction

The correlation analysis showed that the factors, including gender, course of TBI, rehabilitation treatment, epilepsy or hydrocephalus, aphasia, tracheotomy, concurrent dysfunction, balance, and motor function, were significantly correlated with F1 (Table 1).

This study used the neural fitting application in MATLAB 2021b software. The GA-BP neural model was applied to predict the motor function. A one-layer neural network model (Figure 1) and FMA were applied for the normalization of input and output data, respectively. To prevent over-fitting and realize external inspection, authors divided patients into two subgroups, one with 175 (75%) patients to construct and test the model, the other with 58 (25%) patients to inspect the model. The correlations between the predicted and actual values were analyzed. Then, the prediction effects were verified and the prediction differences were calculated (mapping software origin 9.1).

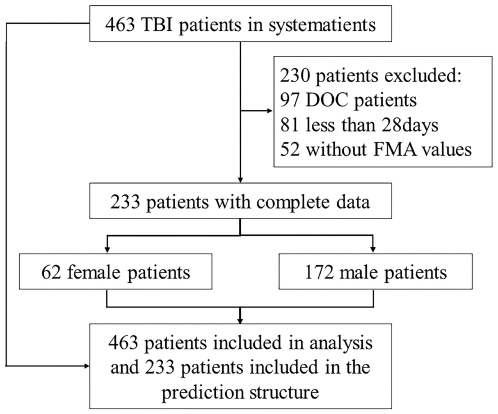

FIGURE 2
Research data source and population. DOC, disturbance of consciousness.

3. Results

This study included a total of 463 patients (**Supplementary material**). Among them, a total of 233 patients were included in the analysis of the neural network model (**Figure 2**).

3.1. General information

Among the patients included in this study, males were significantly more than females (348:115) but did not show significant differences in their ages, courses after TBI, and durations of hospital stay. However, the proportion of smoking and drinking among males was significantly higher as compared to the females (χ^2 = 33.62, P < 0.01, OR = 6.22). Meanwhile, the incidences of concurrent diseases among males, such as hypertension, diabetes, coronary heart disease, and cerebrovascular accident were significantly higher as compared to those among the females (χ^2 = 9.41, P < 0.01, OR = 1.96).

The causes of injuries among males were relatively diverse, among which, the car accident was the major cause, accounting for 47.41% of the causes of injuries. The females showed similar results; car accidents accounted for 84.35% of the causes of injuries, followed by falls (15.65%).

Most cases (98.70%) in this study were identified as severe cases (**Figure 3A**). The incidence of epidural hematoma and diffuse axonal injury among females was significantly higher as compared to those among the males (P < 0.01, OR = 13.14; P < 0.01, OR = 6.30), while the incidence of intracranial hematoma (and brain herniation) among females was significantly lower as compared to that among the males (χ^2 = 27.78, P < 0.01, OR = 1.38; χ^2 = 7.40, P < 0.01, OR = 4.18).

The surgery rate among all the patients was 70.19%, with little gender difference (71.84% *vs.* 65.22%). Most of the surgeries were performed for the removal of hematoma using craniotomy (69.54% *vs.* 60%), followed by hematoma puncture and drainage (2.30% *vs.* 5.22%) (**Figure 3B**). Among all the patients, undergoing surgery, 59 cases (18.15%) went through a second surgical procedure, which included puncture and drainage of hematoma.

Hydrocephalus (46.84%), epilepsy (27.87%), and shoulder subluxation (12.64%) were the most common complications among males (**Figure 3C**). On the other hand, among females, hydrocephalus (45.22%), shoulder subluxation (19.13%), and disuse syndrome (16.52%) were the most common complications, while the incidence of epilepsy was slightly lower among them (15.65%).

Among the types of dysfunctions, both the males and females showed higher consistencies (**Figure 3D**). Cognitive impairment (66.09% *vs.* 62.61%), dyskinesia (61.21% *vs.* 70.43%), and language impairment (32.76% *vs.* 36.52%) were the most common types dysfunctions. Bilateral dyskinesia showed the highest consistency (31.03% *vs.* 32.17%).

3.2. GA-BP neural network model

3.2.1. Construction of GA-BP model

Based on their correlations to the actual FMA, all the 11 prognostic-related factors were included in the prediction model (**Table 1**). After constructed the mode with 175 samples, the GA-BP

TABLE 2 Weights of features to neurons (w1) and neurons to output (w2).

Neuron	Course	Gender	Rehabilitation	Epilepsy	Hydrocephalus	Aphasia	Tracheotomy	Complications	Hands function	FMB	FMA	W2
1	0.13	0.36	−0.24	−0.5	−0.26	−0.26	0.05	−0.57	−0.29	−0.02	0.1	0.16
2	0.42	0.66	−0.34	0.19	0.56	0.38	0.07	0.95	−0.64	−0.2	−0.29	−0.13
3	0.52	−0.58	−0.06	−0.33	0.08	−0.1	−0.69	0.4	−0.03	−0.46	−0.23	−0.37
4	0.37	−0.64	0.25	0.27	−0.7	−0.16	0.3	0.78	0.32	−0.29	−0.43	−0.16
5	−0.62	0.56	0.69	−0.38	0.31	−0.61	0.2	−0.04	0.34	−0.27	−0.6	0.38
6	0.13	−0.89	−0.09	−0.04	−0.65	−0.09	−0.04	−0.16	0.44	0.58	−0.79	0.76
7	0.07	0.29	0.14	−0.06	0.43	−0.62	−0.34	0.28	0.01	−0.43	−0.24	0.26
8	0.01	−0.59	0.17	0.63	−0.45	−0.3	0.47	0.53	0.01	0.69	0.22	0.42
9	−0.75	0.75	0.27	−0.55	0.37	−0.38	0.41	−0.12	−0.66	0.24	0	0.79
10	−0.03	−0.06	0.5	0.21	0.41	−0.25	0.48	−0.23	−0.37	0.56	−0.59	−0.04

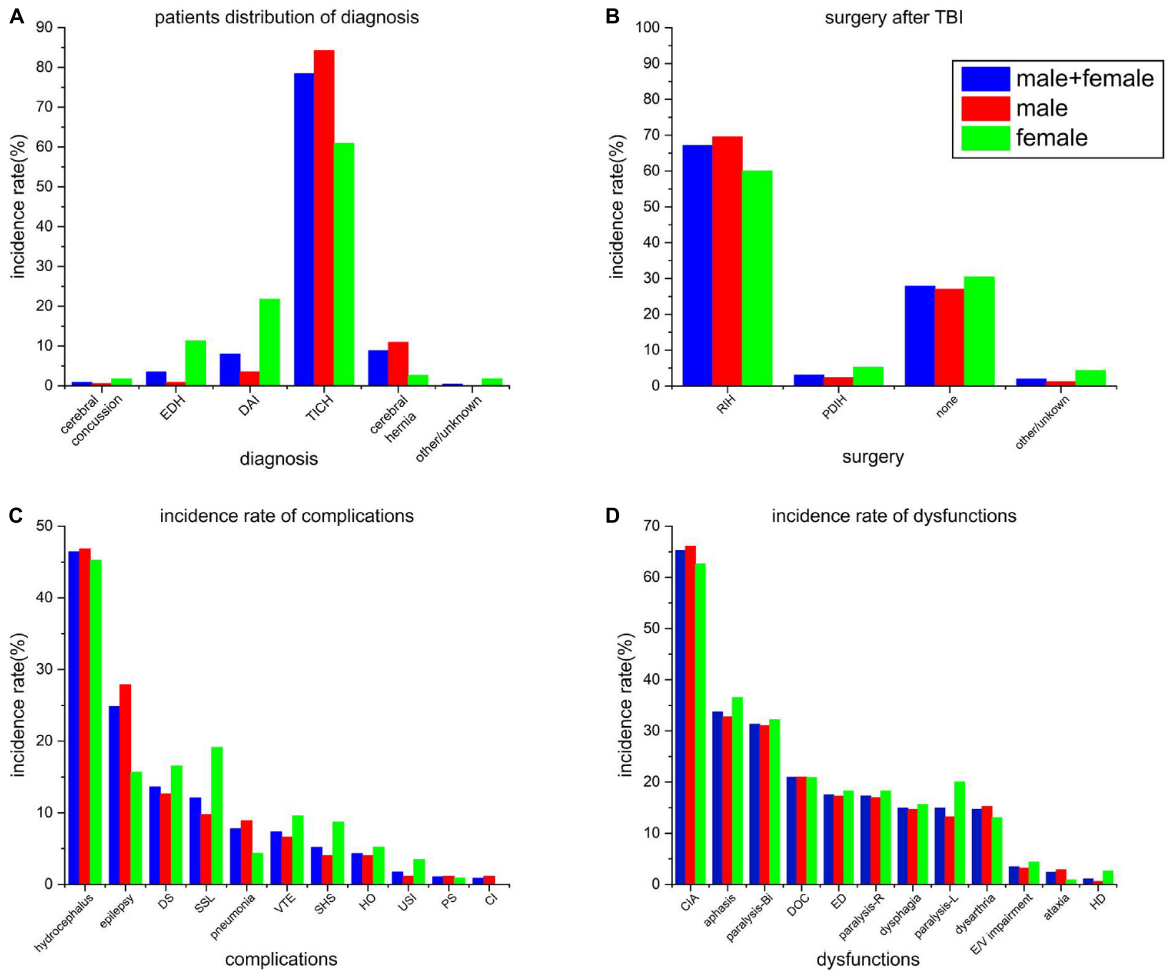

FIGURE 3
(A) Patient distribution of incidence rate of principal diagnosis. **(B)** Rate of the different types of surgeries after TBI. **(C)** Incidence rates of all the complications at the time of admission. **(D)** Incidence rate of all the dysfunctions at the time of admission. EDH, epidural hemorrhage; DAI, diffuse axonal injury; TICH, traumatic intracranial hemorrhage; RIH, removal of intracranial hemorrhage; PDIH, puncture drainage of intracranial hemorrhage; DS, disuse syndrome; SSL, shoulder subluxation; VTE, venous thromboembolism; SHS, shoulder-hand syndrome; HO, heterotopic ossification; USI, urinary system infection; PS, pressure sores; CI, secondary cerebral infarction after stroke; CIA, cognitive impairment assessment; DOC, disturbance of consciousness; ED, emotional disorder; E/V impairment, eyesight/vision impairment; and HD, headache or dizziness.

neural network was built and the code can be found in https://github.com/swlmed/swlmed-public. Pearson correlation between predicted and actual values of the model was $R^2 = 0.97$ and both of these values were shown in **Supplementary Figure 2**. The weight of every features to neurons and neurons to output listed in **Table 2**.

3.2.2. Performance of GA-BP model

Of all the 58 test patients, the predicted and actual FMA values are shown in **Figure 4**. Pearson correlation analysis was used to evaluate the differences between the predicted and actual FMA values ($R^2 = 0.95$, $P < 0.01$, **Figure 5**).

4. Discussion

Backpropagation neural network is a multi-layer feed forward network trained by the error BP algorithm, proposed by Rumelhart et al. (1986). The BP network stores a large number of input-output pattern mapping correlations, describing the mapping correlation without the need for revealing the mathematical equations. Using the gradient descent method, it continuously adjusts the network through BP and minimizes the sum of squared errors of the network. Therefore, it also avoids the use of linear correlations between data. Numerous factors, affecting the degree of injury and prognosis of TBI patients, have unclear correlations among them. Currently, BP neural network is an easily applicable model (Rau et al., 2018).

Although mild TBIs account for the majority of the cases, in this study, moderate to severe TBIs accounted for the majority of the cases (98.70%). The reasons might include the lower hospitalization rate of the patients with mild TBI. Moreover, the patients with concussions mostly complaint about headaches, nervousness, inattention, forgetfulness, etc., which can be cured. The severely affected limb function is mainly manifested in the patients with moderate to severe TBI. Therefore, the improvement of motor function was mainly studied among these patients (Levin and Diaz-Arrastia, 2015; Hon et al., 2019; Silverberg et al., 2020).

In this study, correlation analysis was used to explore the prognostic factors. For this purpose, 11 prognostic-related indicators were investigated. In the current study, age was not included as a prognostic factor, as used in the previously reported mortality

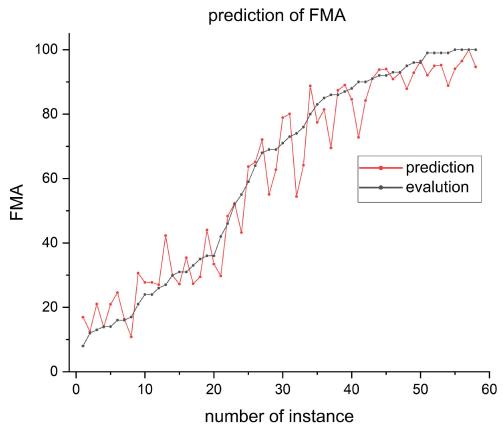

FIGURE 4
Predictive and actual FMA value of 58 patients.

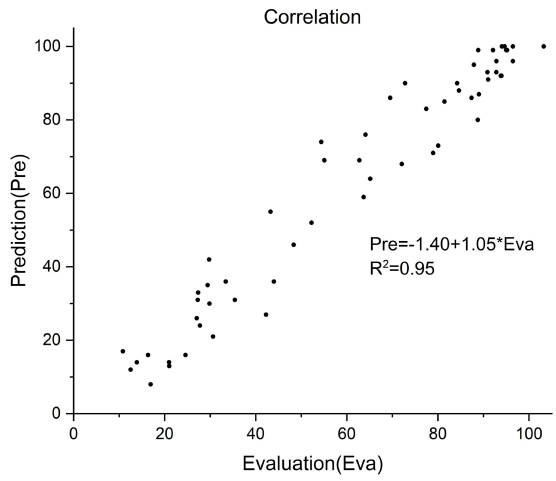

FIGURE 5
Correlation between the predictive and actual FMA value of 58 patients. Prediction value = −1.40 + 1.05 × actual value, R^2 = 0.95.

prediction models, affecting the survival rate of the TBI patients (Gang et al., 2019; Li et al., 2020). After involving the rehabilitation period, the focus of rehabilitation gradually changed from the central nervous system to the rehabilitation of the central-peripheral joint with the weakened effect of neuroplasticity, among which, age might play a less important role than that in the acute period. Unlike the previous prognostic prediction models, this study predicted continuous changes in the FMA, rather than categorizing the results, thereby showing relatively more refinement of the results. As compared to the real results, this prediction model had a satisfying accuracy rate (R^2 = 0.95). The reliability of the results was obtained by the integration of training, validation, and test datasets.

In order to establish the TBI prediction model, ANN was used for predicting the prognosis and complications due to its flexibility and other advantages (DiRusso et al., 2000; Rughani et al., 2010; Hannah et al., 2020; Wang et al., 2021). ANN was superior to the TRISS model in terms of accurate mortality prediction (Matsuo et al., 2020). ANN could achieve higher accuracy than the CRASH and IMPACT models in terms of predicting mortality in patients with moderate to severe TBIs (Rau et al., 2018). ANN was more sensitive than the traditional models in predicting the mortality of the patients with severe cases (Yao et al., 2020), underwent surgery (Shi et al., 2013), mechanical ventilation (Abujaber et al., 2020a,b), septicemia (Kim et al., 2011), as well as in identifying the clinically relevant pediatric TBI (Hale et al., 2018).

The data-driven prediction models, such as CRASH and IMPACT, were based on the databases; as the database updated, their prediction accuracies improved (Hannah et al., 2020). This implied that the data-driven could be continuously improved with the refining of data. Therefore, for these models, the critical point is a database with sufficient data. Although, China collects the TBI information through various systems, such as the Nationally Representative Disease Monitoring Point System (DSP), Hospital Quality Monitoring System (HQMS), and National Injury Monitoring System (NISS), a uniform data system for medical rehabilitation (UDMSR) for the collection of data information in a unified way is currently lacking (Granger et al., 2010; Oyesanya et al., 2021). In this study, a database, containing the rehabilitation information of 463 patients, was established. The outcome measure of this study was FMA, which is one of the most commonly used indices of motor function. In the end, only 233 patients were included in this study. The information in the database was inefficient, which might be due to the following reasons. First, the patients under rehabilitation might have more comorbidities; therefore, numerous factors might affect the rehabilitation treatment. Second, the patients came from different areas in China. Therefore, it was difficult to follow up with the patients after discharge for the follow-up assessment.

This study started with the admission of patients with TBI to a rehabilitation hospital and used the functional assessment as the baseline. The characteristics of TBI were elucidated and the prediction model based on FMA was established to predict the outcome of motor dysfunction. The prediction model had low requirements, strong operation ability, and easy promotion. It had high practicability for the hospitals with fewer research resources and might serve as a reference in the risk and prognosis assessment as well as guiding the clinical decision-making.

5. Limitations

The first limitation of this study was the small sample size obtained from a single medical center. This study lacked the indicators, which directly reflected the severity of TBI in the patients. Therefore, this might have affected the results. Second, the model could not clearly explain which factor was listed at the top. Finally, this study assumed unified rehabilitation therapies for all the patients and did not consider their differences in them.

In addition to the above-mentioned shortcomings, this study used neural network and regression models to predict the prognosis of motor function in patients with TBI and provided novel ideas for the evaluation of the patients with TBI.

Data availability statement

The original contributions presented in this study are included in the article/**Supplementary material**, further inquiries can be directed to the corresponding authors.

Author contributions

HD contributed to the study design, literature search, figures, data extraction, data analysis, and writing. ZT and WS contributed to the figures, data extraction, data interpretation, and writing. HZ and SY contributed to the study design and data interpretation. All authors contributed to the article and approved the submitted version.

Funding

This work was supported by the National Key Research and Development Program of China (Grant No. 2018YFC2001703), the National Natural Science Foundation of China (Grant No. U1809209), and China Rehabilitation Research Center Key Project (Grant Nos. 2021ZX-02 and 2021ZX-19).

Acknowledgments

We thank all the reviewers who participated in the review and MJEditor (www.mjeditor.com) for its linguistic assistance during the preparation of this manuscript.

Conflict of interest

The authors declare that the research was conducted in the absence of any commercial or financial relationships that could be construed as a potential conflict of interest.

Publisher's note

Supplementary material

The Supplementary Material for this article can be found online at: https://www.frontiersin.org/articles/10.3389/fnins.2022.1031712/full#supplementary-material

References

Abujaber, A., Fadlalla, D. G., Abdelrahman, H., Mollazehi, M., and El-Menyar, A. (2020a). Using trauma registry data to predict prolonged mechanical ventilation in patients with traumatic brain injury: Machine learning approach. *PLoS One* 15:e0235231. doi: 10.1371/journal.pone.0235231

Abujaber, A., Fadlalla, D. G., Abdelrahman, H., Mollazehi, M., and El-Menyar, A. (2020b). Prediction of in-hospital mortality in patients on mechanical ventilation post traumatic brain injury: Machine learning approach. *BMC Med. Inform. Decis. Mak.* 20:336. doi: 10.1186/s12911-020-01363-z

Boyd, C. R., Tolson, M. A., and Copes, W. S. (1987). Evaluating trauma care: The TRISS method. trauma score and the injury severity score. *J. Trauma* 27, 370–378.

Brain and Spinal Injury Center (2021). *TRACK-TBI: Transforming research and clinical knowledge in TBI.* San Francisco: University of California. [Accessed 2021 Oct 15]. https://tracktbi.ucsf.edu.

DiRusso, S. M., Sullivan, T., Holly, C., Cuff, S. N., and Savino, J. (2000). An artificial neural network as a model for prediction of survival in trauma patients: Validation for a regional trauma area. *J. Trauma* 49, 212–20;discussion220–3. doi: 10.1097/00005373-200008000-00006

Dodds, T. A., Martin, D. P., Stolov, W. C., and Deyo, R. A. (1993). A validation of the functional independence measurement and its performance among rehabilitation inpatients. *Arch. Phys. Med. Rehabil.* 75, 531–536. doi: 10.1016/0003-9993(93)90119-u

Edwards, P., Arango, M., Balica, L., Cottingham, R., El-Sayed, H., Farrell, B., et al. (2005). Final results of MRC CRASH, a randomised placebo-controlled trial of intravenous corticosteroid in adults with head injury-outcomes at 6 months. *Lancet* 365, 1957–1959. doi: 10.1016/S0140-6736(05)66552-X

Ercole, A., Dixit, A., Nelson, D. W., Bhattacharyay, S., Zeiler, F. A., Nieboer, D., et al. (2021). Imputation strategies for missing baseline neurological assessment covariates after traumatic brain injury: A CENTER-TBI study. *PLoS One* 16:e0253425. doi: 10.1371/journal.pone.0253425

Gang, M. C., Hong, K. J., Shin, S. D., Song, K. J., Ro, Y. S., Kim, T. H., et al. (2019). New prehospital scoring system for traumatic brain injury to predict mortality and severe disability using motor Glasgow Coma Scale, hypotension, and hypoxia: a nationwide observational study. *Clin. Exp. Emerg. Med.* 6, 152–159. doi: 10.15441/ceem.18.027

Gao, G., Wu, X., Feng, J., Hui, J., Mao, Q., Lecky, F., et al. (2020). Clinical characteristics and outcomes in patients with traumatic brain injury in China: A prospective, multicentre, longitudinal, observational study. *Lancet Neurol.* 19, 670–677. doi: 10.1016/s1474-4422(20)30182-4

Granger, V., Markello, S., Graham, J., Deutsch, A., Reistetter, T., and Ottenbacher, K. J. (2010). The uniform data system for medical rehabilitation: report of patients with traumatic brain injury discharged from rehabilitation programs in 2000-2007. *Am. J. Phys. Med. Rehabil.* 89, 265–278. doi: 10.1097/PHM.0b013e3181d3eb20

Hale, T., Stonko, D. P., Lim, J., Guillamondegui, O. D., Shannon, C. N., and Patel, M. B. (2018). Using an artificial neural network to predict traumatic brain injury. *J. Neurosurg. Pediatr.* 23, 219–226. doi: 10.3171/2018.8.PEDS18370

Hannah, L., Radabaugh, J. B., Dietrich, W. D., and Helen, M. (2020). Bramlett, odelia schwartz and dilip sarkar: Development and evaluation of machine learning models for recovery prediction after treatment for traumatic brain injury. *Ann. Int. Conf. IEEE Eng. Med. Biol. Soc.* 2020, 2416–2420. doi: 10.1109/EMBC44109.2020.9175658

Hon, K. L., Leung, A. K. C., and Torres, A. R. (2019). Concussion: A global perspective. *Semin. Pediatr. Neurol.* 30, 117–127. doi: 10.1016/j.spen.2019.03.017

Hukkelhoven, C. W., Steyerberg, E., Dik, J., Habbema, F., Habbema, J., Farace, E., et al. (2005). Predicting outcome after traumatic brain injury: development and validation of a prognostic score based on admission characteristics. *J. Neurotrauma* 22, 1025–1039. doi: 10.1089/neu.2005.22.1025

Kim, S., Kim, W., and Park, R. W. (2011). A comparison of intensive care unit mortality prediction models through the use of data mining techniques. *Healthc. Inform. Res.* 17, 232–243. doi: 10.4258/hir.2011.17.4.232

Levin, H. S., and Diaz-Arrastia, R. R. (2015). Diagnosis, prognosis, and clinical management of mild traumatic brain injury. *Lancet Neurol.* 14, 506–517. doi: 10.1016/s1474-4422(15)00002-2

Li, X., Lü, C., Wang, J., Wan, Y., Dai, S. H., Zhang, L., et al. (2020). Establishment and validation of a model for brain injury state evaluation and prognosis prediction. *Chin. J. Traumatol.* 23, 284–289. doi: 10.1016/j.cjtee.2020.08.006

Maeda, Y., Ichikawa, R., Misawa, J., Shibuya, A., Hishiki, T., Maeda, T., et al. (2019). External validation of the TRISS, CRASH, and IMPACT prognostic models in severe traumatic brain injury in Japan. *PLoS One* 14:e0221791. doi: 10.1371/journal.pone.0221791

Matsuo, K., Aihara, H., Nakai, T., Morishita, A., Tohma, Y., and Kohmura, E. (2020). Machine learning to predict in-hospital morbidity and mortality after traumatic brain injury. *J. Neurotrauma* 37, 202–210. doi: 10.1089/neu.2018.6276

Ottenbacher, K. J., Hsu, Y., Granger, C. V., and Fiedler, R. C. (1996). The reliability of the functional independence measure: A quantitative review. *Arch. Phys. Med. Rehabil.* 77, 1226–1232. doi: 10.1016/s0003-9993(96)90184-7

Oyesanya, T. O., Moran, T. P., Espinoza, T. R., and Wright, D. W. (2021). Regional variations in rehabilitation outcomes of adult patients with traumatic brain injury: A uniform data system for medical rehabilitation investigation. *Arch. Phys. Med. Rehabil.* 102, 68–75. doi: 10.1016/j.apmr.2020.07.011

Perel, P., Arango, M., Clayton, T., Edwards, P., Komolafe, E., Poccock, S., et al. (2008). Predicting outcome after traumatic brain injury: Practical prognostic models based on

large cohort of international patients. *BMJ* 336, 425–429. doi: 10.1136/bmj.39461.643438.25

Perel, P., Edwards, P., Wentz, R., and Roberts, I. (2006). Systematic review of prognostic models in traumatic brain injury. *BMC Med. Inform. Decis. Mak.* 6:38. doi: 10.1186/1472-6947-6-38

Pickelsimer, E. E., Selassie, A., Gu, J., and Langlois, J. A. (2006). A population-based outcomes study of persons hospitalized with traumatic brain injury: Operations of the South Carolina traumatic brain injury follow-up registry. *J. Head Trauma Rehabil.* 21, 491–504. doi: 10.1097/00001199-200611000-00004

Rau, C. S., Kuo, P. J., Chien, P. C., Huang, C. Y., Hsieh, H. Y., and Hsieh, C. H. (2018). Mortality prediction in patients with isolated moderate and severe traumatic brain injury using machine learning models. *PLoS One* 13:e0207192. doi: 10.1371/journal.pone.0207192

Reith, F., Lingsma, H., Gabbe, B., Lecky, F., Roberts, I., and Maas, A. (2017). Differential effects of the glasgow coma scale score and its components: An analysis of 54,069 patients with traumatic brain injury. *Injury* 48, 1932–1943. doi: 10.1016/j.injury.2017.05.038

Roberts, I., Yates, D., Sandercock, P., Farrell, B., Wasserberg, J., Lomas, G., et al. (2004). Effect of intravenous corticosteroids on death within 14 days in 10008 adults with clinically significant head injury (MRC CRASH trial): Randomised placebo-controlled trial. *Lancet* 364, 1321–1328. doi: 10.1016/S0140-6736(04)17188-2

Rogers, S. C., Campbell, B., Saleheen, H., Borrup, K., and Lapidus, G. (2010). Using trauma registry data to guide injury prevention program activities. *J. Trauma* 69(4 Suppl), S209–S213. doi: 10.1097/TA.0b013e3181f1e9fe

Rughani, A. I., Dumont, T. M., Lu, Z., Bongard, J., Horgan, M. A., Penar, P. L., et al. (2010). Use of an artificial neural network to predict head injury outcome. *J. Neurosurg.* 113, 585–590. doi: 10.3171/2009.11.JNS09857

Rumelhart, D. E., Hinton, G. E., and Williams, R. J. (1986). Learning representations by back-propagating errors. *Nature* 323, 533–536. doi: 10.1038/323533a0

Segal, E., Gillard, M., and Schall, R. R. (1996). Telephone and in-person proxy agreement between stroke patients and caregivers for the functional independence measure. *Am. J. Phys. Med. Rehabil.* 75, 208–212. doi: 10.1097/00002060-199605000-00013

Shi, H. Y., Hwang, S. L., Lee, K. T., and Lin, C. L. (2013). In-hospital mortality after traumatic brain injury surgery: A nationwide population-based comparison of mortality predictors used in artificial neural network and logistic regression models. *J. Neurosurg.* 118, 746–752. doi: 10.3171/2013.1.JNS121130

Silverberg, N. D., Iaccarino, M. A., Panenka, W. J., Iverson, G. L., McCulloch, K. L., Dams-O'Connor, K., et al. (2020). Management of concussion and mild traumatic brain injury: A synthesis of practice guidelines. *Arch. Phys. Med. Rehabil.* 101, 382–393. doi: 10.1016/j.apmr.2019.10.179

Steyerberg, E. W., Mushkudiani, N., Perel, P., Butcher, I., Lu, J., McHugh, G., et al. (2008). Predicting outcome after traumatic brain injury: development and international validation of prognostic scores based on admission characteristics. *PLoS Med.* 5:e165;discussione165. doi: 10.1371/journal.pmed.0050165

Subaiya, S., Roberts, I., Komolafe, E., and Perel, P. (2012). Predicting intracranial hemorrhage after traumatic brain injury in low and middle-income countries: A prognostic model based on a large, multi-center, international cohort. *BMC Emerg. Med.* 12:17. doi: 10.1186/1471-227X-12-17

Wang, X., Zhong, J., Lei, T., Chen, D., Wang, H., Zhu, L., et al. (2021). An artificial neural network prediction model for posttraumatic epilepsy: Retrospective cohort study. *J. Med. Internet Res.* 23:e25090. doi: 10.2196/25090

Yao, R. Q., Jin, X., Wang, G. W., Yu, Y., Wu, G. S., Zhu, Y. B., et al. (2020). A machine learning-based prediction of hospital mortality in patients with postoperative sepsis. *Front. Med. (Lausanne)* 7:445. doi: 10.3389/fmed.2020.00445

Yu, J., Tam, H. M., and Lee, T. M. (2015). Traumatic brain injury rehabilitation in Hong Kong: A review of practice and research. *Behav. Neurol.* 2015:274326. doi: 10.1155/2015/274326

Zarshenas, S., Colantonio, A., Horn, S. D., Jaglal, S., and Cullen, N. (2019). Cognitive and motor recovery and predictors of long-term outcome in patients with traumatic brain injury. *Arch Phys Med. Rehabil.* 100, 1274–1282. doi: 10.1016/j.apmr.2018.11.023

frontiers | Frontiers in Neuroscience

TYPE Original Research
PUBLISHED 14 April 2023
DOI 10.3389/fnins.2023.1134330

OPEN ACCESS

EDITED BY
Ping Zheng,
University Hospital Münster, Germany

REVIEWED BY
Yan Zhang,
Department of Orthopedics,
Beijing Luhe Hospital,
Capital Medical University, China
Yankai Dong,
Northwest University, China

*CORRESPONDENCE
Li Li
✉ lili243@mail.sysu.edu.cn
Jianwei Luo
✉ luojw28@mail.sysu.edu.cn

†These authors have contributed equally to this work and share first authorship

SPECIALTY SECTION
This article was submitted to Translational Neuroscience, a section of the journal Frontiers in Neuroscience

RECEIVED 30 December 2022
ACCEPTED 21 March 2023
PUBLISHED 14 April 2023

CITATION
Zeng J, Lai C, Luo J and Li L (2023) Functional investigation and two-sample Mendelian randomization study of neuropathic pain hub genes obtained by WGCNA analysis. *Front. Neurosci.* 17:1134330. doi: 10.3389/fnins.2023.1134330

Functional investigation and two-sample Mendelian randomization study of neuropathic pain hub genes obtained by WGCNA analysis

Jianfeng Zeng[1†], Cong Lai[2†], Jianwei Luo[1*] and Li Li[1*]

[1]Department of Anesthesiology, Sun Yat-sen Memorial Hospital, Sun Yat-sen University, Guangzhou, China, [2]Department of Urology, Sun Yat-sen Memorial Hospital, Sun Yat-sen University, Guangzhou, China

Objective: Neuropathic pain as a complex chronic disease that occurs after neurological injury, however the underlying mechanisms are not clarified in detail, hence therapeutic options are limited. The purpose of this study was to explore potential hub genes for neuropathic pain and evaluate the clinical application of these genes in predicting neuropathic pain.

Methods: Differentially expressed analysis and weighted gene co-expression network analysis (WGCNA) was used to explore new neuropathic pain susceptibility modules and hub genes. KEGG and GO analyses was utilized to explore the potential role of these hub genes. Nomogram model and ROC curves was established to evaluate the diagnostic efficacy of hub genes. Additionally, the correlation of IL-2 with immune infiltration was explored. Finally, a Mendelian randomization study was conducted to determine the causal effect of IL-2 on neuropathic pain based on genome-wide association studies.

Results: WGCNA was performed to establish the networks of gene co-expression, screen for the most relevant module, and screen for 440 overlapping WGCNA-derived key genes. GO and KEGG pathway enrichment analyses demonstrated that the key genes were correlated with cytokine receptor binding, chemokine receptor binding, positive regulation of JAK–STAT cascade, chemokine-mediated signaling pathway, PI3K-AKT pathway and chemokine pathway. Through Cytoscape software, top ten up-regulated genes with high scores were IL2, SMELL, CCL4, CCR3, CXCL1, CCR1, HGF, CXCL2, GATA3, and CRP. In addition, nomogram model performed well in predicting neuropathic pain risk, and with the ROC curve, the model was showed to be effective in diagnosis. Finally, IL2 was selected and we observed that IL2 was causally associated with immune cell infiltrates in trigeminal neuralgia. In inverse variance weighting, we found that IL2 was associated with the risk of trigeminal neuralgia with an OR of 1.203 (95% CI=1.004–1.443, p =0.045).

Conclusion: We constructed a WGCNA-based co-expression network and identified neuropathic pain-related hub genes, which may offer further insight into pre-symptomatic diagnostic approaches and may be useful for the study of molecular mechanisms for understanding neuropathic pain risk genes.

KEYWORDS

neuropathic pain, weighted gene co-expression network analysis, hub genes, IL2, Mendelian randomization

1. Introduction

Neuropathic pain is defined as chronic pain directly or indirectly caused by a pathological disorder or disease of the peripheral or central somatosensory nervous system (Finnerup et al., 2016). Unlike acute pain, which alerts and "protects" the body, neuropathic pain can persist without any benefit to the body and even damage it, seriously affecting the patient's quality of life (St, 2018). The neuropathic pain is divided into central neuropathic pain and peripheral neuropathic pain depending on the site of injury. Neuropathic pain the most common type of chronic pain, has become a commonly seen chronic condition in many countries. The patients' quality of life is seriously affected by neuropathic pain, which brings a heavy economic burden to society and individuals (Moisset and Page, 2021). Its pathogenesis is complex and no effective therapeutic drugs are available. Recently, some researches have combined bioinformatics approaches to elucidate the mechanisms of oxidative stress, neuroinflammation, ion channel alterations, activation of immune cell, glial-derived mediators and epigenetic modulation in neuropathic pain (Finnerup et al., 2021; Golubovic et al., 2021; Seo and Jun, 2021). Nevertheless, none of the various studies detected hub genes related to neuropathic pain by weighted gene co-expression network analysis (WGCNA). Thus, for gaining insight into the molecular mechanisms of neuropathic pain, it is essential to combine bioinformatics approaches to explore neuropathic pain-associated biomarkers.

It is essential to identify expression of specific genes in disorders to understand the microscopic mechanisms of many diseases such as neuropathic pain and to identify biomarkers relevant to diagnosis and therapeutic evaluation (Barclay et al., 2007; von Schack et al., 2011). In fact, several bioinformatics software and databases have been established to recognize disease-associated pathways, such as WGCNA, Kyoto Encyclopedia of Genes and Genomes (KEGG) enrichment analysis, and gene set enrichment analysis (Nangraj et al., 2020). WGCNA has also been applied to a wide variety of data, including proteomics data, genetic marker data, gene expression profiles, metabolomics information, and other high-dimensional data (Nangraj et al., 2020). Furthermore, WGCNA is useful for screening therapeutic targets or candidate biomarkers. Therefore, the current study was conducted to find related genes, new biomarkers, or potential mechanisms related to neuropathic pain.

Mendelian randomization (MR) is a reliable method that has been promoted in recent years to infer potential causal relationships, using single nucleotide polymorphisms (SNPs) as instrumental variables (IVs) to assess the causal relationship between exposure factors and outcomes (Jansen et al., 2014; Emdin et al., 2017). MR uses genetic variations strongly associated with exposure factors as instrumental variables to infer causal effects between exposure factors and study outcomes.

In this work, we identified differentially expressed genes (DEGs) through exploring data from the rattus norvegicus spinal nerve ligation (SNL) and sham groups. WGCNA was then utilized to recognize the most relevant modules for neuropathic pain, which greatly narrowing the scope of genes to screen for. In brief, we identified four hub genes, namely IL2, CCR3, CXCL1, CCL4, and SELL, as potential diagnostic markers that may be useful for the diagnosis of neuropathic pain and further understanding of the underlying mechanisms of neuropathic pain risk genes. Finally, the causal relationship between IL2 and neuropathic pain was explored through MR study.

2. Materials and methods

2.1. Data source

This dataset was created through transcriptome microarray assays in the Dorsal Root Ganglion (DRG) obtained from rattus norvegicus that underwent SNL ($N = 10$) or sham groups ($N = 10$). The expression data of all measured genes can be downloaded from the Gene Expression Omnibus (GEO) database.[1]

2.2. Differentially expressed genes identification

First, we read the data of dataset GSE24982 using *R* software (version 3.6.1) and preprocessed it for batch correction and normalization. Then we performed DEG analysis screening using the "limma" package. After significance analysis of expression levels, the "pheatmap" and "ggplot2" *R* packages were processed to generate volcano maps and DEG expression heat maps.

2.3. Weighted gene co-expression network analysis

WGCNA, a systematic approach to biology, is often applied to characterize patterns of genetic association between different samples. It is used for identifying highly synergistic genomes. Based on the interrelatedness of genomes and the relationship of genomes with phenotypes, it can be applied to identify candidate markers (Langfelder and Horvath, 2008). We constructed a gene co-expression network for neuropathic pain using the "WGCNA" *R* package. Finally, we evaluated the correlation of different modules with the pathogenic mechanism of neuropathic pain and selected the most relevant module as the central gene derived from WGCNA.

2.4. Screening of candidate pivotal genes and Go/KEGG analysis

These intersecting genes are regarded as candidate hub genes relevant for neuropathic pain pathogenesis. KEGG serves as a database resource for systematically analyzing gene function (Kanehisa and Goto, 2000). Subsequently, we performed Gene Ontology (GO) and KEGG enrichment analysis using the "clusterProfiler" *R* package in order to assist us in understanding the potential mechanisms of progression and pathogenesis.

2.5. Protein–protein interaction network hub genes

We predicted and visualized molecular interaction and protein–protein interaction (PPI) networks using STRING[2] and Cytoscape

1 https://www.ncbi.nlm.nih.gov/geo/query/acc.cgi?acc=GSE24982
2 https://string-db.org/

software[3] platform. The Degree algorithm of Cytoscape software was used to to rank the important genes in PPI networks.

2.6. Nomogram model construction

We constructed a nomogram model to predict the risk of neuropathic pain using the "rms" package (Iasonos et al., 2008; Park, 2018). The nomogram model's performance was evaluated through the calculation of Harrell's concordance index, which assessed predictive power (Harrell et al., 1996). After that, we used "ROC" package construct the receiver operator characteristic (ROC) curve to validate the diagnostic effectiveness of the candidate biomarkers. We employed the area under the ROC curve (AUC) to indicate the accuracy. A criterion ($0.9 \leq AUC < 1$) was used to identify excellent accuracy.

2.7. Immune cell analysis

To investigate the function of immune cells in neuropathic pain, we evaluated the level of immune cell infiltration of 22 immunocytes in the neuropathic pain group by CIBERSORT analysis (Chen et al., 2018).

2.8. Mendelian randomization

All the data in this study were used in the open database. Two-sample MR was used to explore the causal association between hub gene and the risk of neuropathic pain with the definition of SNPs as IVs. Hub gene data obtained from the publicly available Genome-Wide Association Study (GWAS) data source. We selected the most critical gene, il-2, and trigeminal neuralgia, as representative diseases of neuropathy, for Mendelian randomization analysis. Data on IL-2 is available at https://gwas.mrcieu.ac.uk/datasets/?gwas_id__icontains=prot-a-1512&year__iexact=&trait__icontains=&consortium__icontains= and data on trigeminal neuralgia is available at https://gwas.mrcieu.ac.uk/datasets/?gwas_id__icontains=finn-b-G6_TRINEU&year__iexact=&trait__icontains=&consortium__icontains=. MR analysis was performed based on the "TwoSampleMR" Package, and inverse variance weighting (IVW) was used to assess the relationship between hub gene levels and the risk of neuropathic pain. MR–Egger was used for additional sensitivity analysis (Emdin et al., 2017; Dudbridge, 2021).

3. Results

3.1. DEGs screening

We first obtained the neuropathic pain dataset (GSE24982) from GEO database and we identified the DEGs of the neuropathic pain dataset. We identified 691 DEGs (449 upregulated and 242 downregulated) in the neuropathic pain group compared to the normal group from the GSE24982 dataset (Figures 1A,B; Supplementary Table S1).

3.2. Construction of WGCNA network and identification of neuropathic pain-related module

To identify whether or not the potential gene modules were associated with neuropathic pain, we performed WGCNA analysis of all candidate genes from neuropathic pain-related datasets (GSE24982) (Figure 2A). We identified five different modules (Figure 2B). After the analysis of the positive correlation coefficients. At last, module turquoise was screened out in the GSE24982 dataset (Figure 2C; Supplementary Table S2).

3.3. Go/KEGG analyses

To search for co-expressed genes between WGCNA-derived hub genes and DEGs. We eventually screened 440 overlapping genes as candidate hub genes that may play an important role in the development and progression of neuropathic pain (Figure 3A). GO and KEGG analyses were conducted to further explore the underlying roles of these 440 overlapping genes (Figures 3B,C). GO enrichment analysis showed that the overlapping genes mainly affect the biological functions of cytokine receptor binding, chemokine receptor binding, cell chemotaxis and positive regulation of JAK STAT cascade. KEGG enrichment analysis showed that the overlapping genes mainly affect cytokine-cytokine receptor interaction, chemokine-mediated signaling pathway, PI3K AKT pathway, chemokine pathway and chemical carcinogenesis.

3.4. PPI network analysis for hub genes

We used the STRING online tool to construct a PPI network of overlapping hub genes (Figure 4A). Subsequently, the top ten highly ranked up-regulated genes were then visualized by using Cytoscape software (Figure 4B). Briefly, IL2, SMELL, CCL4, CCR3, CXCL1, CCR1, HGF, CXCL2, GATA3, and CRP were sorted out. The deeper the color, the higher the score.

3.5. Construction of nomogram model for neuropathic pain risk prediction

We then constructed a nomogram model to predict neuropathic pain risk (Figure 5A). Thus, our nomogram model performs well in neuropathic pain prediction. Subsequently, we calculated ROC curves for the five hub genes (IL2, SELL, CXCL1, CCL4, and CCR3) to assess the diagnostic effect. The AUC of our nomogram could differentiate between neuropathic pain and controls (Figure 5B). The AUC values of IL2, SELL, CXCL1, CCL4, and CCR3 are, respectively, 0.940, 0.950, 0.870, and 0.990.

3 https://cytoscape.org/

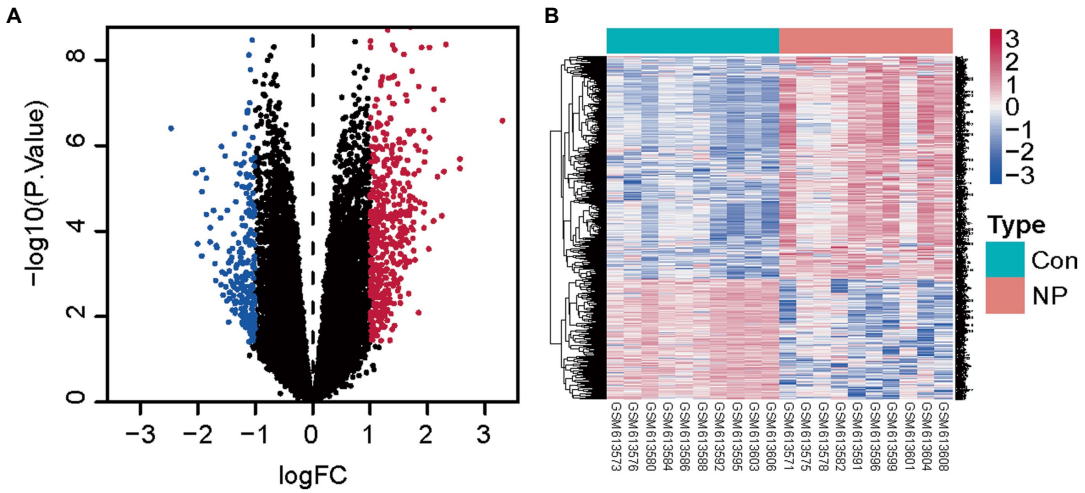

FIGURE 1
Genes differentially expressed between the neuropathic pain and normal groups. **(A)** Volcanic map for differential expression analysis of GSE24982. **(B)** Heat map for differential expression analysis of GSE24982. Blue represents down-regulated genes, red represents up-regulated genes, and black represents undifferentiated genes.

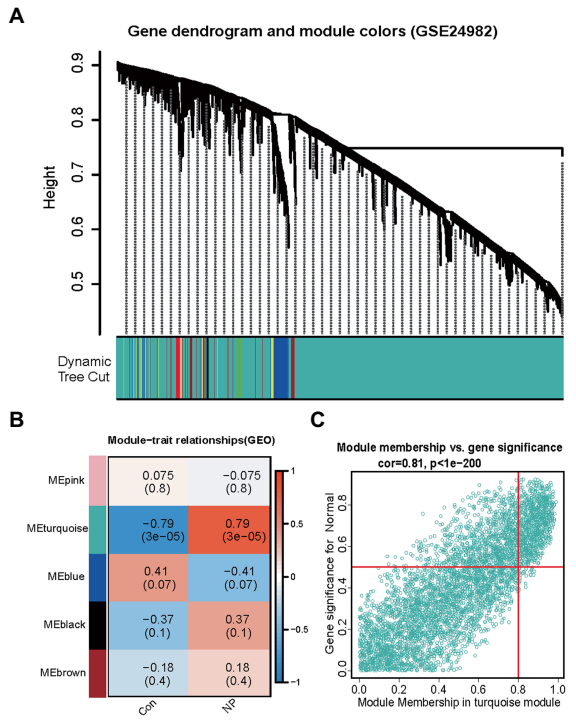

FIGURE 2
Identification of neuropathic pain-associated gene modules in the GEO dataset using WGCNA. **(A)** Dendrogram of all genes in the GSE24982 dataset was clustered on the basis of a topological overlap matrix (1-TOM). Each branch in the clustering tree represents a gene, while co-expression modules were constructed in different colors. **(B)** Module-trait heatmap of the correlation between the clustering gene module and neuropathic pain in the GSE24982 dataset. Each module contains the corresponding correlation coefficient and *p* value. **(C)** Scatter plot of module cyan has the strongest positive correlation with neuropathic pain in the GSE24982 dataset.

3.6. Assessment of immune cell infiltration in neuropathic pain

As KEGG pathway analysis and GO enrichment showed that these hub genes were primarily associated with chemokine-mediated pathways. The results shown that the infiltration levels of CD4 resting memory T cells, activated CD4 resting memory T cells, and resting dendritic cells were higher in IL2-high group compared with IL2-low group, while the infiltration levels of activated NK cells, and eosinophiles were lower in IL2-high group than IL2-low groups (Figures 6A,B). These results demonstrate a direct relationship between the immune cell infiltration and hub gene IL2 in neuropathic pain.

3.7. IL2 was causally associated with the risk of neuropathic pain

The SNP characteristics of IL2 and trigeminal neuralgia are shown in Supplementary Table S3. All SNPs were not weak instrumental variables. The causal effects of each genetic variation on neuropathic pain are shown in Figures 7A,B. We assessed the causal association between IL2 levels and trigeminal neuralgia. Using the IVW method, we found that IL2 was associated with the risk of trigeminal neuralgia with an OR of 1.203 (95% CI = 1.004–1.443, $p = 0.045$). The MR–Egger method showed no significant statistical significance [OR = 1.023, 95% CI = 0.636–1.647, $p = 0.925$]. The causal effect of the funnel plot was roughly symmetrical (Figures 7C), and the intercept of the MR Egger regression did not observe horizontal pleiotropy ($p = 0.480$), further showing that pleiotropy did not bias the causal effect. As shown in Figure 7D, we systematically performed the MR analysis again on the remaining SNPs after removing each SNP. The results remained consistent, suggesting that the calculation results of all SNPs made causality significant. This also indicates that there was no dominant

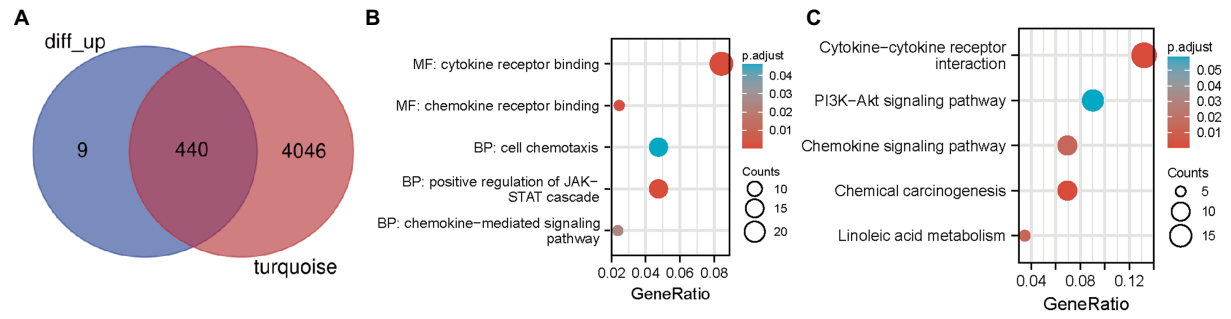

FIGURE 3
Candidate hub genes were screened and validated. **(A)** Venn diagram revealed 440 overlapping candidate hub genes. **(B)** GO enrichment analysis of candidate hub genes. **(C)** KEGG pathway analysis of candidate hub genes.

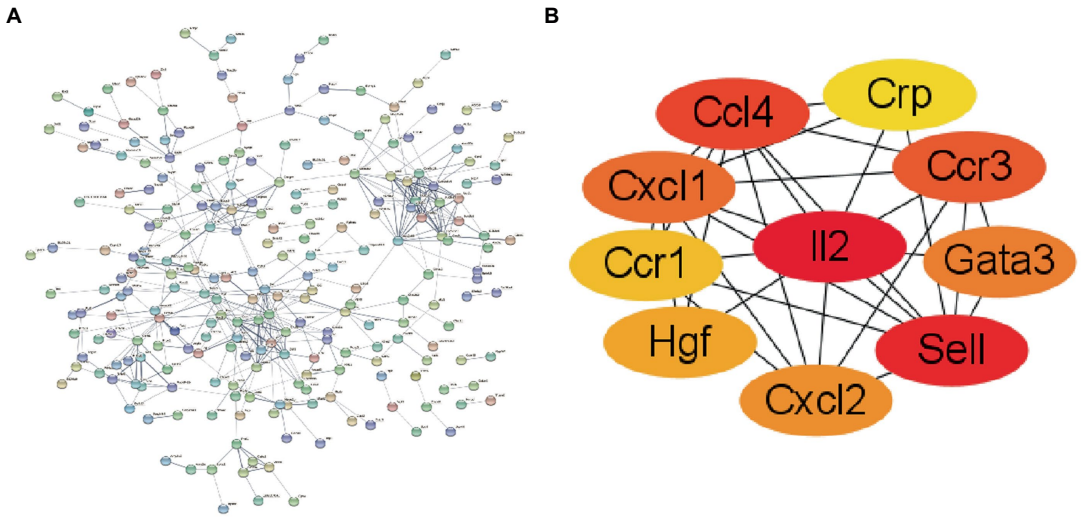

FIGURE 4
The construction of PPI network. **(A)** PPI network of overlapping hub genes. **(B)** The core genes of the interaction network were obtained by degree ssalgorithm.

SNP in IL2 levels and trigeminal neuralgia, and the previous MR results were valid.

4. Discussion

Neuropathic pain is a complicated chronic disease that occurs after neurological injury, its precise mechanism remains unclear. Neuralgia is not a single disorder, but a clinical complex presentation caused by a variety of injuries or diseases, and the pathogenesis is diverse and complex (Torta et al., 2017). There are many recent therapeutic approaches targeting the peripheral and central sensitization of neuropathic pain, including NSAIDs, minimally invasive interventions, and ion channel blockers (Binder and Baron, 2016). Nevertheless, these therapies do not offer significant long-term pain alleviation, so alternative contributing mechanisms to neuropathic pain ought to be investigated. With the advancement of molecular biology techniques, the role of pain-associated genes in the progression of neuropathic pain has emerged as an essential research topic (von Hehn et al., 2012). By quantifying the expression levels of thousands of genes in biological specimens concurrently with the genome-wide expression data gained, we are able to study the intricate regulatory associations between genes and potentially find better targets for treatment of neuropathic pain.

Diagnostic biomarkers are designed to identify patients with pathological changes. Currently, researchers are focused on validating biomarkers associated with neuropathic pain. In a recent research, Robust Rank Aggregation (RRA) method has been employed to identify hub genes of neuropathic pain (Cui et al., 2022). Finally, based on the analysis of RRA and PPI analysis, we identified 2 pivotal genes related to neuropathic pain, including Cav1 and Lep. In an earlier study, SCN10A and SST were identified as biomarkers of neuropathic pain by Zhu et al. (2019). In addition, overexpression of the p53 gene in dorsal root ganglion neurons and ensuing increase of caspase-3 expression leads to an increase in apoptosis in these neurons. p53 has also been shown to be partially responsible for chronic constrictive injury-induced neuropathic pain (Gao et al., 2018). SNAP25 plays a role in extracellular release of neurotransmitters and synaptogenesis (Wu and Nie, 2022). In another research, seven genes (Aif1, Atf3, Gfap, Ctss, Scg2, Vgf, and Jun) were identified as the hub genes for

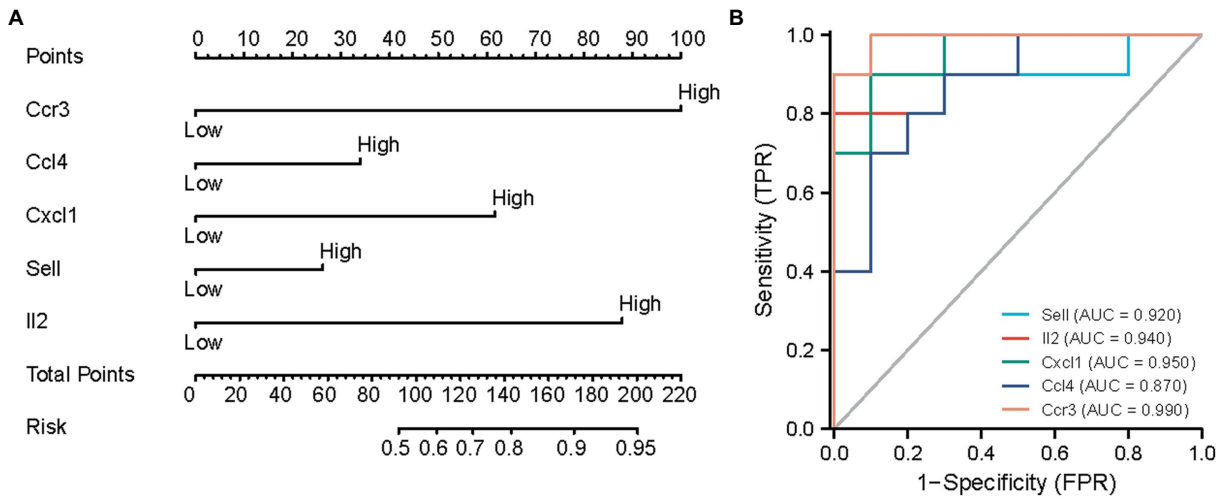

FIGURE 5
Predicting the risk of neuropathic pain using nomograms. **(A)** Nomogram model of hub genes. **(B)** ROC curves to assess the diagnostic efficacy of nomogram model and each hub gene.

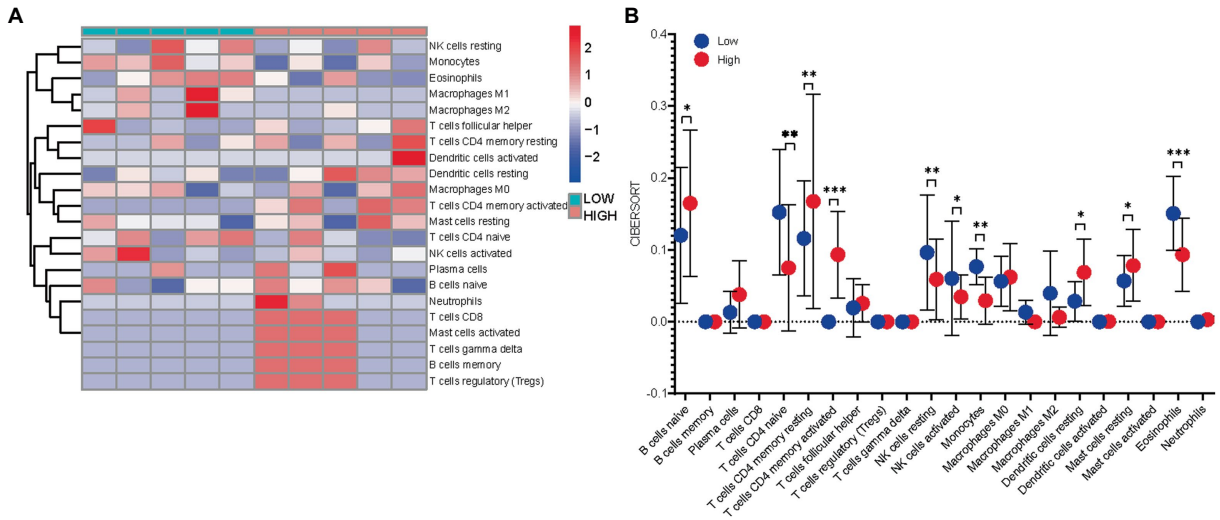

FIGURE 6
Immuno-correlation of IL2 in neuropathic pain. **(A)** Relative distribution of 22 kinds of immune cells in all neuropathic pain samples. **(B)** The difference of immune cell infiltration between high -and low-expression IL2 groups.

neuropathic pain (Xu et al., 2022). However, none of them have validated and assessed the efficacy of candidate biomarkers for diagnosis through mathematical modelling. A more robust and comprehensive design ought to be considered when using these bioinformatics methods to investigate disease. In our research, we first used WGCNA analysis to screen the hub genes of neuropathic pain. We sorted out ten genes, including IL2, SMELL, CCL4, CCR3, CXCL1, CCR1, HGF, CXCL2, GATA3, and CRP as the candidate hub genes for neuropathic pain. Consequently, our nomogram model displayed outstanding performance in the prediction of neuropathic pain. Subsequently, we calculated ROC curves for five hub genes (IL2, SELL, CXCL1, CCL4, and CCR3) to evaluate the diagnostic effect. The AUC of the nomogram can differentiate neuropathic pain from the control group.

There is growing evidence that uninjured DRGs surrounding injured DRGs also act in the onset and progression of neuropathic pain (Fukuoka et al., 2001; He et al., 2014). In this research, we downloaded and analyzed GSE24982 mRNA-seq data and found that 449 genes in the SNL group were up-regulated in comparison to the sham group. Some chemokines (e.g., CCL2, CXCL1, CCL7, CX3CL1, and CCL21) were shown to act on inflammatory and neuropathic pain by mediating neuron-glial interactions in the central nervous system (Imai et al., 2013; Jiang et al., 2016). These results demonstrated once again that chemokines are important in neuropathic pain and may be hub genes influencing the progression of neuropathic pain. The JAK–STAT pathway has been extensively investigated in neurological diseases and has been reported to have a significant role in ischemic stroke (Zhu et al., 2021a,b), glioma (Zhu

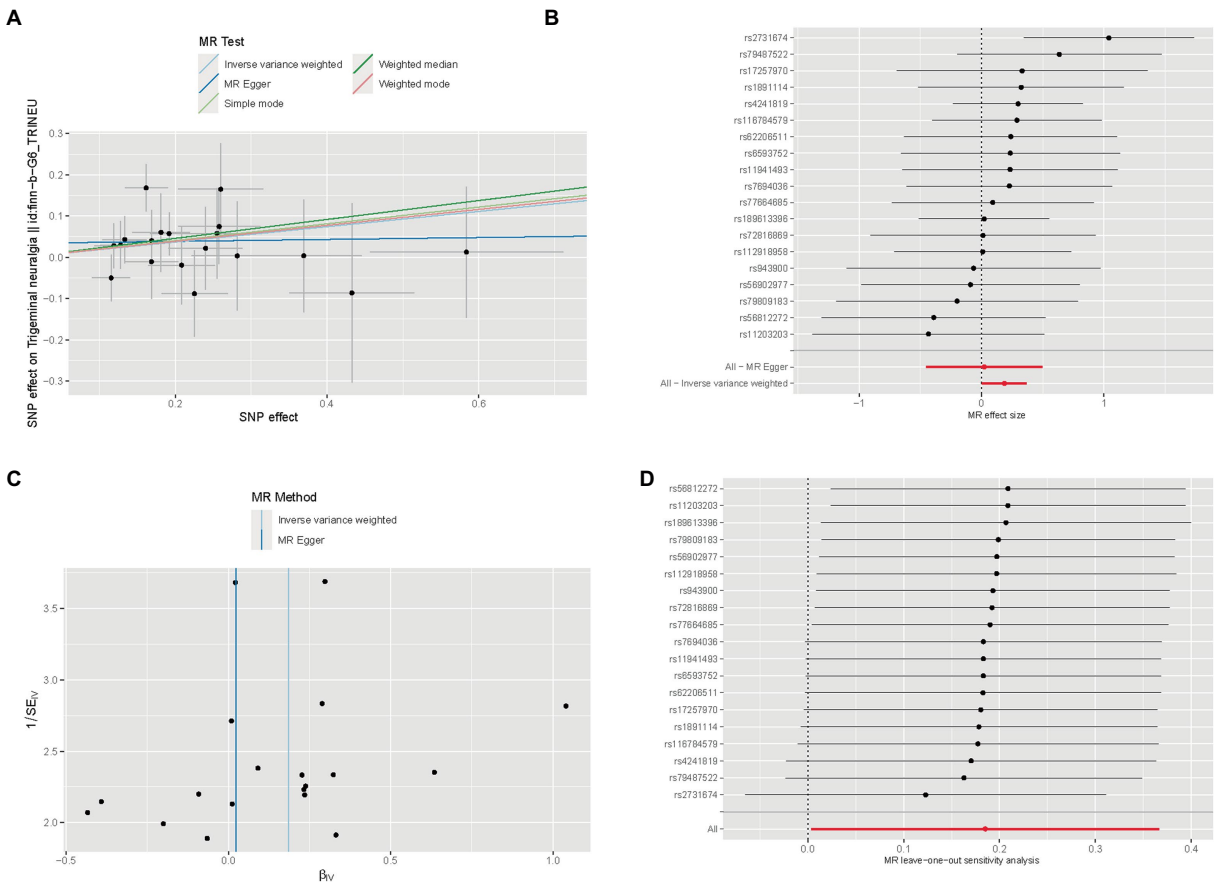

FIGURE 7
Mendelian randomization study results. **(A)** Scatter plot showing the causal effect of IL2 on the risk of trigeminal neuralgia. **(B)** Forest plot showing the causal effect of each SNP on the risk of trigeminal neuralgia. **(C)** Funnel plots to visualize overall heterogeneity of MR estimates for the effect of IL2 on trigeminal neuralgia. **(D)** Leave-one-out plot to visualize causal effect of IL2 on trigeminal neuralgia risk when leaving one SNP out.

et al., 2021c), and neuropathic pain (Dominguez et al., 2008; Li et al., 2018). PI3K/AKT pathway also exert crucial role in the progress of neuropathic pain, some agents have analgesic and anti-inflammatory effects on neuropathic pain through inhibition of the PI3K/Akt signaling pathway, such as cryptotanshinone (Zhang et al., 2019), geniposide (Zhang et al., 2022). This confirms that the JAK–STAT and PI3K-AKT pathways are important in neuropathic pain, but whether chemokines and the JAK–STAT or PI3K-AKT pathway are interlinked in neuropathic pain remains to be further investigated.

Chemokines, a small family of secreted proteins, are regulators of peripheral immune cell transport (Charo and Ransohoff, 2006). Chemokines are also expressed in the CNS and modulate CNS function under pathological and physiological conditions, involving synaptic transmission, neuronal development and neuroinflammation related to neurological diseases (Asensio and Campbell, 1999). A study reported that delivery of CXCL1 shRNA lentiviral vectors in the spinal cord before or after SNL consistently diminished SNL-evoked nociceptive responses. CXCL1 application in the spinal cord caused not only nociceptive hyperalgesia but also rapid activation of neurons, as evidenced by the expression of c-Fos and cAMP response element binding protein and phosphorylated extracellular signal-regulated kinase in spinal cord neurons (Asensio and Campbell, 1999). Our study also confirmed that CXCL1 is one of the key genes in neuropathic pain, and therefore inhibiting CXCL1 signaling may provide a novel treatment for neuropathic pain. In addition, we found that CXCL2 is also one of the key genes in neuropathic pain and previous studies showed that CXCL2 levels were elevated on the first day of neuropathic pain induction and gradually decline. Injection of anti-CXCL2 into the trigeminal ganglion reduces pain, suggesting that anti-CXCL2 is a therapeutic option for neuropathic pain (Iwasa et al., 2019). It has also been reported that cc-chemokine ligand 4 (CCL4) is involved in the induction of neuropathic pain after peripheral nerve injury, confirming our results that CCL4 is one of the hub genes. CCR1 was reported to enhance modification of DGCR8 by SUMO1 through phosphorylation of ERK, thereby promoting activation of spinal microglia and inflammatory responses and increasing pain sensitivity in SNL rats (Shi et al., 2022). Our research provides additional potential therapeutic targets for neuropathic pain.

Through using the Cytoscape software, interleukin-2 (IL-2) was ranked the most important gene in the PPI network, as well as the most important gene of the hub gene. IL-2, also called cell growth factor, is an immunomodulatory cytokine excreted by T lymphocytes in response to antigen stimulation (Zhu et al., 2022). Previous studies have revealed the anti-injurious (analgesic) effects of IL-2 in the peripheral and central nervous system (Yao et al., 2002). The short lifespan of IL-2 *in vivo* unfortunately makes clinical application of IL-2 for analgesia impractical. However, a new approach to single intrathecal injections of IL-2 has to be available as a gene therapy for

the treatment of neuropathic pain (Yao et al., 2002). The effects of adenovirus-mediated IL-2 genes on chronic neuropathic pain and basal nociceptive response in rats have also been investigated. Yao MZ et al. evaluated the anti-injurious effects of adenovirus type 5 (Ad5) and Ad5-IL2 using radiation heat-induced paw withdrawal latency. Intrathecal injection of Ad5-IL2 was found to have a significant anti-injurious effect on chronic neuropathic pain and basal nociceptive response and was sustained for 4 and 3 weeks, respectively (Yao et al., 2003). This study shows that adenovirus-mediated intrathecal delivery of the IL2 gene has a long-lasting anti-injurious effect. In conclusion, IL2 is a potential therapeutic target for neuropathic pain.

This is the first study to explore the causal association between IL2 levels and trigeminal neuralgia risk by a two-sample MR analysis based on a large amount of GWAS data of IL2 (exposure) and trigeminal neuralgia (outcome). This MR study showed that serum IL2 levels might be causally associated with an increased risk of trigeminal neuralgia. MR is similar in concept to prospective randomized controlled trials (RCTs) but reduces systematic biases that affect the results of traditional observational studies, such as confounding factors and reverse causality. The high accuracy of genotyping can effectively avoid regression dilution caused by detection errors. To ensure that SNPs are not related to any confounding factors between IL2 and trigeminal neuralgia, we chose only participants from European populations. Finally, to ensure the stability of the results, we also performed MR–Egger regression test, and no evidence of directional level pleiotropy was observed.

Despite these meaningful findings, our research still has a few shortcomings. Firstly, this study only used one dataset because of the absence of microarray data in the area of neuropathic pain, and the results would have been more convincing if more neuropathic pain-related datasets had been combined. Secondly, this study only used bioinformatics to analyze the hub genes and potential functions associated with the occurrence of neuropathic pain, and more biological experiments are required to validate the specific mechanisms of the hub genes screened.

5. Conclusion

We constructed a WGCNA-based co-expression network and identified neuropathic pain-related hub genes. This may help in the development of pre-symptomatic diagnostics and may provide further insights into the molecular mechanisms for understanding neuropathic pain risk genes.

Data availability statement

The original contributions presented in the study are included in the article/Supplementary material, further inquiries can be directed to the corresponding authors.

Author contributions

LL and JL designed the study and revised the manuscript. JZ and CL acquired the raw data and analyzed the data. JZ wrote the manuscript. All authors contributed to the article and approved the submitted version.

Acknowledgments

The authors thank the editor and reviewers for their kindly help and constructive suggestions to improve the work. Thank you to the researchers who uploaded the raw data to a public database for all to share.

Conflict of interest

The authors declare that the research was conducted in the absence of any commercial or financial relationships that could be construed as a potential conflict of interest.

Publisher's note

Supplementary material

The Supplementary material for this article can be found online at: https://www.frontiersin.org/articles/10.3389/fnins.2023.1134330/full#supplementary-material

References

Asensio, V. C., and Campbell, I. L. (1999). Chemokines in the CNS: Plurifunctional mediators in diverse states. *Trends Neurosci.* 22, 504–512. doi: 10.1016/s0166-2236(99)01453-8

Barclay, J., Clark, A. K., Ganju, P., Gentry, C., Patel, S., Wotherspoon, G., et al. (2007). Role of the cysteine protease cathepsin S in neuropathic hyperalgesia. *Pain* 130, 225–234. doi: 10.1016/j.pain.2006.11.017

Binder, A., and Baron, R. (2016). The pharmacological therapy of chronic neuropathic pain. *Dtsch. Arztebl. Int.* 113, 616–625. doi: 10.3238/arztebl.2016.0616

Charo, I. F., and Ransohoff, R. M. (2006). The many roles of chemokines and chemokine receptors in inflammation. *N. Engl. J. Med.* 354, 610–621. doi: 10.1056/NEJMra052723

Chen, B., Khodadoust, M. S., Liu, C. L., Newman, A. M., and Alizadeh, A. A. (2018). Profiling tumor infiltrating immune cells with CIBERSORT. *Methods Mol. Biol.* 1711, 243–259. doi: 10.1007/978-1-4939-7493-1_12

Cui, C. Y., Liu, X., Peng, M. H., Liu, Q., and Zhang, Y. (2022). Identification of key candidate genes and biological pathways in neuropathic pain. *Comput. Biol. Med.* 150:106135. doi: 10.1016/j.compbiomed.2022.106135

Dominguez, E., Rivat, C., Pommier, B., Mauborgne, A., and Pohl, M. (2008). JAK/STAT3 pathway is activated in spinal cord microglia after peripheral nerve injury and contributes to neuropathic pain development in rat. *J. Neurochem.* 107, 50–60. doi: 10.1111/j.1471-4159.2008.05566.x

Dudbridge, F. (2021). Polygenic Mendelian randomization. *Cold Spring Harb. Perspect. Med.* 11:a039586. doi: 10.1101/cshperspect.a039586

Emdin, C. A., Khera, A. V., and Kathiresan, S. (2017). Mendelian randomization. *JAMA* 318, 1925–1926. doi: 10.1001/jama.2017.17219

Finnerup, N. B., Haroutounian, S., Kamerman, P., Baron, R., Bennett, D. L. H., Bouhassira, D., et al. (2016). Neuropathic pain: An updated grading system for research and clinical practice. *Pain* 157, 1599–1606. doi: 10.1097/j.pain.0000000000000492

Finnerup, N. B., Kuner, R., and Jensen, T. S. (2021). Neuropathic pain: From mechanisms to treatment. *Physiol. Rev.* 101, 259–301. doi: 10.1152/physrev.00045.2019

Fukuoka, T., Kondo, E., Dai, Y., Hashimoto, N., and Noguchi, K. (2001). Brain-derived neurotrophic factor increases in the uninjured dorsal root ganglion neurons in selective spinal nerve ligation model. *J. Neurosci.* 21, 4891–4900. doi: 10.1523/JNEUROSCI.21-13-04891.2001

Gao, Y., Sun, N., Wang, L., Wu, Y., Ma, L., Hong, J., et al. (2018). Bioinformatics analysis identifies p53 as a candidate prognostic biomarker for neuropathic pain. *Front. Genet.* 9:320. doi: 10.3389/fgene.2018.00320

Golubovic, M., Kostic, T., Djordjevic, M., Peric, V., Lazarevic, M., Milic, D. J., et al. (2021). In silico development of potential therapeutic for the pain treatment by inhibiting voltage-gated sodium channel 1.7. *Comput. Biol. Med.* 132:104346. doi: 10.1016/j.compbiomed.2021.104346

Harrell, F. J., Lee, K. L., and Mark, D. B. (1996). Multivariable prognostic models: Issues in developing models, evaluating assumptions and adequacy, and measuring and reducing errors. *Stat. Med.* 15, 361–387. doi: 10.1002/(SICI)1097-0258(19960229)15:4<361::AID-SIM168>3.0.CO;2-4

He, S. Q., Han, L., Li, Z., Xu, Q., Tiwari, V., Yang, F., et al. (2014). Temporal changes in MrgC expression after spinal nerve injury. *Neuroscience* 261, 43–51. doi: 10.1016/j.neuroscience.2013.12.041

Iasonos, A., Schrag, D., Raj, G. V., and Panageas, K. S. (2008). How to build and interpret a nomogram for cancer prognosis. *J. Clin. Oncol.* 26, 1364–1370. doi: 10.1200/JCO.2007.12.9791

Imai, S., Ikegami, D., Yamashita, A., Shimizu, T., Narita, M., Niikura, K., et al. (2013). Epigenetic transcriptional activation of monocyte chemotactic protein 3 contributes to long-lasting neuropathic pain. *Brain* 136, 828–843. doi: 10.1093/brain/aws330

Iwasa, T., Afroz, S., Inoue, M., Arakaki, R., Oshima, M., Raju, R., et al. (2019). IL-10 and CXCL2 in trigeminal ganglia in neuropathic pain. *Neurosci. Lett.* 703, 132–138. doi: 10.1016/j.neulet.2019.03.031

Jansen, H., Samani, N. J., and Schunkert, H. (2014). Mendelian randomization studies in coronary artery disease. *Eur. Heart J.* 35, 1917–1924. doi: 10.1093/eurheartj/ehu208

Jiang, B. C., Cao, D. L., Zhang, X., Zhang, Z. J., He, L. N., Li, C. H., et al. (2016). CXCL13 drives spinal astrocyte activation and neuropathic pain via CXCR5. *J. Clin. Invest.* 126, 745–761. doi: 10.1172/JCI81950

Kanehisa, M., and Goto, S. (2000). KEGG: Kyoto encyclopedia of genes and genomes. *Nucleic Acids Res.* 28, 27–30. doi: 10.1093/nar/28.1.27

Langfelder, P., and Horvath, S. (2008). WGCNA: An R package for weighted correlation network analysis. *BMC Bioinform.* 9:559. doi: 10.1186/1471-2105-9-559

Li, S. F., Ouyang, B. S., Zhao, X., and Wang, Y. P. (2018). Analgesic effect of AG490, a Janus kinase inhibitor, on oxaliplatin-induced acute neuropathic pain. *Neural Regen. Res.* 13, 1471–1476. doi: 10.4103/1673-5374.235305

Moisset, X., and Page, M. G. (2021). Interest of registries in neuropathic pain research. *Rev. Neurol. (Paris)* 177, 843–848. doi: 10.1016/j.neurol.2021.07.011

Nangraj, A. S., Selvaraj, G., Kaliamurthi, S., Kaushik, A. C., Cho, W. C., and Wei, D. Q. (2020). Integrated PPI-and WGCNA-retrieval of hub gene signatures shared between Barrett's esophagus and esophageal adenocarcinoma. *Front. Pharmacol.* 11:881. doi: 10.3389/fphar.2020.00881

Park, S. Y. (2018). Nomogram: An analogue tool to deliver digital knowledge. *J. Thorac. Cardiovasc. Surg.* 155:1793. doi: 10.1016/j.jtcvs.2017.12.107

Seo, H., and Jun, S. C. (2021). Computational exploration of epidural cortical stimulation using a realistic head model. *Comput. Biol. Med.* 135:104290. doi: 10.1016/j.compbiomed.2021.104290

Shi, C., Jin, J., Xu, H., Ma, J., Li, T., Xie, Y., et al. (2022). CCR1 enhances SUMOylation of DGCR8 by up-regulating ERK phosphorylation to promote spinal nerve ligation-induced neuropathic pain. *Gene Ther.* 29, 379–389. doi: 10.1038/s41434-021-00285-3

St, J. S. E. (2018). Advances in understanding nociception and neuropathic pain. *J. Neurol.* 265, 231–238. doi: 10.1007/s00415-017-8641-6

Torta, R., Ieraci, V., and Zizzi, F. (2017). A review of the emotional aspects of neuropathic pain: From comorbidity to co-pathogenesis. *Pain Ther.* 6, 11–17. doi: 10.1007/s40122-017-0088-z

von Hehn, C. A., Baron, R., and Woolf, C. J. (2012). Deconstructing the neuropathic pain phenotype to reveal neural mechanisms. *Neuron* 73, 638–652. doi: 10.1016/j.neuron.2012.02.008

von Schack, D., Agostino, M. J., Murray, B. S., Li, Y., Reddy, P. S., Chen, J., et al. (2011). Dynamic changes in the microRNA expression profile reveal multiple regulatory mechanisms in the spinal nerve ligation model of neuropathic pain. *PLoS One* 6:e17670. doi: 10.1371/journal.pone.0017670

Wu, Y., and Nie, H. (2022). A bioinformatics study of differentially expressed genes in microarrays of dorsal root ganglia from rat models of neuropathic pain. *Med. Sci. Monit.* 28:e934122. doi: 10.12659/MSM.934122

Xu, C., Liu, T., Zhang, Y., and Feng, Y. (2022). Effect of surgical damage to spinal nerve on dorsal-root ganglion gene expressions: Comprehensive analysis of differentially expressed genes. *Asian J. Surg.* 45, 2618–2625. doi: 10.1016/j.asjsur.2021.12.021

Yao, M. Z., Gu, J. F., Wang, J. H., Sun, L. Y., Lang, M. F., Liu, J., et al. (2002). Interleukin-2 gene therapy of chronic neuropathic pain. *Neuroscience* 112, 409–416. doi: 10.1016/S0306-4522(02)00078-7

Yao, M. Z., Gu, J. F., Wang, J. H., Sun, L. Y., Liu, H., and Liu, X. Y. (2003). Adenovirus-mediated interleukin-2 gene therapy of nociception. *Gene Ther.* 10, 1392–1399. doi: 10.1038/sj.gt.3301992

Zhang, D. D., Chen, Q. Q., and Yao, L. (2022). Geniposide alleviates neuropathic pain in CCI rats by inhibiting the EGFR/PI3K/AKT pathway and ca(2+) channels. *Neurotox. Res.* 40, 1057–1069. doi: 10.1007/s12640-022-00531-5

Zhang, W., Suo, M., Yu, G., and Zhang, M. (2019). Antinociceptive and anti-inflammatory effects of cryptotanshinone through PI3K/Akt signaling pathway in a rat model of neuropathic pain. *Chem. Biol. Interact.* 305, 127–133. doi: 10.1016/j.cbi.2019.03.016

Zhu, H., Hu, X., Gu, L., Jian, Z., Li, L., Hu, S., et al. (2021c). TUBA1C is a prognostic marker in low-grade glioma and correlates with immune cell infiltration in the tumor microenvironment. *Front. Genet.* 12:759953. doi: 10.3389/fgene.2021.759953

Zhu, H., Hu, S., Li, Y., Sun, Y., Xiong, X., Hu, X., et al. (2022). Interleukins and ischemic stroke. *Front. Immunol.* 13:828447. doi: 10.3389/fimmu.2022.828447

Zhu, H., Jian, Z., Zhong, Y., Ye, Y., Zhang, Y., Hu, X., et al. (2021b). Janus kinase inhibition ameliorates ischemic stroke injury and neuroinflammation through reducing NLRP3 Inflammasome activation via JAK2/STAT3 pathway inhibition. *Front. Immunol.* 12:714943. doi: 10.3389/fimmu.2021.714943

Zhu, D., Liu, K., Wan, C. L., Lu, J., and Zhao, H. X. (2019). Identification of novel therapeutic targets for neuropathic pain based on gene expression patterns. *J. Cell. Physiol.* 234, 19494–19501. doi: 10.1002/jcp.28448

Zhu, H., Zhang, Y., Zhong, Y., Ye, Y., Hu, X., Gu, L., et al. (2021a). Inflammation-mediated angiogenesis in ischemic stroke. *Front. Cell. Neurosci.* 15:652647. doi: 10.3389/fncel.2021.652647

frontiers | Frontiers in Neuroscience

TYPE Systematic Review
PUBLISHED 17 April 2023
DOI 10.3389/fnins.2023.1120541

OPEN ACCESS

EDITED BY
Bo Li,
Sun Yat-sen Memorial Hospital, Sun Yat-sen University, China

REVIEWED BY
Yi-Ming Ren,
Nankai University, China
Yan Yan,
Sun Yat-sen Memorial Hospital, China
Jiayue Ding,
Tianjin Medical University General Hospital, China

*CORRESPONDENCE
Li Yi
✉ yilitj@hotmail.com

SPECIALTY SECTION
This article was submitted to Translational Neuroscience, a section of the journal Frontiers in Neuroscience

RECEIVED 10 December 2022
ACCEPTED 28 March 2023
PUBLISHED 17 April 2023

CITATION
Zhang X, Song Y, Wei Z, Chen X, Zhuang X and Yi L (2023) The prevalence and risk factors of anxiety in multiple sclerosis: A systematic review and meta-analysis.
Front. Neurosci. 17:1120541.
doi: 10.3389/fnins.2023.1120541

The prevalence and risk factors of anxiety in multiple sclerosis: A systematic review and meta-analysis

Xiaoyun Zhang[1,2], Ying Song[1], Zhiqiang Wei[1], Xiao Chen[1], Xiaojia Zhuang[1] and Li Yi[1]*

[1]Neurology Department, Peking University Shenzhen Hospital, Shenzhen, China, [2]Rehabilitation Department, Shenzhen Longhua District Central Hospital, Shenzhen, China

Background: Patients with multiple sclerosis (MS) suffer from repetitive neurological deterioration, while anxiety may play a significant role in the disease's progression.

Objective: To explore the prevalence of anxiety in MS and to investigate the risk factors related to anxiety in MS patients.

Methods: An analysis of four databases, PubMed, Web of Science, EMBASE, and Cochrane Library, has been conducted to determine the prevalence or risk factors for anxiety in MS published before May 2021.

Results: In total, 32 studies were found to be eligible. Anxiety prevalence was estimated to be 36% based on the pooled estimates [the 95% confidence interval (CI) = [0.30–0.42], I^2 = 98.4%]. Significant risk factors for developing of anxiety were as follows: age at survey [the weighted mean difference (WMD) = 0.96, 95% CI = [0.86–1.06], I^2 = 43.8%], female [the odd ratio (OR) = 1.78, 95% CI = [1.38–2.30], I^2 = 0%], living together (OR 2.83, 95% CI = [1.74–4.59], I^2 = 0%), past psychiatric history (OR 2.42, 95% CI = [1.56–3.75], I^2 = 0%), depression (OR 7.89, 95% CI = [3.71–16.81], I^2 = 0%), not taking MS medication (OR 2.33, 95% CI = [1.29–4.21], I^2 = 77.8%), relapsing-remitting MS (RRMS) (OR 1.50, 95% CI = [0.94–2.37], I^2 = 53.5%), and baseline Expanded Disability Status Scale (EDSS) (OR 0.84, 95% CI = [0.48–1.21], I^2 = 62.2%).

Conclusion: An estimated 36% of people with MS suffer from anxiety. And anxiety rates in MS patients are significantly associated with age, gender, living together, prior psychiatric history, depression, drug compliance, RRMS, and baseline EDSS.

Systematic review registration: https://www.crd.york.ac.uk/PROSPERO/display_record.php?RecordID=287069, identifier CRD42021287069.

KEYWORDS

multiple sclerosis, anxiety, prevalence, risk factor, meta-analysis

Background

The prevalence of MS varies between high-income countries and low-income countries, with a global prevalence of 30 cases per 100,000 population (GBD 2016 Multiple Sclerosis Collaborators, 2019) and world-wide prevalence of 60–120 per 100,000 in working-age adults (Levi et al., 2021), imposing a deterioration of the economy and health care (Browne et al., 2014). There are various neurological deficits associated with multiple sclerosis (MS), such as motor, sensory, cognitive and neuropsychiatric impairments.

According to the clinical course, MS can be classified into clinically isolated syndrome (CIS), relapsing-remitting multiple sclerosis (RRMS), secondary progressive MS (SPMS), primary progressive MS (PPMS), and progressive relapsing MS (PRMS) (Kamm et al., 2014). The most common form is RRMS, affecting around 80% of MS patients (Compston and Coles, 2008). RRMS patients can recover to function for an unpredictable period of time before further attacks lead to progressive deterioration. It is important to note, however, that being disease-free does not necessarily mean that patients with RRMS are symptom-free, because they can still suffer from debilitating condition, such as anxiety and depression. Comorbid anxiety and depression are highly prevalent in chronically ill patients (Scott et al., 2007). Given the unpredictable and fluctuating nature of RRMS, it is not surprising that patients may be anxious about when there will be another episode. In addition, anxiety had a greater impact on disease symptoms as compared to depression. Those with anxiety were much more likely to report fatigue, pain, and sleep problems even with no association with depression (Hanna and Strober, 2020).

Anxiety is a mental state characterized by worry or fear in the face of a stressful event, and is not uncommon for patients with MS. Reports on MS and anxiety started around the 1980s with several studies suggesting that anxiety can reach a lifetime prevalence of up to 50% for MS patients (Olivera et al., 1988). Many factors can lead to anxiety, and ultimately cause poor outcomes in social support and disease duration (Hanna and Strober, 2020). Besides, anxiety, depression and pain are significantly associated with the severity of wheelchair dependence in patients with MS (Janssens et al., 2004). And the negative effect of anxiety on the quality of life (QOL) is the most frequently reported outcome in MS patients (van Tilburg et al., 2021).

Early identification and treatment of anxiety may improve working productivity and extend employment for MS patients (Glanz et al., 2012). However, despite early studies have focused on the prevalence of anxiety and depression in MS, few reviews summarized the risk factors relevant to anxiety in MS patients.

This meta-analysis aims to provide an overview of anxiety prevalence in MS patients and to investigate risk factors that are associated with anxiety development. And to our knowledge, our meta-analysis would be the first to discuss the risk factors for anxiety in MS patients.

Methods

The present systematic review and meta-analysis was conducted in accordance with the Preferred Reporting Items for Systematic Reviews and Meta-Analysis (PRISMA) guidelines (Moher et al., 2009) and has been registered in the PROSPERO database (No. CRD42021287069).

Search strategy

In order to identify studies discussing anxiety among MS patients, articles published before 16th May 2021 were searched in international databases including PubMed, Web of Science, EMBASE, and Cochrane Library. Search items and synonyms were based on the PECO acronym (population: patients with MS, exposure: risk factors and prevalence, outcome: anxiety) and the Boolean operators "AND" and "OR."

As our main focus was set on the MS population, studies with a healthy control group were excluded. Detailed search terms are provided in **Supplementary Appendix 1**. References of eligible studies were also assessed for additional citations.

Eligibility criteria

The following criteria had to be met in order for a study to be included:

1. Inclusion criteria
   Subjects diagnosed with MS by neurologists fulfilling Poser Criteria (Poser et al., 1983), or original or revised McDonald diagnostic criteria for MS (criteria of 2001 or revised McDonald criteria of 2005/2010/2017), or a clinically definite MS based on retrospective medical records;

   1.1 There should be data available to extract to determine the prevalence or risk factors of anxiety in MS, with the diagnosis criteria for anxiety outlined in **Table 1**;
   1.2 Studies were cross-sectional studies or cohort studies.

2. Exclusion criteria

   2.1 Studies not involving humans, case reports, reviews, guidelines, protocols, commentaries, letters, or abstracts;
   2.2 Studies with insufficient or unavailable data;
   2.3 Duplicate studies;
   2.4 Risk factors involving the study of healthy subjects instead of merely MS patients;
   2.5 Risk factors discussed in fewer than two studies;
   2.6 Non-English articles without English abstracts.

Study selection

To determine eligibility, two reviewers (XYZ and YS) independently screened all titles and abstracts using Endnote X10 software after the removal of duplicates. An independent third researcher (LY) resolved all divergences between the two reviewers. Subsequently, to determine whether these full texts met the eligibility criteria, two reviewers (XYZ and YS) screened the included full texts of potential interest.

TABLE 1 Characteristics of included studies.

References	Article type	Nation	Total (*N*)	RR patients (*N*)	Age (*M* ± SD)	M/F	Measurement tool
Askari et al., 2014	Cross-sectional study	Iran	180	142	32.4 ± 8.7	84/236	BAI
Chertcoff et al., 2020	Cross-sectional study	Argentina	83	61	46 ± 13.9	30/53	HADS-A ≥ 8
Garfield and Lincoln, 2012	Cross-sectional study	UK	159	83	50 ± 10.15	47/112	HADS-A ≥ 8
Gascoyne et al., 2019	Cross-sectional study	Australia	1500	858	56 ± 11.2	308/1192	HADS-A ≥ 8
Gay et al., 2017	Cross-sectional study	France	189	107	47.2 ± 12.5	68/121	HADS-A ≥ 8
Gay et al., 2010	Cross-sectional study	France	115	NA	47.22 ± 10.93	36/79	HADS-A ≥ 8
Gill et al., 2019	Cross-sectional study	Canada	128	92	46.32 ± 8.23	33/95	HADS-A ≥ 8
Hanna and Strober, 2020	Cross-sectional study	USA	183	173	44.09 ± 9.51	19/173	STAI
Henry et al., 2019	Cross-sectional study	France	110	70	44.93 ± 12.7	34/76	HADS-A ≥ 8
Jones et al., 2012	Cross-sectional study	UK	4617	2849	50.9 ± 11.5	1355/3253	HADS-A ≥ 8
Karimi et al., 2020	Cross-sectional study	Iran	87	NA	35.5 ± 9.2	26/61	DASS-21 anxiety ≥ 8
Korostil and Feinstein, 2007	Cross-sectional study	Canada	140	78	43.9 ± 10.7	36/104	HADS-A ≥ 10
Kotan et al., 2019	Cross-sectional study	Turkey	227	158	37.0 ± 9.9	64/163	HADS-A
Leonavicius and Adomaitiene, 2013	Cross-sectional study	Lithuania	312	NA	42.01 ± 12.48	116/196	HADS-A
Marck et al., 2016	Cross-sectional study	USA, Canada, Australia, New Zealand, Europe, and others	2399	1472	45.5 ± 10.6	407/1892	SCQ
Marrie et al., 2018	Cross-sectional study	Canada	859	621	48.7 ± 11.3	213/646	HADS-A ≥ 8
Nicholl et al., 2001	Cross-sectional study	UK	96	11	48.7 ± 8.9	11/72	BAI, HADS-A
Noy et al., 1995	Cross-sectional study	Israel	20	NA	41.8 ± 9.0	5/15	HAS ≥ 18
Orr et al., 2018	Cross-sectional study	Canada	251	181	50.9 ± 12.9	47/204	HADS-A ≥ 8
Pham et al., 2018	Cross-sectional study	Canada	244	162	49.5 ± 11.6	99/178	HADS-A ≥ 8
Podda et al., 2020	Cross-sectional study	Italy	608	263	57.9 ± 12.5	200/408	HADS-A ≥ 8
Poder et al., 2009	Cross-sectional study	Canada	245	172	46.1 ± 10.6	45/200	HADS-A ≥ 11
Ramezani et al., 2021	Cross-sectional study	Iran	410	NA	38.60 ± 10.35	84/326	HADS-A ≥ 8
Reyes et al., 2020	Cross-sectional study	UK	236	180	43.5 ± 12.6	68/168	HADS-A ≥ 8
Schiess et al., 2019	Cross-sectional study	USA	416	329	36.6 ± 10.6	148/268	ICD-9
Suh et al., 2010	Cross-sectional study	USA	96	91	42.8 ± 10.2	21/75	HADS-A ≥ 8
Terrill et al., 2015	Cross-sectional study	USA	513	287	51.4 ± 10.9	94/419	GAD-7 ≥ 8
Uguz et al., 2008	Cross-sectional study	Turkey	74	74	34.57 ± 11.93	24/50	SCID-I
van der Hiele et al., 2012	Cross-sectional study	Netherlands	715	251	48.3 ± 10.4	185/530	HADS-A ≥ 8
Wallis et al., 2020	Cross-sectional study	Netherlands	119	79	47.8 ± 9.4	44/75	HADS-A ≥ 8
Zanghì et al., 2020	Cross-sectional study	Italy	432	432	40.4 ± 12.4	155/277	DASS-21 ≥ 8
Panda et al., 2018	Cross-sectional study	India	90	83	38.070 ± 10.470	36/54	HADS-A ≥ 8

RR patients, relapsing and remitting MS patients; M, male; F, female; BAI, Beck Anxiety Inventory; DASS-21, Depression Anxiety and Stress Scale-21; HADS-A, anxiety subscale of the Hospital Anxiety and Depression Scale; ICD-9, International Classification of Diseases, Ninth Revision; HAS, Hamilton Anxiety Scale; SCID-I, Structured Clinical Interview for DSM-IV; SCQ, Self-administered Comorbidity Questionnaire; STAI, State trait anxiety inventory; NA, not available.

Data collection process

In this study, two researchers (XYZ and YS) extracted data using preformulated forms. A third researcher (LY) double-checked their results and resolved any disagreements. Supplementary data concerning risk factors were also screened by the researcher (XYZ). For dichotomization, we requested both numbers of patients with anxiety and those without it for each subgroup. And outcomes that could not be dichotomized were eliminated from our analyses.

Quality assessment

Two researchers (XYZ and ZW) evaluated the methodological quality using the guidance from the Agency for Healthcare

Research and Quality (AHRQ) Evidence-based Practice Center (Berkman et al., 2008) for the included studies (**Figure 1**). Research with a total score of >7 out of 11 was considered high-quality (Berkman et al., 2008). Whenever there was a disagreement, it was resolved by consensus.

Outcome measures

Studies with multiple anxiety evaluation methods were entered as individual study samples. Weighted mean differences (WMDs) were calculated for continuous data, and odds ratios (ORs) were calculated for dichotomous data. And 95% confidence intervals were provided for both WMDs and ORs. A primary outcome measure was anxiety prevalence and ORs with 95% confidence intervals (CIs). The sample sizes or specific values of the subgroups of anxiety and non-anxiety were collected to calculate the WMDs or ORs of each risk factor separately by using the Stata 15.0 (version 15.0, StataCorp, College Station, TX, USA). Sensitivity analyses were run to exclude studies with a high risk of bias.

Statistical analysis

Data analysis was conducted by XYZ, XC, and XJZ. Fixed effects models were used at the beginning of the analysis. I^2 was assessed using the method proposed by Higgins et al. (2003). In cases where $I^2 \leq 50\%$, it was determined that there was no obvious heterogeneity among the studies included, and a fixed effect model was applied. Otherwise, $I^2 > 50\%$ indicated high heterogeneity (Higgins et al., 2003). In this case, random effect models would be used to calculate the effect size, and a sensitivity analysis and subgroup analysis were conducted to clarify the underlying systematic differences and reduce the substantial heterogeneity. Countries of the studies and measurement tools used in the studies were taken into account for subgroup analyses. In order to compare the significance of the heterogeneity among studies, Chi-squared (χ^2) tests were conducted. And a conventional p-value of 0.05 was used as the cut-off for determining the significance of the heterogeneity.

Results

Study selection

Through systematic search, 2,523 articles were found. After excluding duplicate papers and irrelevant articles, 534 potentially eligible studies remained. Finally, 32 articles (Noy et al., 1995; Nicholl et al., 2001; Korostil and Feinstein, 2007; Uguz et al., 2008; Poder et al., 2009; Gay et al., 2010, 2017; Suh et al., 2010; Garfield and Lincoln, 2012; Jones et al., 2012; van der Hiele et al., 2012; Leonavicius and Adomaitiene, 2013; Askari et al., 2014; Terrill et al., 2015; Marck et al., 2016; Marrie et al., 2018; Orr et al., 2018; Panda et al., 2018; Pham et al., 2018; Gascoyne et al., 2019; Gill et al., 2019; Henry et al., 2019; Kotan et al., 2019; Schiess et al., 2019; Chertcoff et al., 2020; Hanna and Strober, 2020; Karimi et al., 2020; Podda et al., 2020; Reyes et al., 2020; Wallis et al., 2020; Zanghì et al., 2020; Ramezani et al., 2021) with 15,853 participants were found to be eligible in the analyses, as shown in **Table 1**. The flow diagram of the search and study selection process was shown in **Figure 2**.

Study characteristics

Among the included studies, sample sizes ranged from 20 (Noy et al., 1995) to 4,617 (Jones et al., 2012). **Table 1** summarized the clinical characteristics of MS patients enrolled in the included studies. As displayed in **Table 1**, most studies were cross-sectional, and most of them were conducted in European and American countries including one multi-countries study, with seven studies conducted in Canada, five in the USA and four in the UK. Twenty-three studies assessed anxiety using the anxiety subscale of the Hospital Anxiety and Depression Scale (HADS-A) as a measurement tool. One study diagnosed anxiety according to 9th Revision of the International Classification of Diseases (ICD-9) and another was based on Structured Clinical Interview for DSM-IV (SCID-I) (First et al., 2007). As for the analysis of risk factors of anxiety in MS patients, only fifteen studies were eligible for further investigation.

Quality of studies

Agency for Healthcare Research and Quality checklists were used to assess the quality of cross-sectional studies. The checklist contains 11 items with the options of "Yes," "No," or "unclear." For each item, the answers of "no" or "unclear" were recorded as "0" and the answer of "yes" was marked as "1" (Landeiro et al., 2011). Based on the total score, the included studies were divided into the following categories: good (8–11), average (4–7), and poor (0–3).

Based on the AHRQ checklist, the included studies' methodological quality was strong with a mean score of 9.78 ± 1.16 out of 11 and a score range of 7 to 11 out of 11 (see **Table 2**). The main weakness of the included studies was that quite a few studies did not mention whether the subjects were consecutive if not population-based.

Prevalence of anxiety in MS

Anxiety is prevalent in MS at 36% (95% CI = [0.30–0.42], $I^2 = 98.4\%$, $p < 0.001$; 32 studies). And high heterogeneity was still observed after subgroup analyses based on geographical country, measurement tool, publication year and sample size (see **Figures 3–6**).

Risk factors for anxiety in MS

Fifteen studies reported more than 50 risk factors for the development of anxiety in MS, as summarized in **Tables 3**, **4**. The risk factors presented in at least two studies are as follows: gender (female or not), prior psychiatric history (past history of psychiatric disorders or psychiatric comorbidity), age at survey, comorbidity with depression, family history of

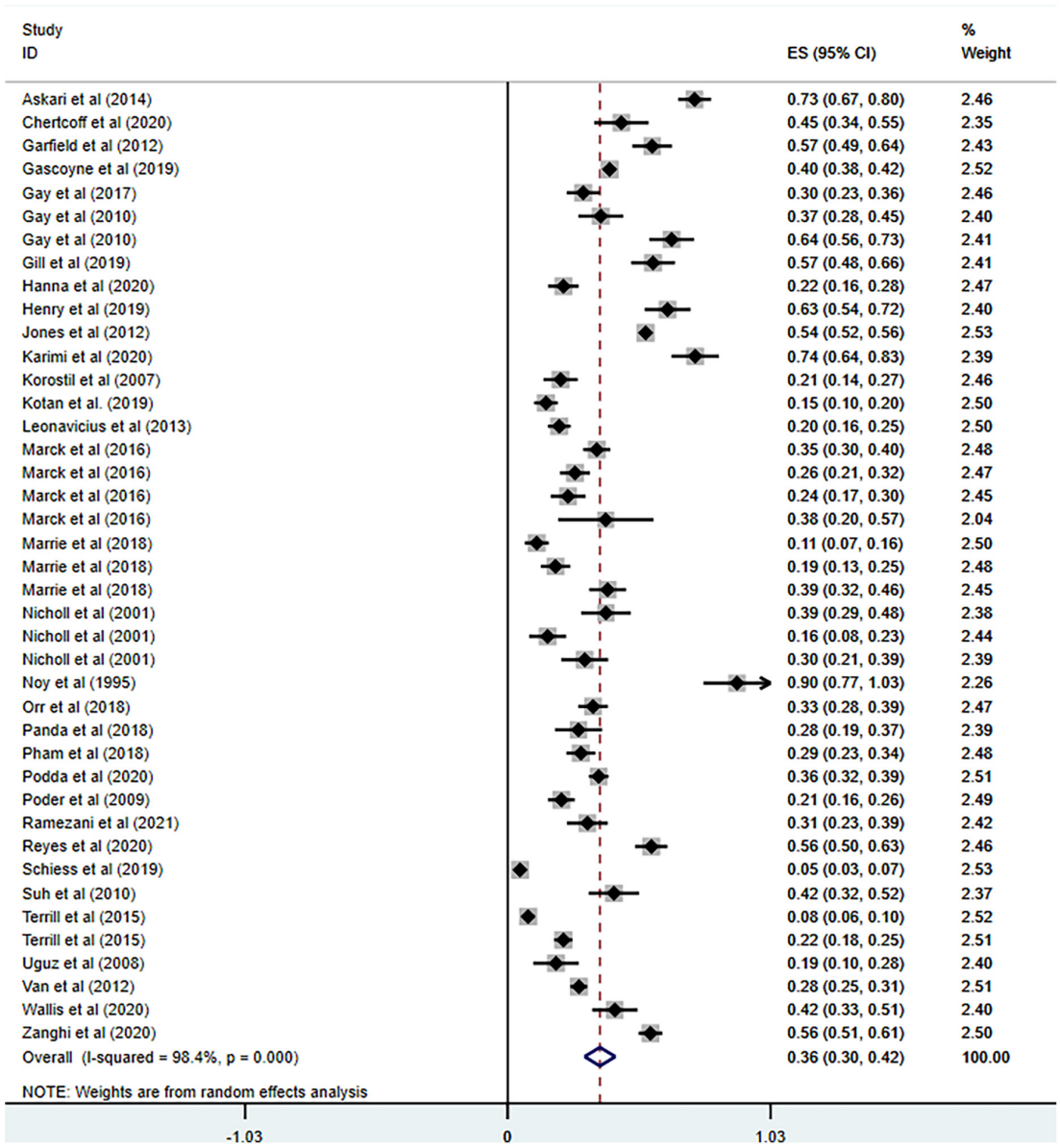

FIGURE 1
Forest plot of meta-analysis on prevalence of anxiety in MS patients.

psychiatric disorders, family status (living together or living alone), employment status (currently working or not), education level, marriage, disease course (type of MS), disease duration (time since diagnosis in years), lack of disease-modifying therapy (DMT) and Expanded Disability Status Scale (EDSS) scores at baseline (T0). Meta analyses were conducted for the risk factors mentioned in more than one study. **Supplementary figures** can be found in **Supplementary Appendix 2**.

Age at survey

Age at survey was discussed in six studies and one study (Podda et al., 2020) with a high risk of bias was withdrawn. Fixed effect model analysis showed that there was no correlation between age and anxiety (WMD 0.96, 95% CI = [0.86–1.06], $p < 0.001$, $I^2 = 43.8\%$) (see **Supplementary Figure 1**).

Gender

Data from eight eligible studies were combined and a sensitivity analysis was carried out with a high-risk bias study (Jones et al., 2012) withdrawn. The analysis results showed that female MS patients were 1.78 times more likely to have anxiety than male MS patients (OR 1.78, 95% CI = [1.38–2.30], $p < 0.001$, $I^2 = 0$) (see **Supplementary Figure 2**).

Depression

Depression was investigated in three studies. After excluding one study (Jones et al., 2012) with a high risk of bias after sensitivity analysis, the heterogeneity remained zero ($I^2 = 0$, $p = 0.560$) with an increase of the intergroup difference. Our result showed that in MS patients who had depression, anxiety was 7.89 times more likely to develop than in those without

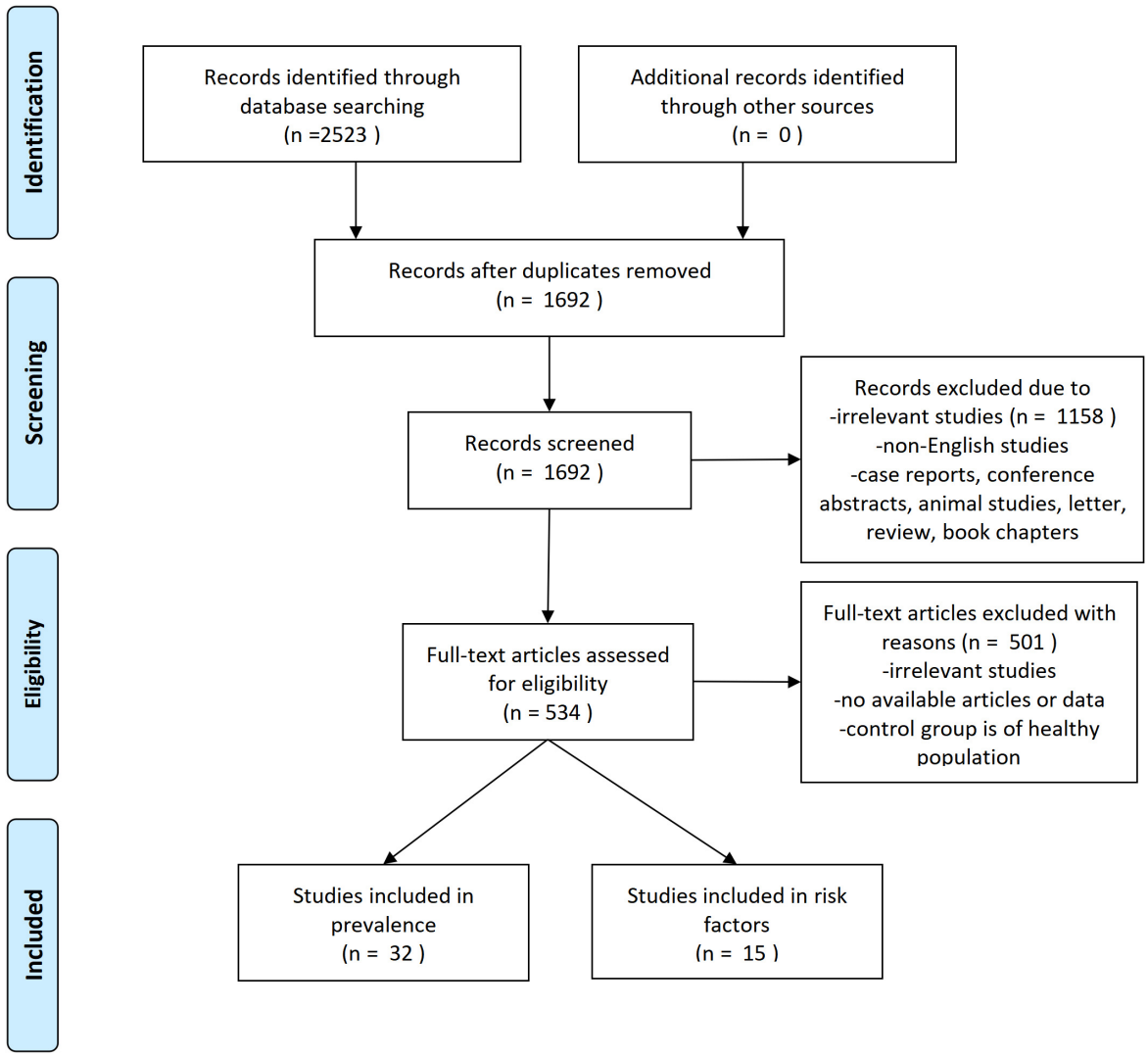

FIGURE 2
Selection process for the studies included in the meta-analysis.

depression (OR 7.89, 95% CI = [3.71–16.81], $p < 0.001$, $I^2 = 0$) (see Supplementary Figure 3).

Marriage status

The combined analysis of marriage status in three studies showed that there was no significant relationship between marriage status and anxiety (OR 0.95, 95% CI = [0.62–1.44], $p = 0.794$) without heterogeneity ($I^2 = 40.7\%$) (see Supplementary Figure 4).

Employment status

The results of three studies concerning employment status were pooled, and no significant association was found between the development of anxiety and employment (OR 0.87, 95% CI = [0.6–1.24], $p = 0.434$) without heterogeneity ($I^2 = 27.5\%$) (see Supplementary Figure 5).

Education

Education was reported in five studies, three of which provided binary variables (education levels) and two provided continuous variables (years of education). The analysis of binary variables showed no significant association between education and the development of anxiety (OR 1.28, 95% CI = [0.52–3.15], $p = 0.830$) (see Supplementary Figure 6) with high heterogeneity ($I^2 = 85.5\%$), while the analysis of continuous variables also showed no significant association between education and anxiety (WMD −0.03, 95% CI = [−0.32 to 0.26], $p = 0.830$) and the between-group heterogeneity was small ($I^2 = 7.9\%$) (see Supplementary Figure 7). Sensitivity analysis of binary variables did not find the cause of heterogeneity.

Disease duration

Four studies reported the effect of disease duration on the development of anxiety in MS patients. After eliminating a study (Jones et al., 2012) with a high risk of bias, the result showed no significant relationship between disease duration and anxiety and the heterogeneity between studies dropped to zero ($I^2 = 0$) with a decreased intergroup difference (WMD 0 95%, CI = [−0.21 to 0.22], $p = 0.966$) (see Supplementary Figure 8).

TABLE 2 Agency for Healthcare Research and Quality assessment of included studies.

References	Item 1	Item 2	Item 3	Item 4	Item 5	Item 6	Item 7	Item 8	Item 9	Item 10	Item 11	Total
Askari et al., 2014	1	1	1	Unclear	1	1	1	1	1	1	1	10
Chertcoff et al., 2020	1	1	1	1	1	1	1	1	1	1	1	11
Garfield and Lincoln, 2012	1	1	1	Unclear	1	1	1	1	1	1	1	10
Gascoyne et al., 2019	1	1	1	1	1	1	1	1	1	1	1	11
Gay et al., 2017	1	0	1	Unclear	1	1	1	1	1	1	1	9
Gay et al., 2010	1	0	0	Unclear	1	1	1	1	1	1	1	8
Gill et al., 2019	1	1	1	0	1	1	1	1	1	1	1	10
Hanna and Strober, 2020	1	1	1	1	1	1	1	1	1	1	1	11
Henry et al., 2019	1	1	0	Unclear	1	1	1	1	1	1	1	9
Jones et al., 2012	1	0	1	1	1	0	0	1	0	1	1	7
Karimi et al., 2020	1	1	1	1	1	1	1	1	1	1	1	11
Korostil and Feinstein, 2007	1	1	0	1	1	1	1	1	1	1	1	10
Kotan et al., 2019	1	1	0	Unclear	1	0	1	1	1	1	1	8
Leonavicius and Adomaitiene, 2013	1	0	1	Unclear	0	0	1	1	1	1	1	7
Marck et al., 2016	1	0	1	1	0	1	1	1	1	1	1	9
Marrie et al., 2018	1	0	1	1	1	1	1	1	1	1	1	10
Nicholl et al., 2001	1	0	1	1	1	1	1	1	1	1	1	10
Noy et al., 1995	1	1	0	Unclear	1	1	1	1	1	1	1	9
Orr et al., 2018	1	1	0	1	1	1	1	1	1	1	1	9
Pham et al., 2018	1	1	1	Unclear	1	1	1	1	1	1	1	10
Podda et al., 2020	1	1	1	1	1	1	1	1	1	1	1	11
Poder et al., 2009	1	1	1	1	1	1	1	1	1	1	1	11
Ramezani et al., 2021	1	0	1	Unclear	1	1	1	1	1	1	1	9
Reyes et al., 2020	1	1	1	Unclear	1	1	1	1	1	1	1	10
Schiess et al., 2019	1	1	1	1	1	1	1	1	1	1	1	11
Suh et al., 2010	1	1	0	Unclear	1	1	1	1	1	1	1	9
Terrill et al., 2015	1	1	1	Unclear	1	1	1	1	1	1	1	10
Uguz et al., 2008	1	1	1	1	1	1	1	1	1	1	1	11
van der Hiele et al., 2012	1	1	1	1	1	1	1	1	1	1	1	11
Wallis et al., 2020	1	1	1	1	1	1	1	1	1	1	1	11
Zanghì et al., 2020	1	1	1	Unclear	1	1	1	1	1	1	1	10
Panda et al., 2018	1	1	0	1	1	1	1	1	1	1	1	10

Disease course

Seven studies reported disease course (types of MS) as a risk factor. After excluding one study (Jones et al., 2012) with a high risk of bias after sensitivity analysis, results demonstrated that RRMS patients were 1.50 times more likely to develop anxiety than those with other types of MS (OR 1.50, 95% CI = [1.14–1.99], $p = 0.004$, $I^2 = 53.5\%$) (see **Supplementary Figure 9**).

Others

The remaining risk factors were discussed in only two studies: past psychiatric history, family psychiatric history, family status, DMT therapy (including interferon beta, glatiramer acetate, fingolimod, dimethyl fumarate, teriflunomide, alemtuzumab, and natalizumab), and baseline EDSS scores. And the results showed that MS patients with prior psychiatric history were 2.83 times more

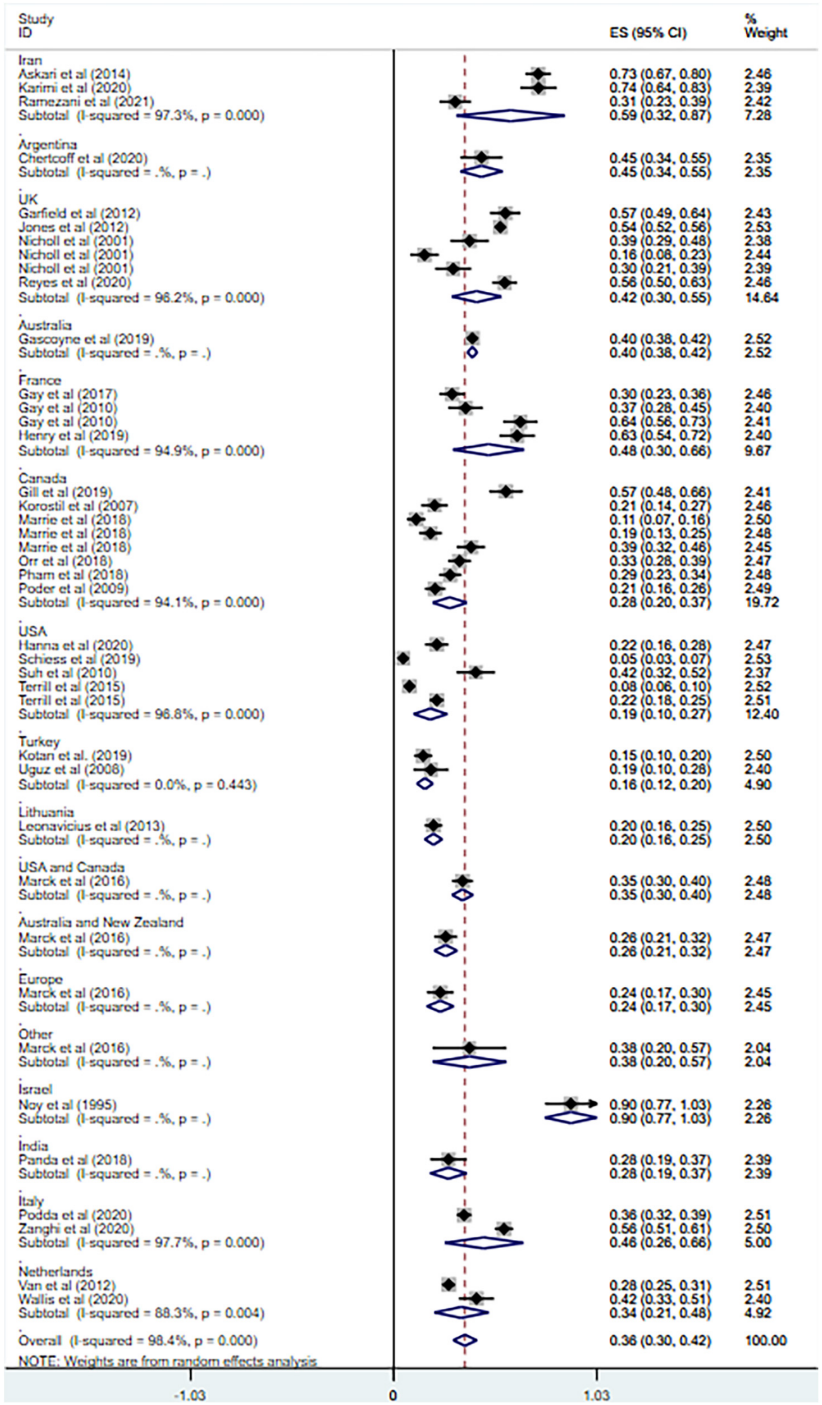

FIGURE 3
Forest plot of subgroup analysis on changes of prevalence of anxiety in MS based on country.

likely to have anxiety (OR 2.83, 95% CI = [1.74–4.59], $p < 0.001$) (see Supplementary Figure 10). And those living with other family members were more anxious than those living alone (OR 2.83, 95% CI = [1.74–4.59], $p < 0.001$) (see Supplementary Figure 11). But no significant effect of family history of psychiatric disorders on anxiety was found (OR 2.42, 95% CI = [1.56–3.75], $p = 0.158$) (see Supplementary Figure 12). No significant heterogeneity was perceived for the above three risk factors ($I^2 = 0$). For EDSS scores at baseline, those with higher scores were probably less likely to have anxiety (WMD 0.84, 95% CI = [0.48–1.21], $p < 0.001$) with heterogeneity ($I^2 = 62.2\%$) (see Supplementary Figure 13). And among patients who did not take DMT medication, anxiety was 2.33 times more common than among those who did (OR 2.33, 95% CI = [1.29–4.21], $p < 0.001$) with a heterogeneity of $I^2 = 77.8\%$ (see Supplementary Figure 14). Other risk factors that were discussed only in one study included COVID-19, comorbidity, races, physical exercise, smoking, drinking, illicit drug use, diet, residency, social status, cognition decline, fatigue severity, etc.

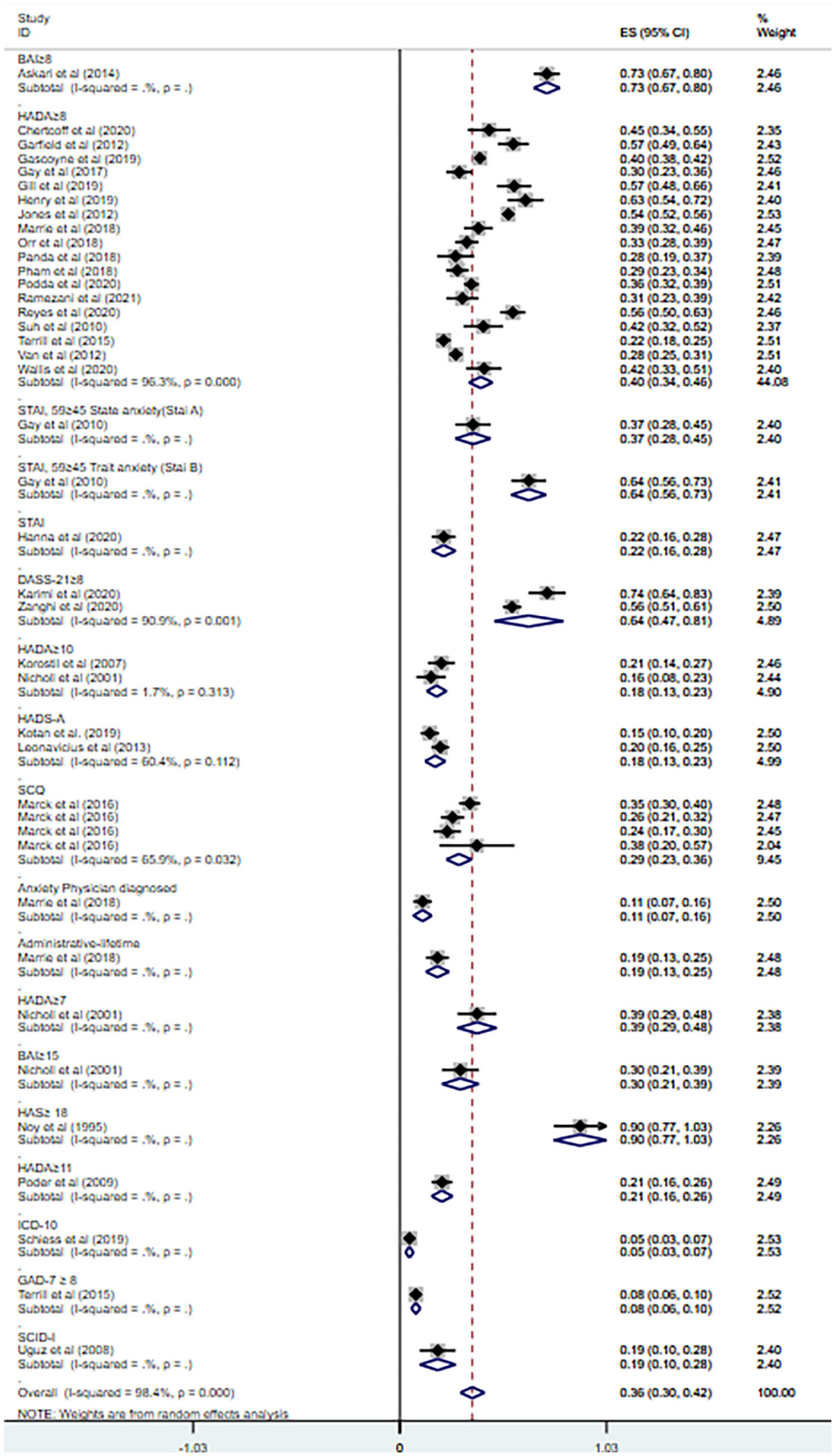

FIGURE 4
Forest plot of subgroup analysis on changes of prevalence of anxiety in MS based on measurement tool.

Publication bias

We evaluated publication bias on the prevalence of anxiety in MS through Egger's and Begg's tests with the use of Stata15. The *p*-values of Egger's and Begg's tests were mixed (Begg's test 0.011, Egger's test 0.121), which appeared that publication bias may exist in our study. Begg's funnel plot for publication bias is shown in Figure 7.

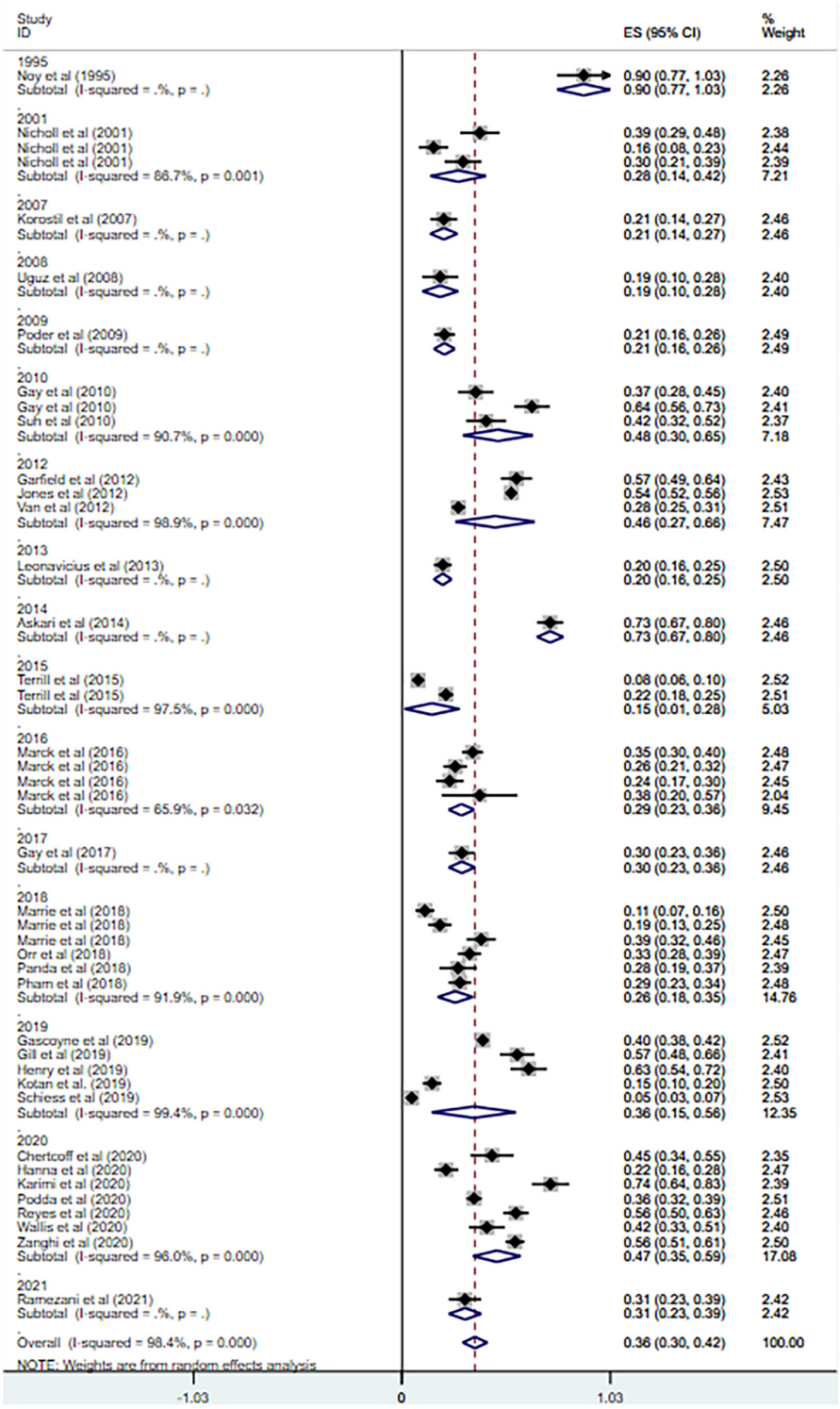

FIGURE 5
Forest plot of subgroup analysis on changes of prevalence of anxiety in MS based on publication year.

Discussion

The current study is the first meta-analysis to investigate both the prevalence and the risk factors in the development of anxiety in MS patients. With a relatively large sample of 15,853 patients in 32 studies conducted in 15 countries, the latest data as of May 2021 on the prevalence of anxiety in MS and comparing anxiety and non-anxiety populations was collected to examine the prevalence and risk factors of anxiety in MS patients.

Overall, the prevalence of anxiety among MS patients was 36% (95% CI = [0.30–0.42]) according to our results, which is in line with previous studies with the range of 22.1%

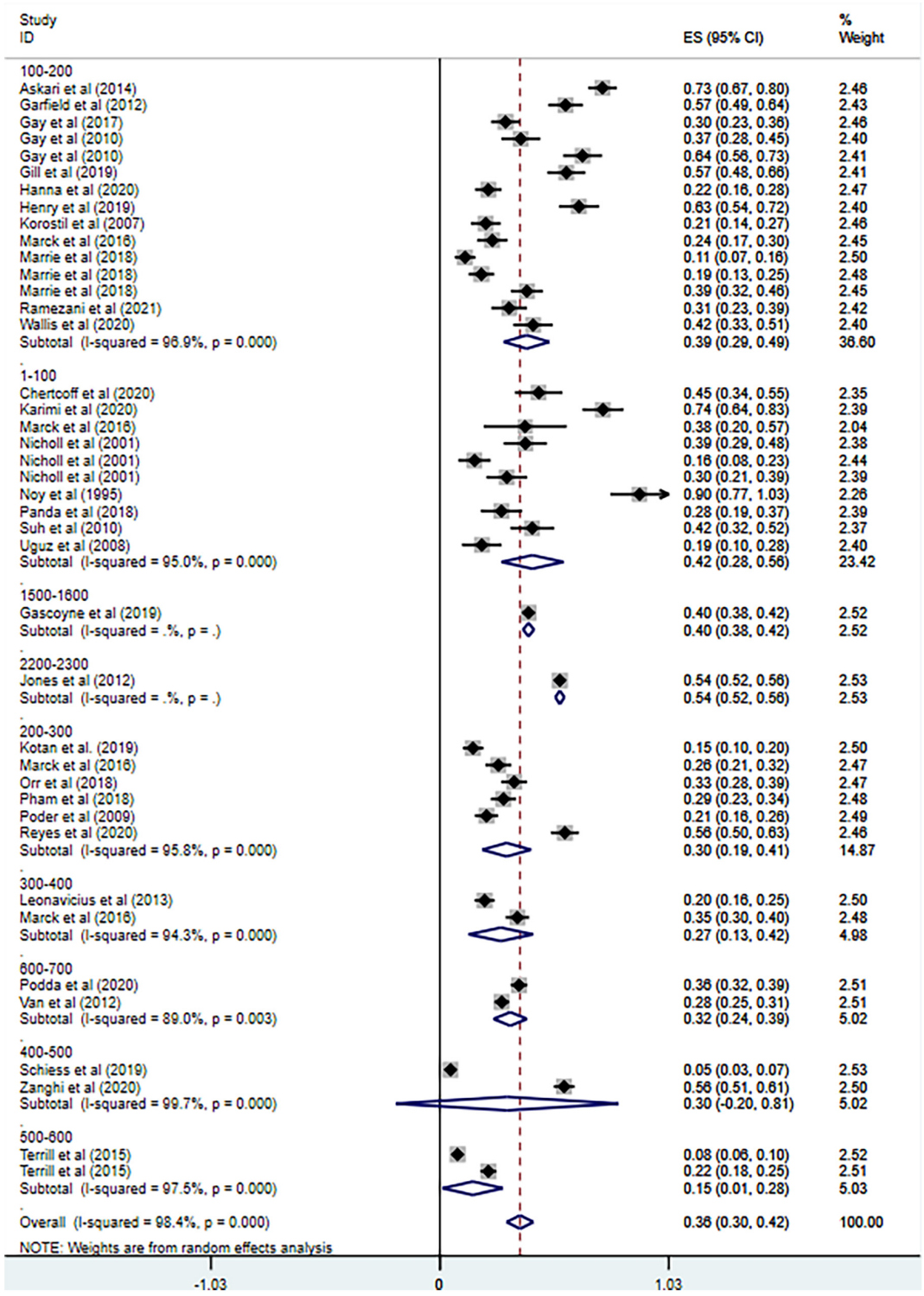

FIGURE 6
Forest plot of subgroup analysis on changes of prevalence of anxiety in MS based on total sample size.

(Boeschoten et al., 2017) to 55% (Hauer et al., 2021). However, the heterogeneity of our study of prevalence was extremely high, and thus subgroup analyses were conducted based on country, measurement tools, publication year, and sample size. The subgroup analysis based on country showed the heterogeneity sharply decreased in the analysis of Turkey, but did not change much in other countries. And the subgroup analysis based on measurement tools resulted in the decrease of heterogeneity in the combined HADA $\geq$ 10 group and HADS-A group (cut-off values not mentioned). As for the analysis of other measurement tools, the heterogeneity remained high. Little change was found after subgroup analysis based on publication year or sample size.

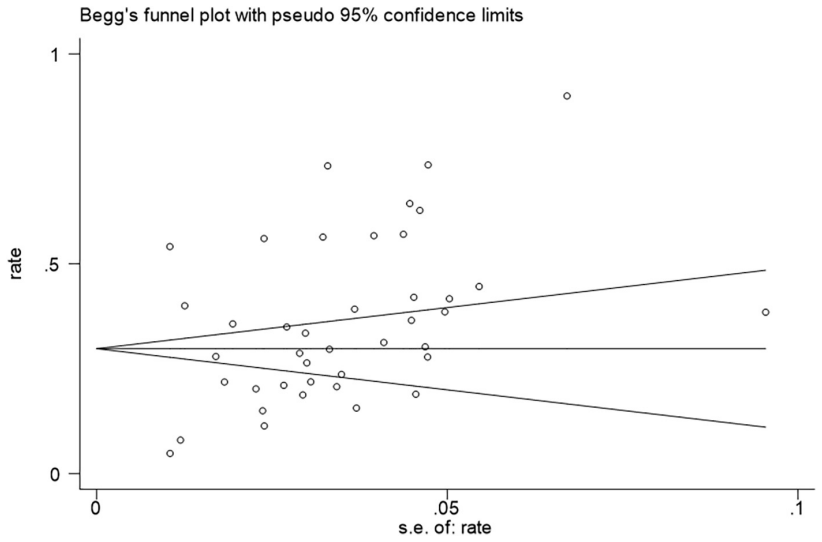

FIGURE 7
Funnel plot of meta-analysis on prevalence of anxiety in MS patients.

The heterogeneity of previous review on anxiety in MS was also high and the variations still presented after subgroup analyses (Boeschoten et al., 2017), which is consistent with our results.

Thus, it seems impossible to provide an exact picture of the prevalence of anxiety among patients with MS considering the significant heterogeneity of the pooled estimates, and various reasons may account for the discrepancies in the prevalence. First of all, the prevalence of MS varies across ethnic groups, regions and countries (Pugliatti et al., 2002) and the diagnostic criteria of MS have been updated over the years (Polman et al., 2005, 2011; Thompson et al., 2018), resulting in differences in the sample population characteristics in the included studies. Secondly, the evaluation of anxiety disorder relies on measurement tools and different cut-off values and is a lack of consolidated standards (Brooks and Kutcher, 2003), and measurement tools may not be objective enough for the diagnosis of anxiety. Thirdly, patients with the same criteria of MS diagnosis may differ in the disease courses, duration, disability level, family, and economic status and past medical history, which would certainly greatly affect anxiety development. And because of that, we also discussed the risk factors of anxiety in our review.

Multiple sclerosis anxiety risk factors were another objective of this review. The following factors were investigated in our study: gender (female or not), prior psychiatric history, age at survey, comorbidity with depression, family history of psychiatric disorders, family status (living together or not), employment status, education, marriage, disease course (disease subtype), disease duration, treatment compliance, and EDSS scores at baseline. Among them, the results showed that age at survey, female, family status, prior psychiatric history, comorbidity with depression, usage of MS medication, and baseline EDSS were significantly correlated with the development of anxiety in patients with MS.

As shown in **Table 4**, age and gender are the most commonly discussed risk factors. Our study showed that female MS patients were prone to have an increased rate of anxiety. According to studies, MS has a female predominance, and anxiety is highly associated with women (Koch-Henriksen and Sørensen, 2010; Sellner et al., 2011). And a multicenter survey of 3,142 adults showed the prevalence rate of anxiety disorders was higher in female populations, but dropped in adults aged 75–84 compared with 65–74 (Canuto et al., 2018). Potential factors contributing to gender discrepancy include anxiety sensitivity (Norr et al., 2015), stress coping style (Altemus et al., 2014; Kiely et al., 2019) or fluctuations in exposure to reproductive hormones and peptides during the menstrual cycle (Altemus et al., 2014; Kiely et al., 2019). However, little data are available on the relationship between age and anxiety. A recent review showed that anxiety symptoms may be more difficult to elicit in the elderly, as they are less accurate in identifying anxiety symptoms and tend to attribute them to physical illness rather than anxiety itself. Another survey indicated that the age-sex pattern for anxiety in the general population was only observed during fertile periods, while the risk for new cases became similar for both genders after menopause (Faravelli et al., 2013). Few articles have addressed the effects of aging on the development of anxiety in MS. Our review found the age disparity, but could not show the prevalence rate among the different age groups of a specific gender owing to the lack of original data from included studies.

Prior psychiatric history and comorbidity of depression were also found to be significantly associated with the prevalence of anxiety in MS patients. Pre-existing mental disorders will increase the prevalence of anxiety after the diagnosis of MS, and anxiety, depression, and fatigue tend to cluster together (Wood et al., 2013; Demyttenaere and Heirman, 2020). The incorporation of phenomenological, psychopathological and evolutionary concepts may be helpful in understanding the articulation between anxiety and depression. From a phenomenological approach, both the diagnostic criteria from classification systems and items of measurement tools for anxiety overlap significantly with those of depression (Tyrer, 2018; Demyttenaere and Heirman, 2020; Konac et al., 2021). From the perspective

TABLE 3 Factors correlated with anxiety status in MS patients.

References	Factor
Ramezani et al., 2021	Age at survey, age at the onset of MS, history of psychiatric disorders, history of taking psychiatric medication, history of COVID-19 in family, education, occupation, immunomodulation, immunosuppressor
Podda et al., 2020	Age at survey, gender, level of education (university, high school, primary school), disease duration, disease course, EDSS at T0, MoCA at T0, HADS-D at T0, HADS-A at T0, FIS at T0
Karimi et al., 2020	Gender, family history, history of the disease, smoking, physical activity, mental status, occupation
Hanna and Strober, 2020	Age, gender, education, disease course, disease duration
Chertcoff et al., 2020	Gender (female),age, education (in years), marital status, currently smoking, prior psychiatric history, family history of psychiatric disorders, time since diagnosis, disease subtype, current DMT, EDSS, depression, COOP/WONCA score
Marrie et al., 2018	Gender, race, education, age, disease duration, EDSS score, clinical score, clinical course, smoking
Marrie et al., 2018	Gender, age, socioeconomic status, region
Terrill et al., 2015	Gender, race, employment status, married, MS type, age, MS duration, PHQ-9 score
Askari et al., 2014	BDI, EDSS, age, gender, disease type
Leonavicius and Adomaitiene, 2013	Age, family status, residence, MS duration
Jones et al., 2012	Gender, MS type, depression level
Garfield and Lincoln, 2012	Age, years since diagnosis, months since last relapse, HADS Depression, GHQ-12, GNDS score, MSSS, MHLC, PSS
Korostil and Feinstein, 2007	Cognitively impaired, depression, disease course, disease duration, EDSS, education, employed, family history of mental illness, gender, HAD, living alone, major depression, married, SSSI, substance abuse, suicidal intent, suicide attempt, taking disease modifying treatments
Zanghì et al., 2020	Marital status, age, psychiatric comorbidity, EDSS score, disease duration, number of relapse in the year before, starting or changing DMT in the last 12 months, line of DMT actually taken
Gascoyne et al., 2019	Age, gender, type of MS at onset, type of MS now, PDDS, prevalent fatigue, years since symptom onset, employed, socio-economic status, rurality
Pham et al., 2018	Gender, education, employment, smoking, alcohol, illicit drug use, disease type, disease modifying medication, adverse medication side effects, EDSS score, depression

MS, multiple sclerosis; COVID-19, Coronavrus Disease 2019; EDSS, Expanded Disability Status Scale; MoCA, Montreal Cognitive Assessment; HAD, Hospital Anxiety and Depression; HADS-D, Hospital Depression and Anxiety Scale Depression subscale; HADS Depression, Hospital Depression and Anxiety Scale Depression subscale; HADS-A, Hospital Depression and Anxiety Scale Anxiety subscale; FIS, Fatigue Impact Scale; T0, at baseline; PHQ-9, Patient Health Questionnaire-Nine; DMT, disease modifying treatments; BDI, Beck Depression Inventory; GHQ-12, General Health Questionnaire-12; GNDS score, General Neuropsychological Deficit Score; MSSS, Multiple Sclerosis Severity Score; MHLC, Multidimensional Health Locus of Control scale; PSS, Perceived Stress Scale; SSSI, Social Stress and Support Interview; PDDS, Patient Determined Disease Steps.

TABLE 4 Comparisons on risk factors for anxiety in patients with MS.

Risk factor	Effect size, confidence interval, p-value, I^2	Total number of studies included
Age at survey (Supplementary Figure 1)	WMD 0.96, 95% CI = [0.86–1.06], $p < 0.001$, $I^2 = 43.8\%$	6
Gender (Supplementary Figure 2)	OR 1.78, 95% CI = [1.38–2.30], $p < 0.001$, $I^2 = 0$	8
Depression (Supplementary Figure 3)	OR 7.89, 95% CI = [3.71–16.81], $p < 0.001$, $I^2 = 0$	3
Marriage status (Supplementary Figure 4)	OR 0.95, 95% CI = [0.62–1.44], $p = 0.794$, $I^2 = 40.7\%$	3
Employment status (Supplementary Figure 5)	OR 0.87, 95% CI = [0.6–1.24], $p = 0.434$, $I^2 = 27.5\%$	3
Education levels (Supplementary Figure 6)	OR 1.28, 95% CI = [0.52–3.15], $p = 0.830$, $I^2 = 85.5\%$	3
Years of education (Supplementary Figure 7)	WMD −0.03, 95% CI = [−0.32 to 0.26], $p = 0.830$, $I^2 = 7.9\%$	2
Disease duration (Supplementary Figure 8)	WMD 0, 95%, CI = [−0.21–0.22], $p = 0.966$, $I^2 = 0$	4
Disease course (Supplementary Figure 9)	OR 1.50, 95% CI = [1.14–1.99], $p = 0.004$, $I^2 = 53.5\%$	7
Past psychiatric history (Supplementary Figure 10)	OR 2.83, 95% CI = [1.74–4.59], $p < 0.001$, $I^2 = 0$	2
Living together (Supplementary Figure 11)	OR 2.83, 95% CI = [1.74–4.59], $p < 0.001$, $I^2 = 0$	2
Baseline EDSS scores (Supplementary Figure 12)	WMD 0.84, 95% CI = [0.48–1.21], $p < 0.001$, $I^2 = 62.2\%$	2
Lack of DMT therapy (Supplementary Figure 13)	OR 2.33, 95% CI = [1.29–4.21], $p < 0.001$, $I^2 = 77.8\%$	2
Family psychiatric history (Supplementary Figure 14)	OR 2.42, 95% CI = [1.56–3.75], $p = 0.158$, $I^2 = 0$	2

of pathophysiological mechanism, anxiety and depression are both characterized by neuroendocrine disorders (Boyer, 2000). Historically, the monoamine hypothesis has dominated anxiety and depression research and treatment. While the research into neuropeptide systems throws greater views on the understanding of the pathogenesis of the comorbidity (Alldredge, 2010). Recent research has also focused on stress on the signal transduction on the pathogenesis of anxiety and depression. Stress-induced pathogenic stimuli activate endothelial and perivascular microglia, and mediate perivascular neurons and peripheral astrocytes,

thereby controlling the formation of pre-inflammatory and anti-inflammatory phenotypes of astrocytes and microglia in the blood brain barrier (Welcome, 2020). The above mechanisms provide insight into prevention and treatment of anxiety and depression for MS patients.

No significant associations between anxiety and the disease duration or disease course of MS patients were found in our study. Nevertheless, our results showed that patients not taking MS medication and those with a higher baseline EDSS tended to have a higher prevalence rate of anxiety. That may imply MS patients with severe symptoms may be more likely to experience anxiety, and medication treatment may alleviate anxiety symptoms to some degree. As previous surveys suggested that anxiety is related to physical severity (Lester et al., 2007), interventions for self-management may improve anxiety and QOL for MS patients (Kidd et al., 2017). Moreover, patients with less changes in severity of symptoms may have less variation in work productivity as well (Bessing et al., 2021). The above findings suggest that MS patients should be more active in the intervention of the disease, which may decrease the prevalence of psychiatric complications and improve their QOL.

Our review also found that family status may probably affect the development of anxiety in MS, but no significant correlations was observed between anxiety and risk factors including employment status, education, and family history of psychiatric in MS patients. In terms of family relationships, living together with family members may increase the prevalence rate of anxiety when compared with living alone. A survey of 2,057 medical students showed that anxiety symptoms had highly significant correlations with family status, social support, and coping style (Shao et al., 2020). And people who had bad relationships with their lovers, classmates or friends scored higher on anxiety tests (Shao et al., 2020), since life-threatening diseases may cause much more severe stress that can lead to marital discord, separation, or divorce (Hakim et al., 2000). Patients who lived together with family members may experience higher level of anxiety due to deteriorated couple relationships and a greater probability of divorce (Glantz et al., 2009).

Compared with depression, anxiety receives less attention from clinicians or researchers, whereas anxiety often accompanies depression and can decrease patients' and caregivers' QOL. Thus, it is necessary to focus on the prevalence and risk factors of anxiety in chronic diseases like MS. Our study demonstrated the prevalence of anxiety in patients with MS and the potential risk factors including age at survey, female, family status, prior psychiatric history, comorbidity with depression, treatment compliance, and baseline EDSS. However, as the reliability of current results is limited by small sample size, outcome measures and cross-sectional designs, our results should be interpreted cautiously and need further validation with more qualitative research. In the future, a more accurate classification and more detailed description of the target population should be provided. Besides, future detection of anxiety should not solely rely on measurement tools, but also on objective evaluation tools or diagnostic markers such as neuroimaging, neurophysiology, and biochemistry (Koch-Henriksen and Sørensen, 2010). Furthermore, longitudinal designs are needed to develop a deeper understanding of the associations between significant risk factors and anxiety in MS patients.

Conclusion

In this meta-analysis, we summarized the prevalence of anxiety in MS and analyzed common significant risk factors that contribute to anxiety development in MS patients. Our study estimated that 36% of MS patients suffer from anxiety. And we found that age at survey, female, living together, past psychiatric history, depression, compliance with MS medications, RRMS, and baseline EDSS are significant risk factors for anxiety in MS patients. Our results help serve as a reminder to both patients and physicians of various risk factors that contribute to anxiety, and highlight the necessity of monitoring patients with modifiable risk factors to prevent further costs and aggravation.

Data availability statement

The original contributions presented in this study are included in the article/**Supplementary material**, further inquiries can be directed to the corresponding author.

Author contributions

XYZ involved in the study's conceptualization and design, and wrote the original draft of the work. XYZ and YS extracted the data using pre-made forms. XYZ, XC, and XJZ carried out the statistical analysis. All authors reviewed, revised, and approved the submitted version of the work.

Conflict of interest

The authors declare that the research was conducted in the absence of any commercial or financial relationships that could be construed as a potential conflict of interest.

Publisher's note

Supplementary material

The Supplementary Material for this article can be found online at: https://www.frontiersin.org/articles/10.3389/fnins.2023.1120541/full#supplementary-material

References

Alldredge, B. (2010). Pathogenic involvement of neuropeptides in anxiety and depression. *Neuropeptides* 44, 215–224. doi: 10.1016/j.npep.2009.12.014

Altemus, M., Sarvaiya, N., and Neill Epperson, C. (2014). Sex differences in anxiety and depression clinical perspectives. *Front. Neuroendocrinol.* 35, 320–330. doi: 10.1016/j.yfrne.2014.05.004

Askari, F., Ghajarzadeh, M., Mohammadifar, M., Azimi, A., Sahraian, M., and Owji, M. (2014). Anxiety in patients with multiple sclerosis: Association with disability, depression, disease type and sex. *Acta Med. Iran.* 52, 889–892.

Berkman, N., Lohr, K., Ansari, M., McDonagh, M., Balk, E., and Whitlock, E. (eds). (2008). "Grading the strength of a body of evidence when assessing health care interventions for the effective health care program of the agency for healthcare research and quality: An update," in *Methods guide for effectiveness and comparative effectiveness reviews*, (Rockville, MD: Agency for Healthcare Research and Quality (US)).

Bessing, B., Hussain, M., Claflin, S., Chen, J., Blizzard, L., van Dijk, P., et al. (2021). Changes in multiple sclerosis symptoms are associated with changes in work productivity of people living with multiple sclerosis. *Mult. Scler.* 27, 2093–2102. doi: 10.1177/1352458521994557

Boeschoten, R., Braamse, A., Beekman, A., Cuijpers, P., van Oppen, P., Dekker, J., et al. (2017). Prevalence of depression and anxiety in multiple sclerosis: A systematic review and meta-analysis. *J. Neurol. Sci.* 372, 331–341. doi: 10.1016/j.jns.2016.11.067

Boyer, P. (2000). Do anxiety and depression have a common pathophysiological mechanism? *Acta Psychiatr. Scand. Suppl.* 406, 24–29.

Brooks, S., and Kutcher, S. (2003). Diagnosis and measurement of anxiety disorder in adolescents: A review of commonly used instruments. *J. Child Adolesc. Psychopharmacol.* 13, 351–400. doi: 10.1089/104454603322572688

Browne, P., Chandraratna, D., Angood, C., Tremlett, H., Baker, C., Taylor, B., et al. (2014). Atlas of multiple sclerosis 2013: A growing global problem with widespread inequity. *Neurology* 83, 1022–1024. doi: 10.1212/WNL.0000000000000768

Canuto, A., Weber, K., Baertschi, M., Andreas, S., Volkert, J., Dehoust, M., et al. (2018). Anxiety disorders in old age: Psychiatric comorbidities, quality of life, and prevalence according to age, gender, and country. *Am. J. Geriatr. Psychiatry* 26, 174–185. doi: 10.1016/j.jagp.2017.08.015

Chertcoff, A., Curbelo, M., Bauer, J., Ferrandina, F., Martinez, A., Steinberg, J., et al. (2020). Anxiety in Argentinian patients with multiple sclerosis: Prevalence and associated factors. *Mult. Scler. Relat. Disord.* 41:102042. doi: 10.1016/j.msard.2020.102042

Compston, A., and Coles, A. (2008). Multiple sclerosis. *Lancet* 372, 1502–1517. doi: 10.1016/S0140-6736(08)61620-7

Demyttenaere, K., and Heirman, E. (2020). The blurred line between anxiety and depression: Hesitations on comorbidity, thresholds and hierarchy. *Int. Rev. Psychiatry* 32, 455–465. doi: 10.1080/09540261.2020.1764509

Faravelli, C., Alessandra Scarpato, M., Castellini, G., and Lo Sauro, C. (2013). Gender differences in depression and anxiety: The role of age. *Psychiatry Res.* 210, 1301–1303. doi: 10.1016/j.psychres.2013.09.027

First, M. B., Spitzer, R. L., Gibbon, M., and Williams, J. (2007). *Structured clinical interview for DSM-IV-TR axis i disorders, clinical trials version (SCID-CT), in New York: Biometrics research*. New York, NY: State Psychiatric Institute.

Garfield, A., and Lincoln, N. (2012). Factors affecting anxiety in multiple sclerosis. *Disabil. Rehabil.* 34, 2047–2052. doi: 10.3109/09638288.2012.667503

Gascoyne, C., Simpson, S., Chen, J., van der Mei, I., and Marck, C. (2019). Modifiable factors associated with depression and anxiety in multiple sclerosis. *Acta Neurol. Scand.* 140, 204–211. doi: 10.1111/ane.13132

Gay, M., Bungener, C., Thomas, S., Vrignaud, P., Thomas, P., Baker, R., et al. (2017). Anxiety, emotional processing and depression in people with multiple sclerosis. *BMC Neurol.* 17:43. doi: 10.1186/s12883-017-0803-8

Gay, M., Vrignaud, P., Garitte, C., and Meunier, C. (2010). Predictors of depression in multiple sclerosis patients. *Acta Neurol. Scand.* 121, 161–170. doi: 10.1111/j.1600-0404.2009.01232.x

GBD 2016 Multiple Sclerosis Collaborators (2019). Global, regional, and national burden of multiple sclerosis 1990-2016: A systematic analysis for the Global Burden of Disease Study 2016. *Lancet Neurol.* 18, 269–285. doi: 10.1016/S1474-4422(18)30443-5

Gill, S., Santo, J., Blair, M., and Morrow, S. (2019). Depressive symptoms are associated with more negative functional outcomes than anxiety symptoms in persons with multiple sclerosis. *J. Neuropsychiatry Clin. Neurosci.* 31, 37–42. doi: 10.1176/appi.neuropsych.18010011

Glantz, M., Chamberlain, M., Liu, Q., Hsieh, C., Edwards, K., Van Horn, A., et al. (2009). Gender disparity in the rate of partner abandonment in patients with serious medical illness. *Cancer* 115, 5237–5242. doi: 10.1002/cncr.24577

Glanz, B., Dégano, I., Rintell, D., Chitnis, T., Weiner, H., and Healy, B. (2012). Work productivity in relapsing multiple sclerosis: Associations with disability, depression, fatigue, anxiety, cognition, and health-related quality of life. *Value Health* 15, 1029–1035. doi: 10.1016/j.jval.2012.07.010

Hakim, E., Bakheit, A., Bryant, T., Roberts, M., McIntosh-Michaelis, S., Spackman, A., et al. (2000). The social impact of multiple sclerosis–a study of 305 patients and their relatives. *Disabil. Rehabil.* 22, 288–293. doi: 10.1080/096382800296755

Hanna, M., and Strober, L. (2020). Anxiety and depression in multiple sclerosis (MS): Antecedents, consequences, and differential impact on well-being and quality of life. *Mult. Scler. Relat. Disord.* 44:102261. doi: 10.1016/j.msard.2020.102261

Hauer, L., Perneczky, J., and Sellner, J. (2021). A global view of comorbidity in multiple sclerosis: A systematic review with a focus on regional differences, methodology, and clinical implications. *J. Neurol.* 268, 4066–4077. doi: 10.1007/s00415-020-10107-y

Henry, A., Tourbah, A., Camus, G., Deschamps, R., Mailhan, L., Castex, C., et al. (2019). Anxiety and depression in patients with multiple sclerosis: The mediating effects of perceived social support. *Mult. Scler. Relat. Disord.* 27, 46–51. doi: 10.1016/j.msard.2018.09.039

Higgins, J., Thompson, S., Deeks, J., and Altman, D. (2003). Measuring inconsistency in meta-analyses. *BMJ* 327, 557–560. doi: 10.1136/bmj.327.7414.557

Janssens, A., van Doorn, P., de Boer, J., van der Meché, F., Passchier, J., and Hintzen, R. (2004). Perception of prognostic risk in patients with multiple sclerosis: The relationship with anxiety, depression, and disease-related distress. *J. Clin. Epidemiol.* 57, 180–186. doi: 10.1016/S0895-4356(03)00260-9

Jones, K., Ford, D., Jones, P., John, A., Middleton, R., Lockhart-Jones, H., et al. (2012). A large-scale study of anxiety and depression in people with Multiple Sclerosis: A survey via the web portal of the UK MS register. *PLoS One* 7:e41910. doi: 10.1371/journal.pone.0041910

Kamm, C., Uitdehaag, B., and Polman, C. (2014). Multiple sclerosis: Current knowledge and future outlook. *Eur. Neurol.* 72, 132–141. doi: 10.1159/000360528

Karimi, S., Andayeshgar, B., and Khatony, A. (2020). Prevalence of anxiety, depression, and stress in patients with multiple sclerosis in Kermanshah-Iran: A cross-sectional study. *BMC Psychiatry* 20:166. doi: 10.1186/s12888-020-02579-z

Kidd, T., Carey, N., Mold, F., Westwood, S., Miklaucich, M., Konstantara, E., et al. (2017). A systematic review of the effectiveness of self-management interventions in people with multiple sclerosis at improving depression, anxiety and quality of life. *PLoS One* 12:e0185931. doi: 10.1371/journal.pone.0185931

Kiely, K., Brady, B., and Byles, J. (2019). Gender, mental health and ageing. *Maturitas* 129, 76–84. doi: 10.1016/j.maturitas.2019.09.004

Koch-Henriksen, N., and Sørensen, P. (2010). The changing demographic pattern of multiple sclerosis epidemiology. *Lancet Neurol.* 9, 520–532. doi: 10.1016/S1474-4422(10)70064-8

Konac, D., Young, K., Lau, J., and Barker, E. (2021). Comorbidity between depression and anxiety in adolescents: Bridge symptoms and relevance of risk and protective factors. *J. Psychopathol. Behav. Assess.* 43, 583–596. doi: 10.1007/s10862-021-09880-5

Korostil, M., and Feinstein, A. (2007). Anxiety disorders and their clinical correlates in multiple sclerosis patients. *Mult. Scler.* 13, 67–72. doi: 10.1177/1352458506071161

Kotan, V. O., Kotan, Z., Aydın, B., Taşkapılıoğlu, Ö, and Alkan, B. (2019). The relationship between psychopathology, psychosocial adjustment, social support and quality of life in multiple sclerosis. *Eur. Res. J.* 5, 20–28.

Landeiro, G. M., Pedrozo, C. C., Gomes, M. J., and Oliveira, E. R. (2011). [Systematic review of studies on quality of life indexed on the SciELO database]. *Cien. Saude Colet.* 16, 4257–4266.

Leonavicius, R., and Adomaitiene, V. (2013). Anxiety and social activities in multiple sclerosis patients. *Cent. Eur. J. Med.* 8, 56–61.

Lester, K., Stepleman, L., and Hughes, M. (2007). The association of illness severity, self-reported cognitive impairment, and perceived illness management with depression and anxiety in a multiple sclerosis clinic population. *J. Behav. Med.* 30, 177–186. doi: 10.1007/s10865-007-9095-6

Levi, I., Gurevich, M., Perlman, G., Magalashvili, D., Menascu, S., Bar, N., et al. (2021). Potential role of indolelactate and butyrate in multiple sclerosis revealed by integrated microbiome-metabolome analysis. *Cell Rep. Med.* 2:100246. doi: 10.1016/j.xcrm.2021.100246

Marck, C., Neate, S., Taylor, K., Weiland, T., and Jelinek, G. (2016). Prevalence of comorbidities, overweight and obesity in an international sample of people with multiple sclerosis and associations with modifiable lifestyle factors. *PLoS One* 11:e0148573. doi: 10.1371/journal.pone.0148573

Marrie, R., Patten, S., Berrigan, L., Tremlett, H., Wolfson, C., Warren, S., et al. (2018). Diagnoses of depression and anxiety versus current symptoms and quality of life in multiple sclerosis. *Int. J. MS Care* 20, 76–84. doi: 10.7224/1537-2073.2016-110

Moher, D., Liberati, A., Tetzlaff, J., and Altman, D. (2009). Preferred reporting items for systematic reviews and meta-analyses: The PRISMA statement. *Ann Intern Med* 151, 264–269. doi: 10.7326/0003-4819-151-4-200908180-00135

Nicholl, C., Lincoln, N., Francis, V., and Stephan, T. (2001). Assessment of emotional problems in people with multiple sclerosis. *Clin. Rehabil.* 15, 657–668. doi: 10.1191/0269215501cr427oa

Norr, A., Albanese, B., Allan, N., and Schmidt, N. (2015). Anxiety sensitivity as a mechanism for gender discrepancies in anxiety and mood symptoms. *J. Psychiatr. Res.* 62, 101–107. doi: 10.1016/j.jpsychires.2015.01.014

Noy, S., Achiron, A., Gabbay, U., Barak, Y., Rotstein, Z., Laor, N., et al. (1995). A new approach to affective symptoms in relapsing-remitting multiple sclerosis. *Compr. Psychiatry* 36, 390–395. doi: 10.1016/s0010-440x(95)90121-3

Olivera, A., Fero, D., and Evans, M. (1988). Major depression, anxiety, and substance abuse in a multiple sclerosis patient: Diagnosis, treatment, and outcome. *J. Clin. Psychiatry* 49:78.

Orr, J., Bernstein, C., Graff, L., Patten, S., Bolton, J., Sareen, J., et al. (2018). Factors associated with perceived need for mental health care in multiple sclerosis. *Mult. Scler. Relat. Disord.* 25, 179–185. doi: 10.1016/j.msard.2018.07.043

Panda, S., Das, R., Srivastava, K., Ratnam, A., and Sharma, N. (2018). Psychiatric comorbidity in multiple sclerosis. *Neurol. Neurochir. Pol.* 52, 704–709. doi: 10.1016/j.pjnns.2018.09.003

Pham, T., Jetté, N., Bulloch, A., Burton, J., Wiebe, S., and Patten, S. (2018). The prevalence of anxiety and associated factors in persons with multiple sclerosis. *Mult. Scler. Relat. Disord.* 19, 35–39. doi: 10.1016/j.msard.2017.11.003

Podda, J., Ponzio, M., Messmer Uccelli, M., Pedullà, L., Bozzoli, F., Molinari, F., et al. (2020). Predictors of clinically significant anxiety in people with multiple sclerosis: A one-year follow-up study. *Mult. Scler. Relat. Disord.* 45:102417. doi: 10.1016/j.msard.2020.102417

Poder, K., Ghatavi, K., Fisk, J., Campbell, T., Kisely, S., Sarty, I., et al. (2009). Social anxiety in a multiple sclerosis clinic population. *Mult. Scler.* 15, 393–398. doi: 10.1177/1352458508099143

Polman, C., Reingold, S., Banwell, B., Clanet, M., Cohen, J., Filippi, M., et al. (2011). Diagnostic criteria for multiple sclerosis: 2010 revisions to the McDonald criteria. *Ann. Neurol.* 69, 292–302. doi: 10.1002/ana.22366

Polman, C., Reingold, S., Edan, G., Filippi, M., Hartung, H., Kappos, L., et al. (2005). Diagnostic criteria for multiple sclerosis: 2005 revisions to the "McDonald Criteria". *Ann. Neurol.* 58, 840–846. doi: 10.1002/ana.20703

Poser, C. M., Paty, D. W., Scheinberg, L., McDonald, W. I., Davis, F. A., Ebers, G. C., et al. (1983). New diagnostic criteria for multiple sclerosis: guidelines for research protocols. *Ann. Neurol.* 13, 227–231. doi: 10.1002/ana.410130302

Pugliatti, M., Sotgiu, S., and Rosati, G. (2002). The worldwide prevalence of multiple sclerosis. *Clin. Neurol. Neurosurg.* 104, 182–191. doi: 10.1016/s0303-8467(02)00036-7

Ramezani, N., Ashtari, F., Bastami, E., Ghaderi, K., Hosseini, S., Naeini, M., et al. (2021). Fear and anxiety in patients with multiple sclerosis during COVID-19 pandemic; report of an Iranian population. *Mult. Scler. Relat. Disord.* 50:102798. doi: 10.1016/j.msard.2021.102798

Reyes, S., Suarez, S., Allen-Philbey, K., Thomson, A., and Giovannoni, G. (2020). The impact of social capital on patients with multiple sclerosis. *Acta Neurol. Scand.* 142, 58–65. doi: 10.1111/ane.13244

Schiess, N., Huether, K., Holroyd, K., Aziz, F., Emam, E., Shahrour, T., et al. (2019). Multiple sclerosis, anxiety, and depression in the United Arab Emirates: Does social stigma prevent treatment? *Int. J. MS Care* 21, 29–34. doi: 10.7224/1537-2073.2017-041

Scott, K., Bruffaerts, R., Tsang, A., Ormel, J., Alonso, J., Angermeyer, M., et al. (2007). Depression-anxiety relationships with chronic physical conditions: Results from the world mental health surveys. *J. Affect. Disord.* 103, 113–120. doi: 10.1016/j.jad.2007.01.015

Sellner, J., Kraus, J., Awad, A., Milo, R., Hemmer, B., and Stüve, O. (2011). The increasing incidence and prevalence of female multiple sclerosis–a critical analysis of potential environmental factors. *Autoimmun. Rev.* 10, 495–502. doi: 10.1016/j.autrev.2011.02.006

Shao, R., He, P., Ling, B., Tan, L., Xu, L., Hou, Y., et al. (2020). Prevalence of depression and anxiety and correlations between depression, anxiety, family functioning, social support and coping styles among Chinese medical students. *BMC Psychol.* 8:38. doi: 10.1186/s40359-020-00402-8

Suh, Y., Motl, R., and Mohr, D. (2010). Physical activity, disability, and mood in the early stage of multiple sclerosis. *Disabil. Health J.* 3, 93–98. doi: 10.1016/j.dhjo.2009.09.002

Terrill, A., Hartoonian, N., Beier, M., Salem, R., and Alschuler, K. (2015). The 7-item generalized anxiety disorder scale as a tool for measuring generalized anxiety in multiple sclerosis. *Int. J. MS Care* 17, 49–56. doi: 10.7224/1537-2073.2014-008

Thompson, A., Banwell, B., Barkhof, F., Carroll, W., Coetzee, T., Comi, G., et al. (2018). Diagnosis of multiple sclerosis: 2017 revisions of the McDonald criteria. *Lancet Neurol.* 17, 162–173. doi: 10.1016/S1474-4422(17)30470-2

Tyrer, P. (2018). Against the stream: Generalised anxiety disorder (GAD) - a redundant diagnosis. *BJPsych Bull.* 42, 69–71. doi: 10.1192/bjb.2017.12

Uguz, F., Akpinar, Z., Ozkan, I., and Tokgoz, S. (2008). Mood and anxiety disorders in patients with multiple sclerosis. *Int. J. Psychiatry Clin. Pract.* 12, 19–24. doi: 10.1080/13651500701330825

van der Hiele, K., Spliethoff-Kamminga, N., Ruimschotel, R., Middelkoop, H., and Visser, L. (2012). Daily hassles reported by Dutch multiple sclerosis patients. *J. Neurol. Sci.* 320, 85–90. doi: 10.1016/j.jns.2012.06.023

van Tilburg, C., Pfaff, E., Pajtler, K., Langenberg, K., Fiesel, P., Jones, B., et al. (2021). The pediatric precision oncology INFORM registry: Clinical outcome and benefit for patients with very high-evidence targets. *Cancer Discov.* 11, 2764–2779. doi: 10.1158/2159-8290.CD-21-0094

Wallis, O., Bol, Y., Köhler, S., and van Heugten, C. (2020). Anxiety in multiple sclerosis is related to depressive symptoms and cognitive complaints. *Acta Neurol. Scand.* 141, 212–218. doi: 10.1111/ane.13191

Welcome, M. (2020). Cellular mechanisms and molecular signaling pathways in stress-induced anxiety, depression, and blood-brain barrier inflammation and leakage. *Inflammopharmacology* 28, 643–665. doi: 10.1007/s10787-020-00712-8

Wood, B., van der Mei, I., Ponsonby, A., Pittas, F., Quinn, S., Dwyer, T., et al. (2013). Prevalence and concurrence of anxiety, depression and fatigue over time in multiple sclerosis. *Mult. Scler.* 19, 217–224. doi: 10.1177/1352458512450351

Zanghì, A., D'Amico, E., Luca, M., Ciaorella, M., Basile, L., and Patti, F. (2020). Mental health status of relapsing-remitting multiple sclerosis Italian patients returning to work soon after the easing of lockdown during COVID-19 pandemic: A monocentric experience. *Mult. Scler. Relat. Disord.* 46:102561. doi: 10.1016/j.msard.2020.102561

Frontiers in Neuroscience

Provides a holistic understanding of brain function from genes to behavior

Part of the most cited neuroscience journal series which explores the brain - from the new eras of causation and anatomical neurosciences to neuroeconomics and neuroenergetics.

Discover the latest Research Topics

See more →

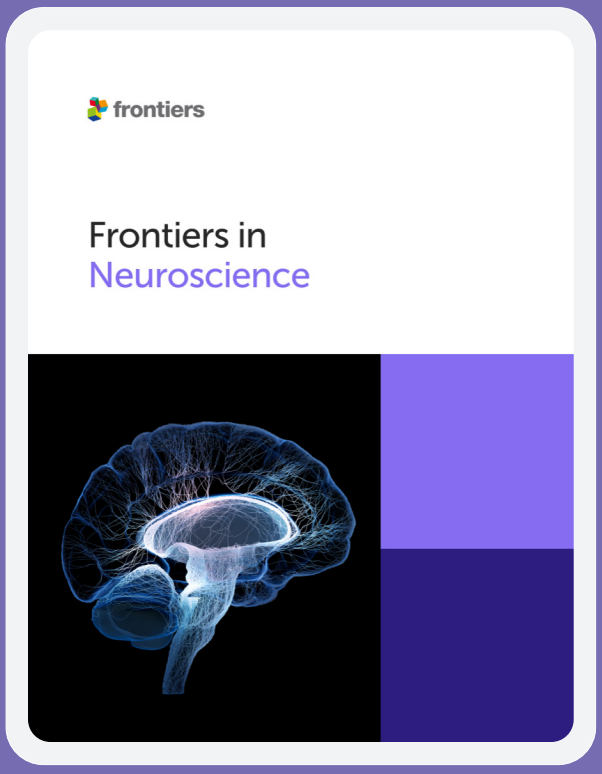

Frontiers

Avenue du Tribunal-Fédéral 34
1005 Lausanne, Switzerland
frontiersin.org

Contact us

+41 (0)21 510 17 00
frontiersin.org/about/contact